

**EFFECT OF DIFFERENT DESIGN PARAMETERS ON
THE CYCLIC RESPONSE OF
REDUCED BEAM SECTIONS (RBS) MOMENT CONNECTIONS**

By

Syed Asad Abbas Naqvi

B.S. (Civil Engineering), SSUET Karachi, Pakistan, 2009

A major research project
presented to Ryerson University
in partial fulfillment of the
requirements for the degree of
Master of Engineering
in the program of
Civil Engineering
Toronto, Ontario, Canada, 2019

© Syed Asad Abbas Naqvi, 2019

AUTHOR'S DECLARATION

I hereby declare that I am the sole author of this report. This is a true copy of the MRP, including any required final revisions.

I authorize Ryerson University to lend this MRP to other institutions or individuals for the purpose of scholarly research

I further authorize Ryerson University to reproduce this MRP by photocopying or by other means, in total or in part, at the request of other institutions or individuals for the purpose of scholarly research.

I understand that my MRP may be made electronically available to the public.

**EFFECT OF DIFFERENT DESIGN PARAMETERS ON THE CYCLIC RESPONSE OF
REDUCED BEAM SECTIONS (RBS) MOMENT CONNECTIONS**

By

Syed Asad Abas Naqvi

Master of Engineering (MEng.) in the Program of Civil Engineering

Ryerson University

2019

ABSTRACT

After the 1994 Northridge earthquake, research has been conducted to develop new types of beam-column moment connections, such as Reduced Beam Section (RBS) connections. This study performs a sensitivity analysis of the cyclic response of RBS connections using detailed finite element simulation. The significance of the effect of twenty-one factors is assessed using a statistical design of experiment method. The input factors are related to the material properties or the geometry of the beam-column connection. A two-level fractional factorial design is used to create factor combinations for the sensitivity analysis. The cyclic response of RBS connections is assessed in terms of five response variables, including: the total dissipated energy, initial stiffness, strength degradation rate, maximum moment capacity and rupture index at 7.5% storey drift. The sensitivity analysis results show that the beam depth has the greatest influence on the cyclic response of RBS connections.

ACKNOWLEDGEMENTS

I would like to acknowledge my supervisor Dr. Saber Moradi for his continuous guidance and support throughout the process of my experiment and completion of this project. I would also like to thank Dr. Thomas Duever for his valuable time and support in regards to his guidance about the design of experiments. It is necessary to mention about the resources that Ryerson University has provided me including all the research papers and tools to carry out my project such as ANSYS APDL that were necessary for this endeavour.

Table of Contents

AUTHOR'S DECLARATION.....	ii
ABSTRACT.....	iii
ACKNOWLEDGEMENTS.....	iv
LIST OF TABLES.....	vii
LIST OF FIGURES.....	viii
CHAPTER – 1.....	1
1. INTRODUCTION.....	1
1.1. Background.....	1
1.1.1. Moment Resisting Frames.....	1
1.1.2. Need for Reduced Beam Sections (RBS).....	2
1.2. Problem Statement.....	2
CHAPTER – 2.....	3
2. LITERATURE REVIEW.....	3
CHAPTER – 3.....	9
3. METHODOLOGY.....	9
3.1. GENERAL.....	9
3.2. FINITE ELEMENT MODEL.....	9
3.2.1. Geometry.....	9
3.2.2. Material.....	12
3.2.3. Meshing.....	13
3.2.4. Boundary Conditions.....	14
3.2.5. Loading Conditions.....	14
3.2.6. Validation of the Finite Element Model.....	15
3.3. IDENTIFICATION OF FACTORS.....	18
3.4. SELECTION OF FACTORS.....	28
3.5. FINALIZATION OF FACTORS.....	30
3.6. DESIGN OF EXPERIMENT.....	33
3.7. ANALYTICAL SPECIMEN GEOMETRIES.....	35
3.8. RESPONSE VARIABLES.....	38
3.8.1. R1: Total Dissipated Energy.....	38
3.8.2. R2: Initial Stiffness (k_i).....	39
3.8.3. R3: Strength Degradation Rate.....	39
3.8.4. R4: Maximum Moment Resistance.....	39
3.8.5. R5: Rupture Index @ 7.5% Total Storey Drift.....	40

CHAPTER – 4	41
4. THE EXPERIMENT	41
4.1. PHASE – 1 RESPONSE PLOTS	41
4.2. INITIAL SENSITIVITY ANALYSIS	43
4.3. SEMI-FOLD OVER AUGMENTED DESIGN (PHASE-2)	51
4.4. PHASE – 2 RESPONSE PLOTS	53
CHAPTER – 5	56
5. RESULTS AND DISCUSSIONS	56
5.1. DEFLECTED GEOMETRIES OF FEA MODELS	56
5.2. OVERALL SENSITIVITY ANALYSIS OF EFFECTS	58
5.2.1. For Response Variable R1 (Total Dissipated Energy)	60
5.2.2. For Response Variable R2 (Initial Stiffness)	71
5.2.3. For Response Variable R3 (Strength Degradation Rate)	76
5.2.4. For Response Variable R4 (Maximum Moment Capacity)	86
5.2.5. For Response Variable R5 (Rupture Index @ 7.5% Total Storey Drift)	91
5.2.6. Overview of the Results	96
5.3. CONCLUSIONS AND RECOMMENDATIONS	99
GLOSSARY OF ACRONYMS AND SYMBOLS	100
APPENDICES	102
APPENDIX A: FEA Models	
APPENDIX B: Response Plots	
APPENDIX C: Deflected Geometries of Specimen	
REFERENCES	

LIST OF TABLES

Table 1: Parameters for Validation Specimen RBS1-S	16
Table 2: Parameters for Validation Specimen RBS2-S	17
Table 3: Selected 2-Level Values of Parameters	29
Table 4: Values of Parameters for Testing 2 Insignificant Factors.....	30
Table 5: Finalized 2-Level Values of Parameters	33
Table 6: Coded Factor Combinations for Experiment Phase 1	34
Table 7: ANOVA of Selected Model for Response R1, Phase-1	46
Table 8: ANOVA of Selected Model for Response R2, Phase-1	47
Table 9: ANOVA of Selected Model for Response R3, Phase-1	48
Table 10: ANOVA of Selected Model for Response R4, Phase-1.....	49
Table 11: ANOVA of Selected Model for Response R5, Phase-1.....	50
Table 12: Coded Factor Combinations for Experiment Phase 2 (Semi-Fold over)	52
Table 13: Results from Both Phases of the Experiment	58
Table 14: Coefficients of Model for Response R1.....	60
Table 15: ANOVA of Selected Model for Response R1	64
Table 16: Coefficients of Model for Response R2.....	72
Table 17: ANOVA of Selected Model for Response R2	74
Table 18: Coefficients of Model for Response R3.....	77
Table 19: ANOVA of Selected Model for Response R3	81
Table 20: Coefficients of Model for Response R4.....	87
Table 21: ANOVA of Selected Model for Response R4	91
Table 22: Coefficients of Model for Response R5.....	93
Table 23: ANOVA of Selected Model for Response R5	96
Table 24: Summary of Contribution of Factors for All Responses	98
Table 25: Overall Ranking of Factors.....	100

LIST OF FIGURES

Figure 1: A Conceptual Sketch of a Moment Resisting Frame (MRF)	1
Figure 2: Type I - RBS with Continuity and Doubler Web Plates.....	10
Figure 3: Type II - RBS with Continuity Plates.....	11
Figure 4: Type III - RBS with Doubler Web Plates.....	11
Figure 5: Type IV - RBS without Continuity and Doubler Web Plates.....	12
Figure 6: Bilinear Stiffness Curve of Material.....	13
Figure 7: A Depiction of Model Meshing and Boundary Conditions.....	14
Figure 8: Loading History.....	15
Figure 9: Response Comparison for RBS1-S (Tabar and Deylami 2005)	16
Figure 10: Response Comparison for RBS2-S (Tabar and Deylami 2005)	17
Figure 11: Comparison of Model 1 & Model 2 Results	31
Figure 12: Comparison of Model 3 & Model 4 Results	31
Figure 13: Comparison of Model 5 & Model 6 Results	32
Figure 14: Comparison of Model 7 & Model 8 Results	32
Figure 15: FEA Model for Specimen RBS-1	35
Figure 16: FEA Model for Specimen RBS-2.....	35
Figure 17: FEA Model for Specimen RBS-3.....	36
Figure 18: FEA Model for Specimen RBS-4.....	36
Figure 19: FEA Model for Specimen RBS-5.....	36
Figure 20: FEA Model for Specimen RBS-6.....	37
Figure 21: Schematic of Response Variables Considered in Sensitivity Study	38
Figure 22: Strength Degradation Rate (Uang and Fan, 2001)	39
Figure 23: Experimental Moment vs Rotation Curve for RBS-1	41
Figure 24: Experimental Moment vs Rotation Curve for RBS-2	41
Figure 25: Experimental Moment vs Rotation Curve for RBS-3	41
Figure 26: Experimental Moment vs Rotation Curve for RBS-4	41
Figure 27: Experimental Moment vs Rotation Curve for RBS-5	42
Figure 28: Experimental Moment vs Rotation Curve for RBS-6	42
Figure 29: Experimental Moment vs Rotation Curve for RBS-7	42
Figure 30: Experimental Moment vs Rotation Curve for RBS-8	42
Figure 31: Experimental Moment vs Rotation Curve for RBS-9	42
Figure 32: Experimental Moment vs Rotation Curve for RBS-10	42

Figure 33: Half-Normal Probability Plot for Response R1 (Total Dissipated Energy) Phase-1.....	43
Figure 34: Half-Normal Probability Plot for Response R2 (Initial Stiffness) Phase-1	44
Figure 35: Half-Normal Probability Plot for Response R3 (Strength Degradation Rate) Phase 1	44
Figure 36: Half-Normal Probability Plot for Response R4 (Max. Moment Capacity) Phase-1	45
Figure 37: Half-Normal Probability Plot for Response R5 (Rupture Index) Phase-1	45
Figure 38: Semi-foldover Augmented Design Dialogue Screen in Design Expert v.11 Software	51
Figure 39: Experimental Moment vs Rotation Curve for RBS-33	53
Figure 40: Experimental Moment vs Rotation Curve for RBS-34	53
Figure 41: Experimental Moment vs Rotation Curve for RBS-35	53
Figure 42: Experimental Moment vs Rotation Curve for RBS-36	53
Figure 43: Experimental Moment vs Rotation Curve for RBS-37	54
Figure 44: Experimental Moment vs Rotation Curve for RBS-38	54
Figure 45: Experimental Moment vs Rotation Curve for RBS-39	54
Figure 46: Experimental Moment vs Rotation Curve for RBS-40	54
Figure 47: Experimental Moment vs Rotation Curve for RBS-41	54
Figure 48: Experimental Moment vs Rotation Curve for RBS-42	54
Figure 49: Experimental Moment vs Rotation Curve for RBS-43	55
Figure 50: Experimental Moment vs Rotation Curve for RBS-44	55
Figure 51: Experimental Moment vs Rotation Curve for RBS-45	55
Figure 52: Experimental Moment vs Rotation Curve for RBS-46	55
Figure 53: Experimental Moment vs Rotation Curve for RBS-47	55
Figure 54: Experimental Moment vs Rotation Curve for RBS-48	55
Figure 55: Deflected Geometry of Specimen RBS-1.....	56
Figure 56: Deflected Geometry of Specimen RBS-2.....	56
Figure 57: Deflected Geometry of Specimen RBS-3.....	57
Figure 58: Deflected Geometry of Specimen RBS-4.....	57
Figure 59: Deflected Geometry of Specimen RBS-5.....	57
Figure 60: Half-Normal Probability Plot for Response R1 (Total Dissipated Energy)	61
Figure 61: Pareto Chart for Response R1 (Total Dissipated Energy).....	61
Figure 62: Percentage Contributions of Factors and Interactions on Response R1	62
Figure 63: Plot of Marginal Means for Interaction AB in Selected Model for Response R1	64
Figure 64: 3D Response Surface and Contour Plots for 2FI AB in Selected Model for Response R1.....	64
Figure 65: Plot of Marginal Means for Interaction AC in Selected Model for Response R1	65
Figure 66: 3D Response Surface and Contour Plots for 2FI AC in Selected Model for Response R1.....	65

Figure 67: Plot of Marginal Means for Interaction AD in Selected Model for Response R1	66
Figure 68: 3D Response Surface and Contour Plots for 2FI AD in Selected Model for Response R1	66
Figure 69: Plot of Marginal Means for Interaction AQ in Selected Model for Response R1	67
Figure 70: 3D Response Surface and Contour Plots for 2FI AQ in Selected Model for Response R1	67
Figure 71: Plot of Marginal Means for Interaction AU in Selected Model for Response R1	68
Figure 72: 3D Response Surface and Contour Plots for 2FI AU in Selected Model for Response R1	68
Figure 73: Plot of Marginal Means for Interaction BC in Selected Model for Response R1	69
Figure 74: 3D Response Surface and Contour Plots for 2FI BC in Selected Model for Response R1	69
Figure 75: Plot of Marginal Means for Interaction BD in Selected Model for Response R1	70
Figure 76: 3D Response Surface and Contour Plots for 2FI BD in Selected Model for Response R1	70
Figure 77: Half-Normal Probability Plot for Response R2 (Initial Stiffness).....	72
Figure 78: Pareto Chart for Response R2 (Initial Stiffness)	72
Figure 79: Percentage Contributions of Factors and Interactions on Response R2	73
Figure 80: Plot of Marginal Means for Interaction BC in Selected Model for Response R2	74
Figure 81: 3D Response Surface and Contour Plots for 2FI BC in Selected Model for Response R2.....	74
Figure 82: Plot of Marginal Means for Interaction BD in Selected Model for Response R2	75
Figure 83: 3D Response Surface and Contour Plots for 2FI BD in Selected Model for Response R2.....	75
Figure 84: Half-Normal Probability Plot for Response R3 (Strength Degradation Rate)	77
Figure 85: Pareto Chart for Response R3 (Strength Degradation Rate)	78
Figure 86: Percentage Contributions of Factors and Interactions on Response R3	78
Figure 87: Plot of Marginal Means for Interaction AF in Selected Model for Response R3	81
Figure 88: 3D Response Surface and Contour Plots for 2FI AF in Selected Model for Response R3	81
Figure 89: Plot of Marginal Means for Interaction AK in Selected Model for Response R3	82
Figure 90: 3D Response Surface and Contour Plots for 2FI AK in Selected Model for Response R3	82
Figure 91: Plot of Marginal Means for Interaction AL in Selected Model for Response R3	83
Figure 92: 3D Response Surface and Contour Plots for 2FI AL in Selected Model for Response R3.....	83
Figure 93: Plot of Marginal Means for Interaction AR in Selected Model for Response R3	84
Figure 94: 3D Response Surface and Contour Plots for 2FI AR in Selected Model for Response R3.....	84
Figure 95: Plot of Marginal Means for Interaction BE in Selected Model for Response R3	85
Figure 96: 3D Response Surface and Contour Plots for 2FI BE in Selected Model for Response R3	85
Figure 97: Half-Normal Probability Plot for Response R4 (Maximum Moment Capacity).....	87
Figure 98: Pareto Chart for Response R4 (Maximum Moment Capacity)	87
Figure 99: Percentage Contributions of Factors and Interactions on Response R4	88
Figure 100: Plot of Marginal Means for Interaction BD in Selected Model for Response R4	90

Figure 101: 3D Response Surface and Contour Plots for 2FI BD in Selected Model for Response R4..... 90
Figure 102: Half-Normal Probability Plot for Response R5 (Rupture Index @ 7.5% Total Storey Drift). 92
Figure 103: Pareto Chart for Response R5 (Rupture Index @ 7.5% Total Storey Drift) 92
Figure 104: Percentage Contributions of Factors and Interactions on Response R5 93
Figure 105: Plot of Marginal Means for Interaction AD in Selected Model for Response R5 95
Figure 106: 3D Response Surface and Contour Plots for 2FI AD in Selected Model for Response R5 95
Figure 107: Graphical Representation of Aggregate Percentile Contribution of Factors 97

CHAPTER – 1

1. INTRODUCTION

1.1. Background

1.1.1. Moment Resisting Frames

A structural system consisting of beam column arrangement for moment resistance is generally termed as moment resisting frame. The concept of steel frames emerged with the construction of high-rise structures in Chicago and New York City in 1880's when those steel frames were used as a system to carry gravity loads, and the lateral stiffness was provided by claddings and beams. The requirement of addressing lateral loads such as seismic and wind loads were established after 1906 San Francisco earthquake followed by the evolution of moment resisting frame system over the decades (Bruneau et al., 2011). The Moment Resisting Frames (MRFs) that are subjected to cyclic loading (e.g. lateral loads induced by seismic activities) are design and detailed specially to restrain the rotation of beam element at the connection and dissipate the energy resulted by the beam deflection due to applied loadings. A simple Moment Resisting Frame (MRF) is depicted in **Figure 1**.

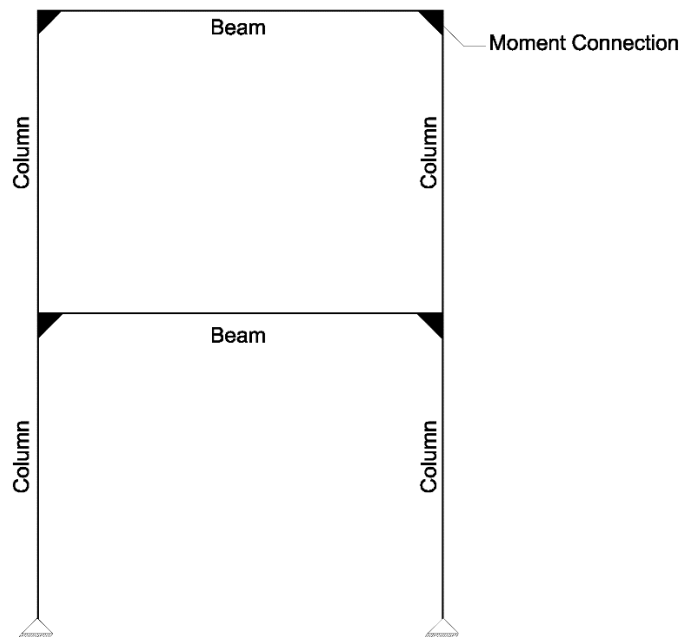


Figure 1: A Conceptual Sketch of a Moment Resisting Frame (MRF)

1.1.2. Need for Reduced Beam Sections (RBS)

The unexpected brittle failure of beam to column welded moment connection reported across the greater Los Angeles area during 1994 Northridge, California earthquake triggered the researches to improve the behavior of the moment connections in MRFs. An approach of reducing the beam flexure capacity by reducing the beam section at certain point near the connection was adopted and named as reduced beam section or dog-bone connections (Paul Popov et al., 1998).

1.2. Problem Statement

The idea of developing such connections was introduced to deal with the cyclic loadings that may cause a brittle failure in the system due to stress concentrations at welded zones. Several efforts have been made to understand the effectiveness of RBS connections in comparison to a regular moment connection under cyclic loadings. However, to design the RBS connections efficiently, understanding the effects of different parameters on the performance of these connections under cyclic loadings is essential. These parameters will be discussed in detail in section 3.3 to 3.5 of this document. To achieve these objectives, a statistical design of experiment was required to analyze these effects and identifying individual and interactive effects of these parameters on the system and its sensitivity towards these parameters. The design of experiment will be discussed in section 3.6 of this document followed by the experimental procedure and its outcomes.

CHAPTER – 2

2. LITERATURE REVIEW

In mid 90's, a study by (Chen and Chu, 1996) was carried out to observe the effectiveness of flange cut RBS connections in steel beams as a means of introducing plastic hinge in steel section ensuring the yielding to initiate from the steel section instead of weld to avoid stress concentrations in the welded zone. This was due to an uncertain behaviour of welded parts as observed in past. The experiment carried out for a 4% beam rotation suggested that by predefining an enlarged yielding zone by means of flange cuts, the energy dissipation was more predictable and reliable and resulted in an ultimate strength of the moment connection 1.29 times more than nominal values along with a drop in the stiffness by an acceptable difference of 3%. The study recommended the determination of point of inflection by means of inelastic analysis under seismic and gravity loads.

Two years later, another experiment (Paul Popov et al., 1998) was completed that studied the fracture locations and failure modes of pre (traditional) vs post (RBS/ dog-bone) 1994 Northridge Earthquake connections. The elastic-plastic FEA of the beam-column welded junction explained the sudden brittle failure of weak beam flange at the welded section due to triaxial action. The study concluded that a connection of beam directly welded to the column fails with a brittle behaviour before attaining the plastic moment of the beam due to triaxial stresses and not because of the material properties and a RBS connection was found to be a viable solution to this problem of not being able to control the demand of ductility by material properties by introducing a plastic hinge in steel section. Some design recommendations were presented for these type of (radial cut) RBS connections in the compliance with SAC advisory 1 and AWS D1.1-98 codes of practises by (Engelhardt, 1999).

Another study (Uang et al., 2000) was conducted to evaluate the effectiveness of implementation of reduced beam sections for seismic rehabilitation of conventional moment connections that were used commonly before the Northridge earthquake. As the design of special moment resisting frames (SMRFs) is usually governed by story drift that is controlled by stiffnesses of lateral structural members rather than their strengths, the design might have larger sections than the required strength and hence can be reduced without posing any significant effect on overall stiffness of the frame resulting in the reduction in shear force in

the panel zone, reduced force demand in column continuity plates and easier fulfilment of strong column – weak beam system requirement. Therefore, a RBS was introduced to the beam by reducing its bottom flange by 50% to induce the phenomenon of plastic hinge formation in the beam at specified location under the loading condition and the welds it was observed that providing RBS at bottom flange alone doesn't exhibit the ductile behavior of the connection unless welds developed with low toughness electrode (E70T-4) at top flange are replaced by welds made with a notch-tough electrode (E71T-8) (Uang et al., 2000).

At this point, the effectiveness of RBS over a conventional beam-column moment connection was proven and RBS were becoming more adaptable. That triggered need of new researches to study different aspects of RBS behaviour and ways to make it more efficient. Such an effort was made by (Uang and Fan, 2001) to assess if additional bracing is required near RBS region by analyzing the effects of slenderness ratio on plastic rotational capacity and strength degradation rate with the consideration of effects of slab on these responses statistically. The experiment was conducted on a database of 55 full scale RBS moment connection specimens tested under cyclic loading conditions by means of regression analysis. The study suggested that the slenderness ratio of web local buckling was most significant for the responses followed by the flange local buckling and lateral torsional buckling being the least significant for both linear and non-linear regression analysis for individual and combined effects. A regression model was developed using web and flange local buckling slenderness ratios as independent variables and plastic rotation capacity as response variable that recommended the limiting h/t_w ratio for web local buckling to be $\frac{11,00}{\sqrt{F_y}}$ for seismic provisions. It was also concluded that concrete slab under positive bending contributed towards an increased plastic rotation capacity of RBS. These observations were later on verified as a result of experiment carried out by (Jones et al., 2002) on RBS connections with weak, balanced and very strong types of panel zones.

Another study (Chi and Uang, 2002) was conducted to assess the behaviour of RBS moment connection under cyclic loading with deep columns having wide-flange sections. Three specimens, namely DC-1, DC-2 and DC-3 with beam sections W36x150, W36x150, W27x194 and column sections W27x146, W27x194 and W27x194 respectively, were experimentally examined and it was observed that DC-1 and DC-2 were able to achieve 3% plastic rotation

while specimen DC-3 had a brittle failure at 2.8% plastic rotation. Twisting in deep columns was also observed during the experiment and it was explained as a result of higher warping stresses in deep column sections due to their torsional properties and tendency of RBS connections to buckle laterally inducing torsion and out-of-plane bending effects in deep columns. A calculation procedure for the subject connection type considering the combined effects of in-plane, out-of-plane and warping stresses was also presented to verify the adequacy of the connection. Four years later, (Zhang et al., 2006) conducted more detailed experiment on RBS connections with deep columns that verified the findings of (Chi and Uang, 2002). In another similar study, (Zhang and Ricles, 2006) tested six full scale specimens to observe the effects of four parameters namely column size, beam size, floor slab and supplemental lateral brace at the end of RBS and presented more refined criteria to predict stress distribution in beam and column flanges.

The effects of introducing a RBS in a beam to column weak axis connection were studied by (Gilton and Uang, 2002) and it was observed that introduction of RBS to such connection type prevented a brittle failure in welded section due to stress concentration in groove weld at the edges of beam flange as observed in past. The RBS reduced the strain concentration at the edges of beam flange near the groove weld by three times. Also, the total plastic rotation of 3% was achieved without any yielding in column or panel zone as most of the plastic rotation occurred near RBS. It was also concluded that the far-side continuity plate was insignificant in reducing any stress concentrations in tested specimen. However, the near side continuity plate was suggested to be protruded at least 75 mm from the tips of the column flanges due to its tendency to reduce tensile force in beam flange. It was also suggested that if beam width is less than 70% of width of continuity plate, the plate should be trimmed at the edges to help reducing stress concentration near welds. This study also gave a design procedure for the connection type experimented. (Oh et al., 2015) also evaluated the weak axis column tree connection with RBS that yielded 5% of story drift with more stable deformation capacity curve for RBS as compared to conventional connections.

Efficiency of RBS in connections without continuity plates were investigated by (Pantelides et al., 2004) under ASIC 1997 and 2002 Seismic Provisions and it was found by testing four specimens that these specimen met the requirement of FEMA-350 for special moment frames.

Also, the failure sequence showed a local buckling in beam web followed by buckling and failure in bottom flange of the beam. It was concluded that with strong panel zone and suitably thicker column flanges, effect of continuity plates on performance of RBS is insignificant.

The effect of panel zone on the performance of RBS were presented by (Lee et al., 2005) suggesting that a panel zone can develop 1% of plastic rotation without effecting the groove welds at beam flange resulting in a drop of lateral torsional buckling of the beam up to 50% of its value. The relation of panel zone to RBS was further explored by (Tabar and Deylami, 2005) that observed a reduction in flexural moment capacity of RBS with strong PZ due to lateral and local buckling. The hysteric response in slender beams is controlled by lateral torsional buckling as compared to web local buckling. The study recommended to implement a reduction factor of 0.85 to ultimate shear strength of PZ recommended by AISC seismic provision.

The idea of reduced section was tested on reduced flange plate type connection by (Chou and Wu, 2007) when they evaluated 4 specimens that exhibited similar responses to past studies. Statistical analysis showed that the buckling force of reduced flange plate is highly sensitive to minimum width and slenderness ratio.

The formulation of non-prismatic beam element was presented by (Kim et al., 2007) to accommodate the effect of RBS while modeling a non-prismatic beam that can effectively predict elastic story drift of moment frames with RBS connections. An increase of 6 to 8% in story drift was observed for a 50% flange reduction while the increase in story drift for a 40% flange reduction was reported as 4.5 to 6%. Another study (Lee and Kim, 2007) presented the design procedure for RBS steel moment connections with bolted web attachments having a much higher slip-critical bolt requirement as compared to conventional methods. The specimen exhibited a story drift of 5% without fracture.

The geometrical characteristics of RBS for European profiles were evaluated by (Pachoumis et al., 2009, 2010) with the help of 2 specimens. FEA was also performed for these specimens and results were compared to find out that geometrical characteristics of RBS are required to be readjusted to be applied on European profiles. This need of including RBS geometrical characteristics consideration to be included in European standards was also suggested by (Sophianopoulos, 2011).

(Li et al., 2009) studied the local buckling of reduced beam section under cyclic loading by means of different specimen of RBS with 1, 2, 3 and no set of stiffeners at RBS portion. The experiment presented an in-depth analysis of the behavior of laterally braced and unbraced RBS. A deterioration in the strength of the beam was observed even when there wasn't any significant lateral buckling observed in laterally unbraced length of 73.2ry. It was also noticed that with stiffened RBS, the last strength under cyclic loading was increased from under 80% of plastic moment which was observed with no stiffener case, to over 80% of plastic moment. It was also concluded that the thickness of stiffener effects least on the strength of RBS and a sufficient strength can be achieved by using a stiffener thickness equal to beam web thickness. Also, the maximum stress at RBS portion of stiffened RBS beam was noted to be more than a non-stiffened RBS beam while it didn't differ much at the fixed support location for both stiffened and un-stiffened conditions (Li et al., 2009).

Two specimen for end plate moment connection with RBS were analyzed by (Sofias et al., 2014) to observe the effect of RBS on end plate moment connection elements and it was concluded that due to development of a plastic hinge at predetermined location, the end plate, bolts, column flange, stiffeners and other connection elements did not experience any plasticizing and failures.

A low cycle fatigue damage model of RBS in beams with out-of-plane skew were evaluated by (Prinz and Richards, 2016) to see the effects of the angle of skew on the connection and the results from the experiment showed that the skew induced increased twisting in column and minor yielding at column flanges.

The behavior of RBS with floor slab system was studied by (Li et al., 2017) by designing, constructing and testing 6 specimen including 1 reference specimen. The reference specimen was developed without slab while the other specimens were designed and constructed with slabs. A composite hollow core steel column filled with concrete was used in all specimens while the beams had 3 types of cross-sections in different specimens. The study concluded that through-diaphragms were adequate to connect RBS beams to the composite columns considered in the study. Also, it was observed that the influence of RBS on flexural stiffness of connection was more significant under hogging moments as compared to sagging moment.

Moreover, the flange cut depth didn't affect the seismic behavior of the connection, however, a deeper cut resulted in abrupt strength degradation of the beam flange.

CHAPTER – 3

3. METHODOLOGY

3.1. GENERAL

In order to study the effects of different factors on any process, experiments are conducted with number of tests dealing with different combinations of these factors to observe the correlations and significance of these factors as well as the sensitivity and variability of the outcome of the experiments. However, an ill-designed experiment can result in a significant number of redundant tests, thus, to address this problem, an experiment can be designed to mitigate these efforts and conduct the experiment more efficiently to achieve desired objectives. In this study, a computer experiment was planned, designed and conducted to observe the behaviour through variation of different responses as the factors vary.

It is also important to select a reliable and adequate method to carry out the experiment so that the results would be error free and consistent. A finite element analysis approach was adopted using a renowned and reliable finite element analysis software package ANSYS Mechanical APDL 18.1 (Canonsburg, 2012). The design and the means to conduct the experiment are discussed in the following sections.

3.2. FINITE ELEMENT MODEL

As mentioned in section 3.1, a parametric finite element model was developed by using Solid 185 3D 8 nodes homogenous structural solid element type in ANSYS Mechanical APDL. Details of the model development process are explained in following sections while a sample parametric code for analytical model on ANSYS APDL is presented in Appendix A.

3.2.1. Geometry

The model consisted of a beam connected monolithically with the flange of a column. The beam had 2 radial cuts in its flange to form the dog-bone section type while the column had continuity plates and doubler web plates, however, the experiment had required such scenarios where either continuity plate or doubler

plate or both were not provided. Therefore, the model can be divided into 4 generic types. These types can be identified as shown in **Figures 2** through **5**.

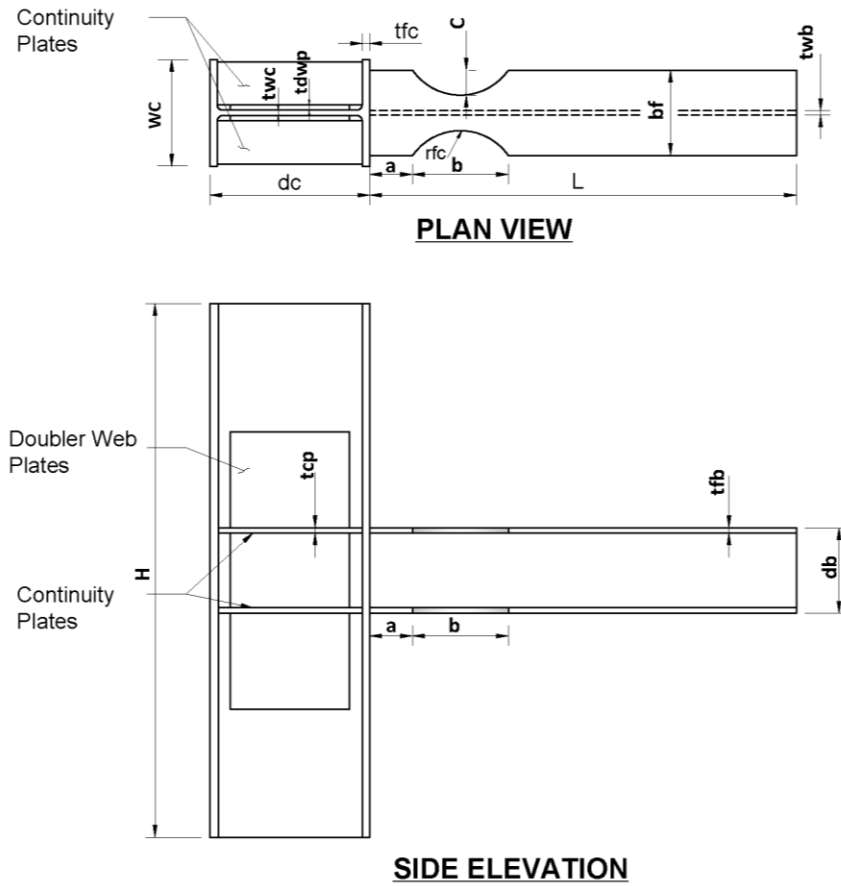


Figure 2: Type I - RBS with Continuity and Doubler Web Plates

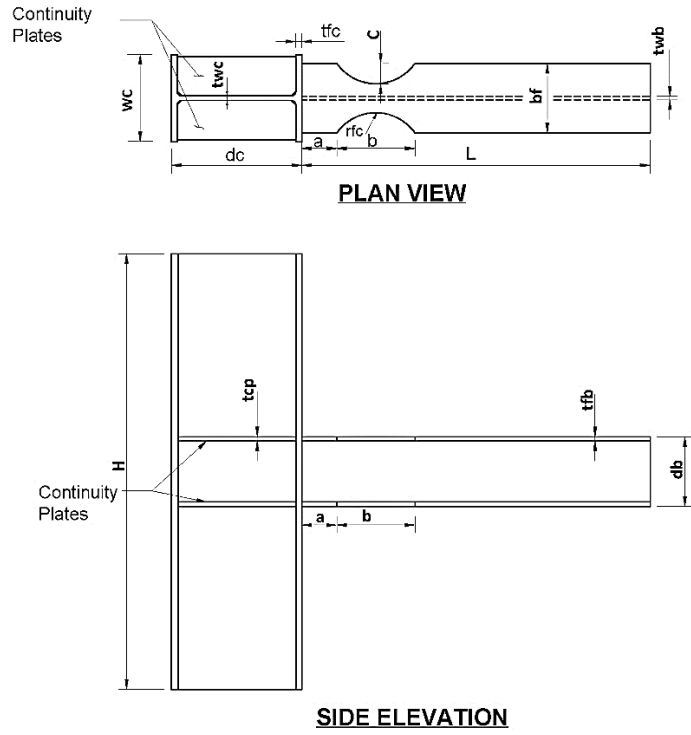


Figure 3: Type II - RBS with Continuity Plates

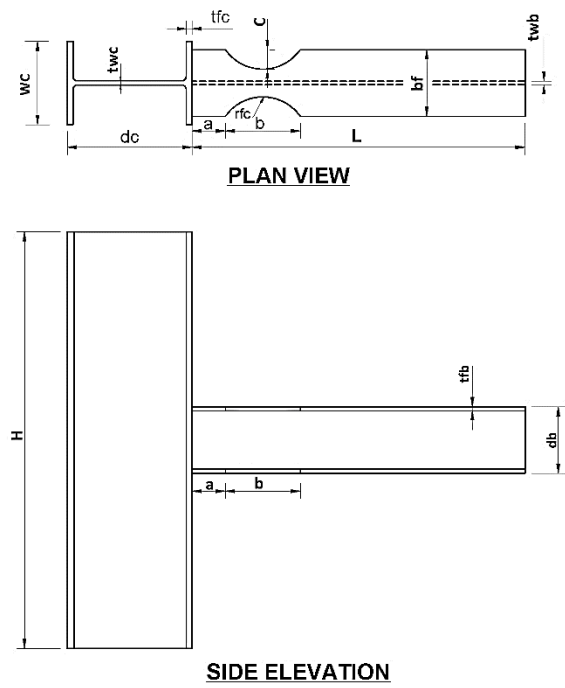


Figure 4: Type III - RBS with Doubler Web Plates

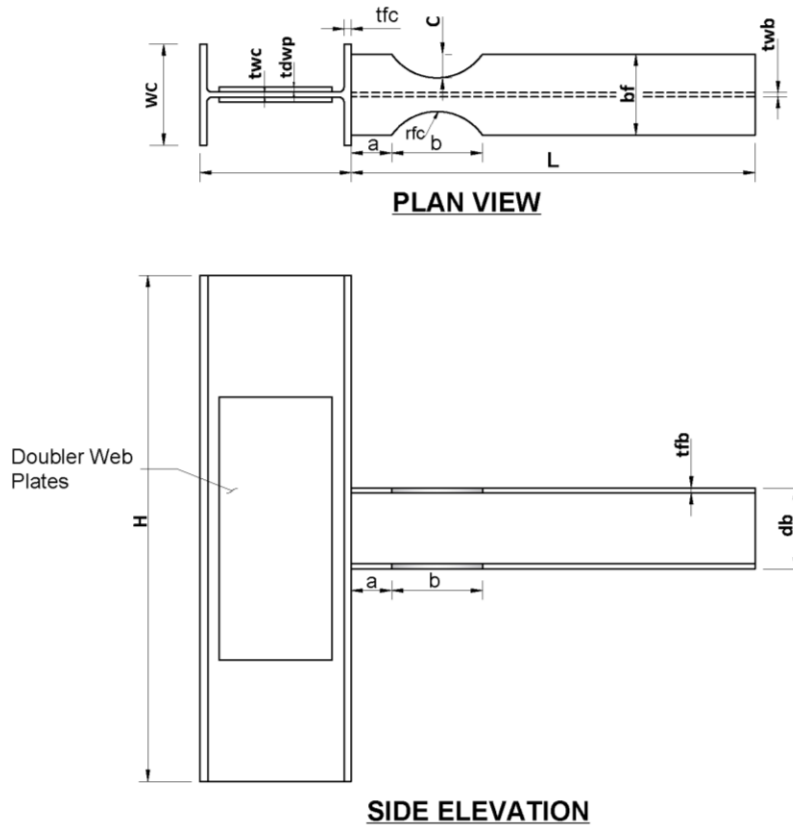


Figure 5: Type IV - RBS without Continuity and Doubler Web Plates

3.2.2. Material

The material for the specimen was selected as steel with a minimum and maximum values of modulus of elasticity that are shown in sections 3.3 to 3.5 and a Poisson's ratio of 0.3 was selected for the all cases. For non-linear analysis, bilinear stiffness was considered with a post-yielding modulus of elasticity as 1% of pre-yielding modulus elasticity (1% E). The bilinear stiffness curve of the material is depicted in **Figure 6**.

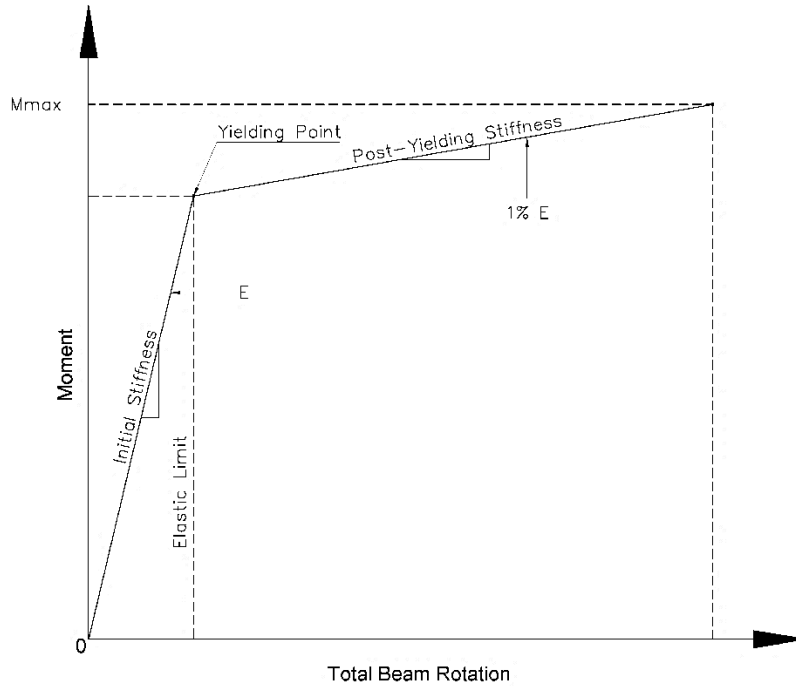


Figure 6: Bilinear Stiffness Curve of Material

3.2.3. Meshing

The model was meshed using mapped meshing to ensure better stress and deformation distribution amongst elements. Since, our area of interest was more specifically the area of beam from face of column to slightly farther the end of RBS flange cut and column panel zone, these portions were meshed using a finer mesh as compared to the tip of the beam and top and bottom portions of column as depicted in **Figure 7**.

3.2.4. Boundary Conditions

The tip of the beam was restrained against out of plane displacement in lateral direction (parallel to weak axis of beam) while the column was fixed at bottom and restrained against lateral displacements in both directions (weak and strong axes of column) as shown in **Figure 7**.

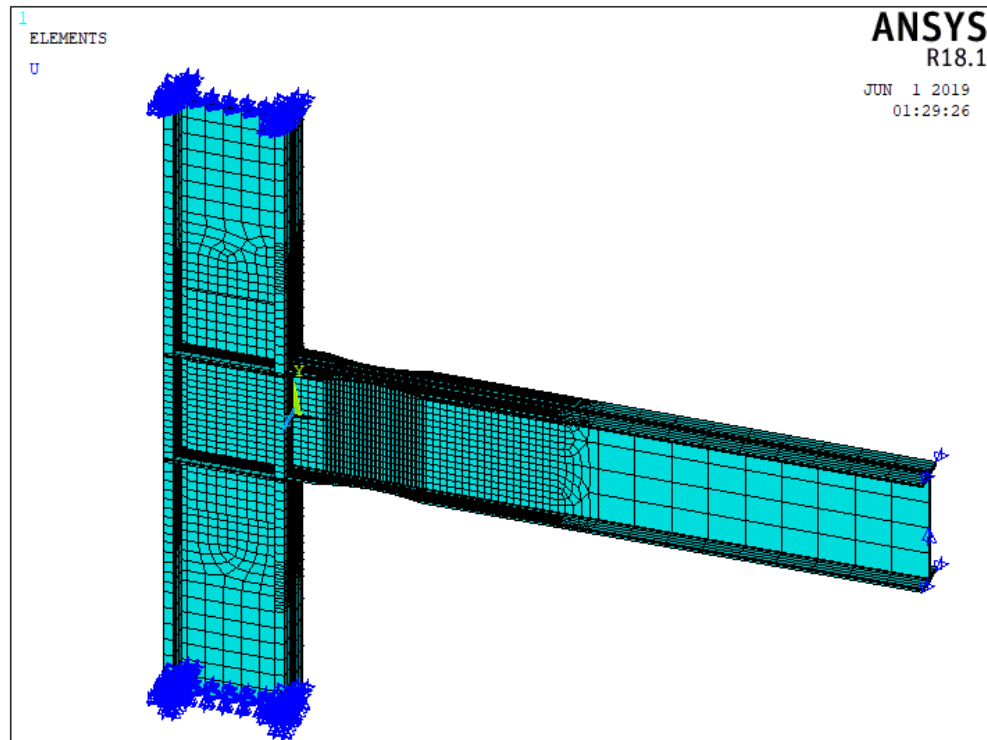


Figure 7: A Depiction of Model Meshing and Boundary Conditions

3.2.5. Loading Conditions

The beam was loaded at its tip with cyclic deflection as per SAC loading protocol as shown in **Figure 8**. Every run was performed with a consistent loading history of 11 cycles with a maximum of 7.5% deflection at the tip of the beam to record the responses for the static analysis with non linear geometric effects considerations.

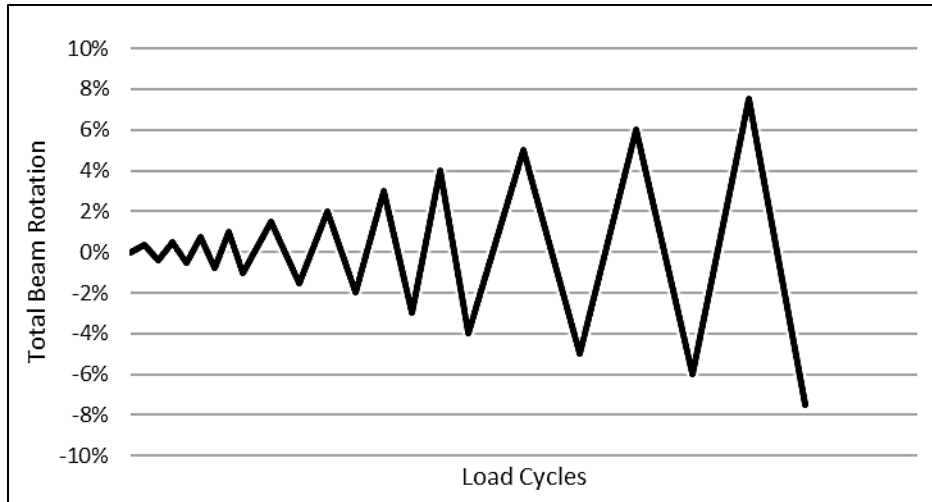


Figure 8: Loading History

3.2.6. Validation of the Finite Element Model

The process of validation is a vital part of the process to ensure that the experiment is error free and yields accurate results, in this regard, the analytical model was validated by analyzing 2 specimens referred as RBS1-S and RBS2-S in a study by Tabar and Deylami (2005) and comparing the results to the results of source study. These specimens were loaded as per SAC loading protocol as shown in **Figure 8** up to rotations recorded by the reference study for both specimens. The parameters used in the analysis are presented in **Tables 1** and **2**. The comparison of responses for RBS1-S and RBS2-S are presented in **Figures 9** and **10**, respectively.

Table 1: Parameters for Validation Specimen RBS1-S

BEAM PARAMETERS	S. No.	PARAMETER	Value	COLUMN PARAMETERS	S. No.	PARAMETER	Value
	1	bf (mm)	150.00		13	wc (mm)	200.00
	2	db (mm)	300.00		14	dc (mm)	200.00
	3	tfb (mm)	10.70		15	tfc (mm)	15.00
	4	twb (mm)	7.10		16	twc (mm)	9.00
	5	a (mm)	80.00		17	H (mm)	3000
	6	b (mm)	200.00		18	tdwp (mm)	10.00
	7	c (mm)	32.00		19	tcp (mm)	11.00
	8	L (mm)	2500		20	Escf (MPa)	2.10E+05
	9	Esbf (MPa)	2.10E+05		21	Fycf (MPa)	250.00
	10	Fybf (MPa)	250.00		22	Escw (MPa)	2.10E+05
	11	Esbw (MPa)	2.10E+05		23	Fycw (MPa)	250.00
12	Fybw (MPa)	250.00					

Note: For acronyms, refer to section 3.3 or glossary of acronyms and symbols

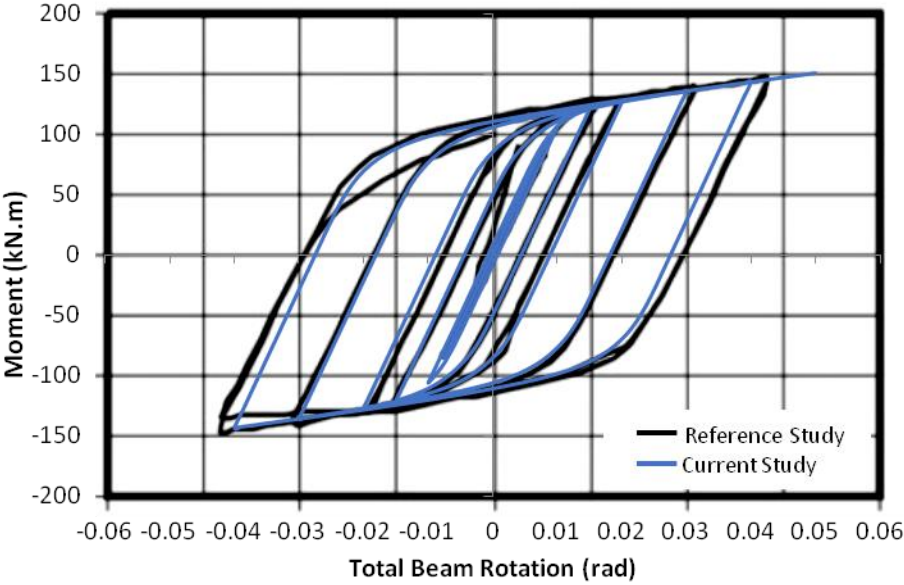


Figure 9: Response Comparison for RBS1-S (Tabar and Deylami 2005)

Table 2: Parameters for Validation Specimen RBS2-S

BEAM PARAMETERS	S. No.	PARAMETER	Value	COLUMN PARAMETERS	S. No.	PARAMETER	Value
	1	bf (mm)	190.00		13	wc (mm)	300.00
	2	db (mm)	450.00		14	dc (mm)	300.00
	3	tfb (mm)	14.60		15	tfc (mm)	19.00
	4	twb (mm)	19.40		16	twc (mm)	11.00
	5	a (mm)	120.00		17	H (mm)	3000
	6	b (mm)	350.00		18	tdwp (mm)	10.00
	7	c (mm)	45.00		19	tcp (mm)	19.00
	8	L (mm)	2500		20	Escf (MPa)	2.10E+05
	9	Esbf (MPa)	2.10E+05		21	Fycf (MPa)	250.00
	10	Fybf (MPa)	250.00		22	Escw (MPa)	2.10E+05
	11	Esbw (MPa)	2.10E+05		23	Fycw (MPa)	250.00
12	Fybw (MPa)	250.00					

Note: For acronyms, refer to section 3.3 or glossary of acronyms and symbols

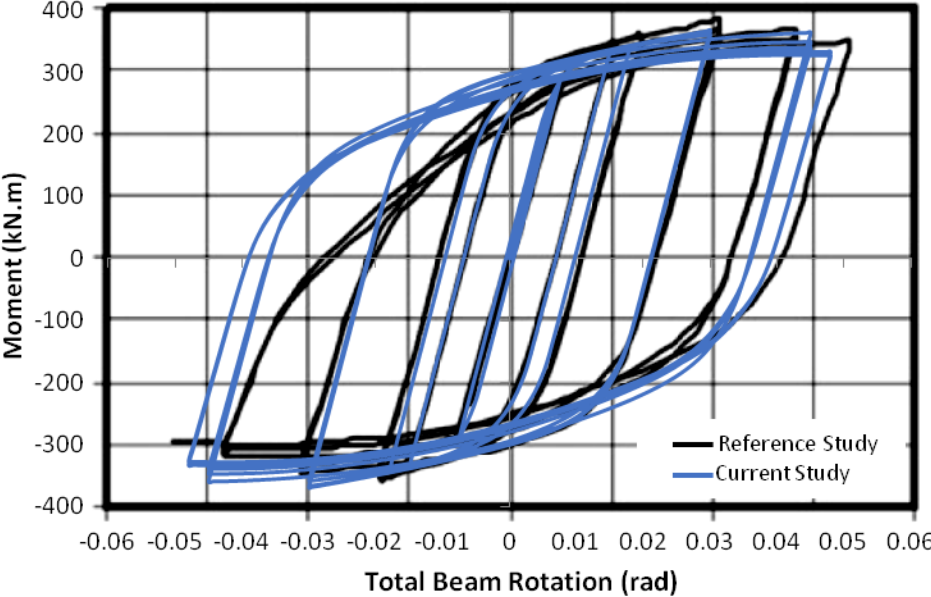


Figure 10: Response Comparison for RBS2-S (Tabar and Deylami 2005)

As a result of this validation process, it was evident that the FEA model developed for this study exhibits tendencies to perform analysis under cyclic loading conditions precisely and it was adequate and valid to be used for the experiment.

3.3. IDENTIFICATION OF FACTORS

Past studies on the behaviour of RBS under cyclic loading have shown that there are several parameters that may potentially affect the performance of RBS under these loading conditions. Those parameters were collected from such studies to develop a range of levels as shown in **Table 3.**

Table 3: Selected 2-Level Values of Parameters (Continued)

Reference	bf (mm)		db (mm)		tfb (mm)		twb (mm)		a (mm)		b (mm)		c (mm)	
	Min.	Max.	Min.	Max.	Min.	Max.	Min.	Max.	Min.	Max.	Min.	Max.	Min.	Max.
(Paul Popov et al. 1998)	304.80	419.10	904.24	916.94	20.07	711.20	15.24	20.32	203.20	279.40	711.20	635.00	60.96	86.36
(Uang et al. 2000)	304.80	304.80	911.86	911.86	23.88	686.00	15.88	15.88	152.40	152.40	686.00	686.00	76.00	76.00
(Uang and Fan 2001)	178.82	178.82	601.98	601.98	14.99	508.00	10.92	10.92	177.80	177.80	508.00	508.00	66.68	66.68
(Chi and Uang 2002)	304.80	355.60	911.86	713.74	23.88	609.60	15.88	19.05	266.70	228.60	609.60	762.00	69.85	76.20
(Gilton and Uang 2002)	178.82	304.80	601.98	911.86	14.99	406.00	10.92	15.88	127.00	229.00	406.00	762.00	44.00	76.00
(Jones et al. 2002)	304.80	304.80	911.86	911.86	23.88	685.00	15.88	15.88	230.00	230.00	685.00	685.00	76.00	76.00
(Pantelides et al. 2004)	266.70	266.70	769.62	769.62	25.40	531.04	15.62	15.62	152.02	165.35	531.04	531.04	69.34	69.34
(Tabar and Deylami 2005)	150.00	220.00	300.00	600.00	10.70	200.00	7.10	12.00	80.00	140.00	200.00	400.00	32.00	55.00
(Zhang and Ricles 2006)	304.80	304.80	911.86	911.86	23.88	525.00	15.88	15.88	175.00	175.00	525.00	525.00	75.00	75.00
(Lee and Kim 2007)	300.00	300.00	700.00	700.00	24.00	525.00	13.00	13.00	175.00	175.00	525.00	525.00	75.00	75.00
(Li et al. 2009)	228.35	307.34	607.06	927.10	17.27	494.00	11.18	19.43	114.00	154.00	494.00	773.00	57.00	77.00
(Pachoumis et al. 2009)	240.00	240.00	230.00	230.00	12.00	184.00	7.50	7.50	156.00	156.00	184.00	184.00	36.00	60.00
(Pachoumis et al. 2010)	180.00	180.00	171.00	171.00	9.50	102.60	6.00	6.00	72.00	144.00	102.60	128.25	22.50	36.00
(Sofias et al. 2014)	152.00	152.00	160.00	160.00	9.00	114.00	6.00	6.00	96.00	96.00	114.00	114.00	40.00	40.00
(Oh et al. 2015)	200.00	200.00	600.00	600.00	17.00	450.00	11.00	11.00	120.00	120.00	450.00	450.00	40.00	40.00
(Li et al. 2017)	133.00	124.00	203.00	248.00	7.80	180.00	5.80	5.00	80.00	80.00	180.00	220.00	26.00	31.00
(Sophianopoulos and Deri 2017)	110.00	220.00	217.00	210.00	7.70	81.38	5.00	7.00	66.00	132.00	81.38	78.75	25.00	48.00

N/A: Not Applicable

NG: Not Given

Table 3: Selected 2-Level Values of Parameters (Continued)

Reference	s (mm)		rfc (mm)		L (mm)		Esbf (MPa)		Fybf (MPa)		Esbw (MPa)	
	Min.	Max.	Min.	Max.	Min.	Max.	Min.	Max.	Min.	Max.	Min.	Max.
(Paul Popov et al. 1998)	558.80	596.90	1066.80	626.82	3416.30	3416.30	NG	NG	4.30E+02	3.90E+02	NG	NG
(Uang et al. 2000)	495.40	495.40	813.00	813.00	3128.00	3128.00	NG	NG	3.38E+02	3.38E+02	NG	NG
(Uang and Fan 2001)	431.80	431.80	517.53	517.53	NG	NG	NG	NG	2.50E+02	4.50E+02	NG	NG
(Chi and Uang 2002)	571.50	609.60	699.94	990.60	3233.02	3224.13	2.00E+05	2.00E+05	4.00E+02	4.27E+02	2.00E+05	2.00E+05
(Gilton and Uang 2002)	330.00	610.00	486.00	991.00	3381.61	3370.18	2.07E+05	2.07E+05	2.86E+02	4.00E+02	2.07E+05	2.07E+05
(Jones et al. 2002)	572.50	572.50	810.00	810.00	3416.30	3416.30	2.07E+05	2.07E+05	3.74E+02	3.74E+02	2.07E+05	2.07E+05
(Pantelides et al. 2004)	417.54	430.87	533.40	533.40	3737.61	3687.19	2.07E+05	2.07E+05	3.82E+02	3.82E+02	2.07E+05	2.07E+05
(Tabar and Deylami 2005)	180.00	340.00	172.25	391.13	2500.00	2500.00	2.10E+05	2.10E+05	3.70E+02	3.70E+02	2.10E+05	2.10E+05
(Zhang and Ricles 2006)	437.50	437.50	497.00	497.00	4040.00	4264.00	NG	NG	3.45E+02	3.45E+02	NG	NG
(Lee and Kim 2007)	437.50	437.50	497.00	497.00	4297.00	4297.00	NG	NG	3.30E+02	3.30E+02	NG	NG
(Li et al. 2009)	361.00	540.50	563.67	1008.51	3580.00	4816.00	2.10E+05	2.10E+05	2.35E+02	3.45E+02	2.10E+05	2.10E+05
(Pachoumis et al. 2009)	248.00	248.00	135.56	100.53	1200.00	1200.00	2.07E+05	2.07E+05	3.05E+02	3.05E+02	2.07E+05	2.07E+05
(Pachoumis et al. 2010)	123.30	208.13	69.73	75.11	1200.00	1200.00	2.09E+05	2.09E+05	3.10E+02	3.10E+02	2.09E+05	2.09E+05
(Sofias et al. 2014)	153.00	153.00	60.61	60.61	1200.00	1200.00	2.15E+05	2.20E+05	3.70E+02	4.30E+02	2.15E+05	2.20E+05
(Oh et al. 2015)	345.00	345.00	654.29	654.29	3510.00	3510.00	2.04E+05	2.07E+05	2.35E+02	3.25E+02	2.04E+05	2.07E+05
(Li et al. 2017)	170.00	190.00	168.77	210.66	1625.00	1625.00	2.02E+05	2.02E+05	3.00E+02	3.00E+02	2.04E+05	2.04E+05
(Sophianopoulos and Deri 2017)	106.69	171.38	45.61	40.15	3000.00	3000.00	2.10E+05	2.10E+05	2.35E+02	2.35E+02	2.10E+05	2.10E+05

N/A: Not Applicable

NG: Not Given

Table 3: Selected 2-Level Values of Parameters (Continued)

Reference	Fybw (MPa)		wc (mm)		dc (mm)		tfc (mm)		twc (mm)		H (mm)	
	Min.	Max.	Min.	Max.	Min.	Max.	Min.	Max.	Min.	Max.	Min.	Max.
(Paul Popov et al. 1998)	4.30E+02	3.90E+02	406.40	421.64	416.56	464.82	48.01	72.39	29.97	44.96	3505.20	3505.20
(Uang et al. 2000)	3.28E+02	3.28E+02	424.18	424.18	474.98	474.98	77.22	77.22	47.75	47.75	3658.00	3658.00
(Uang and Fan 2001)	2.50E+02	4.50E+02	398.78	398.78	386.08	386.08	33.27	33.27	21.08	21.08	NG	NG
(Chi and Uang 2002)	3.59E+02	4.35E+02	355.60	355.60	695.96	713.74	24.77	34.04	15.37	19.05	3810.00	3810.00
(Gilton and Uang 2002)	3.14E+02	3.59E+02	398.78	421.64	386.08	464.82	33.27	72.39	21.08	44.96	3810.00	3810.00
(Jones et al. 2002)	4.10E+02	4.10E+02	408.94	421.64	424.18	464.82	52.58	72.39	32.77	44.96	3708.00	3708.00
(Pantelides et al. 2004)	3.90E+02	3.90E+02	408.94	293.50	424.18	525.02	52.58	48.51	32.77	26.92	4925.06	4925.06
(Tabar and Deylami 2005)	3.70E+02	3.70E+02	200.00	300.00	200.00	400.00	15.00	24.00	9.00	13.50	3000.00	3000.00
(Zhang and Ricles 2006)	3.45E+02	3.45E+02	421.64	419.10	464.82	911.86	72.39	32.00	44.96	19.30	3962.00	3962.00
(Lee and Kim 2007)	3.43E+02	3.43E+02	407.00	407.00	428.00	428.00	35.00	35.00	20.00	20.00	3500.00	3500.00
(Li et al. 2009)	2.35E+02	3.45E+02	N/A	N/A	N/A	N/A	N/A	N/A	N/A	N/A	N/A	N/A
(Pachoumis et al. 2009)	3.05E+02	3.05E+02	300.00	300.00	300.00	300.00	19.00	19.00	11.00	11.00	1797.00	1797.00
(Pachoumis et al. 2010)	3.10E+02	3.10E+02	300.00	300.00	300.00	300.00	19.00	19.00	11.00	11.00	1797.00	1797.00
(Sofias et al. 2014)	3.70E+02	4.30E+02	300.00	300.00	300.00	300.00	19.00	19.00	11.00	11.00	1797.00	1797.00
(Oh et al. 2015)	2.35E+02	3.25E+02	400.00	400.00	400.00	400.00	21.00	21.00	13.00	13.00	3500.00	3500.00
(Li et al. 2017)	3.45E+02	3.45E+02	N/A	N/A	N/A	N/A	N/A	N/A	N/A	N/A	N/A	N/A
(Sophianopoulos and Deri 2017)	2.35E+02	2.35E+02	300.00	300.00	350.00	500.00	17.50	28.00	10.00	14.50	4000.00	4000.00

N/A: Not Applicable

NG: Not Given

Table 3: Selected 2-Level Values of Parameters (Continued)

Reference	tdwp (mm)		tcp (mm)		Escf (MPa)		Fycf (MPa)		Escw (MPa)		Fycw (MPa)	
	Min.	Max.	Min.	Max.	Min.	Max.	Min.	Max.	Min.	Max.	Min.	Max.
(Paul Popov et al. 1998)	N/A	N/A	NG	NG	NG	NG	3.70E+02	3.70E+02	NG	NG	3.70E+02	3.70E+02
(Uang et al. 2000)	10.00	10.00	25.00	25.00	NG	NG	4.21E+02	4.21E+02	NG	NG	4.21E+02	4.21E+02
(Uang and Fan 2001)	N/A	N/A	19.05	19.05	NG	NG	3.45E+02	3.45E+02	NG	NG	3.45E+02	3.45E+02
(Chi and Uang 2002)	10.00	25.00	25.00	25.00	2.00E+05	2.00E+05	3.58E+02	4.27E+02	2.00E+05	2.00E+05	3.44E+02	4.35E+02
(Gilton and Uang 2002)	N/A	N/A	16.00	22.00	2.07E+05	2.07E+05	2.86E+02	4.00E+02	2.07E+05	2.07E+05	3.14E+02	3.59E+02
(Jones et al. 2002)	N/A	N/A	25.00	25.00	2.07E+05	2.07E+05	3.80E+02	3.52E+02	2.07E+05	2.07E+05	3.76E+02	3.31E+02
(Pantelides et al. 2004)	N/A	N/A	N/A	N/A	2.07E+05	2.07E+05	3.95E+02	3.82E+02	2.07E+05	2.07E+05	4.10E+02	3.87E+02
(Tabar and Deylami 2005)	6.00	10.00	NG	NG	2.10E+05	2.10E+05	3.70E+02	3.70E+02	2.10E+05	2.10E+05	3.70E+02	3.70E+02
(Zhang and Ricles 2006)	12.50	19.00	24.00	24.00	NG	NG	3.45E+02	3.45E+02	NG	NG	3.45E+02	3.45E+02
(Lee and Kim 2007)	10.00	10.00	24.00	24.00	NG	NG	NG	NG	NG	NG	4.02E+02	4.02E+02
(Li et al. 2009)	N/A	N/A	N/A	N/A	2.10E+05	2.10E+05	2.35E+02	3.45E+02	2.10E+05	2.10E+05	2.35E+02	3.45E+02
(Pachourmis et al. 2009)	12.00	12.00	12.00	12.00	2.07E+05	2.07E+05	3.05E+02	3.05E+02	2.07E+05	2.07E+05	3.05E+02	3.05E+02
(Pachourmis et al. 2010)	12.00	12.00	10.00	10.00	2.09E+05	2.09E+05	3.10E+02	3.10E+02	2.09E+05	2.09E+05	3.10E+02	3.10E+02
(Sofias et al. 2014)	12.00	12.00	10.00	10.00	2.15E+05	2.20E+05	3.70E+02	4.30E+02	2.15E+05	2.20E+05	3.70E+02	4.30E+02
(Oh et al. 2015)	N/A	N/A	20.00	20.00	2.04E+05	2.07E+05	2.35E+02	3.25E+02	2.04E+05	2.07E+05	2.35E+02	3.25E+02
(Li et al. 2017)	N/A	N/A	N/A	N/A	2.02E+05	2.02E+05	3.00E+02	3.00E+02	2.04E+05	2.04E+05	3.45E+02	3.45E+02
(Sophianopoulos and Deri 2017)	N/A	N/A	12.00	12.00	2.10E+05	2.10E+05	2.35E+02	2.35E+02	2.10E+05	2.10E+05	2.35E+02	2.35E+02

N/A: Not Applicable

NG: Not Given

Table 3: Selected 2-Level Values of Parameters (Continued)

Reference	bf (mm)		db (mm)		tfb (mm)		twb (mm)		a (mm)		b (mm)		c (mm)	
	Min.	Max.	Min.	Max.	Min.	Max.	Min.	Max.	Min.	Max.	Min.	Max.	Min.	Max.
(Paul Popov et al. 1998)	304.80	419.10	904.24	916.94	20.07	711.20	15.24	20.32	203.20	279.40	711.20	635.00	60.96	86.36
(Uang et al. 2000)	304.80	304.80	911.86	911.86	23.88	686.00	15.88	15.88	152.40	152.40	686.00	686.00	76.00	76.00
(Uang and Fan 2001)	178.82	178.82	601.98	601.98	14.99	508.00	10.92	10.92	177.80	177.80	508.00	508.00	66.68	66.68
(Chi and Uang 2002)	304.80	355.60	911.86	713.74	23.88	609.60	15.88	19.05	266.70	228.60	609.60	762.00	69.85	76.20
(Gilton and Uang 2002)	178.82	304.80	601.98	911.86	14.99	406.00	10.92	15.88	127.00	229.00	406.00	762.00	44.00	76.00
(Jones et al. 2002)	304.80	304.80	911.86	911.86	23.88	685.00	15.88	15.88	230.00	230.00	685.00	685.00	76.00	76.00
(Pantelides et al. 2004)	266.70	266.70	769.62	769.62	25.40	531.04	15.62	15.62	152.02	165.35	531.04	531.04	69.34	69.34
(Tabar and Deylami 2005)	150.00	220.00	300.00	600.00	10.70	200.00	7.10	12.00	80.00	140.00	200.00	400.00	32.00	55.00
(Zhang and Ricles 2006)	304.80	304.80	911.86	911.86	23.88	525.00	15.88	15.88	175.00	175.00	525.00	525.00	75.00	75.00
(Lee and Kim 2007)	300.00	300.00	700.00	700.00	24.00	525.00	13.00	13.00	175.00	175.00	525.00	525.00	75.00	75.00
(Li et al. 2009)	228.35	307.34	607.06	927.10	17.27	494.00	11.18	19.43	114.00	154.00	494.00	773.00	57.00	77.00
(Pachoumis et al. 2009)	240.00	240.00	230.00	230.00	12.00	184.00	7.50	7.50	156.00	156.00	184.00	184.00	36.00	60.00
(Pachoumis et al. 2010)	180.00	180.00	171.00	171.00	9.50	102.60	6.00	6.00	72.00	144.00	102.60	128.25	22.50	36.00
(Sofias et al. 2014)	152.00	152.00	160.00	160.00	9.00	114.00	6.00	6.00	96.00	96.00	114.00	114.00	40.00	40.00
(Oh et al. 2015)	200.00	200.00	600.00	600.00	17.00	450.00	11.00	11.00	120.00	120.00	450.00	450.00	40.00	40.00
(Li et al. 2017)	133.00	124.00	203.00	248.00	7.80	180.00	5.80	5.00	80.00	80.00	180.00	220.00	26.00	31.00
(Sophianopoulos and Deri 2017)	110.00	220.00	217.00	210.00	7.70	81.38	5.00	7.00	66.00	132.00	81.38	78.75	25.00	48.00

N/A: Not Applicable

NG: Not Given

Table 3: Selected 2-Level Values of Parameters (Continued)

Reference	s (mm)		rfc (mm)		L (mm)		Esbf (MPa)		Fybf (MPa)		Esbw (MPa)	
	Min.	Max.	Min.	Max.	Min.	Max.	Min.	Max.	Min.	Max.	Min.	Max.
(Paul Popov et al. 1998)	558.80	596.90	1066.80	626.82	3416.30	3416.30	NG	NG	4.30E+02	3.90E+02	NG	NG
(Uang et al. 2000)	495.40	495.40	813.00	813.00	3128.00	3128.00	NG	NG	3.38E+02	3.38E+02	NG	NG
(Uang and Fan 2001)	431.80	431.80	517.53	517.53	NG	NG	NG	NG	2.50E+02	4.50E+02	NG	NG
(Chi and Uang 2002)	571.50	609.60	699.94	990.60	3233.02	3224.13	2.00E+05	2.00E+05	4.00E+02	4.27E+02	2.00E+05	2.00E+05
(Gilton and Uang 2002)	330.00	610.00	486.00	991.00	3381.61	3370.18	2.07E+05	2.07E+05	2.86E+02	4.00E+02	2.07E+05	2.07E+05
(Jones et al. 2002)	572.50	572.50	810.00	810.00	3416.30	3416.30	2.07E+05	2.07E+05	3.74E+02	3.74E+02	2.07E+05	2.07E+05
(Pantelides et al. 2004)	417.54	430.87	533.40	533.40	3737.61	3687.19	2.07E+05	2.07E+05	3.82E+02	3.82E+02	2.07E+05	2.07E+05
(Tabar and Deylami 2005)	180.00	340.00	172.25	391.13	2500.00	2500.00	2.10E+05	2.10E+05	3.70E+02	3.70E+02	2.10E+05	2.10E+05
(Zhang and Ricles 2006)	437.50	437.50	497.00	497.00	4040.00	4264.00	NG	NG	3.45E+02	3.45E+02	NG	NG
(Lee and Kim 2007)	437.50	437.50	497.00	497.00	4297.00	4297.00	NG	NG	3.30E+02	3.30E+02	NG	NG
(Li et al. 2009)	361.00	540.50	563.67	1008.51	3580.00	4816.00	2.10E+05	2.10E+05	2.35E+02	3.45E+02	2.10E+05	2.10E+05
(Pachoumis et al. 2009)	248.00	248.00	135.56	100.53	1200.00	1200.00	2.07E+05	2.07E+05	3.05E+02	3.05E+02	2.07E+05	2.07E+05
(Pachoumis et al. 2010)	123.30	208.13	69.73	75.11	1200.00	1200.00	2.09E+05	2.09E+05	3.10E+02	3.10E+02	2.09E+05	2.09E+05
(Sofias et al. 2014)	153.00	153.00	60.61	60.61	1200.00	1200.00	2.15E+05	2.20E+05	3.70E+02	4.30E+02	2.15E+05	2.20E+05
(Oh et al. 2015)	345.00	345.00	654.29	654.29	3510.00	3510.00	2.04E+05	2.07E+05	2.35E+02	3.25E+02	2.04E+05	2.07E+05
(Li et al. 2017)	170.00	190.00	168.77	210.66	1625.00	1625.00	2.02E+05	2.02E+05	3.00E+02	3.00E+02	2.04E+05	2.04E+05
(Sophianopoulos and Deri 2017)	106.69	171.38	45.61	40.15	3000.00	3000.00	2.10E+05	2.10E+05	2.35E+02	2.35E+02	2.10E+05	2.10E+05

N/A: Not Applicable

NG: Not Given

Table 3: Selected 2-Level Values of Parameters (Continued)

Reference	Fybw (MPa)		wc (mm)		dc (mm)		tfc (mm)		twc (mm)		H (mm)	
	Min.	Max.	Min.	Max.	Min.	Max.	Min.	Max.	Min.	Max.	Min.	Max.
(Paul Popov et al. 1998)	4.30E+02	3.90E+02	406.40	421.64	416.56	464.82	48.01	72.39	29.97	44.96	3505.20	3505.20
(Uang et al. 2000)	3.28E+02	3.28E+02	424.18	424.18	474.98	474.98	77.22	77.22	47.75	47.75	3658.00	3658.00
(Uang and Fan 2001)	2.50E+02	4.50E+02	398.78	398.78	386.08	386.08	33.27	33.27	21.08	21.08	NG	NG
(Chi and Uang 2002)	3.59E+02	4.35E+02	355.60	355.60	695.96	713.74	24.77	34.04	15.37	19.05	3810.00	3810.00
(Gilton and Uang 2002)	3.14E+02	3.59E+02	398.78	421.64	386.08	464.82	33.27	72.39	21.08	44.96	3810.00	3810.00
(Jones et al. 2002)	4.10E+02	4.10E+02	408.94	421.64	424.18	464.82	52.58	72.39	32.77	44.96	3708.00	3708.00
(Pantelides et al. 2004)	3.90E+02	3.90E+02	408.94	293.50	424.18	525.02	52.58	48.51	32.77	26.92	4925.06	4925.06
(Tabar and Deylami 2005)	3.70E+02	3.70E+02	200.00	300.00	200.00	400.00	15.00	24.00	9.00	13.50	3000.00	3000.00
(Zhang and Ricles 2006)	3.45E+02	3.45E+02	421.64	419.10	464.82	911.86	72.39	32.00	44.96	19.30	3962.00	3962.00
(Lee and Kim 2007)	3.43E+02	3.43E+02	407.00	407.00	428.00	428.00	35.00	35.00	20.00	20.00	3500.00	3500.00
(Li et al. 2009)	2.35E+02	3.45E+02	N/A	N/A	N/A	N/A	N/A	N/A	N/A	N/A	N/A	N/A
(Pachoumis et al. 2009)	3.05E+02	3.05E+02	300.00	300.00	300.00	300.00	19.00	19.00	11.00	11.00	1797.00	1797.00
(Pachoumis et al. 2010)	3.10E+02	3.10E+02	300.00	300.00	300.00	300.00	19.00	19.00	11.00	11.00	1797.00	1797.00
(Sofias et al. 2014)	3.70E+02	4.30E+02	300.00	300.00	300.00	300.00	19.00	19.00	11.00	11.00	1797.00	1797.00
(Oh et al. 2015)	2.35E+02	3.25E+02	400.00	400.00	400.00	400.00	21.00	21.00	13.00	13.00	3500.00	3500.00
(Li et al. 2017)	3.45E+02	3.45E+02	N/A	N/A	N/A	N/A	N/A	N/A	N/A	N/A	N/A	N/A
(Sophianopoulos and Deri 2017)	2.35E+02	2.35E+02	300.00	300.00	350.00	500.00	17.50	28.00	10.00	14.50	4000.00	4000.00

N/A: Not Applicable

NG: Not Given

Table 3: Selected 2-Level Values of Parameters (Continued)

Reference	tdwp (mm)		tcp (mm)		Escf (MPa)		Fycf (MPa)		Escw (MPa)		Fycw (MPa)	
	Min.	Max.	Min.	Max.	Min.	Max.	Min.	Max.	Min.	Max.	Min.	Max.
(Paul Popov et al. 1998)	N/A	N/A	NG	NG	NG	NG	3.70E+02	3.70E+02	NG	NG	3.70E+02	3.70E+02
(Uang et al. 2000)	10.00	10.00	25.00	25.00	NG	NG	4.21E+02	4.21E+02	NG	NG	4.21E+02	4.21E+02
(Uang and Fan 2001)	N/A	N/A	19.05	19.05	NG	NG	3.45E+02	3.45E+02	NG	NG	3.45E+02	3.45E+02
(Chi and Uang 2002)	10.00	25.00	25.00	25.00	2.00E+05	2.00E+05	3.58E+02	4.27E+02	2.00E+05	2.00E+05	3.44E+02	4.35E+02
(Gilton and Uang 2002)	N/A	N/A	16.00	22.00	2.07E+05	2.07E+05	2.86E+02	4.00E+02	2.07E+05	2.07E+05	3.14E+02	3.59E+02
(Jones et al. 2002)	N/A	N/A	25.00	25.00	2.07E+05	2.07E+05	3.80E+02	3.52E+02	2.07E+05	2.07E+05	3.76E+02	3.31E+02
(Pantelides et al. 2004)	N/A	N/A	N/A	N/A	2.07E+05	2.07E+05	3.95E+02	3.82E+02	2.07E+05	2.07E+05	4.10E+02	3.87E+02
(Tabar and Deylami 2005)	6.00	10.00	NG	NG	2.10E+05	2.10E+05	3.70E+02	3.70E+02	2.10E+05	2.10E+05	3.70E+02	3.70E+02
(Zhang and Ricles 2006)	12.50	19.00	24.00	24.00	NG	NG	3.45E+02	3.45E+02	NG	NG	3.45E+02	3.45E+02
(Lee and Kim 2007)	10.00	10.00	24.00	24.00	NG	NG	NG	NG	NG	NG	4.02E+02	4.02E+02
(Li et al. 2009)	N/A	N/A	N/A	N/A	2.10E+05	2.10E+05	2.35E+02	3.45E+02	2.10E+05	2.10E+05	2.35E+02	3.45E+02
(Pachourmis et al. 2009)	12.00	12.00	12.00	12.00	2.07E+05	2.07E+05	3.05E+02	3.05E+02	2.07E+05	2.07E+05	3.05E+02	3.05E+02
(Pachourmis et al. 2010)	12.00	12.00	10.00	10.00	2.09E+05	2.09E+05	3.10E+02	3.10E+02	2.09E+05	2.09E+05	3.10E+02	3.10E+02
(Sofias et al. 2014)	12.00	12.00	10.00	10.00	2.15E+05	2.20E+05	3.70E+02	4.30E+02	2.15E+05	2.20E+05	3.70E+02	4.30E+02
(Oh et al. 2015)	N/A	N/A	20.00	20.00	2.04E+05	2.07E+05	2.35E+02	3.25E+02	2.04E+05	2.07E+05	2.35E+02	3.25E+02
(Li et al. 2017)	N/A	N/A	N/A	N/A	2.02E+05	2.02E+05	3.00E+02	3.00E+02	2.04E+05	2.04E+05	3.45E+02	3.45E+02
(Sophianopoulos and Deri 2017)	N/A	N/A	12.00	12.00	2.10E+05	2.10E+05	2.35E+02	2.35E+02	2.10E+05	2.10E+05	2.35E+02	2.35E+02

N/A: Not Applicable

NG: Not Given

The following symbols are used in **Tables 1 to 3**.

bf	=	Width of beam flange (mm)
db	=	Depth of beam section (mm)
tfb	=	Thickness of beam flange (mm)
twb	=	Thickness of beam web (mm)
a	=	Distance from face of the column flange to starting point of beam flange cut (mm)
b	=	Length of beam flange cut (mm)
c	=	Depth of beam flange cut (mm)
s	=	Distance from face of the column flange to middle of beam flange cut (mm)
r _{fc}	=	Radius of beam flange cut (mm)
L	=	Length of beam (mm)
E _{sbf}	=	Young's modulus of beam flange (MPa)
F _{ybf}	=	Yield strength of beam flange (MPa)
E _{sbw}	=	Young's modulus of beam web (MPa)
F _{ybw}	=	Yield strength of beam web (MPa)
w _c	=	Width of column flange (mm)
d _c	=	Depth of column section (mm)
t _{fc}	=	Thickness of column flange (mm)
t _{wc}	=	Thickness of column web (mm)
H	=	Total height of column (mm)
t _{dwp}	=	Thickness of doubler web plate (mm)
t _{cp}	=	Thickness of continuity plate (mm)
E _{scf}	=	Young's modulus of column flange (MPa)
F _{y_{cf}}	=	Yield strength of column flange (MPa)
E _{scw}	=	Young's modulus of column web (MPa)
F _{y_{cw}}	=	Yield strength of column web (MPa)

A total of 756 values for 25 factors/ parameters were noted from 17 different studies to define a practical range of values to be set for a two-level factorial design of experiment that will be discussed later in section 3.4 of this document.

3.4. SELECTION OF FACTORS

A prerequisite of carrying out a good experiment is that all the factors are independent and not correlated so that results can effectively portray a clear picture based on statistical analysis regarding the effects of individual factors on the response of the process. Therefore, those factors which are dependent on other factors were dropped. There were 2 such factors; namely:

- Factor s: Dependent of factors a and b
- Factor rfc: Dependent of factors b and c

Dropping these 2 factors resulted in 23 independent factors. In ideal scenario, minimum and maximum level values for these factors would be the highest and lowest values recorded from the past studies, however, that approach would have lead to incompatibility between the factors (for example a maximum value of depth of beam flange cut “c” was more than half of minimum value of beam flange width “bf” excluding thickness of beam web “twb”), therefore, the values were set to cover a maximum possible range with a balance of factors’ compatibility as mentioned in **Table 3**.

Table 3: Selected 2-Level Values of Parameters

BEAM PARAMETERS	S. No.	PARAMETER	Min	Max	COLUMN PARAMETERS	S. No.	PARAMETER	Min	Max
	1	bf (mm)	178.82	304.80		13	wc (mm)	355.60	424.18
	2	db (mm)	160.00	927.10		14	dc (mm)	406.40	911.86
	3	tfb (mm)	7.70	34.29		15	tfc (mm)	24.77	72.39
	4	twb (mm)	5.00	20.32		16	twc (mm)	15.37	44.96
	5	a (mm)	66.00	228.60		17	H (mm)	3000	5000
	6	b (mm)	78.75	773.00		18	tdwp (mm)	6.00	25.00
	7	c (mm)	22.50	60.00		19	tcp (mm)	0.00	25.00
	8	L (mm)	1200	4816.00		20	Escf (MPa)	2.02E+05	2.12E+05
	9	Esbf (MPa)	1.85E+05	2.12E+05		21	Fycf (MPa)	235.00	430.00
	10	Fybf (MPa)	235.00	450.00		22	Escw (MPa)	2.04E+05	2.12E+05
	11	Esbw (MPa)	1.85E+05	2.12E+05		23	Fycw (MPa)	235.00	430.00
	12	Fybw (MPa)	235.00	450.00					

3.5. FINALIZATION OF FACTORS

As discussed in section 3.4, there were 23 potentially significant factors that can affect the performance of RBS, however, a two-level factorial design of experiment can be carried out up to 21 factors using Design Expert v.11 software (Anderson et al., 2017); Therefore, 2 factors that are of least significance had to be dropped after an analytical investigation of their affect on the response of RBS under cyclic loading conditions. Incidentally, 8 models were analyzed for a total beam rotation of up to 2% under cyclic loads to study the significance of effect of Young’s modulus of beam web, beam flange, column web and column flange separately with a high and low value for each of these variables. All other values were kept constant as mentioned in **Table 4**.

Table 4: Values of Parameters for Testing 2 Insignificant Factors

	S. No.	PARAMETER	Min	Max		S. No.	PARAMETER	Min	Max
	BEAM PARAMETERS	1	bf (mm)	241.81		241.81	COLUMN PARAMETERS	13	wc (mm)
2		db (mm)	543.55	543.55	14	dc (mm)		659.13	659.13
3		tfb (mm)	20.995	20.995	15	tfc (mm)		48.58	48.58
4		twb (mm)	12.66	12.66	16	twc (mm)		30.165	30.165
5		a (mm)	147.3	147.3	17	H (mm)		4000	4000
6		b (mm)	425.875	425.875	18	tdwp (mm)		15.5	15.5
7		c (mm)	41.25	41.25	19	tcp (mm)		12.5	12.5
8		L (mm)	3008	3008	20	Escf (MPa)		2.02E+05	2.12E+05
9		Esbf (MPa)	1.85E+05	2.12E+05	21	Fycf (MPa)		332.5	332.5
10		Fybf (MPa)	342.5	342.5	22	Escw (MPa)		2.04E+05	2.12E+05
11		Esbw (MPa)	1.85E+05	2.12E+05	23	Fycw (MPa)		332.5	332.5
12		Fybw (MPa)	342.5	342.5					

The values for the 4 subject variables for 8 tests were as follows, while the rest of the parameters were equal to the mean of the ranges defined in **Table 3**:

- Model 1: Value of Esbf = 1.85E+05 MPa
- Model 2: Value of Esbf = 2.12E+05 MPa
- Model 3: Value of Esbw = 1.85E+05 MPa
- Model 4: Value of Esbw = 2.12E+05 MPa
- Model 5: Value of Escf = 2.02E+05 MPa

- Model 6: Value of $E_{scf} = 2.12E+05$ MPa
- Model 7: Value of $E_{scw} = 2.04E+05$ MPa
- Model 8: Value of $E_{scw} = 2.12E+05$ MPa

The test responses were recorded and matched in pairs of Model 1 & 2, Model 3 & 4, Model 5 & 6 and Model 7 & 8 as shown in **Figures 11** through **14**.

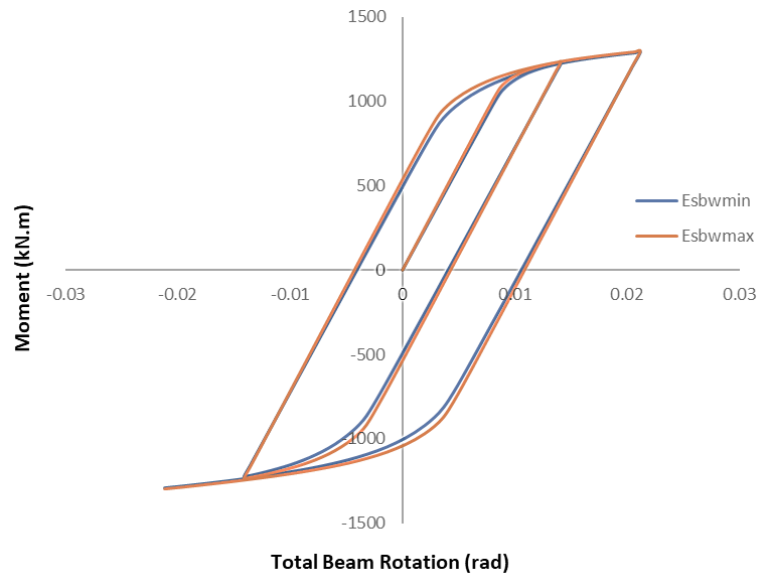


Figure 11: Comparison of Model 1 & Model 2 Results

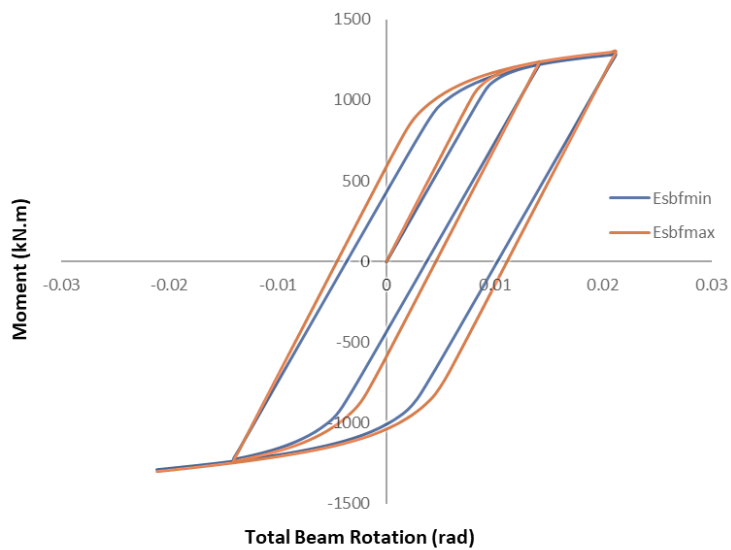


Figure 12: Comparison of Model 3 & Model 4 Results

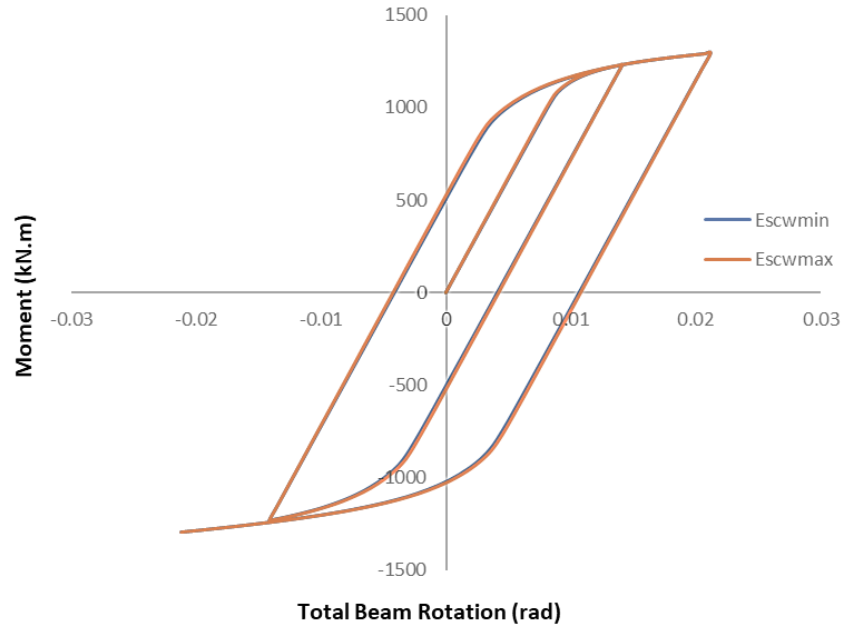


Figure 13: Comparison of Model 5 & Model 6 Results

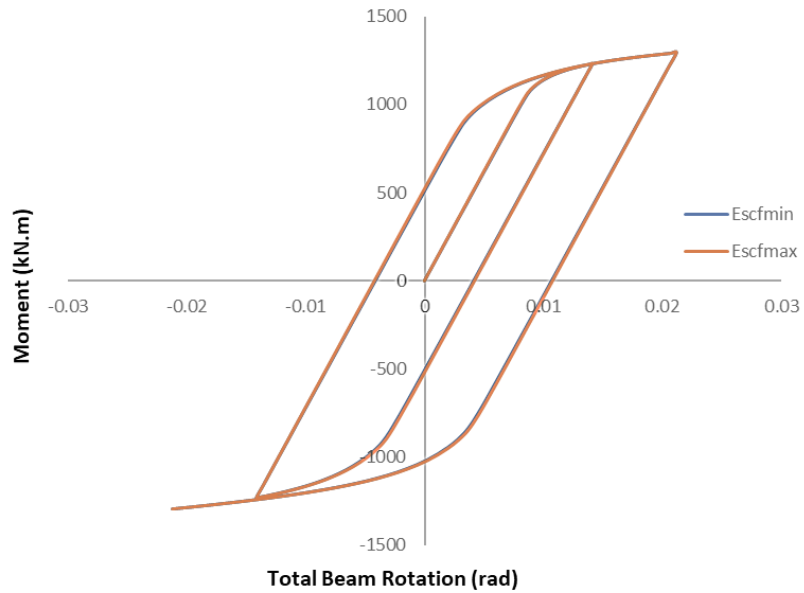


Figure 14: Comparison of Model 7 & Model 8 Results

The tests yielded a difference of 0.413%, 1.3%, 0.073% and 0.005% between models 1 & 2, models 3 & 4, models 5 & 6 and models 7 & 8, respectively. Therefore, it was safe to conclude that the value of young's modulus of column web and column flange had minimum effect on the response and there fore can be dropped from the factors.

With the help of these tests, the final 21 factors to be considered for experiment were set to be as mentioned in **Table 5**.

Table 5: Finalized 2-Level Values of Parameters

BEAM PARAMETERS	S. No.	PARAMETER	SYMBOL	Min	Max	COLUMN PARAMETERS	S. No.	PARAMETER	SYMBOL	Min	Max
	1	bf (mm)	A	178.82	304.80		13	wc (mm)	N	355.60	424.18
	2	db (mm)	B	160.00	927.10		14	dc (mm)	O	406.40	911.86
	3	tfb (mm)	C	7.70	34.29		15	tfc (mm)	P	24.77	72.39
	4	twb (mm)	D	5.00	20.32		16	twc (mm)	Q	15.37	44.96
	5	a (mm)	E	66.00	228.60		17	H (mm)	R	3000	5000
	6	b (mm)	F	78.75	773.00		18	tdwp (mm)	S	6.00	25.00
	7	c (mm)	G	22.50	60.00		19	tcp (mm)	T	0.00	25.00
	8	L (mm)	H	1200	4816.00		20	Fycf (MPa)	U	235.00	430.00
	9	Esbf (MPa)	J	1.85E+05	2.12E+05		21	Fycw (MPa)	V	235.00	430.00
	10	Fybf (MPa)	K	235.00	450.00						
	11	Esbw (MPa)	L	1.85E+05	2.12E+05						
12	Fybw (MPa)	M	235.00	450.00							

3.6. DESIGN OF EXPERIMENT

In order to study the cause and effect relationships between the parameters/ factors and response of the connection more efficiently in a systematic way, a computer experiment for 21 factors was designed with Two-Level 2^k Factorial design approach to optimize the experiment efficiency by reducing number of required runs from $2^{21} = 2097152$ runs to just 32 runs. This design of the experiment and analysis of the results were performed with the aid of renowned statistical computer software package Stat-Ease[®] Design-Expert[®]. To verify the effects of the main factors on responses and unravel the combined effects of multi-factor interactions, a semi-fold over augmented design was added to the existing design with 16 more combinations. In the first phase of experiment, 32 combinations of factors were generated for 32 randomized model runs as shown in **Table 6**, each test was named as RBS-N, where “N” stands for the number of model.

Table 6: Coded Factor Combinations for Experiment Phase 1

RBS	bf mm	db mm	tfb mm	twb mm	a mm	b mm	c mm	L mm	Esbf MPa	Fybf MPa	Esbw MPa	Fybw MPa	wc mm	dc mm	tfc mm	twc mm	H mm	tdwp mm	tcp mm	Fycf MPa	Fycw MPa
1	-1	-1	-1	-1	-1	-1	-1	-1	-1	1	-1	-1	-1	1	-1	-1	1	-1	1	1	-1
2	1	-1	-1	-1	-1	1	1	1	-1	-1	1	1	-1	-1	1	-1	-1	-1	-1	1	1
3	-1	1	-1	-1	-1	1	1	-1	1	-1	1	-1	1	-1	-1	1	-1	-1	1	-1	1
4	1	1	-1	-1	-1	-1	-1	1	1	1	-1	1	1	1	1	1	1	-1	-1	-1	-1
5	-1	-1	1	-1	-1	1	-1	1	1	-1	-1	1	1	-1	-1	-1	1	1	-1	-1	1
6	1	-1	1	-1	-1	-1	1	-1	1	1	1	-1	1	1	1	-1	-1	1	1	-1	-1
7	-1	1	1	-1	-1	-1	1	1	-1	1	1	1	-1	1	-1	1	-1	1	-1	1	-1
8	1	1	1	-1	-1	1	-1	-1	-1	-1	-1	-1	-1	-1	1	1	1	1	1	1	1
9	-1	-1	-1	1	-1	-1	1	1	1	-1	-1	-1	-1	1	1	1	-1	1	-1	-1	1
10	1	-1	-1	1	-1	1	-1	-1	1	1	1	1	-1	-1	-1	1	1	1	1	-1	-1
11	-1	1	-1	1	-1	1	-1	1	-1	1	1	-1	1	-1	1	-1	1	1	-1	1	-1
12	1	1	-1	1	-1	-1	1	-1	-1	-1	-1	1	1	1	-1	-1	-1	1	1	1	1
13	-1	-1	1	1	-1	1	1	-1	-1	1	-1	1	1	-1	1	1	-1	-1	1	1	-1
14	1	-1	1	1	-1	-1	-1	1	-1	-1	1	-1	1	1	-1	1	1	-1	-1	1	1
15	-1	1	1	1	-1	-1	-1	-1	1	-1	1	1	-1	1	1	-1	1	-1	1	-1	1
16	1	1	1	1	-1	1	1	1	1	1	-1	-1	-1	-1	-1	-1	-1	-1	-1	-1	-1
17	-1	-1	-1	-1	1	-1	-1	-1	-1	1	1	1	1	-1	1	1	-1	1	-1	-1	1
18	1	-1	-1	-1	1	1	1	1	-1	-1	-1	-1	1	1	-1	1	1	1	1	-1	-1
19	-1	1	-1	-1	1	1	1	-1	1	-1	-1	1	-1	1	1	-1	1	1	-1	1	-1
20	1	1	-1	-1	1	-1	-1	1	1	1	1	-1	-1	-1	-1	-1	-1	1	1	1	1
21	-1	-1	1	-1	1	1	-1	1	1	-1	1	-1	-1	1	1	1	-1	-1	1	1	-1
22	1	-1	1	-1	1	-1	1	-1	1	1	-1	1	-1	-1	-1	1	1	-1	-1	1	1
23	-1	1	1	-1	1	-1	1	1	-1	1	-1	-1	1	-1	1	-1	1	-1	1	-1	1
24	1	1	1	-1	1	1	-1	-1	-1	-1	1	1	1	1	-1	-1	-1	-1	-1	-1	-1
25	-1	-1	-1	1	1	-1	1	1	1	-1	1	1	1	-1	-1	-1	1	-1	1	1	-1
26	1	-1	-1	1	1	1	-1	-1	1	1	-1	-1	1	1	1	-1	-1	-1	-1	1	1
27	-1	1	-1	1	1	1	-1	1	-1	1	-1	1	-1	1	-1	1	-1	-1	1	-1	1
28	1	1	-1	1	1	-1	1	-1	-1	-1	1	-1	-1	-1	1	1	1	-1	-1	-1	-1
29	-1	-1	1	1	1	1	1	-1	-1	1	1	-1	-1	1	-1	-1	1	1	-1	-1	1
30	1	-1	1	1	1	-1	-1	1	-1	-1	-1	1	-1	-1	1	-1	-1	1	1	-1	-1
31	-1	1	1	1	1	-1	-1	-1	1	-1	-1	-1	1	-1	-1	1	-1	1	-1	1	-1
32	1	1	1	1	1	1	1	1	1	1	1	1	1	1	1	1	1	1	1	1	1

Note: -1 and 1 indicate the minimum and maximum values respectively as mentioned in **Table 5**.

3.7. ANALYTICAL SPECIMEN GEOMETRIES

For all 48 test runs (i.e. from RBS-1 to RBS 48), the FEA models were created. The geometries of specimens RBS-1 to RBS-6 are shown in **Figures 15** through **20**. Graphical representation of rest of the FEA models are presented in Appendix A of this document.

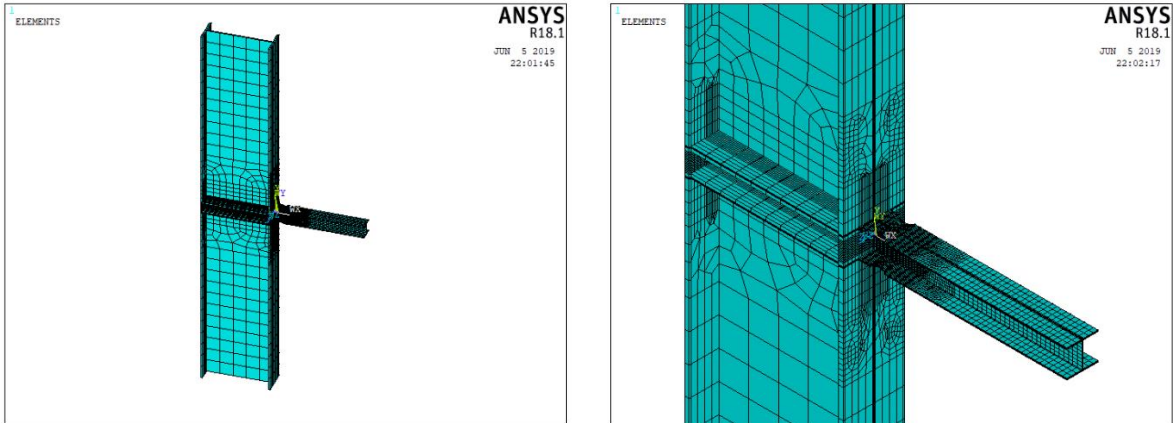


Figure 15: FEA Model for Specimen RBS-1

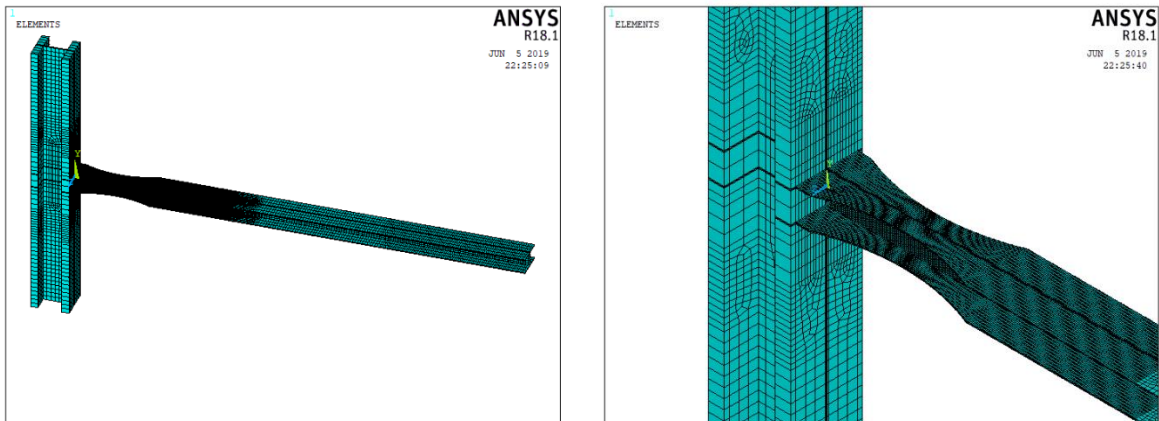


Figure 16: FEA Model for Specimen RBS-2

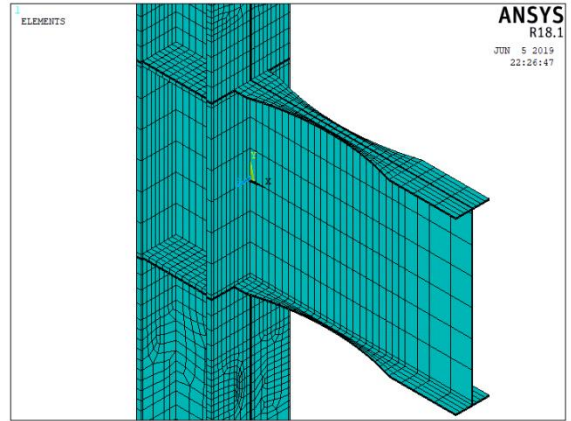
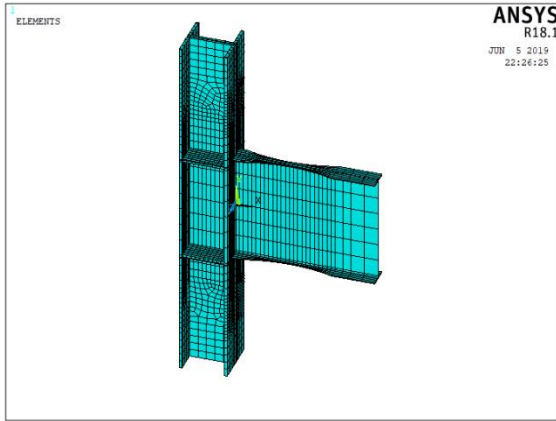


Figure 17: FEA Model for Specimen RBS-3

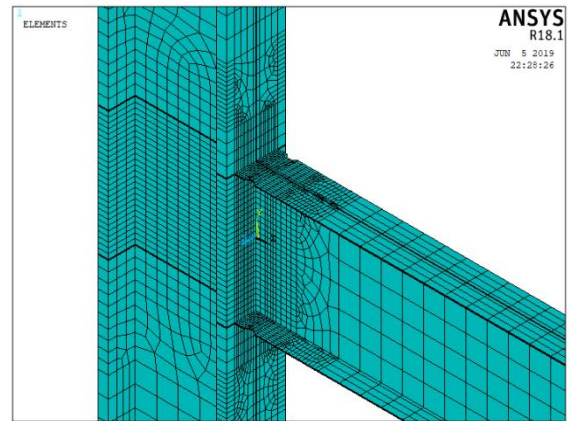
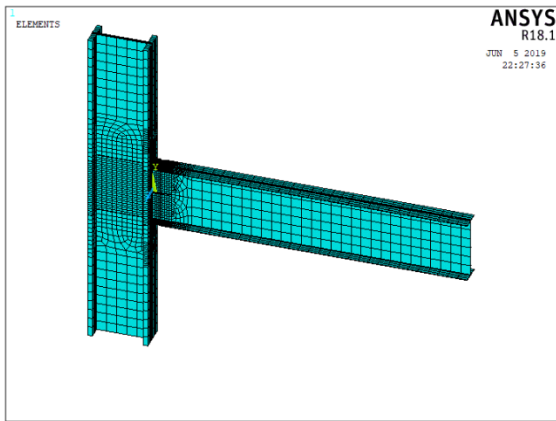


Figure 18: FEA Model for Specimen RBS-4

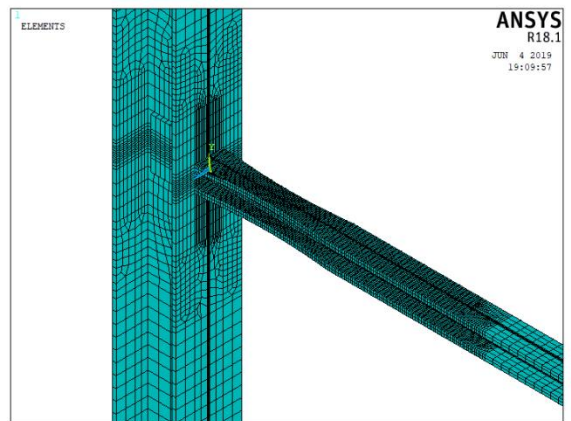
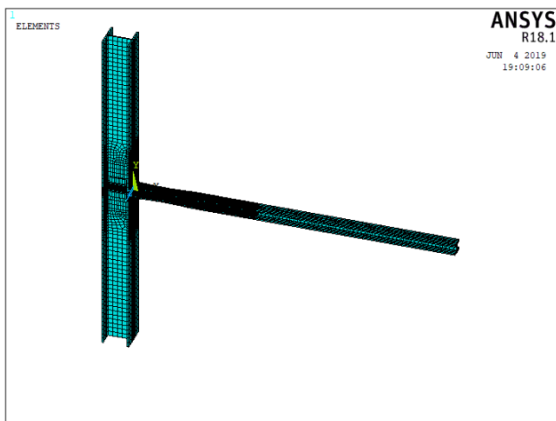


Figure 19: FEA Model for Specimen RBS-5

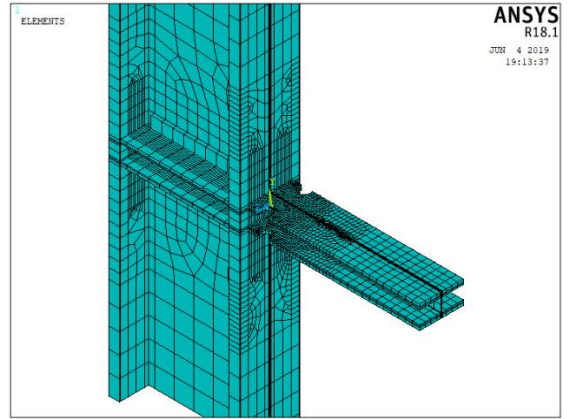
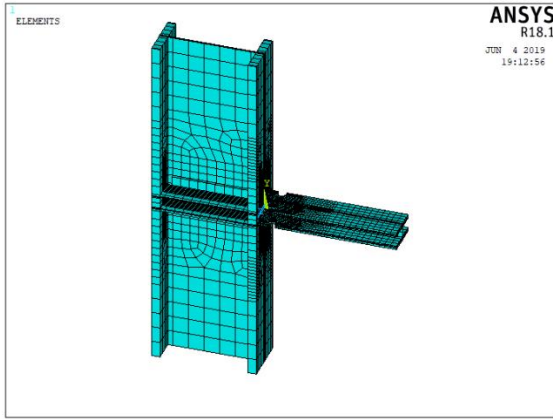


Figure 20: FEA Model for Specimen RBS-6

3.8. RESPONSE VARIABLES

The tests were carried out to record five response variables to assess the sensitivity of RBS connections towards the parameters under considerations. These response variables are depicted in **Figure 21** and discussed in following sections.

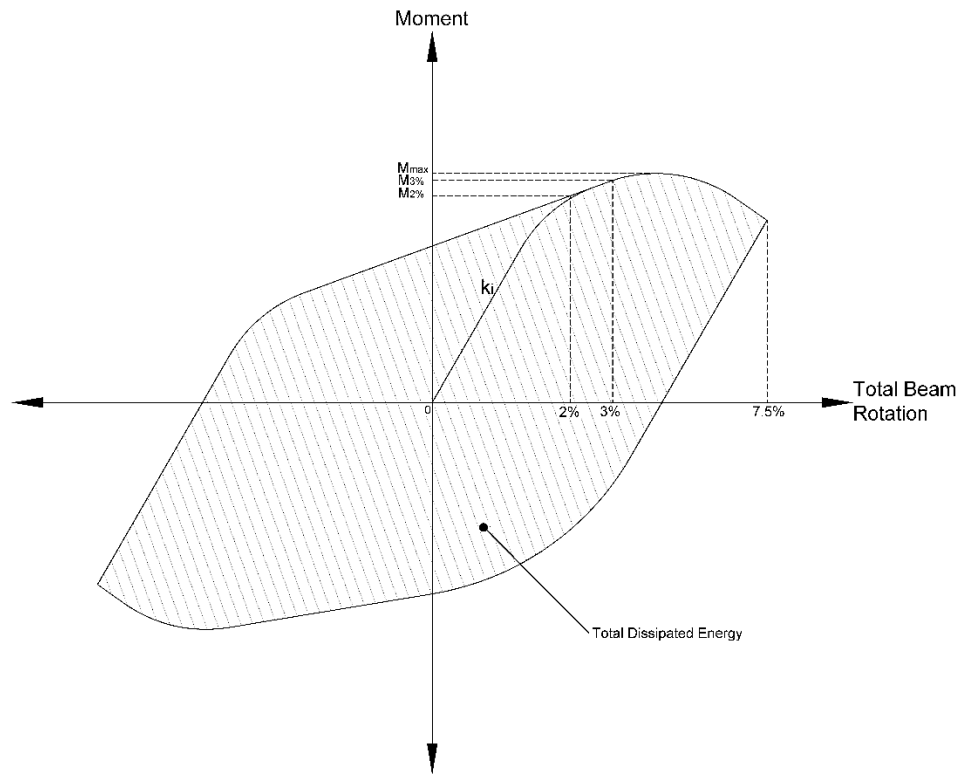


Figure 21: Schematic of Response Variables Considered in Sensitivity Study

3.8.1. R1: Total Dissipated Energy

The dissipation of energy in the subject system under cyclic loading is caused by yielding and wearing of steel (Dastfan et al., 2018), hence it was calculated as the area enclosed by the hysteric curve of each test by the trapezoidal method.

3.8.2. R2: Initial Stiffness (k_i)

The resistance of the beam to deformation before yielding is called initial stiffness and was set as another measure to the subject system's performance under the applied conditions.

3.8.3. R3: Strength Degradation Rate

Degradation in the strength caused by buckling was calculated by Strength Degradation Rate (SDR) as a ratio of maximum moment resistance of RBS at 2% rotation to maximum moment resistance of RBS at 3% rotation as depicted in **Figure 22** (Uang and Fan, 2001).

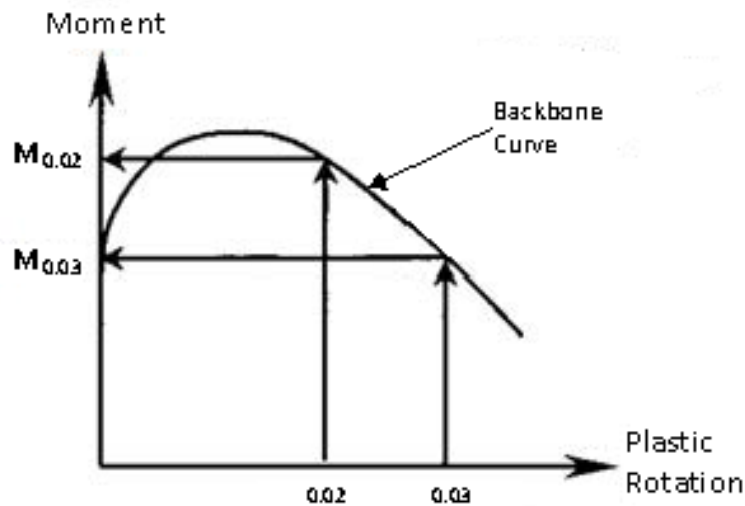


Figure 22: Strength Degradation Rate (Uang and Fan, 2001)

3.8.4. R4: Maximum Moment Resistance

Maximum resistance in each complete hysteric response was set as another measure of the performance of RBS in the terms of peak moment for each test as depicted in **Figure 21**.

3.8.5. R5: Rupture Index @ 7.5% Total Storey Drift

Vulnerability of a section to rupture is calculated by Rupture Index (RI) as the ratio of the equivalent plastic strain index to the ductile fracture strain (Rahnavard et al. 2015; Moradi and Alam, 2017). RI can be written as:

$$RI = \frac{PEEQ/\varepsilon_f}{\exp(1.5 \frac{p}{q})}$$

Where;

RI = Rupture Index

PEEQ = Equivalent Plastic Strain Index

ε_f = Ductile Fracture Strain

p = Hydrostatic Pressure

q = Von Mises Stress

CHAPTER – 4

4. THE EXPERIMENT

4.1. PHASE – 1 RESPONSE PLOTS

In Phase – 1 of the experiment, 32 specimens were analyzed as explained in section 3 and the hysteric responses for first 10 runs are shown in **Figures 23** through **32** while rest of the response plots for Phase – 1 of this experiment are presented in Appendix B of this document.

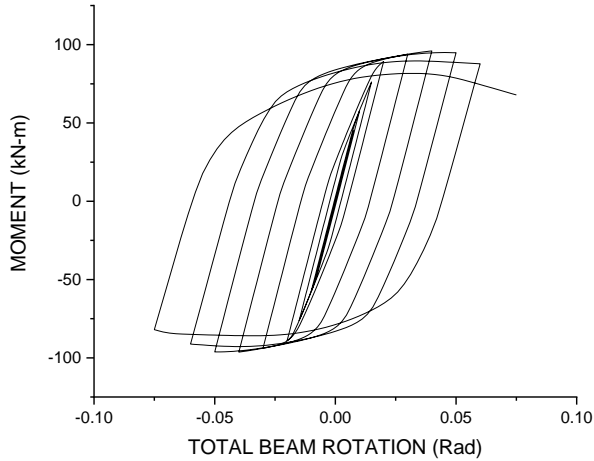


Figure 23: Experimental Moment vs Rotation Curve for RBS-1

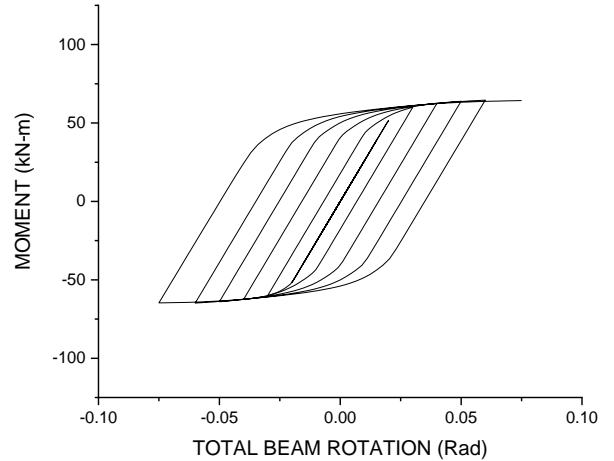


Figure 24: Experimental Moment vs Rotation Curve for RBS-2

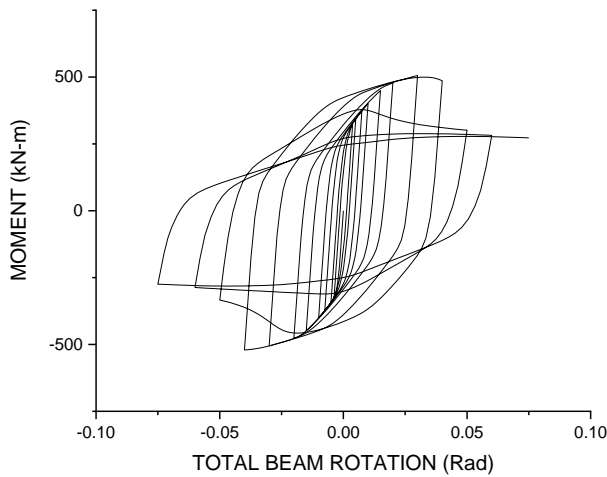


Figure 25: Experimental Moment vs Rotation Curve for RBS-3

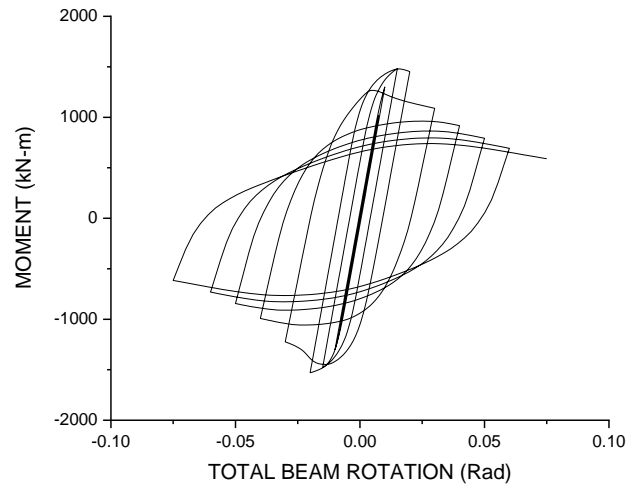


Figure 26: Experimental Moment vs Rotation Curve for RBS-4

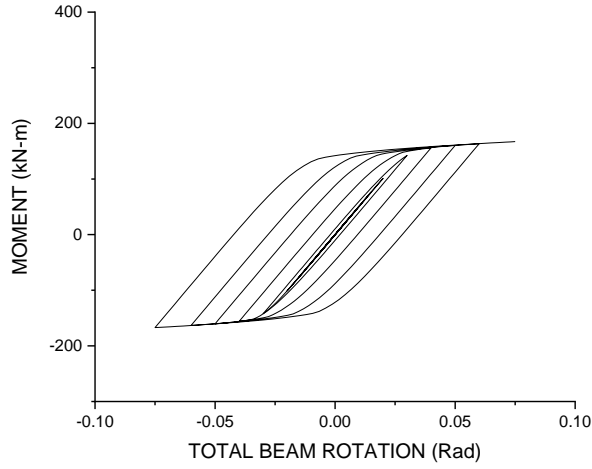


Figure 27: Experimental Moment vs Rotation Curve for RBS-5

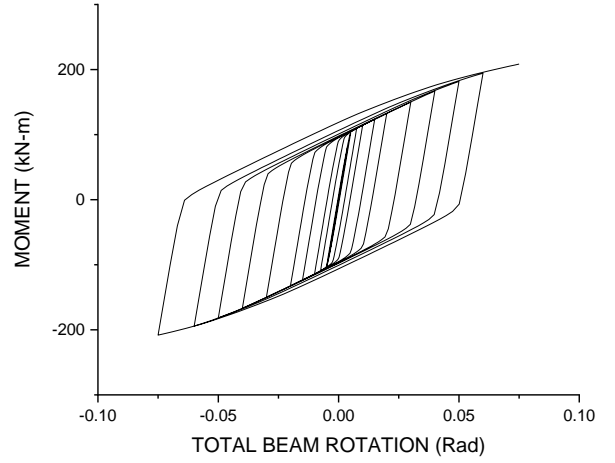


Figure 28: Experimental Moment vs Rotation Curve for RBS-6

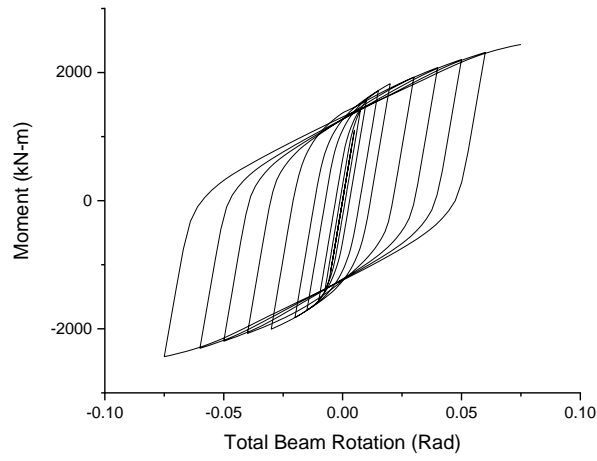


Figure 29: Experimental Moment vs Rotation Curve for RBS-7

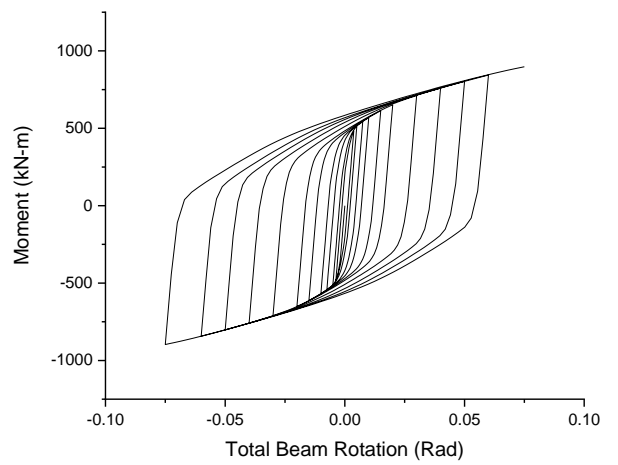


Figure 30: Experimental Moment vs Rotation Curve for RBS-8

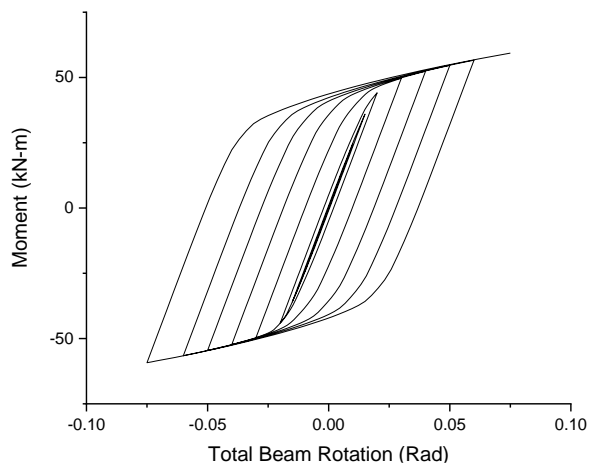


Figure 31: Experimental Moment vs Rotation Curve for RBS-9

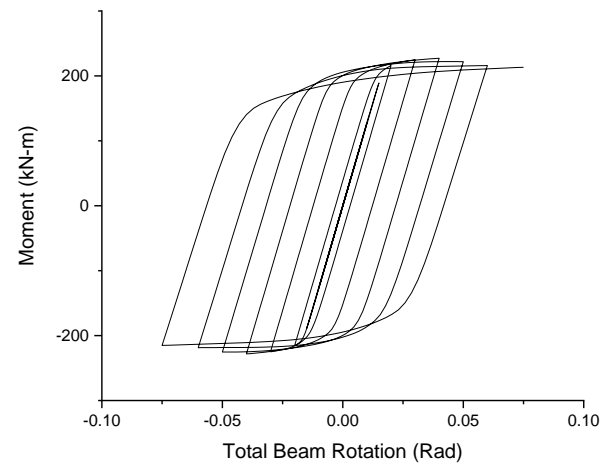


Figure 32: Experimental Moment vs Rotation Curve for RBS-10

4.2. INITIAL SENSITIVITY ANALYSIS

The response variables from phase-I were analyzed to observe the sensitivity of the behaviour of RBS connection. Each response represents a regression model that determines the sensitivity of the response towards certain significant factors considered in the model. To identify the significant independent variables of each regression model, half-normal distribution plots were created for all 5 regression analyses. According to Central Limit Theorem, the distribution of averages is likely to exhibit a normal distribution, therefore, in a half-normal plot of absolute values of the estimated effects versus their respective cumulative normal probabilities, insignificant factors accumulate over a straight line pattern (Montgomery, 2013) leaving the significant ones to be identified with ease as they fall distant from the linear trend. The half normal plots of the 5 responses are presented in **Figures 33** through **37**.

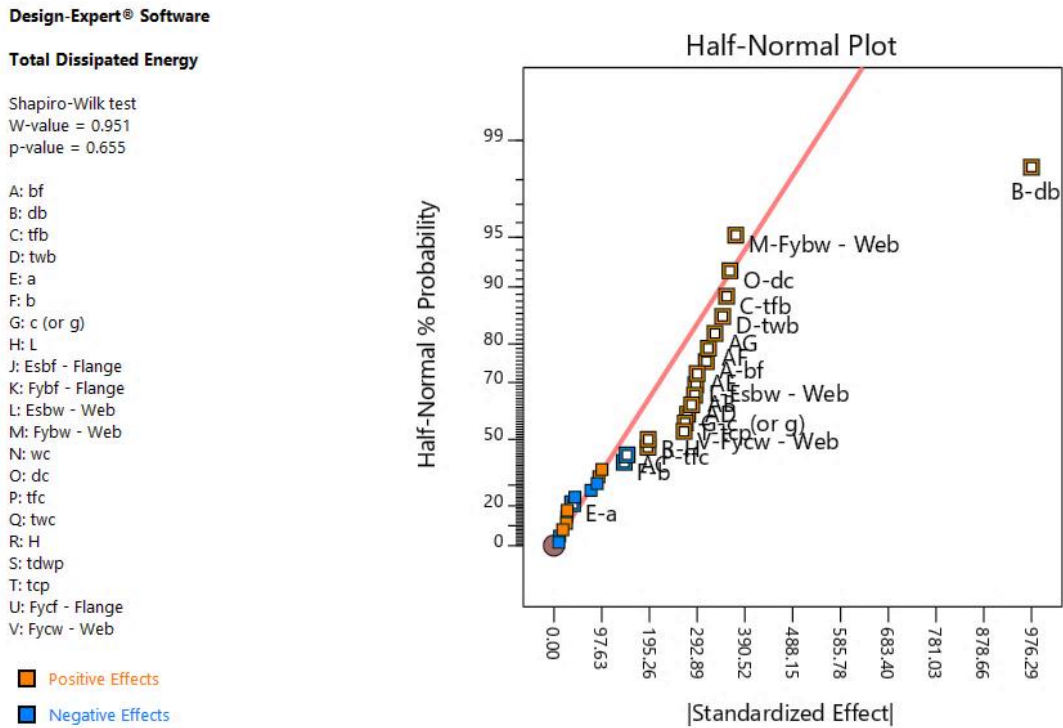


Figure 33: Half-Normal Probability Plot for Response R1 (Total Dissipated Energy) Phase-1

Design-Expert® Software

Initial Stiffness

Shapiro-Wilk test
W-value = 0.721
p-value = 0.000

- A: bf
- B: db
- C: tfb
- D: twb
- E: a
- F: b
- G: c (or g)
- H: L
- J: Esbf - Flange
- K: Fybf - Flange
- L: Esbw - Web
- M: Fybw - Web
- N: wc
- O: dc
- P: tfc
- Q: twc
- R: H
- S: tdwp
- T: tcp
- U: Fycf - Flange
- V: Fycw - Web

- Positive Effects
- Negative Effects

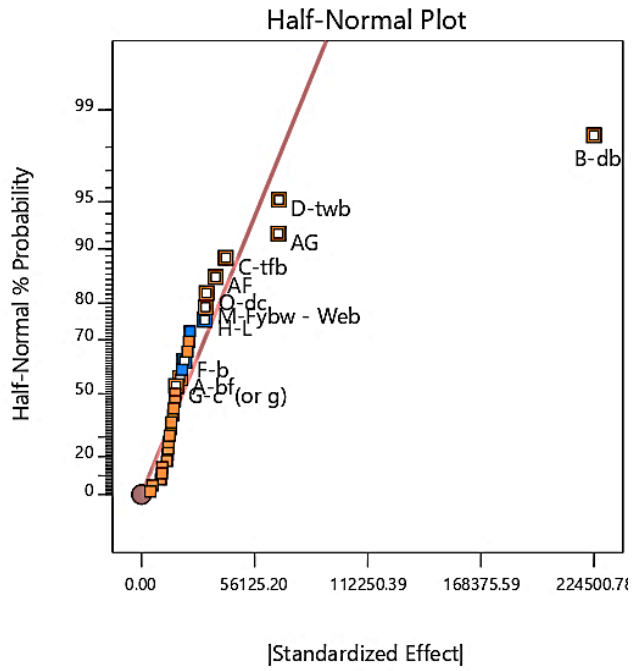


Figure 34: Half-Normal Probability Plot for Response R2 (Initial Stiffness) Phase-1

Design-Expert® Software

Strength Degradation Rate

Shapiro-Wilk test
W-value = 0.963
p-value = 0.768

- A: bf
- B: db
- C: tfb
- D: twb
- E: a
- F: b
- G: c (or g)
- H: L
- J: Esbf - Flange
- K: Fybf - Flange
- L: Esbw - Web
- M: Fybw - Web
- N: wc
- O: dc
- P: tfc
- Q: twc
- R: H
- S: tdwp
- T: tcp
- U: Fycf - Flange
- V: Fycw - Web

- Positive Effects
- Negative Effects

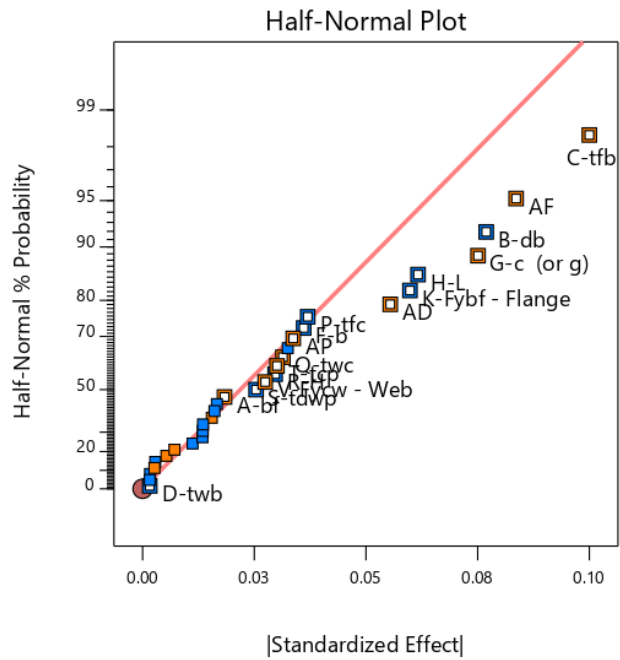


Figure 35: Half-Normal Probability Plot for Response R3 (Strength Degradation Rate) Phase 1

Design-Expert® Software

Max Moment Capacity

Shapiro-Wilk test
 W-value = 0.953
 p-value = 0.469

- A: bf
- B: db
- C: tfb
- D: twb
- E: a
- F: b
- G: c (or g)
- H: L
- J: Esbf - Flange
- K: Fybf - Flange
- L: Esbw - Web
- M: Fybw - Web
- N: wc
- O: dc
- P: tfc
- Q: twc
- R: H
- S: tdwp
- T: tcp
- U: Fycf - Flange
- V: Fycw - Web

- Positive Effects
- Negative Effects

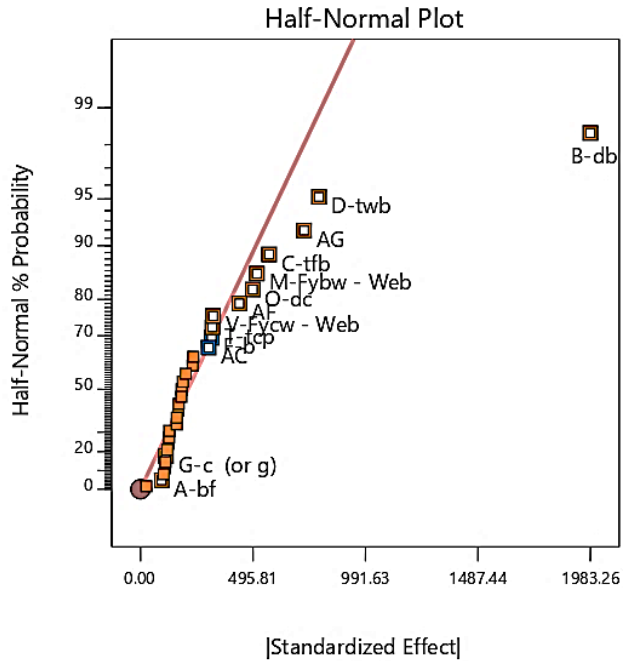


Figure 36: Half-Normal Probability Plot for Response R4 (Max. Moment Capacity) Phase-1

Design-Expert® Software

Rupture Index @ 7.5% rotation

Shapiro-Wilk test
 W-value = 0.864
 p-value = 0.044

- A: bf
- B: db
- C: tfb
- D: twb
- E: a
- F: b
- G: c (or g)
- H: L
- J: Esbf - Flange
- K: Fybf - Flange
- L: Esbw - Web
- M: Fybw - Web
- N: wc
- O: dc
- P: tfc
- Q: twc
- R: H
- S: tdwp
- T: tcp
- U: Fycf - Flange
- V: Fycw - Web

- Positive Effects
- Negative Effects

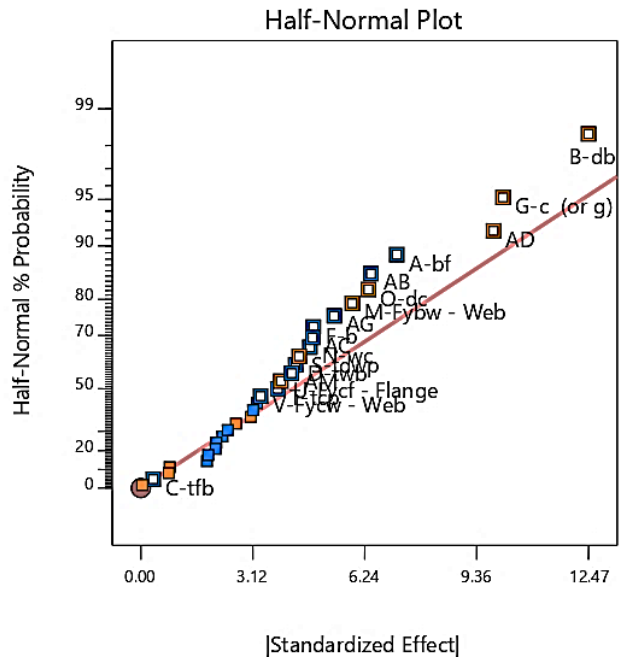


Figure 37: Half-Normal Probability Plot for Response R5 (Rupture Index) Phase-1

These results can be evaluated rationally by Analysis of Variance (ANOVA) tables (from **Tables 7 to 11**) for each response as follows.

Table 7: ANOVA of Selected Model for Response R1, Phase-1

SOURCE	SUM OF SQUARES	df	MEAN SQUARE	F-VALUE	P-VALUE	
Model	19506075.88	20	975303.7942	37.07362	2.31E-07	Significant
A-bf	777664.2951	1	777664.2951	29.56088	0.000205	
B-db	7625170.638	1	7625170.638	289.8509	2.98E-09	
C-tfb	998088.8188	1	998088.8188	37.93974	7.11E-05	
D-twb	952622.6759	1	952622.6759	36.21146	8.7E-05	
E-a	11839.31024	1	11839.31024	0.45004	0.516154	
F-b	165483.8401	1	165483.8401	6.290436	0.029086	
G-c (or g)	596436.4771	1	596436.4771	22.67197	0.000589	
L-Esbw - Web	672414.5054	1	672414.5054	25.56008	0.000369	
M-Fybw - Web	1106380.707	1	1106380.707	42.05617	4.52E-05	
O-dc	1035646.848	1	1035646.848	39.36741	6.05E-05	
P-tfc	295542.4004	1	295542.4004	11.23427	0.006457	
R-H	297434.0326	1	297434.0326	11.30618	0.006336	
T-tcp	576540.1943	1	576540.1943	21.91567	0.00067	
V-Fycw - Web	566483.4793	1	566483.4793	21.53339	0.000716	
AB	662925.503	1	662925.503	25.19938	0.00039	
AC	178878.9383	1	178878.9383	6.799615	0.024361	
AD	634053.417	1	634053.417	24.10188	0.000465	
AE	686996.6958	1	686996.6958	26.11438	0.000339	
AF	798077.6802	1	798077.6802	30.33684	0.000184	
AG	867395.4281	1	867395.4281	32.97177	0.00013	
Residual	289379.3579	11	26307.21435			
Cor Total	19795455.24	31				

Table 8: ANOVA of Selected Model for Response R2, Phase-1

SOURCE	SUM OF SQUARES	df	MEAN SQUARE	F-VALUE	P-VALUE	
Model	5.35235E+11	11	48657741995	25.51525	2.2587E-09	Significant
A-bf	2931570374	1	2931570374	1.53726	0.22937662	
B-db	4.03205E+11	1	4.03205E+11	211.43341	4.2639E-12	
C-tfb	13948371264	1	13948371264	7.31427	0.01364318	
D-twb	37196295746	1	37196295746	19.50507	0.00026581	
F-b	3614657880	1	3614657880	1.89546	0.1838046	
G-c (or g)	2349195942	1	2349195942	1.23187	0.2802095	
H-L	7868373219	1	7868373219	4.12603	0.0557313	
M-Fybw - Web	8078685468	1	8078685468	4.23631	0.0528358	
O-dc	8355611604	1	8355611604	4.38153	0.0492818	
AF	10812230837	1	10812230837	5.66974	0.0273115	
AG	36875363899	1	36875363899	19.33678	0.0002779	
Residual	38140121715	20	1907006086			
Cor Total	5.73375E+11	31				

Table 9: ANOVA of Selected Model for Response R3, Phase-1

SOURCE	SUM OF SQUARES	df	MEAN SQUARE	F-VALUE	P-VALUE	
Model	0.396062246	17	0.023297779	14.96589	0.00000	Significant
A-bf	0.002814055	1	0.002814055	1.80768	0.20017	
B-db	0.049525085	1	0.049525085	31.81364	0.00006	
C-tfb	0.083703973	1	0.083703973	53.76927	0.00000	
D-twb	2.16136E-05	1	2.16136E-05	0.01388	0.90788	
F-b	0.010888384	1	0.010888384	6.99442	0.01923	
G-c (or g)	0.047188566	1	0.047188566	30.31272	0.00008	
H-L	0.031815242	1	0.031815242	20.43729	0.00048	
K-Fybf - Flange	0.029973575	1	0.029973575	19.25425	0.00062	
P-tfc	0.01143883	1	0.01143883	7.34801	0.01690	
Q-twc	0.008262938	1	0.008262938	5.30790	0.03708	
R-H	0.007370626	1	0.007370626	4.73470	0.04718	
S-tdwp	0.005405669	1	0.005405669	3.47246	0.08351	
T-tcp	0.007578574	1	0.007578574	4.86828	0.04456	
V-Fycw - Web	0.006303686	1	0.006303686	4.04932	0.06384	
AD	0.025735019	1	0.025735019	16.53151	0.00116	
AF	0.058516283	1	0.058516283	37.58935	0.00003	
AP	0.009520129	1	0.009520129	6.11549	0.02683	
Residual	0.021794152	14	0.001556725			
Cor Total	0.417856398	31				

Table 10: ANOVA of Selected Model for Response R4, Phase-1

SOURCE	SUM OF SQUARES	df	MEAN SQUARE	F-VALUE	P-VALUE	
Model	52031482.27	13	4002421.713	19.9861	0.0000	Significant
A-bf	70133.42716	1	70133.42716	0.3502	0.5614	
B-db	31466547.48	1	31466547.48	157.1285	0.0000	
C-tfb	2569583.146	1	2569583.146	12.8312	0.0021	
D-twb	4952480.826	1	4952480.826	24.7303	0.0001	
F-b	787818.7096	1	787818.7096	3.9340	0.0628	
G-c (or g)	100318.6572	1	100318.6572	0.5009	0.4882	
M-Fybw - Web	2104680.754	1	2104680.754	10.5097	0.0045	
O-dc	1959800.789	1	1959800.789	9.7863	0.0058	
T-tcp	805571.8361	1	805571.8361	4.0226	0.0602	
V-Fycw - Web	818783.8993	1	818783.8993	4.0886	0.0583	
AC	719474.3712	1	719474.3712	3.5927	0.0742	
AF	1520238.512	1	1520238.512	7.5913	0.0130	
AG	4156049.864	1	4156049.864	20.7533	0.0002	
Residual	3604678.175	18	200259.8986			
Cor Total	55636160.45	31				

Table 11: ANOVA of Selected Model for Response R5, Phase-1

SOURCE	SUM OF SQUARES	df	MEAN SQUARE	F-VALUE	P-VALUE	
Model	5630.02956	17	331.1782094	7.660786	0.000198	Significant
A-bf	406.5377033	1	406.5377033	9.403995	0.008370	
B-db	1244.792276	1	1244.792276	28.794427	0.000100	
C-tfb	0.951366877	1	0.951366877	0.022007	0.884184	
D-twb	148.7905317	1	148.7905317	3.441810	0.084743	
F-b	184.753254	1	184.753254	4.273696	0.057714	
G-c (or g)	814.9194129	1	814.9194129	18.850645	0.000677	
M-Fybw - Web	277.7565243	1	277.7565243	6.425040	0.023810	
N-wc	177.359864	1	177.359864	4.102673	0.062316	
O-dc	321.5553786	1	321.5553786	7.438191	0.016358	
S-tdwp	155.823094	1	155.823094	3.604486	0.078432	
T-tcp	116.4424939	1	116.4424939	2.693538	0.123021	
U-Fycf - Flange	121.6192038	1	121.6192038	2.813285	0.115662	
AB	328.9774037	1	328.9774037	7.609877	0.015383	
AC	183.4130916	1	183.4130916	4.242696	0.058518	
AD	772.8599927	1	772.8599927	17.877730	0.000843	
AG	232.5222893	1	232.5222893	5.378685	0.036014	
AM	140.9556788	1	140.9556788	3.260575	0.092506	
Residual	605.2244767	14	43.23031976			
Cor Total	6235.254036	31				

At this point, it was observed that where the half-normal distributions of all responses exhibited remarkable significance of factor B (depth of beam – db), they also showed no (in models for R1, R2, R3 and R4) or minimum (in model of R4) significance of factor U (Yield Strength of Column Flange – Fycf – Flange) and considerably high significance of combined effects of certain factors which was an ambiguous situation i.e. it is hard to tell if the effect is significant because of either one of factors in the interaction or both. On observing these combined effects, it was evident that all of the combined effects included factor A (width of beam flange – bf) that gives a logical hint that it might be factor A controlling these effects but the F-Values for factor A in models 2, 3 and 4 were found to be significantly lower than other significant factors.

In order to clarify the significance of factor A in models 2, 3 and 4; and confirm other results on the basis of concrete evidence, a semi-foldover augmented design of experiment was carried out as a Phase-2 of experiment and are discussed in following sections. This design was folded on factor A that was needed to be clarified and since factor U was found to be of minimum significance, it was set to its higher level as depicted in **Figure 38**. The semi-foldover design and its responses are discussed in detail in the following sections.

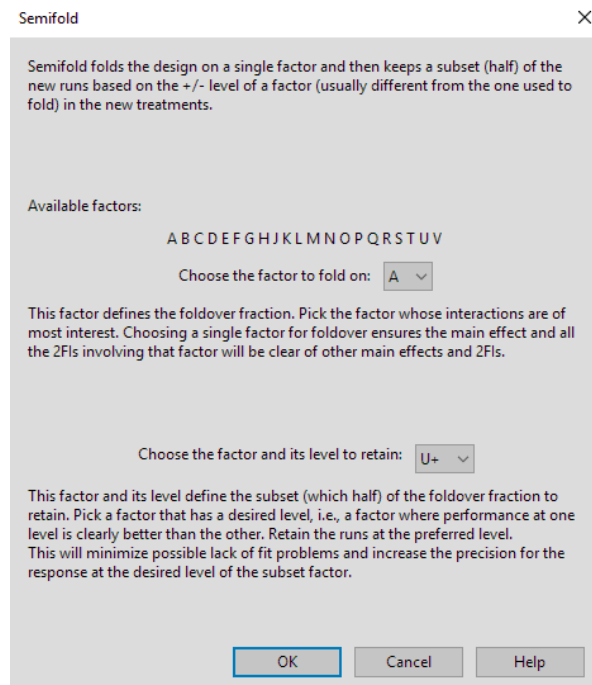


Figure 38: Semi-foldover Augmented Design Dialogue Screen in Design Expert v.11 Software

4.3. SEMI-FOLD OVER AUGMENTED DESIGN (PHASE-2)

As discussed in section 4.2, the results from phase-1 have shown some significant 2 factors interactions (2FIs) that had factor A (bf) in common. Therefore, by carrying out semi-foldover augmented design, 16 more test combinations were generated using Design Expert software as presented in **Table 12**.

Table 12: Coded Factor Combinations for Experiment Phase 2 (Semi-Fold over)

RBS	bf mm	db mm	tfb mm	twb mm	a mm	b mm	c mm	L mm	Esbf MPa	Fybf MPa	Esbw MPa	Fybw MPa	wc mm	dc mm	tfc mm	twc mm	H mm	tdwp mm	tcp mm	Fycf MPa	Fycw MPa
34	1	-1	-1	-1	-1	-1	-1	-1	-1	1	-1	-1	-1	1	-1	-1	1	-1	1	1	-1
35	-1	-1	-1	-1	-1	1	1	1	-1	-1	1	1	-1	-1	1	-1	-1	-1	-1	1	1
36	1	1	1	-1	-1	-1	1	1	-1	1	1	1	-1	1	-1	1	-1	1	-1	1	-1
37	-1	1	1	-1	-1	1	-1	-1	-1	-1	-1	-1	-1	-1	1	1	1	1	1	1	1
38	1	1	-1	1	-1	1	-1	1	-1	1	1	-1	1	-1	1	-1	1	1	-1	1	-1
39	-1	1	-1	1	-1	-1	1	-1	-1	-1	-1	1	1	1	-1	-1	-1	1	1	1	1
40	1	-1	1	1	-1	1	1	-1	-1	1	-1	1	1	-1	1	1	-1	-1	1	1	-1
41	-1	-1	1	1	-1	-1	-1	1	-1	-1	1	-1	1	1	-1	1	1	-1	-1	1	1
42	1	1	-1	-1	1	1	1	-1	1	-1	-1	1	-1	1	1	-1	1	1	-1	1	-1
43	-1	1	-1	-1	1	-1	-1	1	1	1	1	-1	-1	-1	-1	-1	-1	1	1	1	1
44	1	-1	1	-1	1	1	-1	1	1	-1	1	-1	-1	1	1	1	-1	-1	1	1	-1
45	-1	-1	1	-1	1	-1	1	-1	1	1	-1	1	-1	-1	-1	1	1	-1	-1	1	1
46	1	-1	-1	1	1	-1	1	1	1	-1	1	1	1	-1	-1	-1	1	-1	1	1	-1
47	-1	-1	-1	1	1	1	-1	-1	1	1	-1	-1	1	1	1	-1	-1	-1	-1	1	1
48	1	1	1	1	1	-1	-1	-1	1	-1	-1	-1	1	-1	-1	1	-1	1	-1	1	-1

Note: -1 and 1 indicate the minimum and maximum values respectively as mentioned in **Table 5**.

4.4. PHASE – 2 RESPONSE PLOTS

In Phase – 2 of the experiment, 16 new test runs were conducted to verify the observations of Phase – 1 and clarify the significance of factor A (bf). The response plots for these test runs are presented in **Figures 39** through **54**.

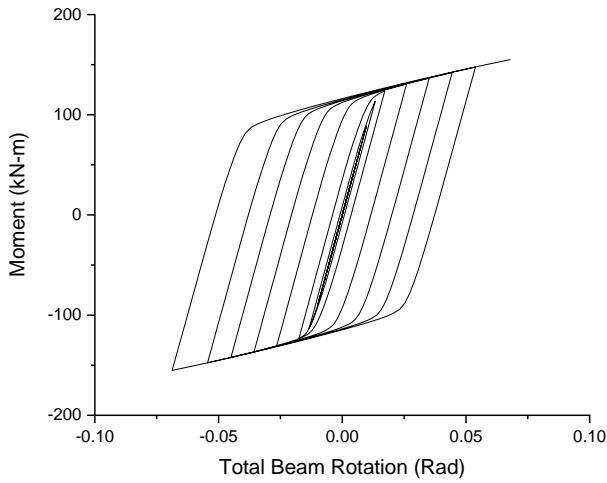


Figure 39: Experimental Moment vs Rotation Curve for RBS-33

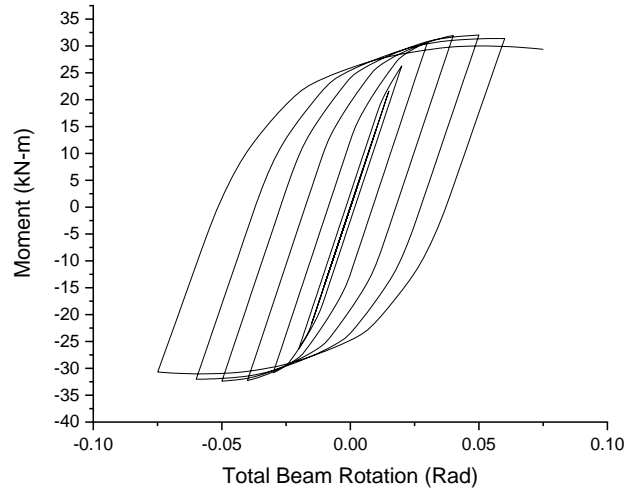


Figure 40: Experimental Moment vs Rotation Curve for RBS-34

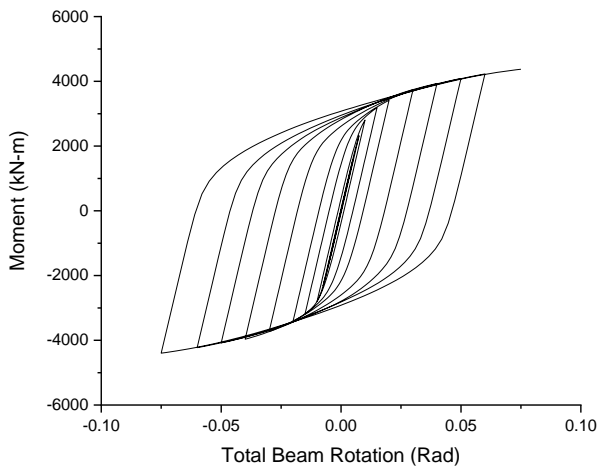


Figure 41: Experimental Moment vs Rotation Curve for RBS-35

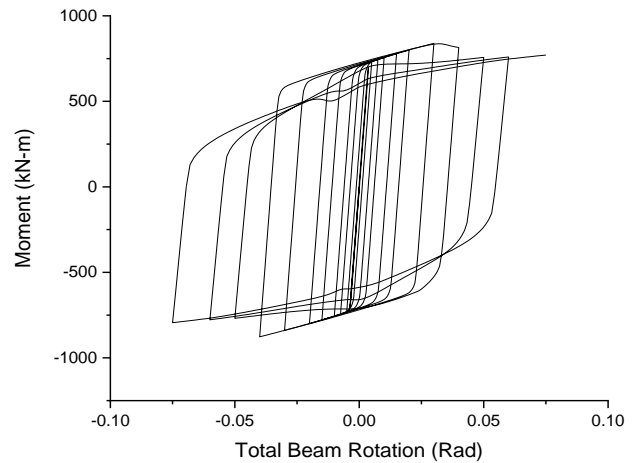


Figure 42: Experimental Moment vs Rotation Curve for RBS-36

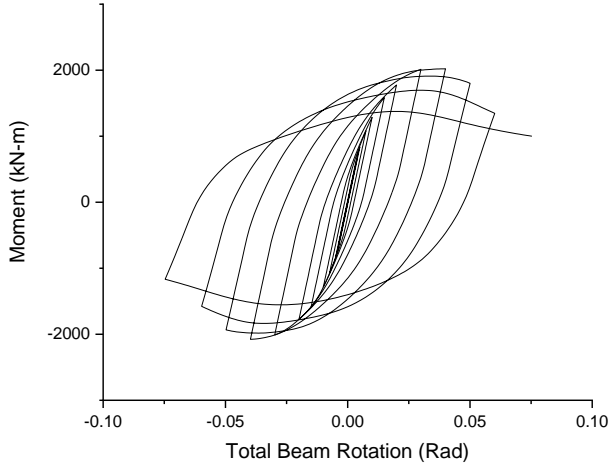


Figure 43: Experimental Moment vs Rotation Curve for RBS-37

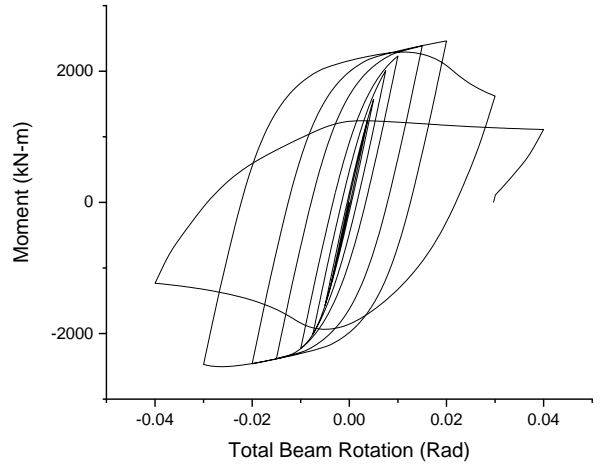


Figure 44: Experimental Moment vs Rotation Curve for RBS-38

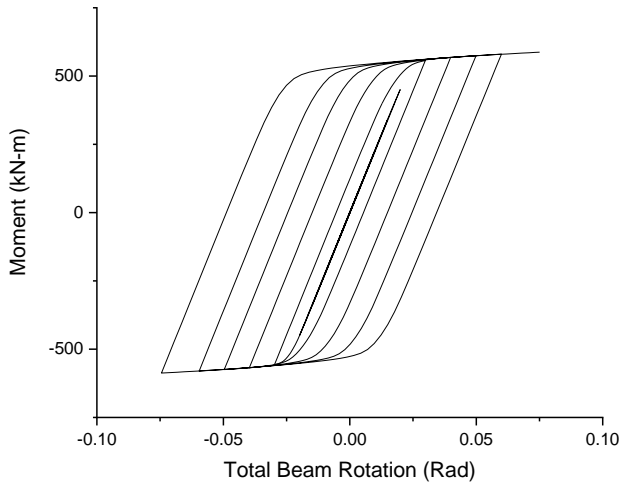


Figure 45: Experimental Moment vs Rotation Curve for RBS-39

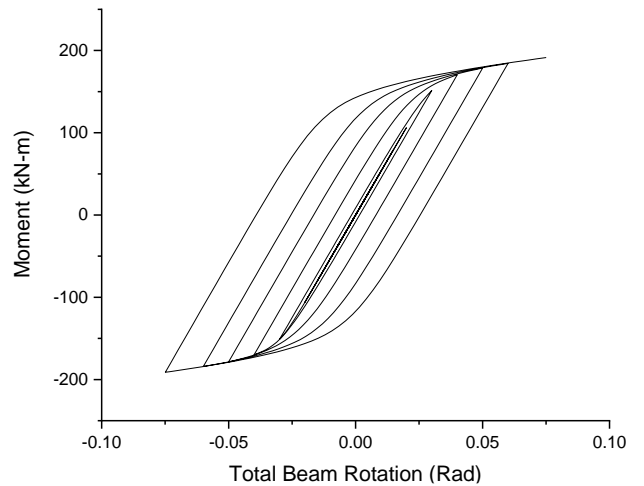


Figure 46: Experimental Moment vs Rotation Curve for RBS-40

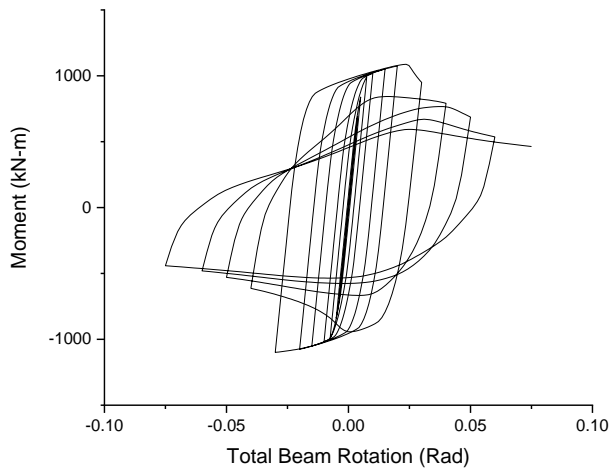


Figure 47: Experimental Moment vs Rotation Curve for RBS-41

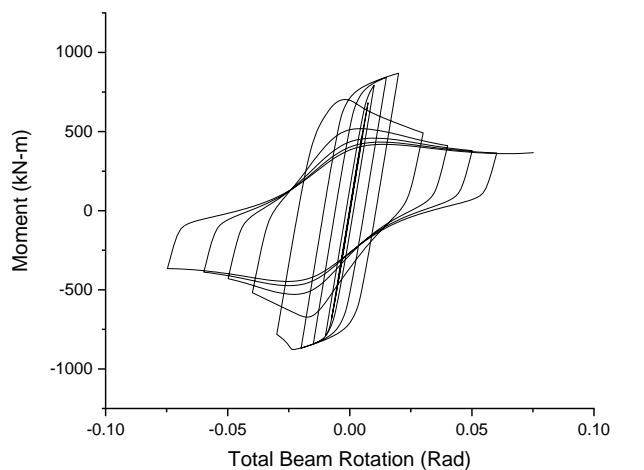


Figure 48: Experimental Moment vs Rotation Curve for RBS-42

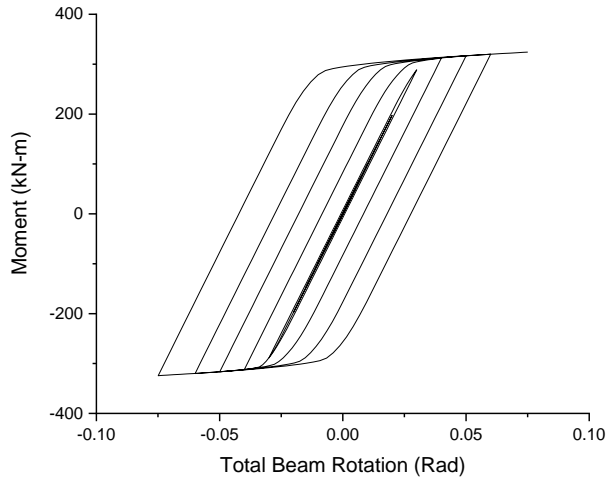


Figure 49: Experimental Moment vs Rotation Curve for RBS-43

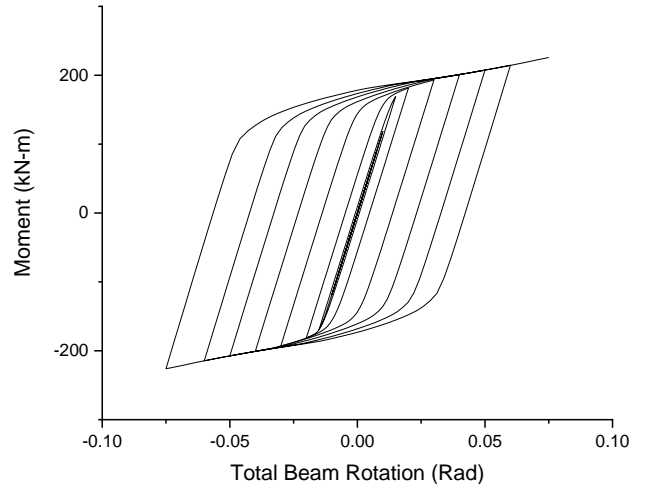


Figure 50: Experimental Moment vs Rotation Curve for RBS-44

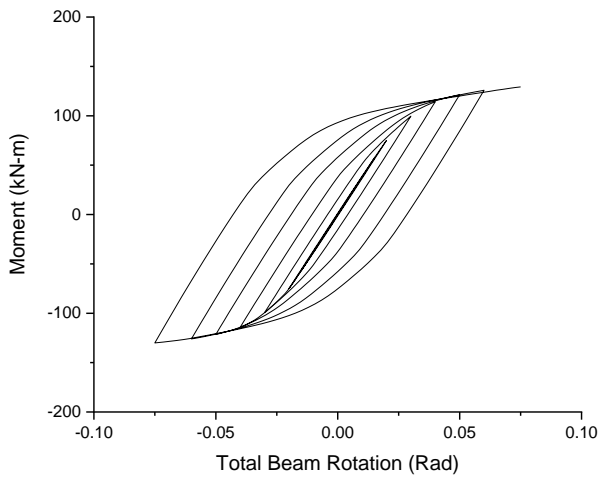


Figure 51: Experimental Moment vs Rotation Curve for RBS-45

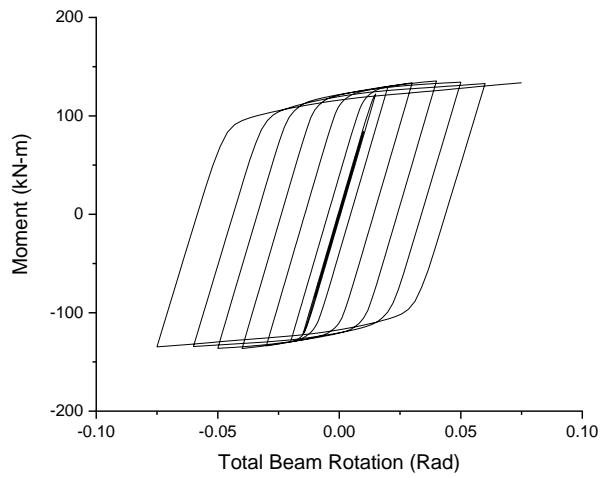


Figure 52: Experimental Moment vs Rotation Curve for RBS-46

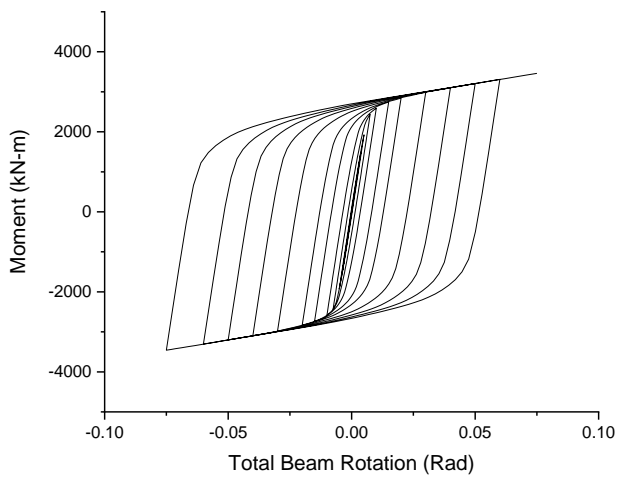


Figure 53: Experimental Moment vs Rotation Curve for RBS-47

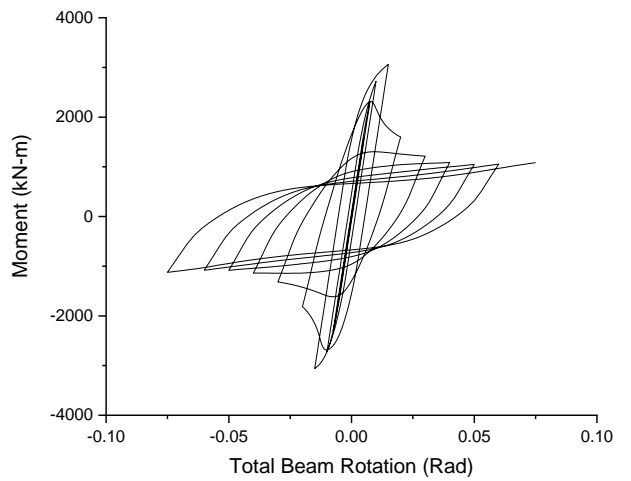


Figure 54: Experimental Moment vs Rotation Curve for RBS-48

CHAPTER – 5

5. RESULTS AND DISCUSSIONS

5.1. DEFLECTED GEOMETRIES OF FEA MODELS

The post processing maximum deflection modes under the cyclic loading are presented in this section for specimen RBS-1 to RBS-5 whereas rest of the deflected geometries are presented in Appendix C.

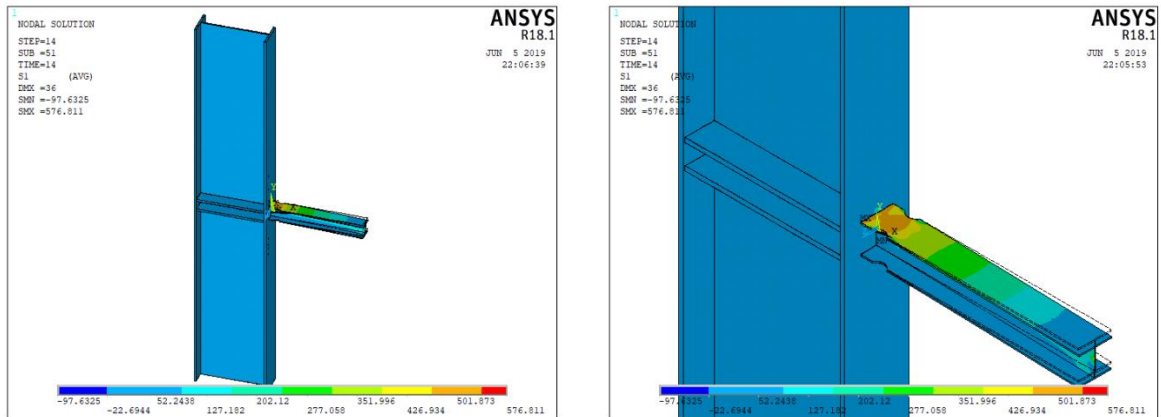


Figure 55: Deflected Geometry of Specimen RBS-1

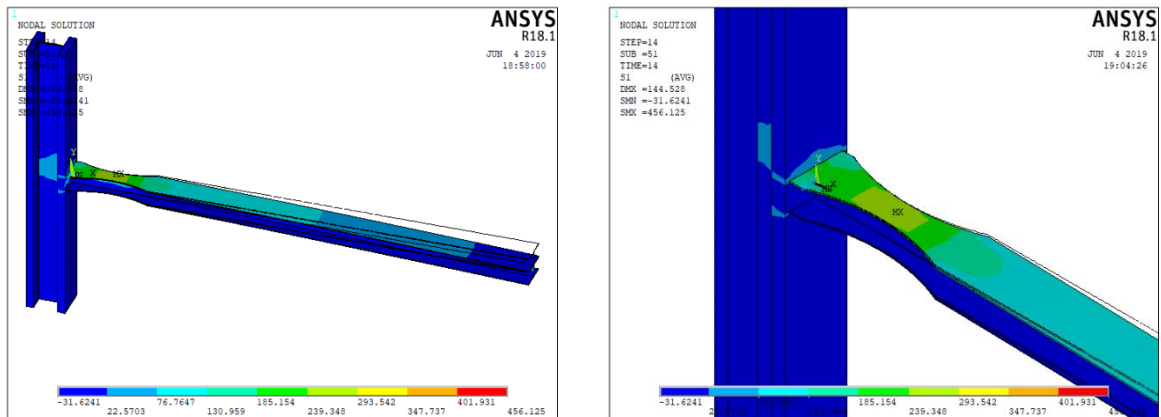


Figure 56: Deflected Geometry of Specimen RBS-2

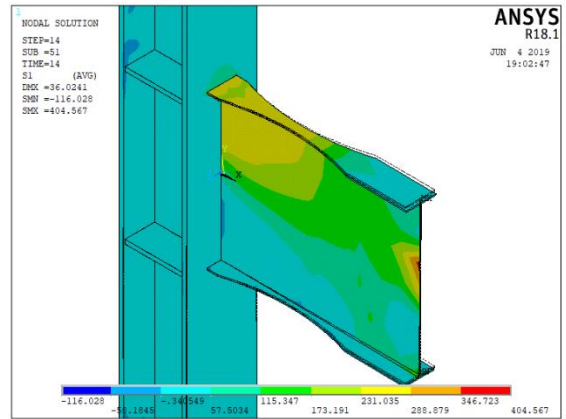
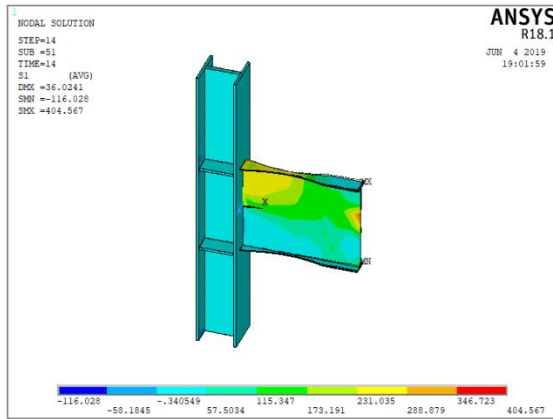


Figure 57: Deflected Geometry of Specimen RBS-3

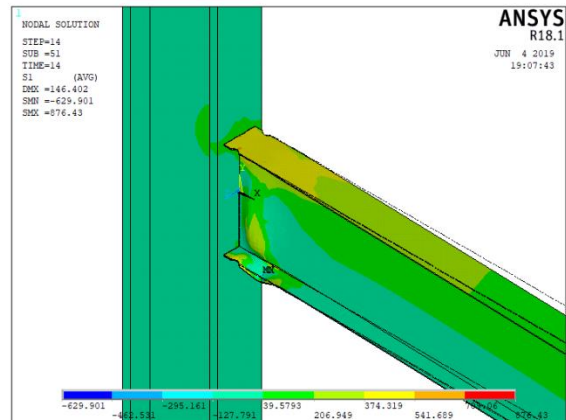
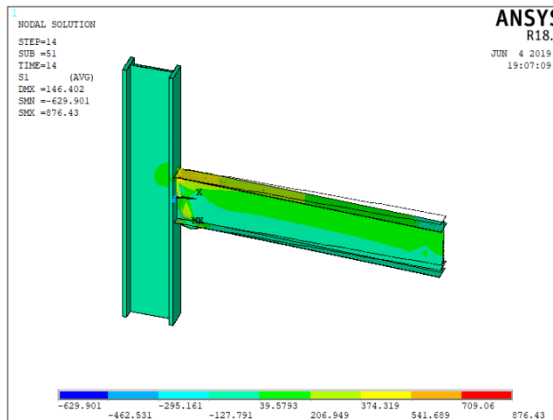


Figure 58: Deflected Geometry of Specimen RBS-4

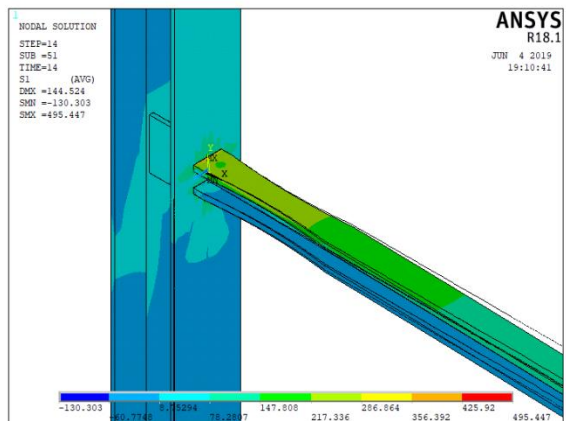
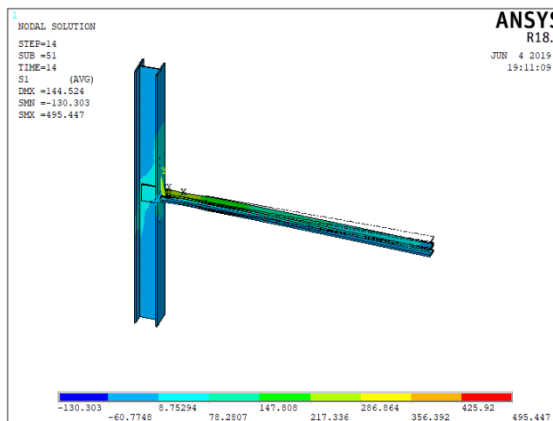


Figure 59: Deflected Geometry of Specimen RBS-5

5.2. OVERALL SENSITIVITY ANALYSIS OF EFFECTS

The second phase of experiment using semi-foldover augmented design yielded the results that helped in understanding the effects of the significant factors independently. However, solution for model no. 38 was not able to converge beyond 4% total beam rotation because of excessive deformation as depicted in deflected geometry shown for RBS-38 presented in Appendix C of this document and therefore the results from this model were not included in the sensitivity analysis which was conducted for results yielded at 7.5% total beam rotation. These results are presented in **Table 13** and the analysis of these results is discussed in the following sub-sections.

Table 13: Results from Both Phases of the Experiment

Phase	Run	Response 1 R1 (kJ/m)	Response 2 R2 (kN-m)	Response 3 R3 -	Response 4 R4 (kN-m)	Response 5 R5 -
PHASE I	1	53.744	6032.00	1.029	96.331	1.480
	2	28.733	2634.21	1.023	64.819	0.537
	3	299.911	132416.00	1.027	520.700	3.312
	4	636.742	136271.94	0.750	1529.446	4.925
	5	55.679	5139.91	1.020	167.178	0.458
	6	104.087	21856.00	1.078	208.470	0.351
	7	1201.633	221208.99	1.085	2438.456	49.063
	8	559.076	185504.00	1.061	897.390	0.947
	9	25.400	2441.46	1.040	59.319	2.637
	10	127.577	12720.00	1.018	228.254	1.896
	11	366.872	154582.87	0.542	1572.385	1.084
	12	2113.492	377648.00	1.036	3121.184	25.041
	13	122.093	11360.00	1.021	232.639	0.944
	14	79.684	8288.11	1.045	312.578	1.227
	15	2472.888	368528.00	1.035	4130.528	16.181
	16	1098.735	209322.94	1.048	1742.862	2.562
	17	68.890	6576.00	1.015	116.932	1.359
	18	31.896	2826.95	1.022	73.839	0.498
	19	170.566	156176.00	0.831	773.075	58.061
	20	509.016	124578.63	0.768	1268.414	0.486
	21	66.276	5846.65	1.018	173.983	0.266
	22	141.630	16080.00	1.050	285.936	0.369
	23	1101.264	149892.70	1.056	2215.962	30.610

	24	1248.835	213808.00	1.025	1643.977	0.837
	25	25.042	2505.71	1.036	84.237	1.571
	26	103.373	12464.00	0.987	204.624	1.182
	27	250.751	181427.50	0.852	2320.633	0.767
	28	1400.861	287000.47	1.050	2201.200	16.983
	29	101.331	10576.00	1.047	250.613	3.782
	30	92.819	8994.85	1.026	343.511	0.709
	31	161.994	364496.00	1.040	2867.322	0.644
	32	3256.290	465492.29	1.008	5391.878	3.480
PHASE 2	33	70.604	9125.393	1.044	155.137	0.201
	34	14.541	1477.725	1.057	32.388	0.595
	35	2366.737	318160.595	1.068	4398.024	12.987
	36	215.763	202092.632	1.034	850.961	0.572
	37	1089.375	173825.065	1.024	2076.996	0.070
	38	N/C	N/C	N/C	N/C	N/C
	39	260.534	22704.000	1.013	587.581	0.425
	40	55.198	5332.659	1.035	191.388	1.093
	41	552.845	187136.000	0.963	1099.554	5.738
	42	327.202	93612.980	0.597	877.413	0.719
	43	110.662	9894.332	1.012	324.281	0.164
	44	117.412	11872.000	1.031	225.931	3.176
	45	39.624	3790.686	1.037	130.061	1.491
	46	82.014	8432.000	1.019	136.350	1.858
	47	2365.757	403488.000	1.037	3460.198	3.543
	48	727.069	318353.342	0.401	3061.107	3.110

N/C: Solution not Converged

5.2.1. For Response Variable R1 (Total Dissipated Energy)

The final predictive model for response variable R1 having a coefficient of determination (R^2) of 0.9552 can be written as a coded equation as follows:

$$\begin{aligned}
 R1 = & \beta_0 + \beta_1A + \beta_2B + \beta_3C + \beta_4D + \beta_5E + \beta_6F + \beta_7J + \beta_8K + \beta_9L + \beta_{10}M \\
 & + \beta_{11}O + \beta_{12}Q + \beta_{13}S + \beta_{14}U + \beta_{15}AB + \beta_{16}AC + \beta_{17}AD \\
 & + \beta_{18}AE + \beta_{19}AJ + \beta_{20}AQ + \beta_{21}AS + \beta_{22}AU + \beta_{23}BC + \beta_{24}BD \\
 & + \beta_{25}ABD
 \end{aligned}$$

Where values of all β are given in **Table 14**.

Table 14: Coefficients of Model for Response R1

Coefficient	Value	Coefficient	Value
β_0	561.98717	β_{13}	-11.273586
β_1	159.37976	β_{14}	-4.9423484
β_2	482.62068	β_{15}	143.48346
β_3	197.77191	β_{16}	-31.268507
β_4	142.40859	β_{17}	150.46106
β_5	-21.259977	β_{18}	146.52183
β_6	-105.44805	β_{19}	-104.8402
β_7	11.51335	β_{20}	139.90719
β_8	117.68004	β_{21}	133.77843
β_9	109.03266	β_{22}	136.5399
β_{10}	177.22434	β_{23}	165.66373
β_{11}	170.20163	β_{24}	131.96968
β_{12}	-16.828696	β_{25}	145.24099

The half-normal plot (**Figure 60**) and Pareto chart (**Figure 61**) show the marginal significance of factor B over all other factors with a contribution of 35.47%. A graphical representation of the percentage contribution of factors in the energy dissipation is also presented in **Figure 62**.

Design-Expert® Software

Total Dissipated Energy

Shapiro-Wilk test
W-value = 0.906
p-value = 0.053

- A: bf
- B: db
- C: tfb
- D: twb
- E: a
- F: b
- G: c (or g)
- H: L
- J: Esbf - Flange
- K: Fybf - Flange
- L: Esbw - Web
- M: Fybw - Web
- N: wc
- O: dc
- P: tfc
- Q: twc
- R: H
- S: tdwp
- T: tcp
- U: Fyfc - Flange
- V: Fywc - Web

- Positive Effects
- Negative Effects

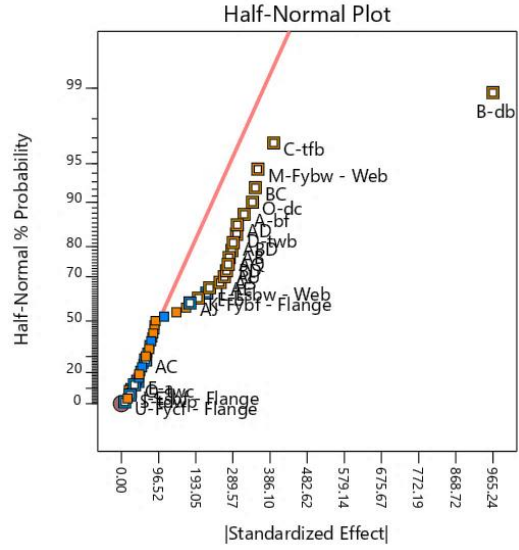


Figure 60: Half-Normal Probability Plot for Response R1 (Total Dissipated Energy)

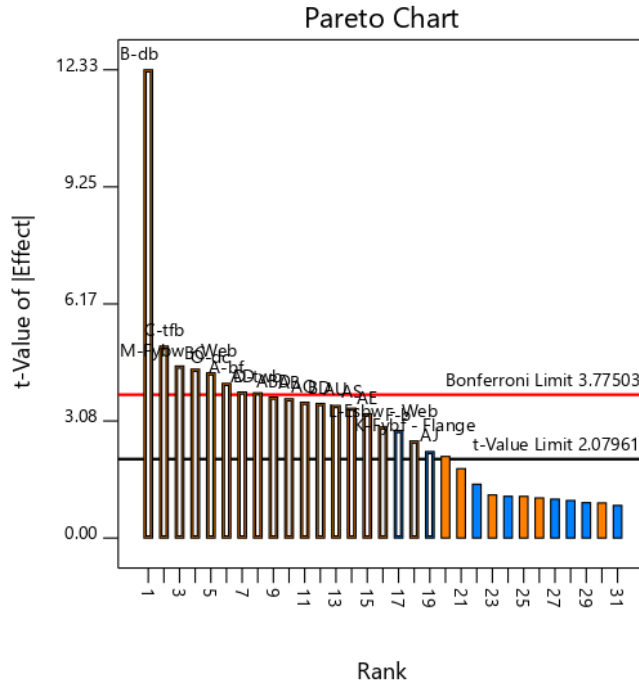


Figure 61: Pareto Chart for Response R1 (Total Dissipated Energy)

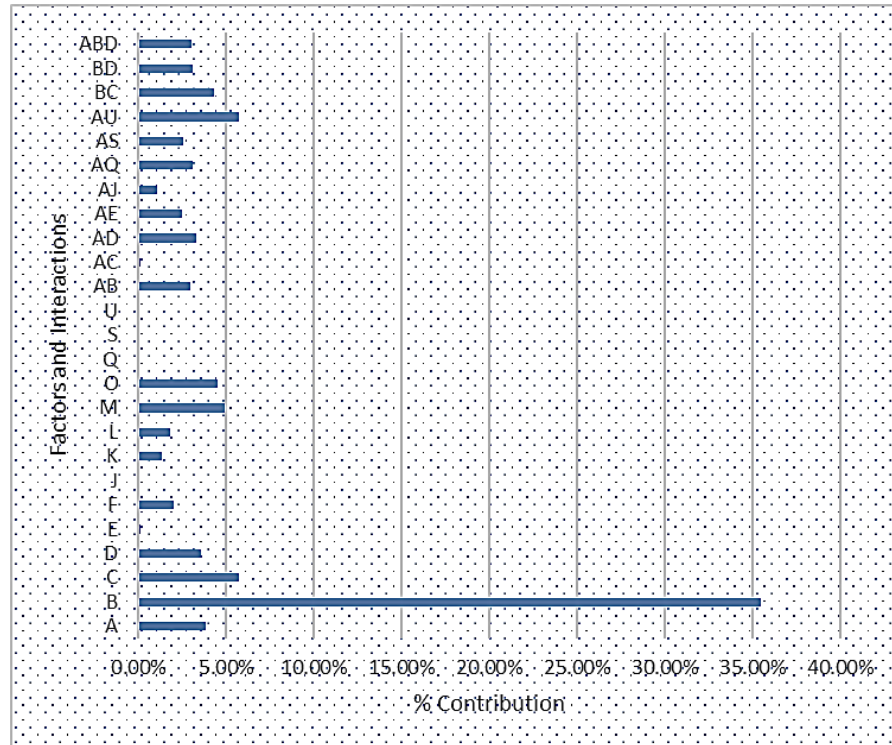


Figure 62: Percentage Contributions of Factors and Interactions on Response R1

The Analysis of Variance for the selected model confirmed the acute sensitivity of the response R1 to the factor B with the highest F-value of 152.09. It is also to be noted that factors with considerably lower F-values like factors E, J, Q, S and U were included in the model just to maintain hierarchy i.e. it can be seen by the ANOVA presented in **Table 15** that factor Q has an F-Value as small as 0.1849 was included in the model because the 2FI AQ had a higher F-Value of 12.78.

Table 15: ANOVA of Selected Model for Response R1

SOURCE	SUM OF SQUARES	df	MEAN SQUARE	F-VALUE	P-VALUE	
Block	278.5705278	1	278.5705278			
Model	27298838.08	25	1091953.523	17.04637	0.00000	Significant
A-bf	1062563.529	1	1062563.529	16.58756	0.00059	
B-db	9743172.77	1	9743172.77	152.09959	0.00000	
C-tfb	1636129.879	1	1636129.879	25.54144	0.00006	
D-twb	936009.5962	1	936009.5962	14.61194	0.00106	
E-a	18906.63028	1	18906.63028	0.29515	0.59294	
F-b	513198.0269	1	513198.0269	8.01148	0.01034	
J-Esbf - Flange	5544.877806	1	5544.877806	0.08656	0.77163	
K-Fybf - Flange	418070.7193	1	418070.7193	6.52646	0.01889	
L-Esbw - Web	548682.526	1	548682.526	8.56542	0.00834	
M-Fybw - Web	1313818.158	1	1313818.158	20.50987	0.00020	
O-dc	1211758.159	1	1211758.159	18.91662	0.00031	
Q-twc	11846.48428	1	11846.48428	0.18493	0.67176	
S-tdwp	5316.339209	1	5316.339209	0.08299	0.77625	
U-Fycf - Flange	781.6578462	1	781.6578462	0.01220	0.91314	
AB	861176.6211	1	861176.6211	13.44373	0.00153	
AC	40898.07153	1	40898.07153	0.63846	0.43366	
AD	946971.1925	1	946971.1925	14.78306	0.00101	
AE	686996.6958	1	686996.6958	10.72463	0.00379	
AJ	331817.8826	1	331817.8826	5.17997	0.03400	
AQ	818782.5769	1	818782.5769	12.78192	0.00189	
AS	748618.8323	1	748618.8323	11.68661	0.00272	
AU	779843.9247	1	779843.9247	12.17406	0.00231	
BC	1266667.955	1	1266667.955	19.77381269	0.000247666	
BD	803815.1853	1	803815.1853	12.54826953	0.002044335	
ABD	882402.8955	1	882402.8955	13.77509354	0.001379823	
Residual	1281157.028	20	64057.85142			
Cor Total	28580273.68	46				

The effect of interaction between factor A and B on the total dissipated energy as shown in **Figures 63** and **64** demonstrated that the total dissipated energy was increased by 81.7% as values of factor A (bf) was increased from low-level to high-level at low-level value of factor B (db). For high-level value of factor B, the rise in total dissipated energy was dropped from 81.7% to 50.1% with increase in the

value of factor A from low to high-level. That indicates sensitivity of effect of factor A on energy dissipation towards the value of factor B.

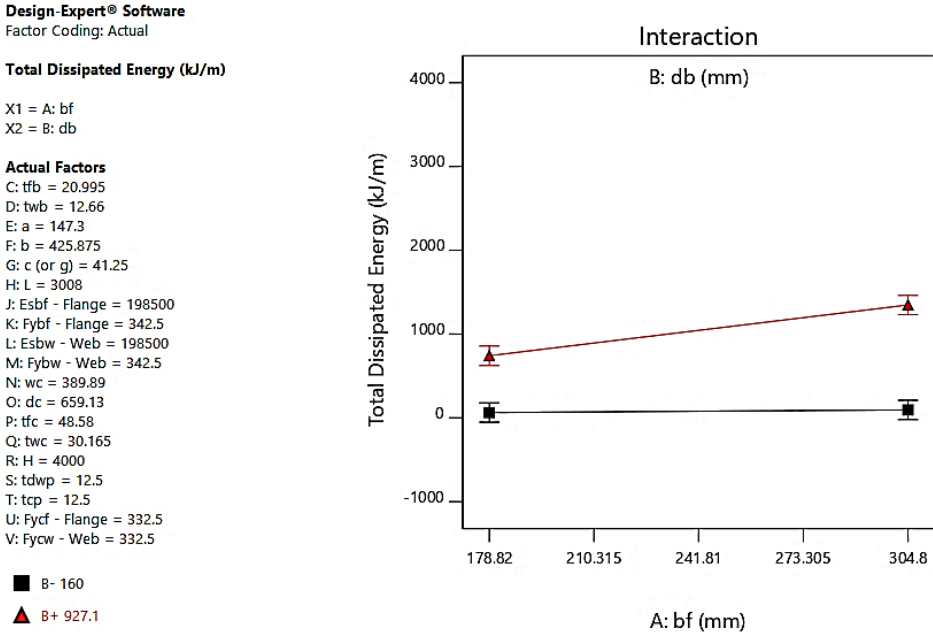


Figure 63: Plot of Marginal Means for Interaction AB in Selected Model for Response R1

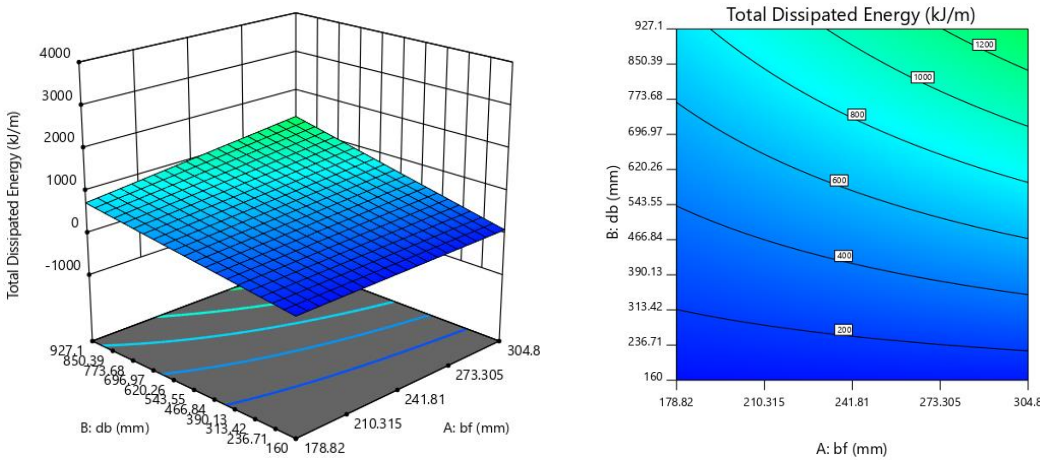


Figure 64: 3D Response Surface and Contour Plots for 2FI AB in Selected Model for Response R1

On the other hand, the 2FI interaction between factor A and C provides evidence that the total energy dissipation was increased at a lower rate (by 40.56%) with the increase in value of factor A (bf) at low-level value of factor C (tfb) as compared to the rate, it rise with the increase in value of factor A at high-level value of factor C (219.68%) as presented in **Figures 65 and 66**. In other words, factor C has an inverse relation with effect of factor A on total energy dissipation.

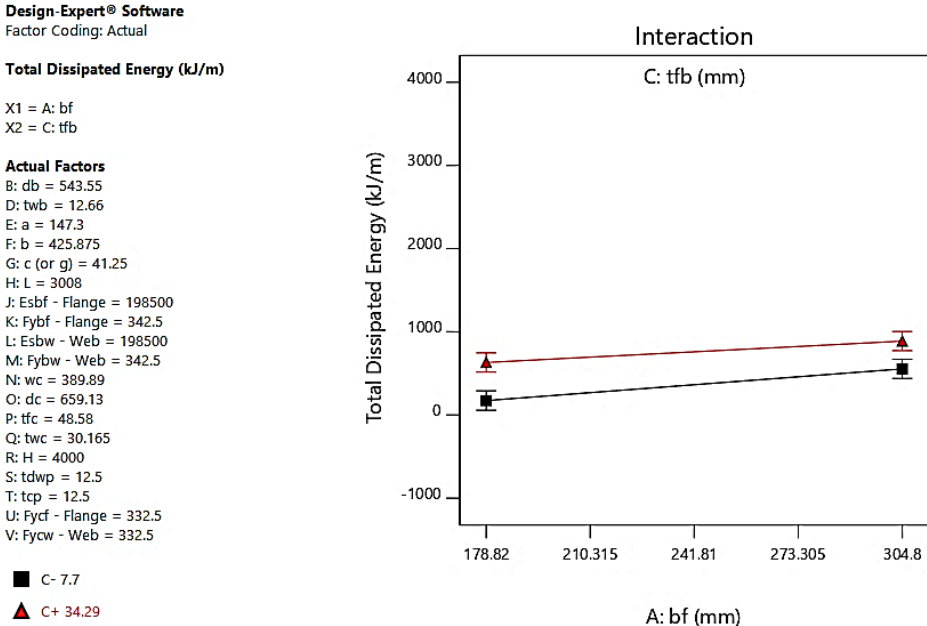


Figure 65: Plot of Marginal Means for Interaction AC in Selected Model for Response R1

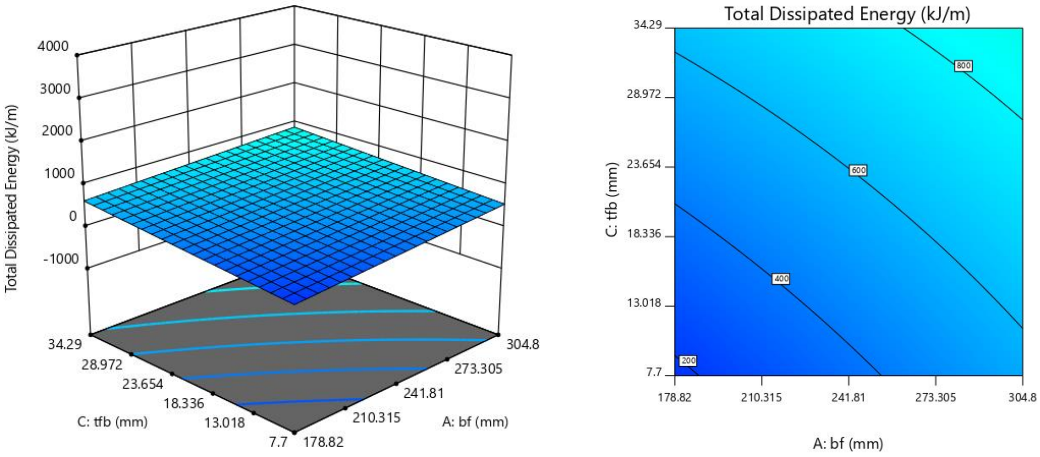


Figure 66: 3D Response Surface and Contour Plots for 2FI AC in Selected Model for Response R1

Interaction between factors A and D was found to be similar to but more sensitive than that of factors A and B, i.e. increase in value of factor A resulted in an increase in the total dissipated energy by 150% at a high-level value of factor D while this rate was decreased to 4.34% for a rise in total dissipated energy with a rise in the value of factor A from low-level to high-level as shown in **Figures 67** and **68**.

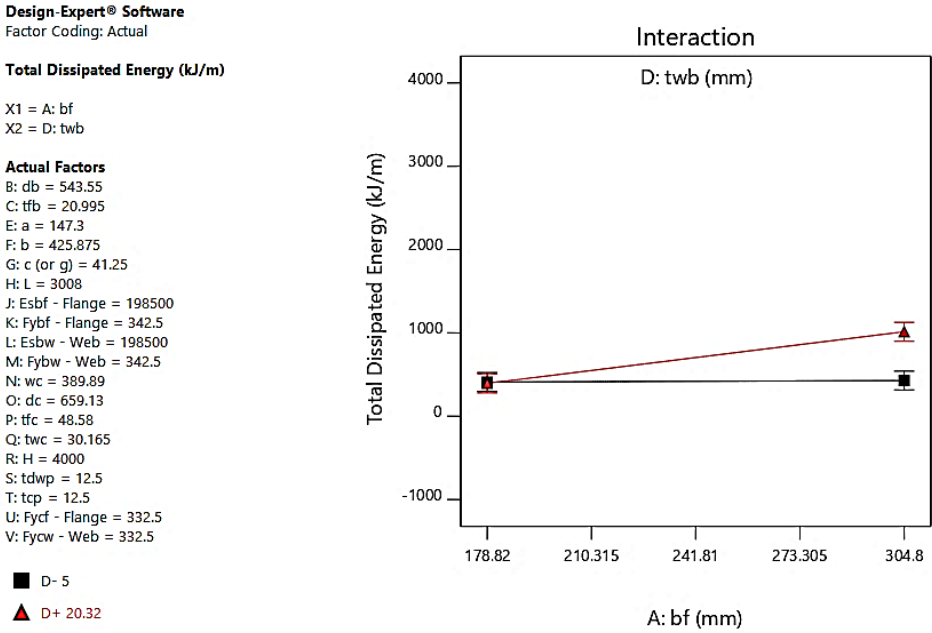


Figure 67: Plot of Marginal Means for Interaction AD in Selected Model for Response R1

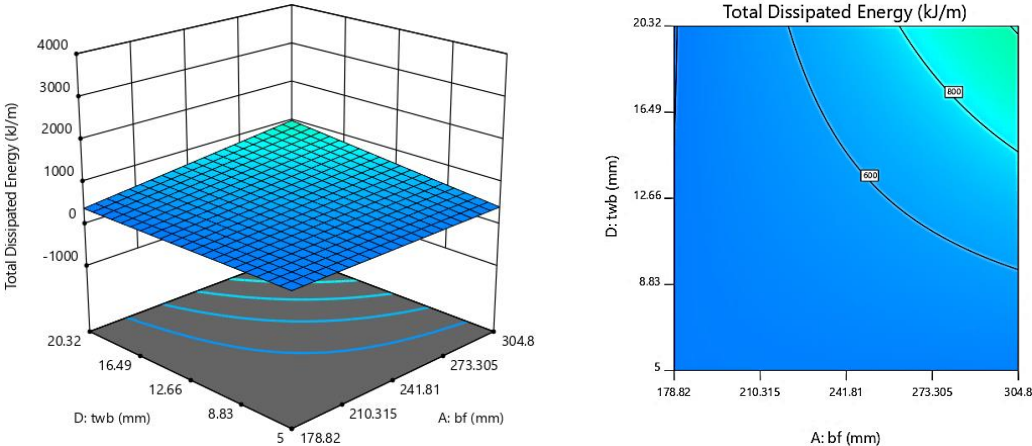


Figure 68: 3D Response Surface and Contour Plots for 2FI AD in Selected Model for Response R1

The interaction AQ in **Figures 69** and **70** had shown a direct relation of value of factor Q (twc) on the effect of value of factor A on total dissipated energy as increasing the value of factor A from low-level to high-level increases total dissipated energy by 6.96% at low-level value of factor Q and by 243.45% at high-level value of factor Q.

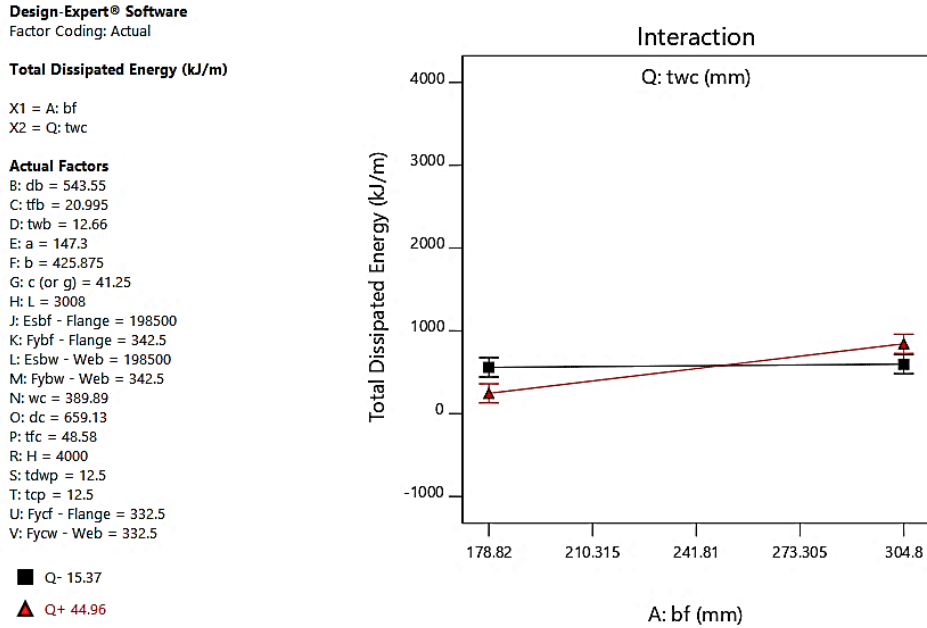


Figure 69: Plot of Marginal Means for Interaction AQ in Selected Model for Response R1

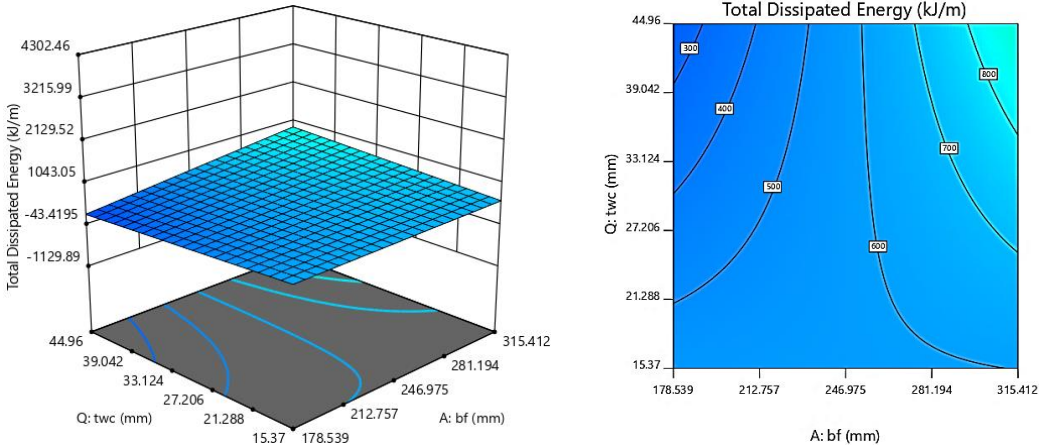


Figure 70: 3D Response Surface and Contour Plots for 2FI AQ in Selected Model for Response R1

The 2FI of factor A and U as illustrated in **Figures 71** and **72** shows a direct relation of factor U (Fycf) to the effect of value of factor A on total dissipated energy. Increase in the value of factor A has increased total dissipated energy by 8.40% at low-level value of factor E and this value was increased to 226.65% at high-level value of factor E.

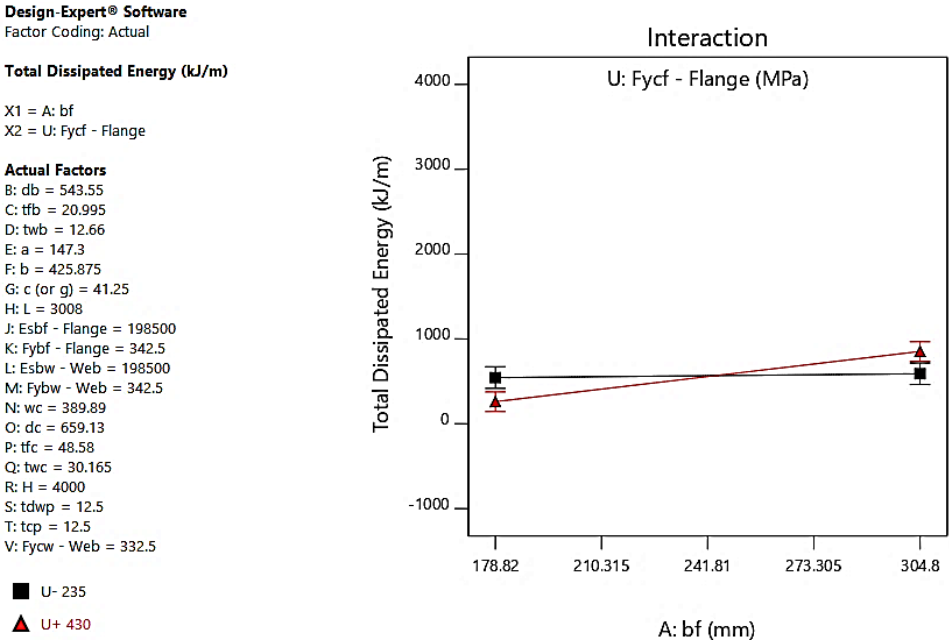


Figure 71: Plot of Marginal Means for Interaction AU in Selected Model for Response R1

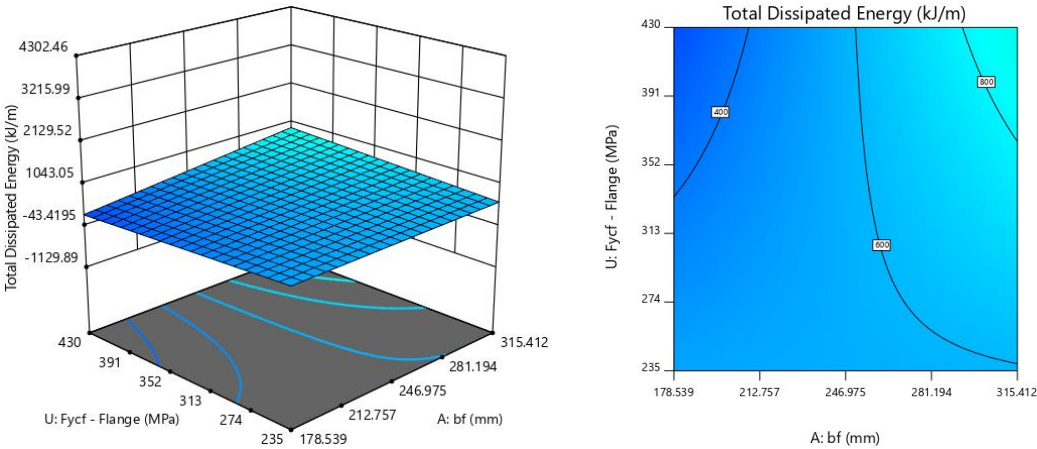


Figure 72: 3D Response Surface and Contour Plots for 2FI AU in Selected Model for Response R1

Also, the interactions BC and BD suggested that direct relation of total dissipated energy to value of factor A is influenced positively by values of C and D as shown in **Figures 73** and **76**. The increase in total dissipated energy with increase in value of factor B (db) was observed to be 1341.38% and 2879.46% for low- and high-level values of factor C and 1017.45% and 1813.59% for low- and high-level values of factor D respectively.

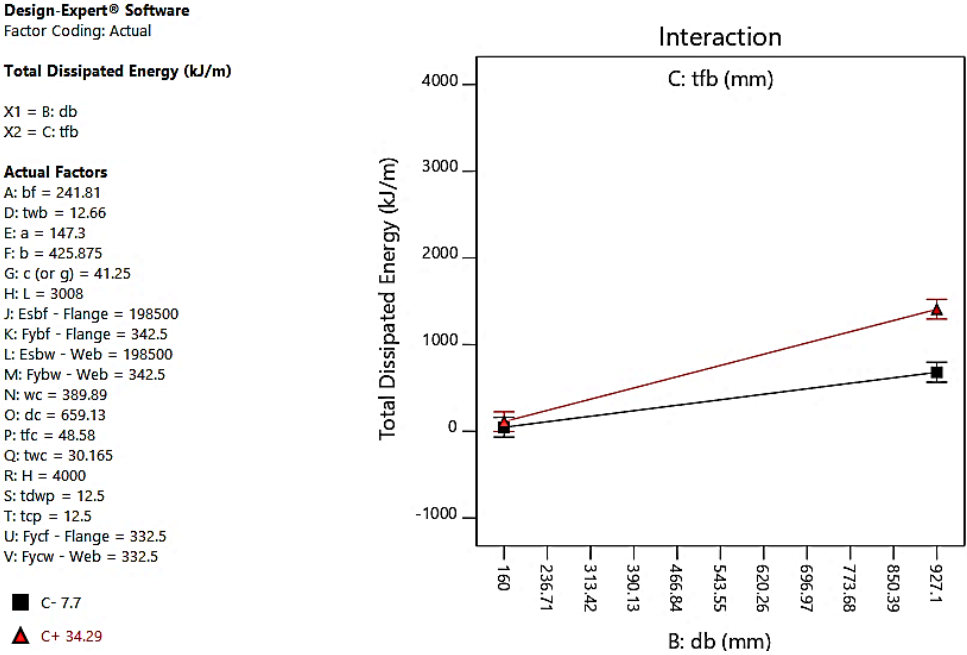


Figure 73: Plot of Marginal Means for Interaction BC in Selected Model for Response R1

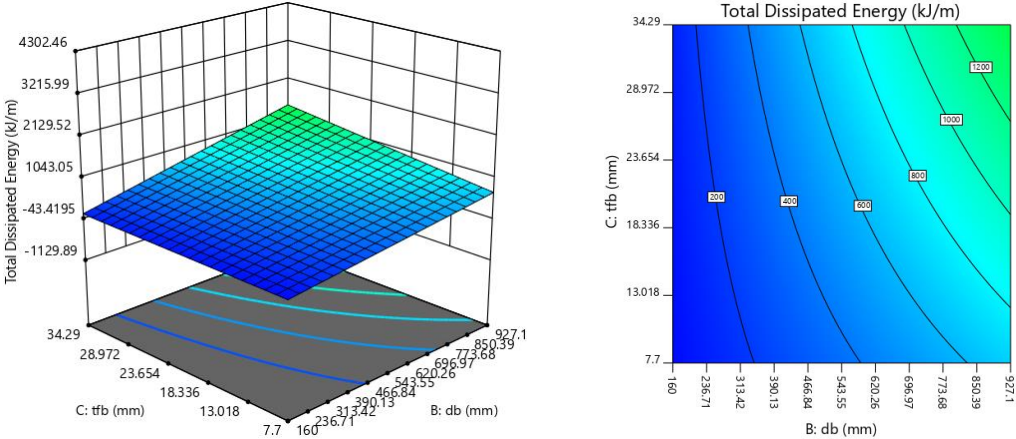


Figure 74: 3D Response Surface and Contour Plots for 2FI BC in Selected Model for Response R1

Design-Expert® Software
Factor Coding: Actual

Total Dissipated Energy (kJ/m)

X1 = B: db
X2 = D: twb

Actual Factors

A: bf = 241.81
C: tfb = 20.995
E: a = 147.3
F: b = 425.875
G: c (or g) = 41.25
H: L = 3008
J: Esbf - Flange = 198500
K: Fybf - Flange = 342.5
L: Esbw - Web = 198500
M: Fybw - Web = 342.5
N: wc = 389.89
O: dc = 659.13
P: tfc = 48.58
Q: twc = 30.165
R: H = 4000
S: tdwp = 12.5
T: tcp = 12.5
U: Fycf - Flange = 332.5
V: Fycw - Web = 332.5

■ D- 5
▲ D+ 20.32

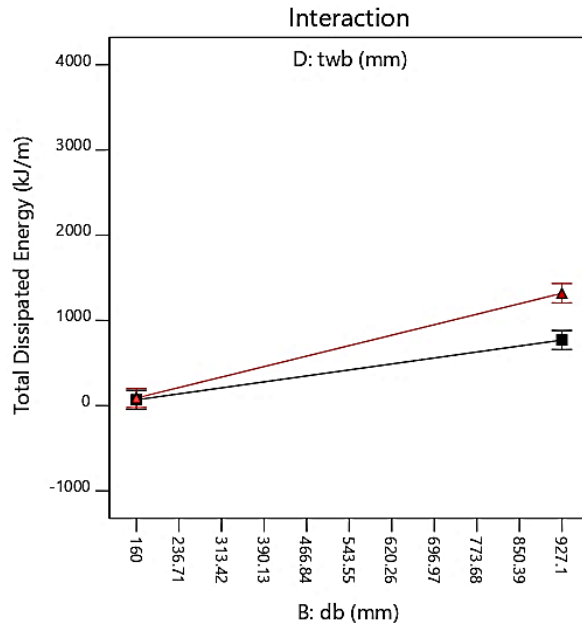


Figure 75: Plot of Marginal Means for Interaction BD in Selected Model for Response R1

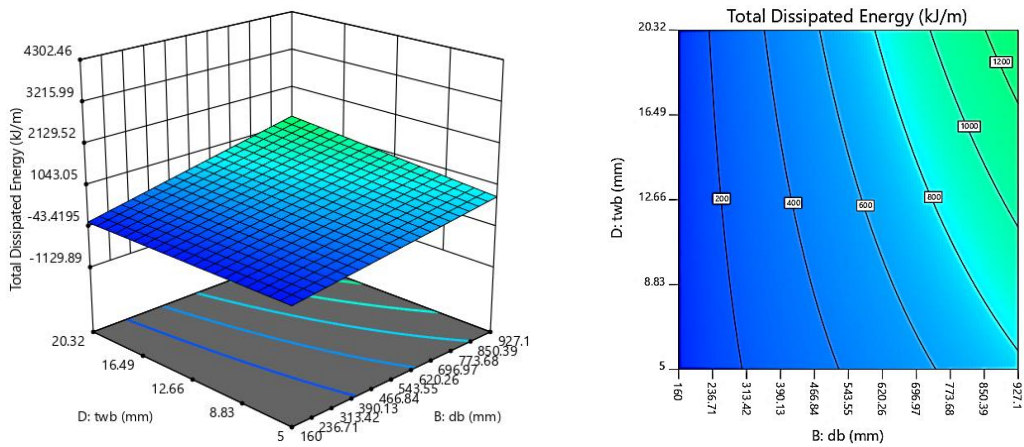


Figure 76: 3D Response Surface and Contour Plots for 2FI BD in Selected Model for Response R1

5.2.2. For Response Variable R2 (Initial Stiffness)

The selected model for response variable R2 had an R² value of 0.91 and can be written as:

$$R2 = \beta_0 + \beta_1 B + \beta_2 C + \beta_3 D + \beta_4 H + \beta_5 M + \beta_6 BC + \beta_7 BD$$

Where values of all β are given in **Table 16**.

Table 16: Coefficients of Model for Response R2

Coefficient	Value	Coefficient	Value
β_0	124679.3312	β_4	-14797.51035
β_1	114669.6962	β_5	15713.14532
β_2	24885.36107	β_6	22097.09506
β_3	30867.65431	β_7	30440.64194

It is evident from the half-normal probability plot and Pareto chart as presented in **Figures 77** and **78**, that similar to model 1, B is the most significant factor for regression model 2 as well with a total contribution of 71.53%. A graphical representation of the percentage contribution of factors in the initial stiffness is presented in **Figure 79**.

Initial Stiffness

Shapiro-Wilk test
 W-value = 0.960
 p-value = 0.184

- A: bf
- B: db
- C: tfb
- D: twb
- E: a
- F: b
- G: c (or g)
- H: L
- J: Esbf - Flange
- K: Fybf - Flange
- L: Esbw - Web
- M: Fybw - Web
- N: wc
- O: dc
- P: tfc
- Q: twc
- R: H
- S: tdwp
- T: tcp
- U: Fycf - Flange
- V: Fycw - Web

- Positive Effects
- Negative Effects

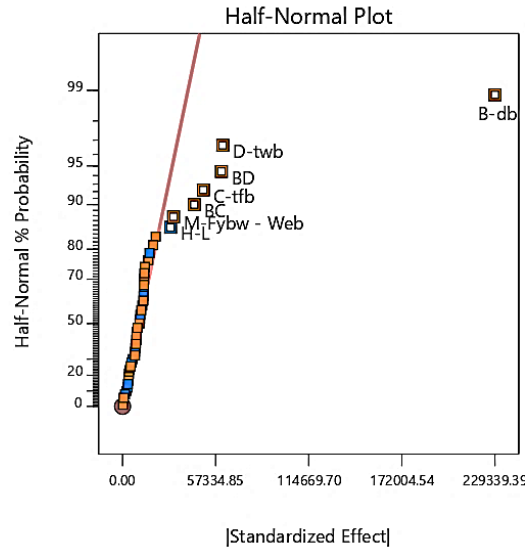


Figure 77: Half-Normal Probability Plot for Response R2 (Initial Stiffness)

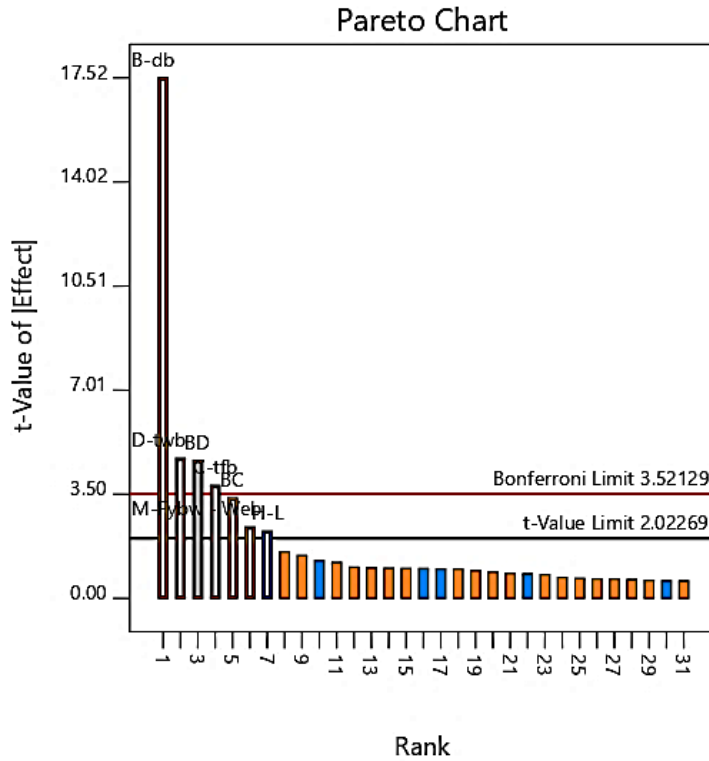


Figure 78: Pareto Chart for Response R2 (Initial Stiffness)

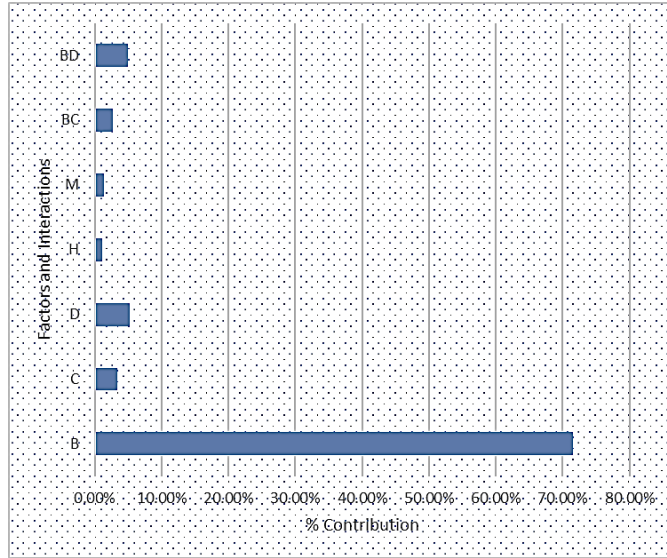


Figure 79: Percentage Contributions of Factors and Interactions on Response R2

ANOVA for model 2 (R2) as shown in **Table 17** verified factor B as the most significant one with an F-value of 307.109.

Table 17: ANOVA of Selected Model for Response R2

SOURCE	SUM OF SQUARES	df	MEAN SQUARE	F-VALUE	P-VALUE	
Block	81135099.13	1	81135099.13			
Model	7.69758E+11	7	1.09965E+11	54.91498	0.00000	Significant
B-db	6.14975E+11	1	6.14975E+11	307.10861	0.00000	
C-tfb	28963305137	1	28963305137	14.46380	0.00050	
D-twb	44562288160	1	44562288160	22.25368	0.00003	
H-L	10240886003	1	10240886003	5.11413	0.02954	
M-Fybw - Web	11547460384	1	11547460384	5.76661	0.02133	
BC	22836555300	1	22836555300	11.40421	0.00170	
BD	43337897739	1	43337897739	21.64224	0.00004	
Residual	76093780146	38	2002467899			
Cor Total	8.45933E+11	46				

Similar to response R1, interactions between main factors BC and BD show that effect of factor B (db) on initial stiffness is directly affected by factors C and D as the initial stiffness increases with rise of value of factor B from low- to high-level

by 2563.86% and 3865.05% for low- and high-level values of factor C and by 1757.96% and 3037.52% for low- and high-level values of factor D respectively as depicted in **Figures 80 through 83**.

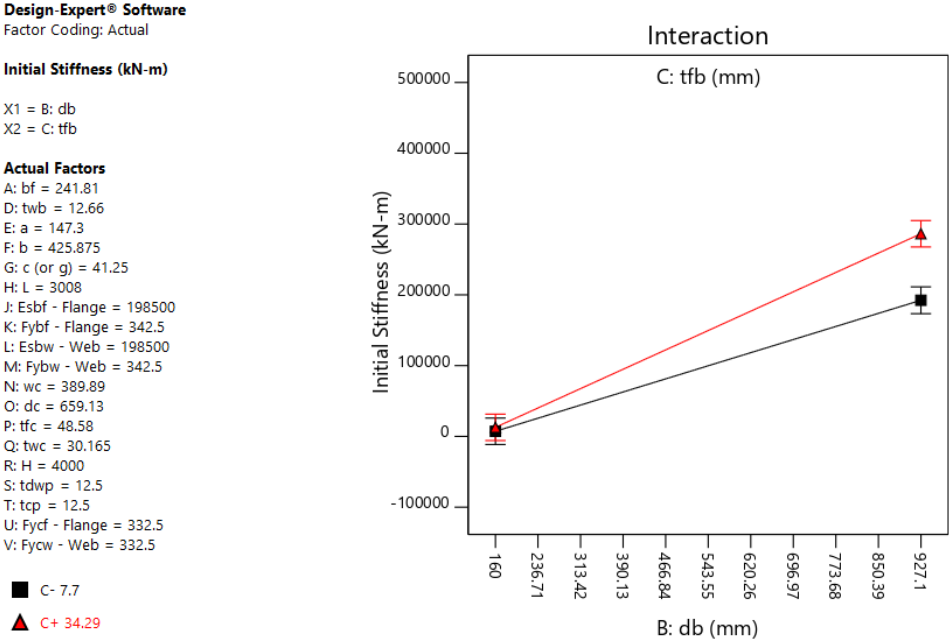


Figure 80: Plot of Marginal Means for Interaction BC in Selected Model for Response R2

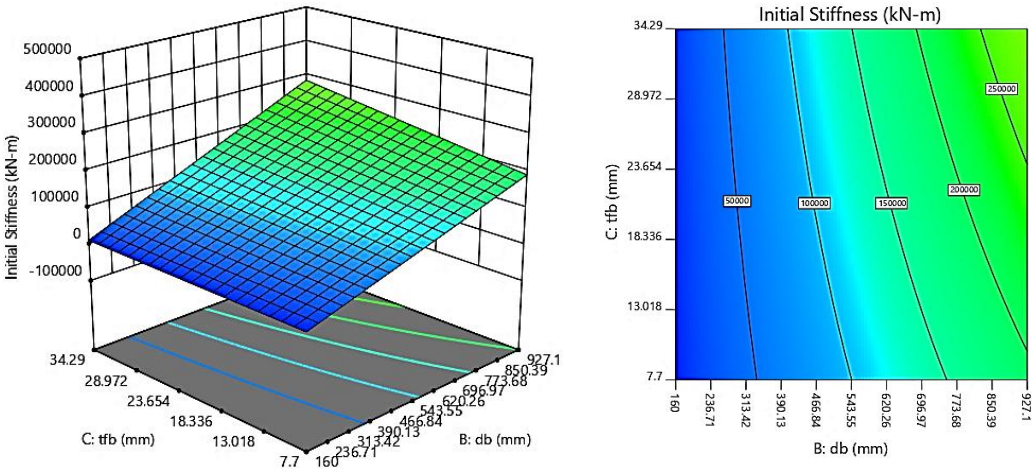


Figure 81: 3D Response Surface and Contour Plots for 2FI BC in Selected Model for Response R2

Design-Expert® Software
Factor Coding: Actual

Initial Stiffness (kN-m)

X1 = B: db
X2 = D: twb

Actual Factors

A: bf = 241.81
C: tfb = 20.995
E: a = 147.3
F: b = 425.875
G: c (or g) = 41.25
H: L = 3008
J: Esbf - Flange = 198500
K: Fybf - Flange = 342.5
L: Esbw - Web = 198500
M: Fybw - Web = 342.5
N: wc = 389.89
O: dc = 659.13
P: tfc = 48.58
Q: twc = 30.165
R: H = 4000
S: tdwp = 12.5
T: tcp = 12.5
U: Fycf - Flange = 332.5
V: Fycw - Web = 332.5

■ D- 5
▲ D+ 20.32

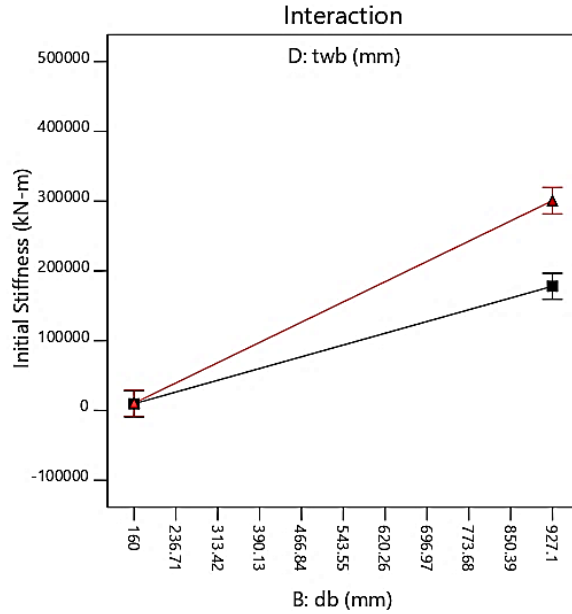


Figure 82: Plot of Marginal Means for Interaction BD in Selected Model for Response R2

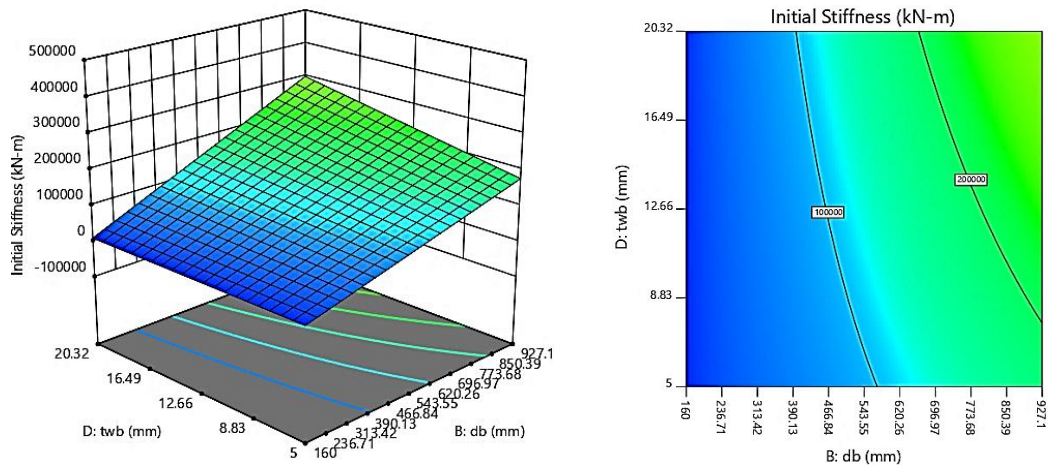


Figure 83: 3D Response Surface and Contour Plots for 2FI BD in Selected Model for Response R2

5.2.3. For Response Variable R3 (Strength Degradation Rate)

The coded model selected for response variable R3 with an R² value of 0.9163 can be written as:

$$\begin{aligned}
 R3 = & \beta_0 + \beta_1A + \beta_2B + \beta_3C + \beta_4D + \beta_5E + \beta_6F + \beta_7G + \beta_8H + \beta_9J + \beta_{10}K \\
 & + \beta_{11}L + \beta_{12}N + \beta_{13}O + \beta_{14}P + \beta_{15}Q + \beta_{16}R + \beta_{17}AB \\
 & + \beta_{18}AD + \beta_{19}AE + \beta_{20}AF + \beta_{21}AJ + \beta_{22}AK + \beta_{23}AL + \beta_{24}AN \\
 & + \beta_{25}AQ + \beta_{26}AR + \beta_{27}BE + \beta_{28}ABE
 \end{aligned}$$

Where values of all β are given in **Table 18**.

Table 18: Coefficients of Model for Response R3

Coefficient	Value	Coefficient	Value
β_0	0.993	β_{15}	-0.0381
β_1	0.016	β_{16}	-0.0321
β_2	-0.038	β_{17}	0.0166
β_3	0.051	β_{18}	0.0284
β_4	0.006	β_{19}	-0.0069
β_5	-0.001	β_{20}	0.0395
β_6	-0.023	β_{21}	0.0358
β_7	0.032	β_{22}	0.0507
β_8	-0.032	β_{23}	0.0527
β_9	-0.056	β_{24}	-0.0210
β_{10}	-0.066	β_{25}	0.0169
β_{11}	-0.031	β_{26}	0.0542
β_{12}	-0.001	β_{27}	-0.0490
β_{13}	0.024	β_{28}	0.0292
β_{14}	-0.023		

The analysis of this model suggested that strength degradation rate of the connection does not exhibit a behaviour that can be attributed as sensitive towards just a single factor, however, the most significant factor in this scenario was found to be yield strength of beam flange material i.e. factor K as can be observed through half-normal plot (**Figure 84**) and Pareto chart (**Figure 85**) with a total contribution of 10.18% and an F-value of 28.18, but we can see here that 2FI of factors A & L (AL), Single Factor J, 2FIs of factors B & E (BE) and A & R (AR) and Single

Factor C are not that far behind with a contribution of 8.30%, 7.34%, 7.19%, 6.78%, 6.6% as shown in Figure 86 and F-values of 22.96, 20.31, 19.89, 18.76 and 18.27 respectively in Table 19 and the percentage contributions of factors in the response variable R3 (Strength Degradation Rate) is depicted in **Figure 86**.

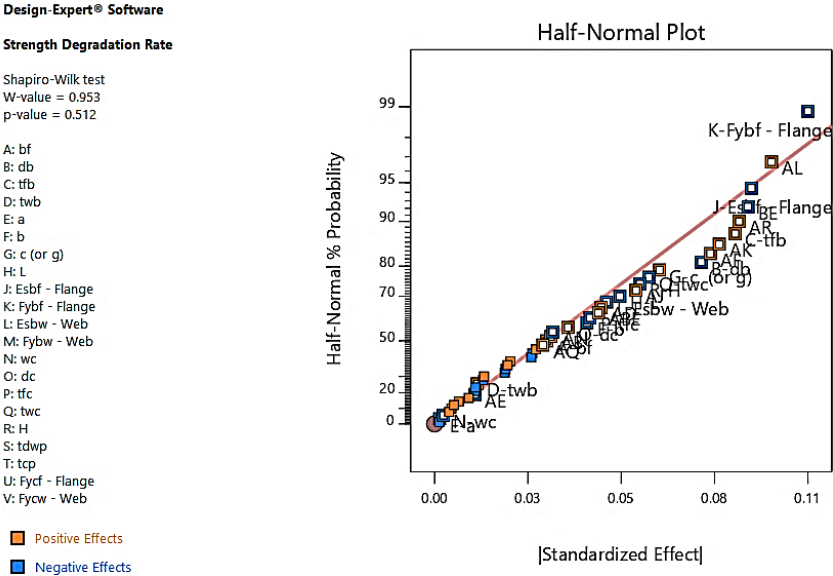


Figure 84: Half-Normal Probability Plot for Response R3 (Strength Degradation Rate)

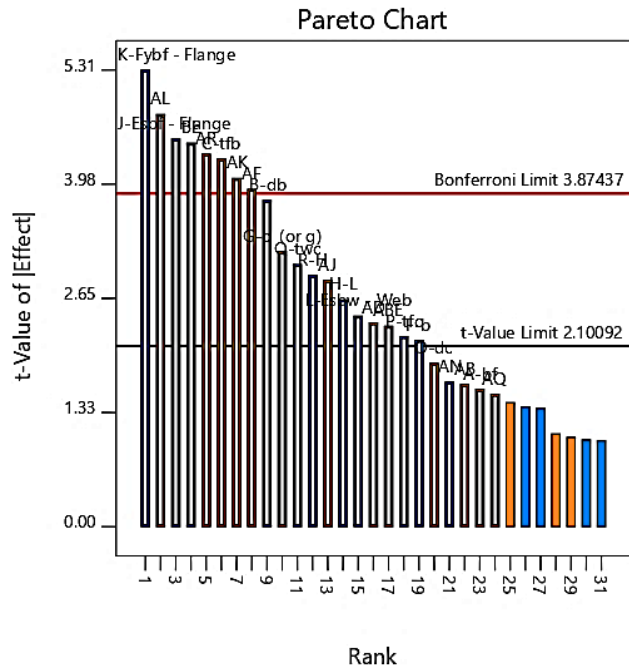


Figure 85: Pareto Chart for Response R3 (Strength Degradation Rate)

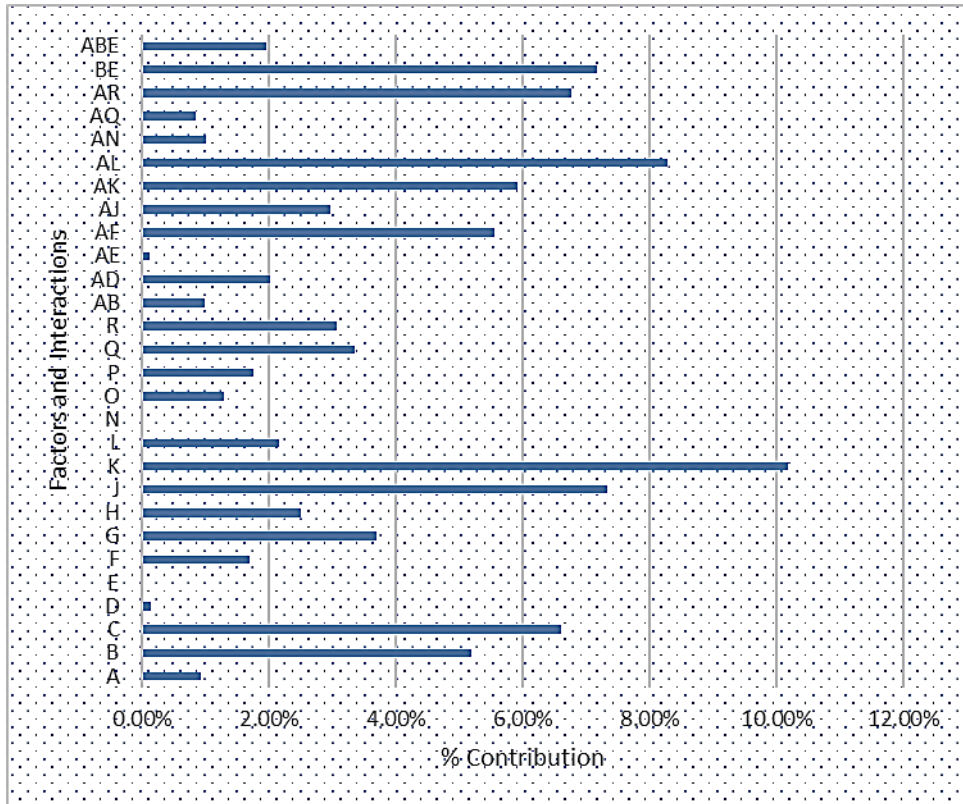


Figure 86: Percentage Contributions of Factors and Interactions on Response R3

It can be observed here that factors that contributed more than 5% i.e. B, C, J, K and 2FIs AF, AK, AL, AR and BE were considerably more influential than other factors as the difference between percentage contribution of the least significant factor amongst these (B: 5.2%) and the next most significant factor (G: 3.7%). The ANOVA shown in **Table 19** verifies this observation with a sudden drop in F-value from factor B (F-value: 14.39) to next most significant factor G (F-value: 10.23)

Table 19: ANOVA of Selected Model for Response R3

SOURCE	SUM OF SQUARES	df	MEAN SQUARE	F-VALUE	P-VALUE	
Block	0.01055	1	0.01055			
Model	0.85257	28	0.03045	6.64625	0.00008	Significant
A-bf	0.01168	1	0.01168	2.54956	0.12875	
B-db	0.06592	1	0.06592	14.38948	0.00145	
C-tfb	0.08370	1	0.08370	18.27045	0.00051	
D-twb	0.00168	1	0.00168	0.36742	0.55242	
E-a	0.00002	1	0.00002	0.00509	0.94395	
F-b	0.02150	1	0.02150	4.69346	0.04478	
G-c (or g)	0.04690	1	0.04690	10.23651	0.00525	
H-L	0.03182	1	0.03182	6.94446	0.01737	
J-Esbf - Flange	0.09303	1	0.09303	20.30536	0.00031	
K-Fybf - Flange	0.12912	1	0.12912	28.18285	0.00006	
L-Esbw - Web	0.02744	1	0.02744	5.98997	0.02555	
N-wc	0.00007	1	0.00007	0.01548	0.90244	
O-dc	0.01650	1	0.01650	3.60055	0.07488	
P-tfc	0.02238	1	0.02238	4.88499	0.04109	
Q-twc	0.04255	1	0.04255	9.28808	0.00728	
R-H	0.03907	1	0.03907	8.52721	0.00955	
AB	0.01251	1	0.01251	2.72976	0.11684	
AD	0.02574	1	0.02574	5.61730	0.02988	
AE	0.00151	1	0.00151	0.32944	0.57351	
AF	0.07049	1	0.07049	15.38613	0.00110	
AJ	0.03755	1	0.03755	8.19679	0.01077	
AK	0.07510	1	0.07510	16.39256	0.00083	
AL	0.10520	1	0.10520	22.96297	0.00017	
AN	0.01292	1	0.01292	2.82045	0.11135	
AQ	0.01086	1	0.01086	2.36940	0.14214	
AR	0.08597	1	0.08597	18.76421	0.00045	
BE	0.09111	1	0.09111	19.88623	0.00034	
ABE	0.02489	1	0.02489	5.43360	0.03232	
Residual	0.07788	17	0.00458			
Cor Total	0.94100	46				

The interaction of factors A and F shows that for low-level value of factor F (b), strength degradation rate was decreased by 4.51% as factor A was increased from low-level value to high-level value but the effect of high-level value of factor F is

opposite on the relation of factor A to SDR i.e. response R3 as it was increased with the rise in value of factor A from low- to high-level value by 12.16% as shown in **Figures 87** and **88**. It can be observed here that the effect of factor A on the response is more sensitive to higher value of factor F.

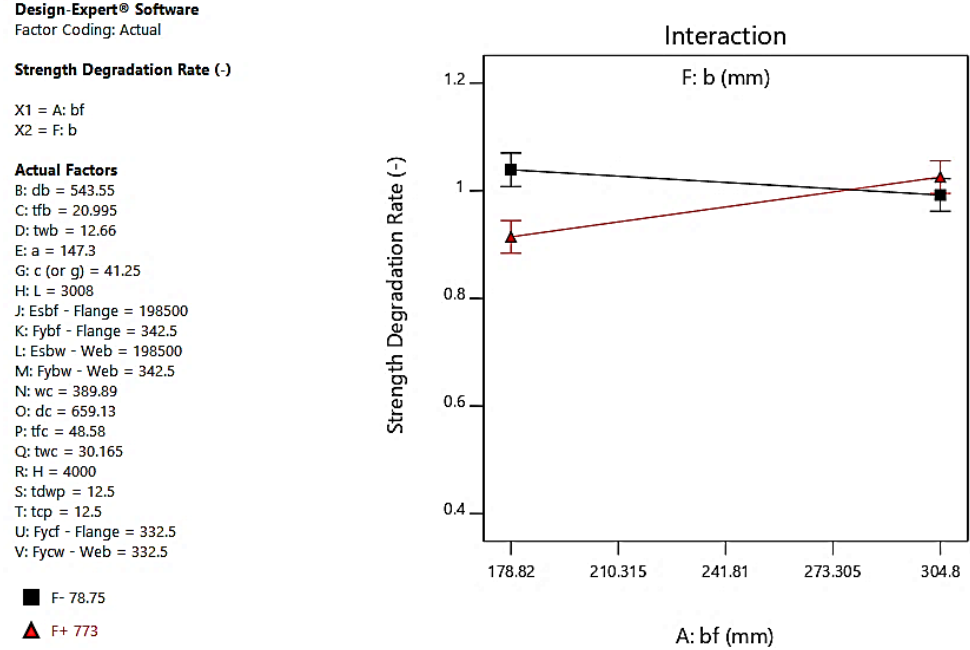


Figure 87: Plot of Marginal Means for Interaction AF in Selected Model for Response R3

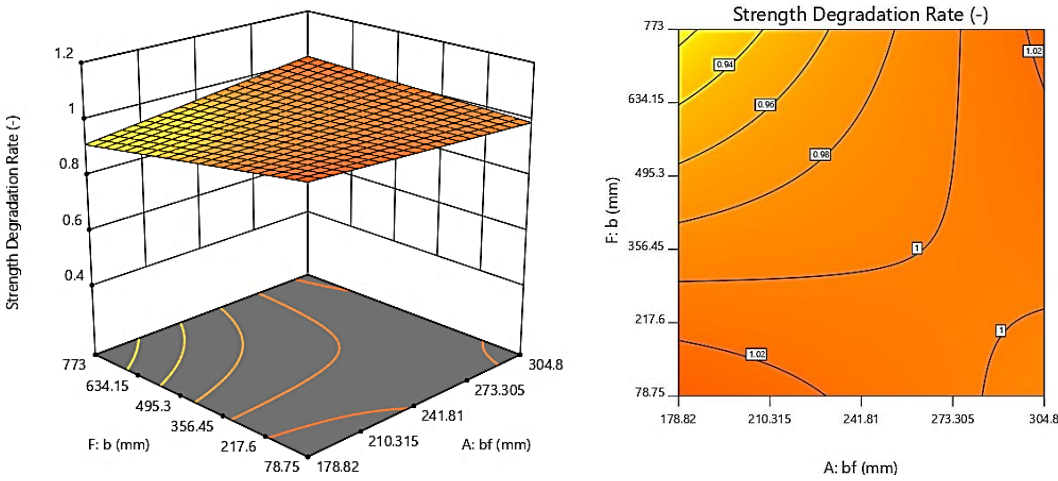


Figure 88: 3D Response Surface and Contour Plots for 2FI AF in Selected Model for Response R3

Effect of factor K (Fybf) on strength degradation rate in interaction with factor A represented in **Figures 89** and **90** suggested that at low-level value of factor K, increase in values of factor A decreased the SDR by 6.32% while for high-level value of K factor, the scenario was reversed as the SDR increased by 15.53% with the increase in value of factor A from low- to high-level.

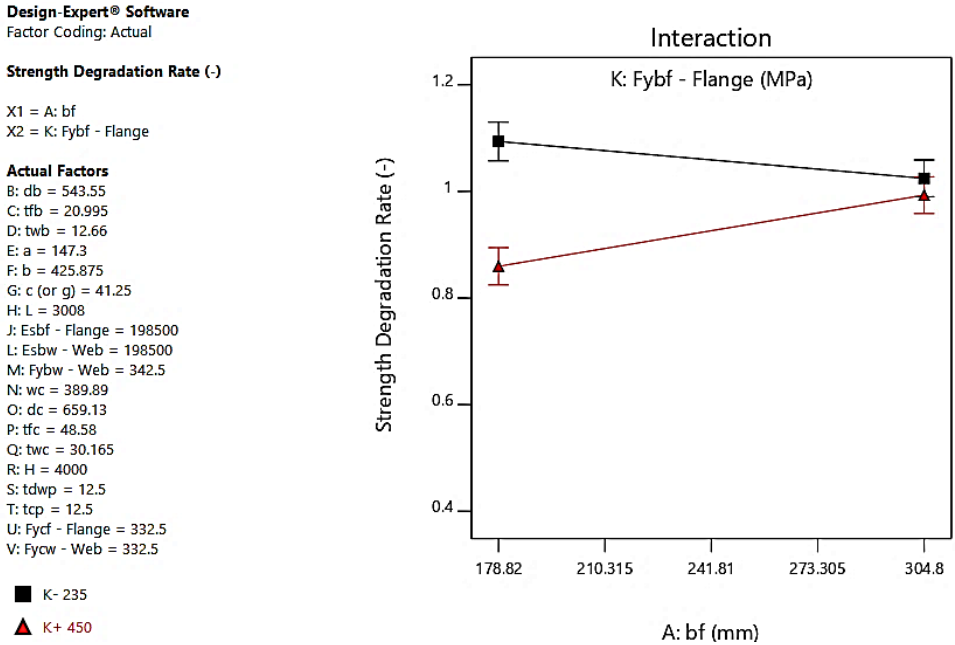


Figure 89: Plot of Marginal Means for Interaction AK in Selected Model for Response R3

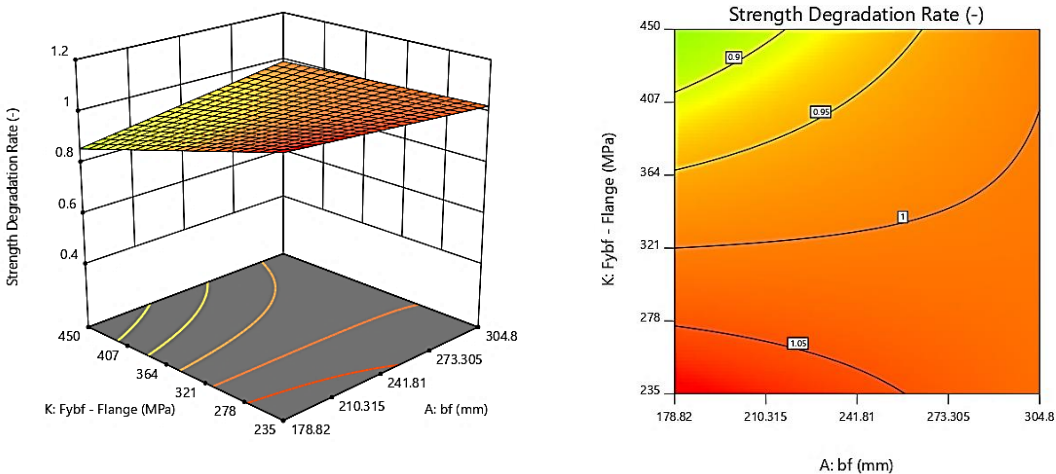


Figure 90: 3D Response Surface and Contour Plots for 2FI AK in Selected Model for Response R3

The 2FIs of AL and AR exhibited similar behaviour as for low-level values of L and R, the SDR dropped with the rise in the value of A from low-level to high-level by 6.9% and 7.17% respectively, while for the high-level values of L and R, the response became directly proportional to value of factor A and increased by 15.39% and 15.79% respectively as shown in **Figures 91** through **94**.

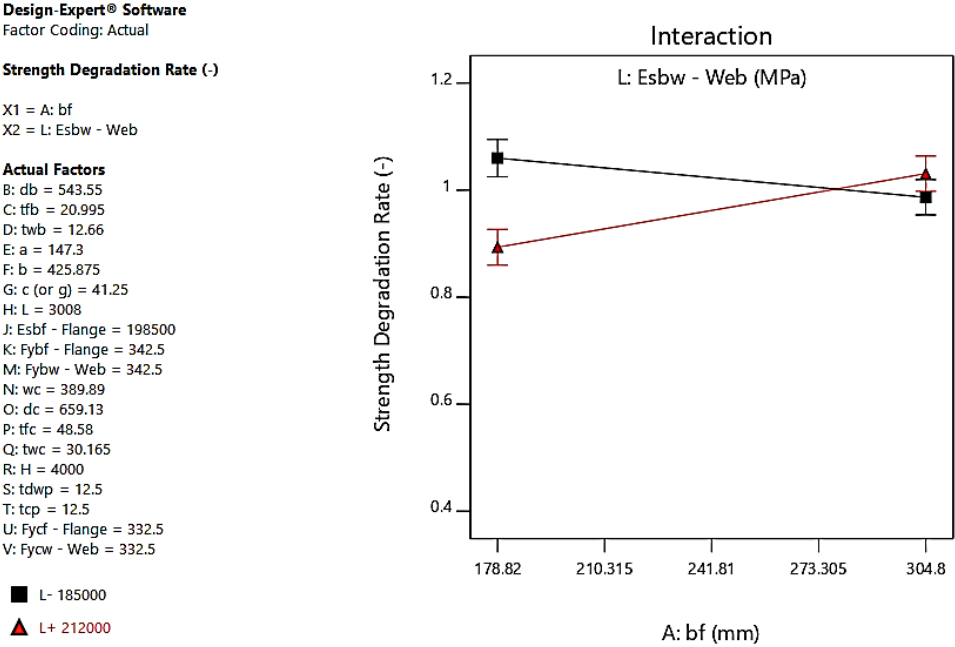


Figure 91: Plot of Marginal Means for Interaction AL in Selected Model for Response R3

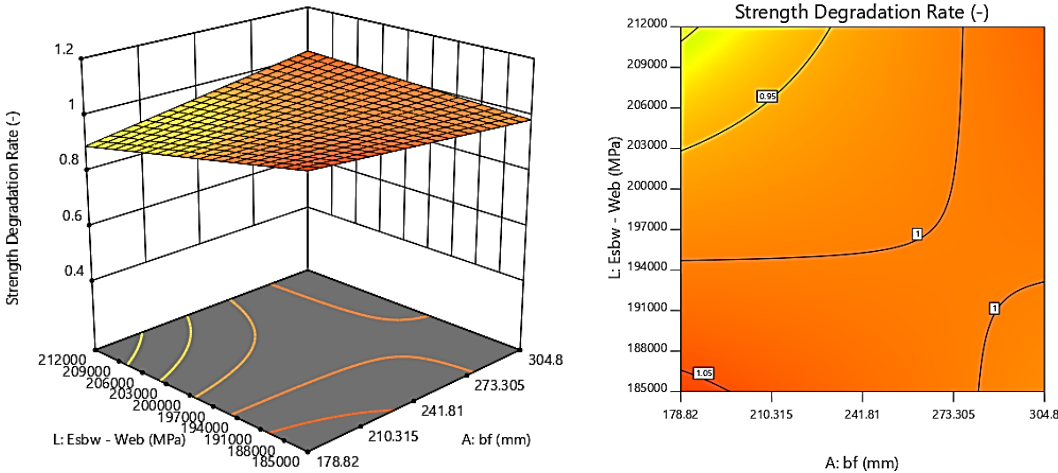


Figure 92: 3D Response Surface and Contour Plots for 2FI AL in Selected Model for Response R3

Design-Expert® Software
Factor Coding: Actual

Strength Degradation Rate (-)

X1 = A: bf
X2 = R: H

Actual Factors

- B: db = 543.55
- C: tfb = 20.995
- D: twb = 12.66
- E: a = 147.3
- F: b = 425.875
- G: c (or g) = 41.25
- H: L = 3008
- J: Esbf - Flange = 198500
- K: Fybf - Flange = 342.5
- L: Esbw - Web = 198500
- M: Fybw - Web = 342.5
- N: wc = 389.89
- O: dc = 659.13
- P: tfc = 48.58
- Q: twc = 30.165
- S: tdwp = 12.5
- T: tcp = 12.5
- U: Fycf - Flange = 332.5
- V: Fycw - Web = 332.5

- R- 3000
- ▲ R+ 5000

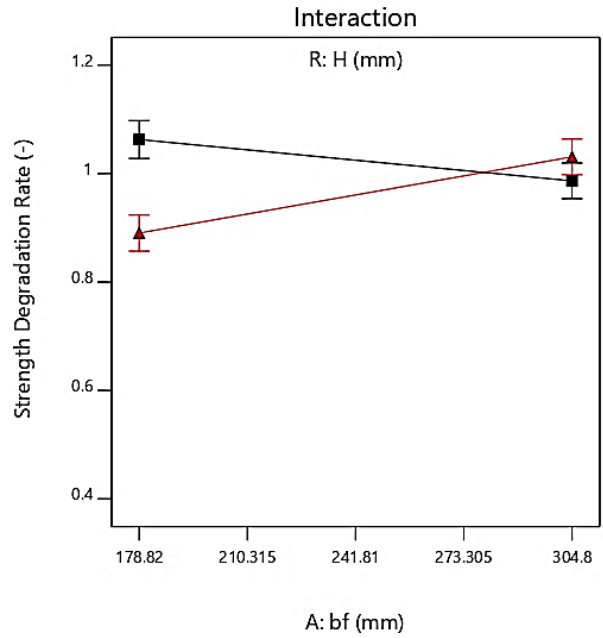


Figure 93: Plot of Marginal Means for Interaction AR in Selected Model for Response R3

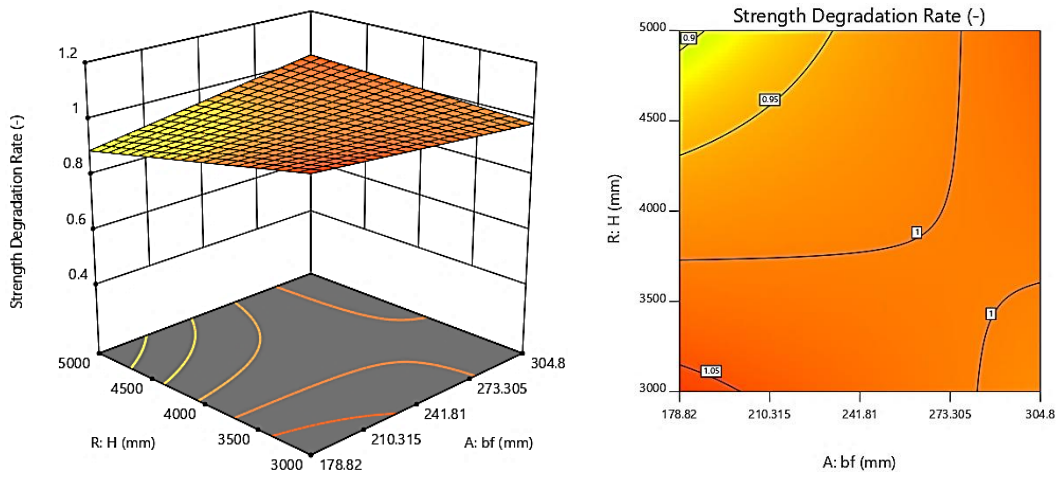


Figure 94: 3D Response Surface and Contour Plots for 2FI AR in Selected Model for Response R3

It was observed from the interaction of factors B and E that low-level value of E has lesser but direct effect on the relation of SDR to factor B as increasing the value of factor B from low- to high-level resulted in an increase in SDR by 2.20% while at high-level value of factor B poses reverse and more vigorous effect as SDR drops by 16.16% with an increase in value of factor B from low- to high-level as shown in **Figures 95** and **96** below.

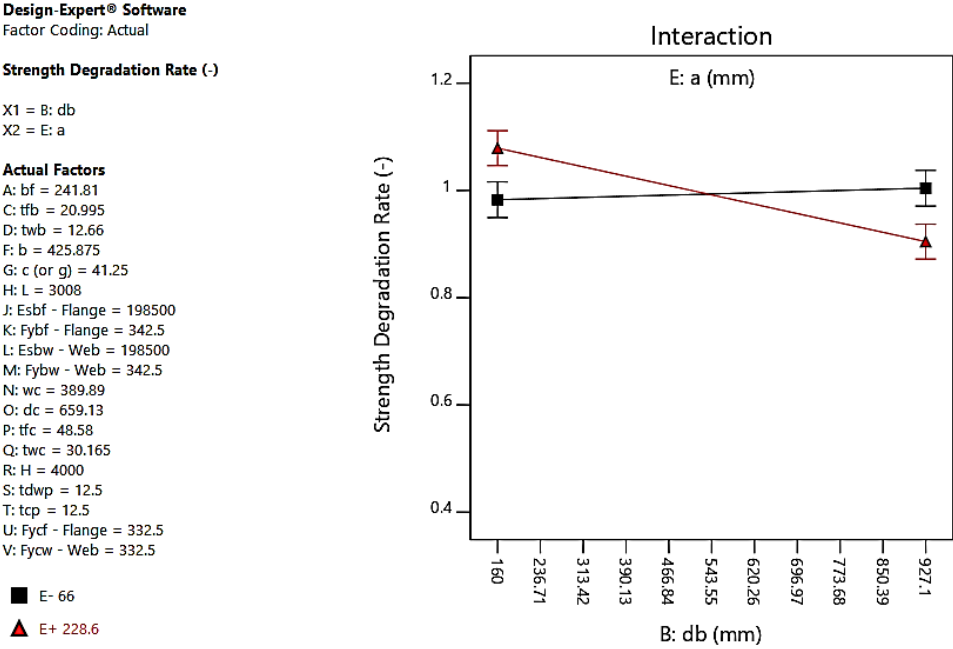


Figure 95: Plot of Marginal Means for Interaction BE in Selected Model for Response R3

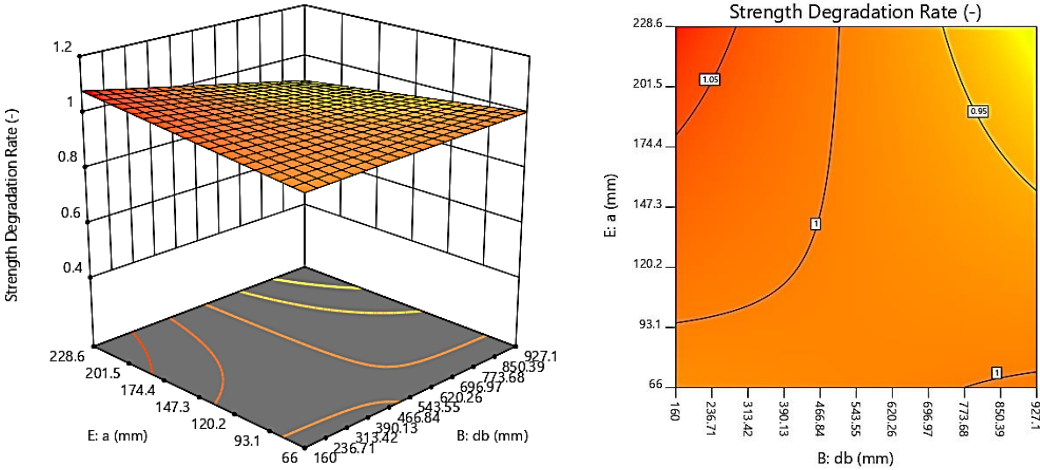


Figure 96: 3D Response Surface and Contour Plots for 2FI BE in Selected Model for Response R3

5.2.4. For Response Variable R4 (Maximum Moment Capacity)

The selected model for response variable R4 with an R² value of 0.915 can be written as a coded equation as follows:

$$R4 = \beta_0 + \beta_1A + \beta_2B + \beta_3C + \beta_4D + \beta_5F + \beta_6M + \beta_7O + \beta_8Q + \beta_9S \\ + \beta_{10}AQ + \beta_{11}AS + \beta_{12}BC + \beta_{13}BD$$

β values are provided in **Table 20**.

Table 20: Coefficients of Model for Response R4

Coefficient	Value	Coefficient	Value
β_0	1233.44	β_7	252.85
β_1	109.60	β_8	56.37
β_2	995.68	β_9	67.11
β_3	284.67	β_{10}	166.70
β_4	361.71	β_{11}	158.71
β_5	-195.48	β_{12}	223.39
β_6	265.87	β_{13}	326.88

The half-normal probability distribution plot for response R4 shows an acute sensitivity for maximum moment capacity towards factor B i.e. depth of beam as shown in **Figures 97** and **98** with a largest contribution of 54.68% towards the response as presented in **Figure 99**.

Design-Expert® Software

Max Moment Capacity

Shapiro-Wilk test
W-value = 0.976
p-value = 0.682

- A: bf
- B: db
- C: tfb
- D: twb
- E: a
- F: b
- G: c (or g)
- H: L
- J: Esbf - Flange
- K: Fybf - Flange
- L: Esbw - Web
- M: Fybw - Web
- N: wc
- O: dc
- P: tfc
- Q: twc
- R: H
- S: tdwp
- T: tcp
- U: Fycf - Flange
- V: Fycw - Web

- Positive Effects
- Negative Effects

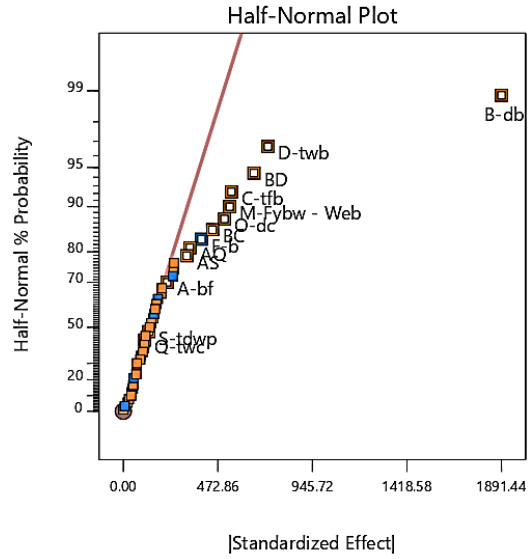


Figure 97: Half-Normal Probability Plot for Response R4 (Maximum Moment Capacity)

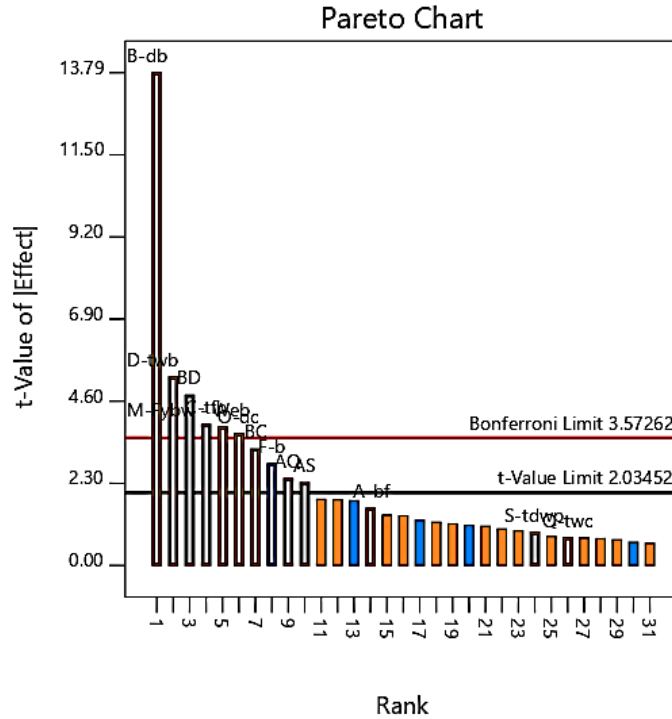


Figure 98: Pareto Chart for Response R4 (Maximum Moment Capacity)

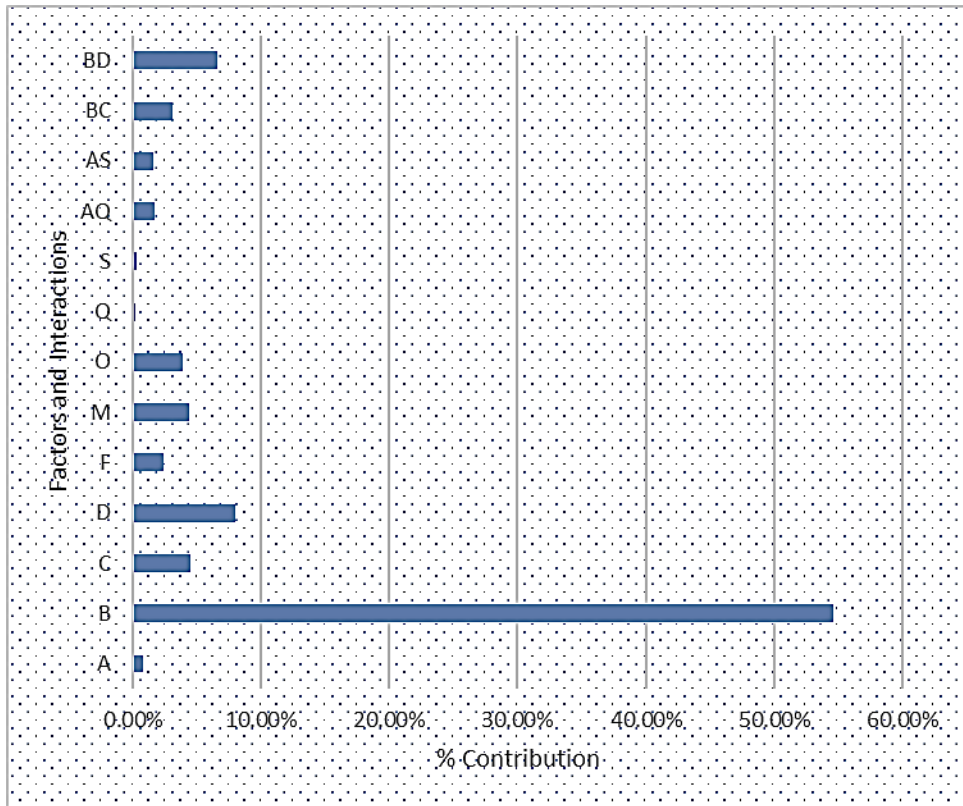


Figure 99: Percentage Contributions of Factors and Interactions on Response R4

It can be clearly observed here that B is the controlling factor in response R4 i.e. maximum moment capacity. An F-value of 190.287 for factor B in comparison to second highest F-value of 27.836 for factor D as shown in ANOVA **Table 21** verifies the distinctive influence of factor B on the response R4.

Table 21: ANOVA of Selected Model for Response R4

SOURCE	SUM OF SQUARES	df	MEAN SQUARE	F-VALUE	P-VALUE	
Block	5.608	1	5.608			
Model	76262618.559	13	5866355.274	26.790	0.000	significant
A-bf	559675.858	1	559675.858	2.556	0.120	
B-db	41667900.877	1	41667900.877	190.287	0.000	
C-tfb	3405979.708	1	3405979.708	15.554	0.000	
D-twb	6095414.145	1	6095414.145	27.836	0.000	
F-b	1780331.376	1	1780331.376	8.130	0.008	
M-Fybw - Web	3293279.511	1	3293279.511	15.040	0.000	
O-dc	2978556.945	1	2978556.945	13.602	0.001	
Q-twc	133560.632	1	133560.632	0.610	0.441	
S-tdwp	189293.224	1	189293.224	0.864	0.359	
AQ	1294579.785	1	1294579.785	5.912	0.021	
AS	1173534.231	1	1173534.231	5.359	0.027	
BC	2324811.014	1	2324811.014	10.617	0.003	
BD	4978039.390	1	4978039.390	22.733	0.000	
Residual	7007167.986	32	218974.000			
Cor Total	83269792.152	46				

The 2FI of factors B and D show that at factor D has a direct effect on the sensitivity of relation between maximum moment capacity and value of factor B. As it can be observed in **Figures 100** and **101**, at low-level value of factor D, the maximum moment capacity was increased by 659.17% as value of factor B was increased from low- to high-level value while this percentage was increased to 1337.84% for high-level value of factor D.

Design-Expert® Software
Factor Coding: Actual

Max Moment Capacity (kN-m)

X1 = B: db
X2 = D: twb

Actual Factors

- A: bf = 241.81
- C: tfb = 20.995
- E: a = 147.3
- F: b = 425.875
- G: c (or g) = 41.25
- H: L = 3008
- J: Esbf - Flange = 198500
- K: Fybf - Flange = 342.5
- L: Esbw - Web = 198500
- M: Fybw - Web = 342.5
- N: wc = 389.89
- O: dc = 659.13
- P: tfc = 48.58
- Q: twc = 30.165
- R: H = 4000
- S: tdwp = 12.5
- T: tcp = 12.5
- U: Fycf - Flange = 332.5
- V: Fycw - Web = 332.5

- D- 5
- ▲ D+ 20.32

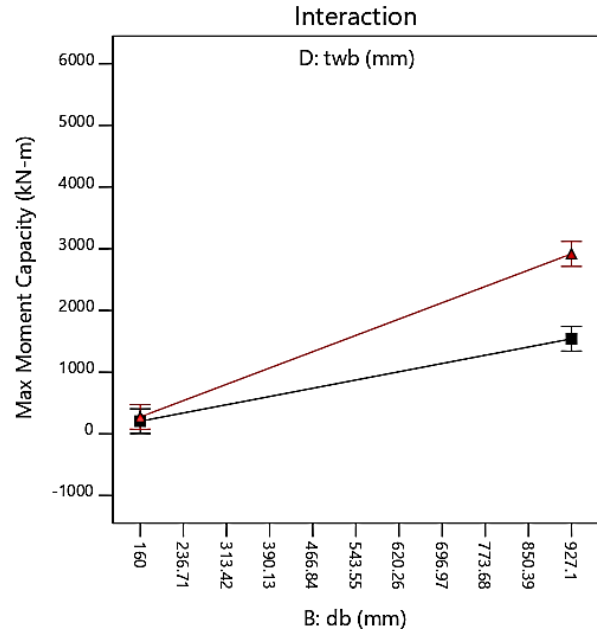


Figure 100: Plot of Marginal Means for Interaction BD in Selected Model for Response R4

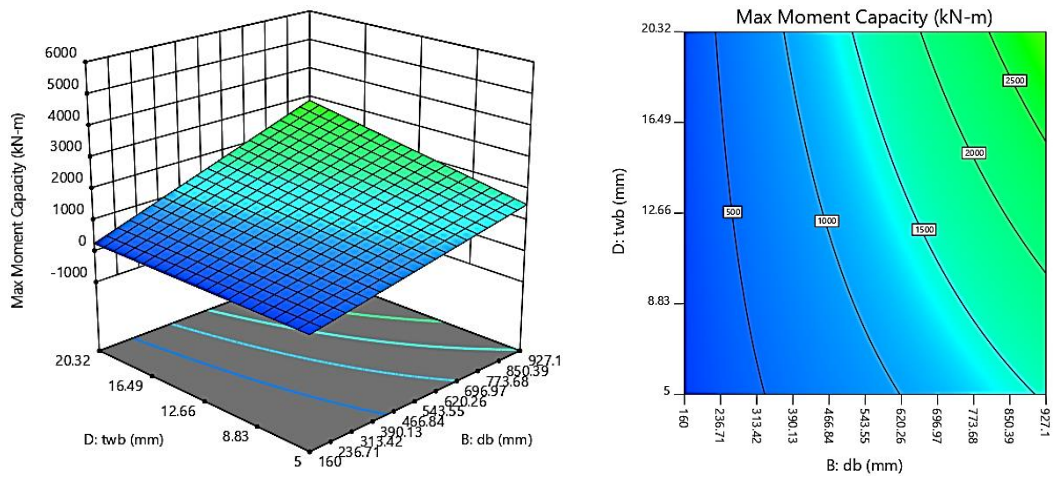


Figure 101: 3D Response Surface and Contour Plots for 2FI BD in Selected Model for Response R4

5.2.5. For Response Variable R5 (Rupture Index @ 7.5% Total Storey Drift)

The coded equation of selected model for response variable R5 with an R² value of 0.9069 is:

$$R5 = \beta_0 + \beta_1A + \beta_2B + \beta_3C + \beta_4D + \beta_5F + \beta_6G + \beta_7M + \beta_8N + \beta_9O + \beta_{10}P \\ + \beta_{11}Q + \beta_{12}T + \beta_{13}U + \beta_{14}AB + \beta_{15}AC + \beta_{16}AD + \beta_{17}AM + \beta_{18}AN \\ + \beta_{19}AO + \beta_{20}AP + \beta_{21}AQ + \beta_{22}AT + \beta_{23}BD + \beta_{24}ABD$$

Coefficient β values are presented in **Table 22**.

Table 22: Coefficients of Model for Response R5

Coefficient	Value	Coefficient	Value
β_0	4.29	β_{13}	1.83
β_1	-2.30	β_{14}	-2.62
β_2	5.60	β_{15}	-1.83
β_3	0.23	β_{16}	5.04
β_4	-2.28	β_{17}	-2.36
β_5	-2.45	β_{18}	-1.75
β_6	2.08	β_{19}	-2.41
β_7	3.067084	β_{20}	-1.10736
β_8	-0.0638	β_{21}	2.09657
β_9	5.045768	β_{22}	2.602347
β_{10}	1.274103	β_{23}	-2.67257
β_{11}	-1.21898	β_{24}	3.086337
β_{12}	-2.24715		

The half-normal probability distribution plot for response R5 suggest the significance of factors B and O and 2FI of factors A and D (AD) as can be observed from **Figures 102 and 103**.

Design-Expert® Software

Rupture Index @ 7.5% Total Storey Drift

Shapiro-Wilk test
W-value = 0.874
p-value = 0.011

- A: bf
- B: db
- C: tfb
- D: twb
- E: a
- F: b
- G: c (or g)
- H: L
- J: Esbf - Flange
- K: Fybf - Flange
- L: Esbw - Web
- M: Fybw - Web
- N: wc
- O: dc
- P: tfc
- Q: twc
- R: H
- S: tdwp
- T: tcp
- U: Fycf - Flange
- V: Fycw - Web

- Positive Effects
- Negative Effects

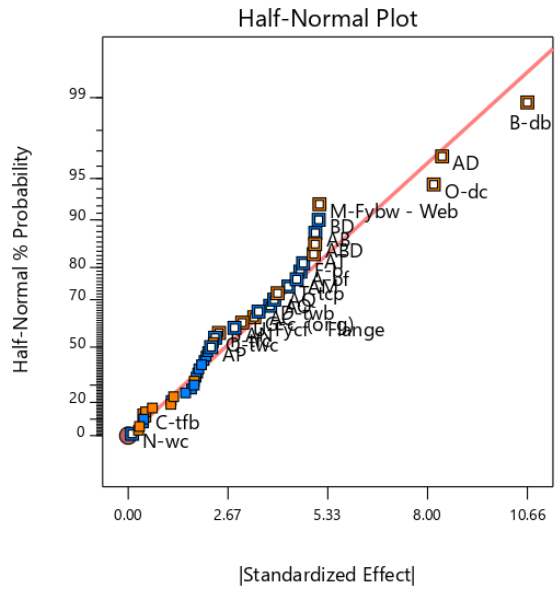


Figure 102: Half-Normal Probability Plot for Response R5 (Rupture Index @ 7.5% Total Storey Drift)

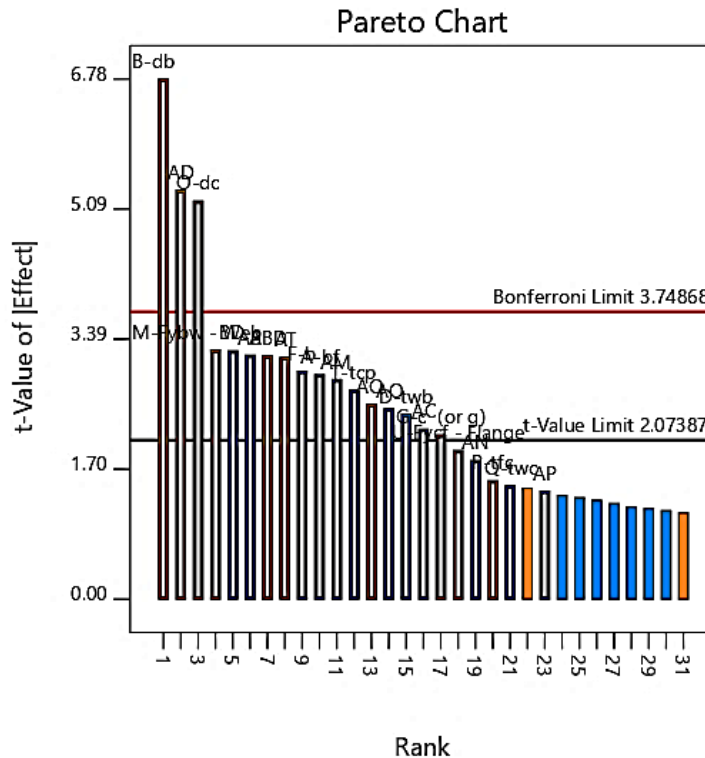


Figure 103: Pareto Chart for Response R5 (Rupture Index @ 7.5% Total Storey Drift)

It is evident that the most influential factor amongst these was factor B with a total contribution of 18.69% towards response R5 followed by 2FI AD and factor O with contributions of 11.56% and 10.95% respectively as depicted in **Figure 104**.

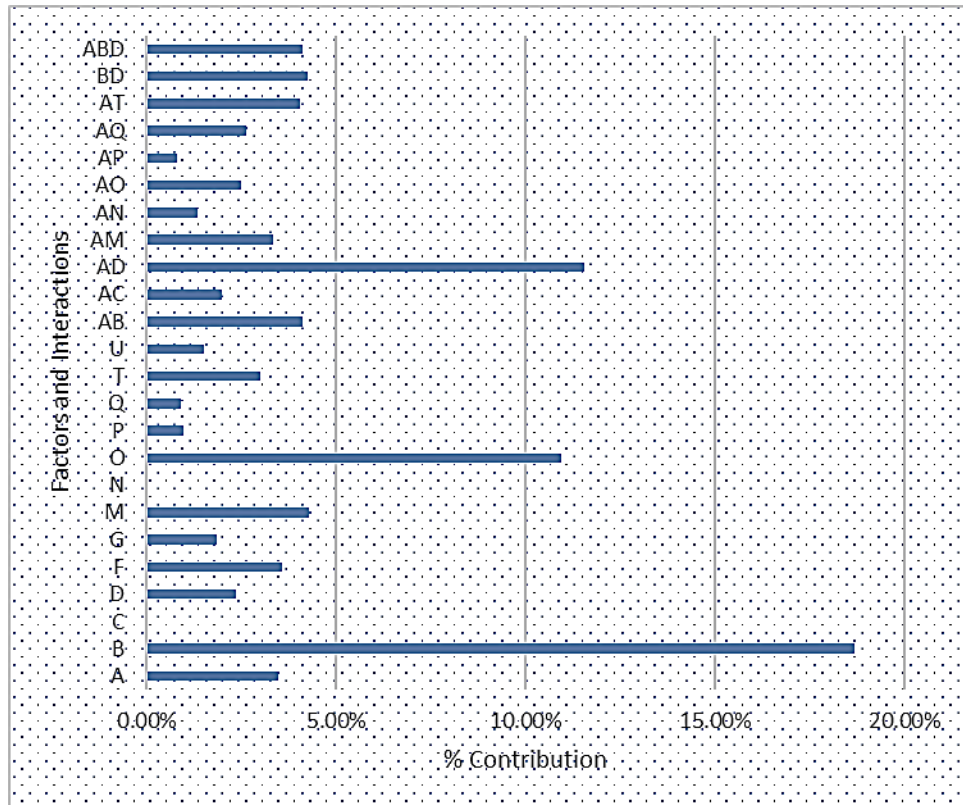


Figure 104: Percentage Contributions of Factors and Interactions on Response R5

The ANOVA for the selected model for response R5 as shown in **Table 23** represents the significance of factor B over other factors with the highest F-value of 46.007 followed by 2FI of A and D (AD) and factor O with F-values of 28.461 and 26.961 respectively.

Table 23: ANOVA of Selected Model for Response R5

SOURCE	SUM OF SQUARES	df	MEAN SQUARE	F-VALUE	P-VALUE	
Block	248.978	1	248.978			
Model	5830.810	24	242.950	8.522	0.000	Significant
A-bf	244.050	1	244.050	8.561	0.008	
B-db	1311.543	1	1311.543	46.007	0.000	
C-tfb	2.129	1	2.129	0.075	0.787	
D-twb	165.946	1	165.946	5.821	0.025	
F-b	251.814	1	251.814	8.833	0.007	
G-c (or g)	130.733	1	130.733	4.586	0.044	
M-Fybw - Web	301.024	1	301.024	10.559	0.004	
N-wc	0.123	1	0.123	0.004	0.948	
O-dc	768.597	1	768.597	26.961	0.000	
P-tfc	67.904	1	67.904	2.382	0.138	
Q-twc	62.156	1	62.156	2.180	0.155	
T-tcp	211.229	1	211.229	7.410	0.013	
U-Fycf - Flange	107.000	1	107.000	3.753	0.066	
AB	288.216	1	288.216	10.110	0.005	
AC	139.834	1	139.834	4.905	0.038	
AD	811.360	1	811.360	28.461	0.000	
AM	233.698	1	233.698	8.198	0.009	
AN	92.971	1	92.971	3.261	0.085	
AO	175.538	1	175.538	6.158	0.022	
AP	56.596	1	56.596	1.985	0.173	
AQ	183.869	1	183.869	6.450	0.019	
AT	283.282	1	283.282	9.937	0.005	
BD	298.778	1	298.778	10.481	0.004	
ABD	287.562	1	287.562	10.087	0.005	
Residual	598.662	21	28.508			
Cor Total	6678.450	46				

It was observed from the interaction plots of 2FI AD that higher value of factor D (20.32 mm) in combination with low-level value of factor A yields a lower value of rupture index as represented in **Figures 105** and **106**. In other words, at low-level value of factor D, factor A has an inverse effect on RI @ 7.5% total storey drift that is explained by the decrease in the response when the value of factor A was

increased from low- to high-level at low-level value of factor D. On the other hand, factor A has a direct effect on RI @ 7.5% storey drift at high-level value of factor D.

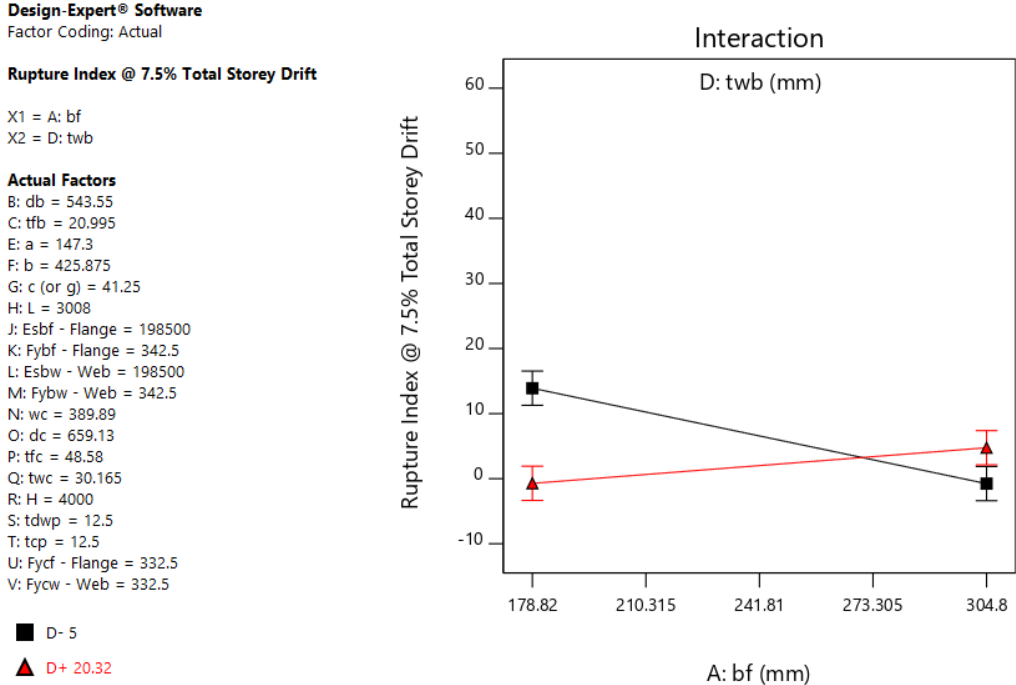


Figure 105: Plot of Marginal Means for Interaction AD in Selected Model for Response R5

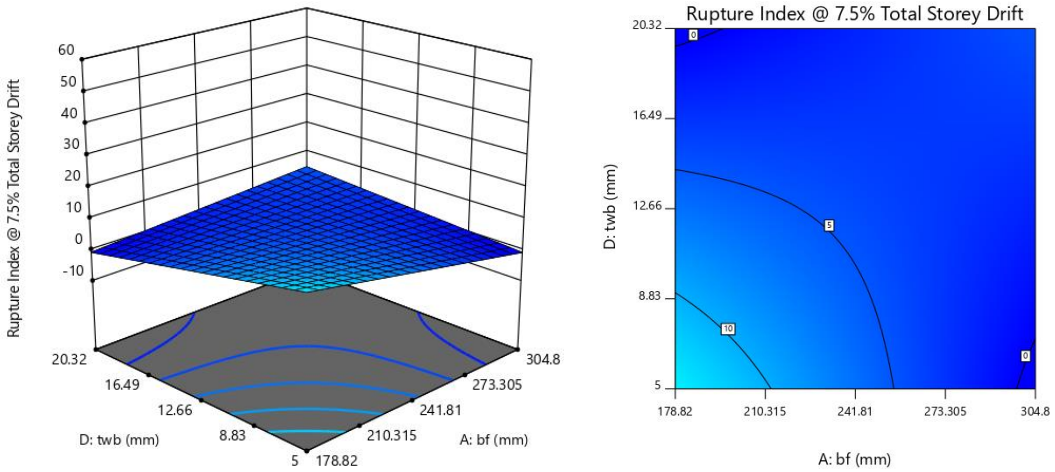


Figure 106: 3D Response Surface and Contour Plots for 2FI AD in Selected Model for Response R5

5.2.6. Overview of the Results

The summary of actual percentage contributions for all factors of selected models is presented in **Table 24**. All of the rows were summed up and divided individually by grand total of all the values of % contribution for responses for all factors as given in **Table 24** to get an aggregate overall percentage effectiveness which is graphically represented in **Figure 107**.

Table 24: Summary of Contribution of Factors for All Responses

FACTORS	% CONTRIBUTION FOR RESPONSES					SUM OF ROWS	OVERALL %
	R1	R2	R3	R4	R5		
A	3.82%	-	0.92%	0.73%	3.48%	8.95%	1.93%
B	35.47%	71.53%	5.20%	54.68%	18.69%	185.58%	40.09%
C	5.70%	3.37%	6.60%	4.47%	0.03%	20.17%	4.36%
D	3.57%	5.18%	0.13%	8.00%	2.37%	19.24%	4.16%
E	0.09%	-	0.00%	-	-	0.09%	0.02%
F	1.99%	-	1.70%	2.34%	3.59%	9.61%	2.08%
G	-	-	3.70%	-	1.86%	5.56%	1.20%
H	-	1.19%	2.51%	-	-	3.70%	0.80%
J	0.01%	-	7.34%	-	-	7.35%	1.59%
K	1.35%	-	10.18%	-	-	11.53%	2.49%
L	1.83%	-	2.16%	-	-	3.99%	0.86%
M	4.89%	1.34%	-	4.32%	4.29%	14.84%	3.21%
N	-	-	0.01%	-	0.00%	0.01%	0.00%
O	4.52%	-	1.30%	3.91%	10.95%	20.68%	4.47%
P	-	-	1.77%	-	0.97%	2.73%	0.59%
Q	0.06%	-	3.36%	0.18%	0.89%	4.48%	0.97%
R	-	-	3.08%	-	-	3.08%	0.67%
S	0.01%	-	-	0.25%	-	0.26%	0.06%
T	-	-	-	-	3.01%	3.01%	0.65%
U	0.00%	-	-	-	1.53%	1.53%	0.33%
AB	2.96%	-	0.99%	-	4.11%	8.06%	1.74%
AC	0.12%	-	-	-	1.99%	2.11%	0.46%
AD	3.26%	-	2.03%	-	11.56%	16.86%	3.64%
AE	2.47%	-	0.12%	-	-	2.59%	0.56%
AF	-	-	5.56%	-	-	5.56%	1.20%
AJ	1.06%	-	2.96%	-	-	4.02%	0.87%
AK	-	-	5.92%	-	-	5.92%	1.28%
AL	-	-	8.30%	-	-	8.30%	1.79%
AM	-	-	-	-	3.33%	3.33%	0.72%

AN	-	-	1.02%	-	1.33%	2.34%	0.51%
AO	-	-	-	-	2.50%	2.50%	0.54%
AP	-	-	-	-	0.81%	0.81%	0.17%
AQ	3.08%	-	0.86%	1.70%	2.62%	8.25%	1.78%
AR	-	-	6.78%	-	-	6.78%	1.46%
AS	2.57%	-	-	1.54%	-	4.11%	0.89%
AT	-	-	-	-	4.04%	4.04%	0.87%
AU	5.71%	-	-	-	-	5.71%	1.23%
BC	4.33%	2.66%	-	3.05%	-	10.04%	2.17%
BD	3.08%	5.04%	-	6.53%	4.26%	18.91%	4.08%
BE	-	-	7.19%	-	-	7.19%	1.55%
ABD	3.04%	-	-	-	4.10%	7.13%	1.54%
ABE	-	-	1.96%	-	-	1.96%	0.42%
						Total	462.88%

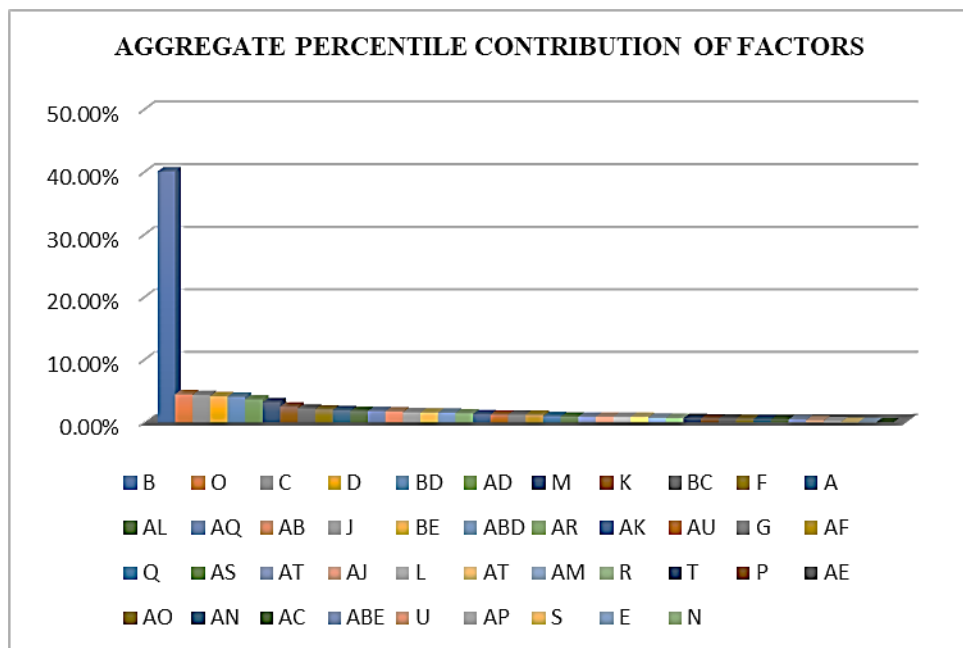


Figure 107: Graphical Representation of Aggregate Percentile Contribution of Factors

These factors were therefore ranked on the basis of their aggregate percentile effect for all 5 responses as presented in **Table 25** . There were some factors that were significantly affective for all responses with a higher percentage contribution and hence were ranked higher than those factors that were effective just for certain responses.

Table 25: Overall Ranking of Factors

RANK	FACTOR(s)	OVERALL %
1	B	40.09%
2	O	4.47%
3	C	4.36%
4	D	4.16%
5	BD	4.08%
6	AD	3.64%
7	M	3.21%
8	K	2.49%
9	BC	2.17%
10	F	2.08%
11	A	1.93%
12	AL	1.79%
13	AQ	1.78%
14	AB	1.74%
15	J	1.59%
16	BE	1.55%
17	ABD	1.54%
18	AR	1.46%
19	AK	1.28%
20	AU	1.23%
21	G	1.20%
22	AF	1.20%
23	Q	0.97%
24	AS	0.89%
25	AT	0.87%
26	AJ	0.87%
27	L	0.86%
27	AT	0.87%
29	AM	0.72%
30	R	0.67%
31	T	0.65%
32	P	0.59%
33	AE	0.56%
34	AO	0.54%
35	AN	0.51%
36	AC	0.46%
37	ABE	0.42%
38	U	0.33%

39	AP	0.17%
40	S	0.06%
41	E	0.02%
42	N	0.00%

5.3. CONCLUSIONS AND RECOMMENDATIONS

In this study, performance of radial flange cut type RBS connections was analyzed under cyclic loading conditions for different combinations of 21 factors. These combinations were designed by adopting 2-Level factorial design of experiment approach. The statistical analysis of the results suggested that:

1. The most significant factor in the performance of RBS connection under cyclic loading conditions is the depth of the beam (factor B) that had contributions of 35.47%, 71.53%, 5.20%, 54.68% and 18.69% towards responses R1 (Total Dissipated Energy), R2 (Initial Stiffness), R3 (Strength Degradation Rate), R4 (Maximum Moment Capacity) and R5 (Rupture Index @ 7.5% Total Storey Drift), therefore making the RBS connection most sensitive to this factor.
2. Strength degradation rate was influenced by various factors amongst which, yield strength of beam flange was the most significant one.
3. Width of beam flange (factor A) can not only impact total dissipated energy positively with higher value of elastic modulus of beam flange, but it can also affect strength degradation rate more significantly at higher values of factors F (length of flange cut: b), L (elastic modulus of beam web: Esbw) and R (height of the column: H).
4. Depth of the column (factor O) significantly affects rupture index.

The findings of this study can be useful for proceeding studies on a similar topic. Also, this study provides an insight of several factors effecting the cyclic response of RBS connections that might help the professionals in the design field to come up with more economical and optimal design solutions.

GLOSSARY OF ACRONYMS AND SYMBOLS

2FIs	2 Factor Interactions
a	Distance from face of the column flange to starting point of beam flange cut (mm)
ANOVA	Analysis of Variance
b	Length of beam flange cut (mm)
bf	Width of beam flange (mm)
c	Depth of beam flange cut (mm)
db	Depth of beam section (mm)
dc	Depth of column section (mm)
E _{sbf}	Young's modulus of beam flange (MPa)
E _{sbw}	Young's modulus of beam web (MPa)
E _{scf}	Young's modulus of column flange (MPa)
E _{scw}	Young's modulus of column web (MPa)
FEMA	Federal Emergency Management Agency
F _{ybf}	Yield strength of beam flange (MPa)
F _{ybw}	Yield strength of beam web (MPa)
F _{ycf}	Yield strength of column flange (MPa)
F _{ycw}	Yield strength of column web (MPa)
H	Total height of column (mm)
L	Length of beam (mm)
MRF(s)	Moment Resisting Frame(s)
PEEQ	Equivalent Plastic Strain
PZ	Panel Zone

RBS	Reduced Beam Section
r _{fc}	Radius of beam flange cut (mm)
RI	Rupture Index
s	Distance from face of the column flange to middle of beam flange cut (mm)
SDR	Strength Degradation Rate
t _{cp}	Thickness of continuity plate (mm)
t _{dwp}	Thickness of doubler web plate (mm)
t _{fb}	Thickness of beam flange (mm)
t _{fc}	Thickness of column flange (mm)
t _{wb}	Thickness of beam web (mm)
t _{wc}	Thickness of column web (mm)
w _c	Width of column flange (mm)

APPENDICES

APPENDIX A: FEA Models

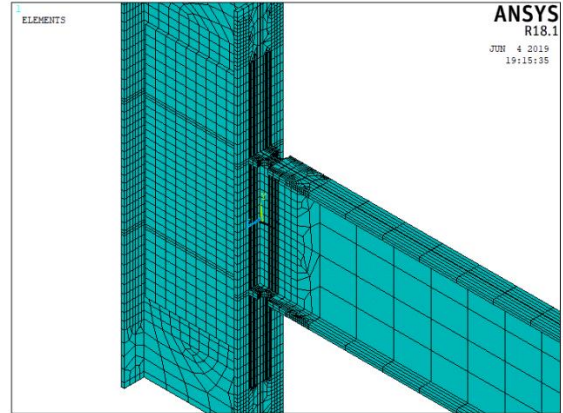
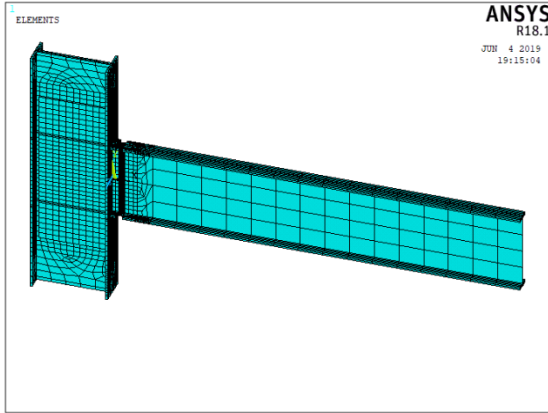


Figure A1: FEA Model for Specimen RBS-7

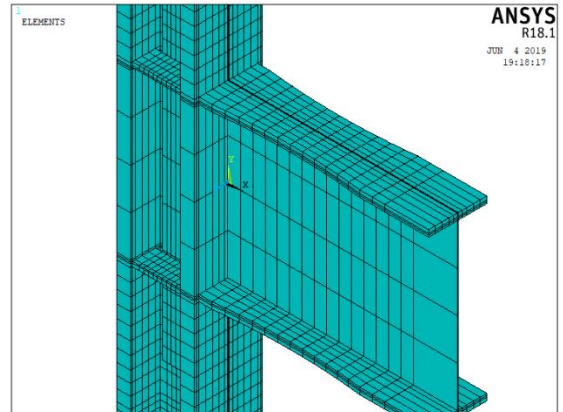
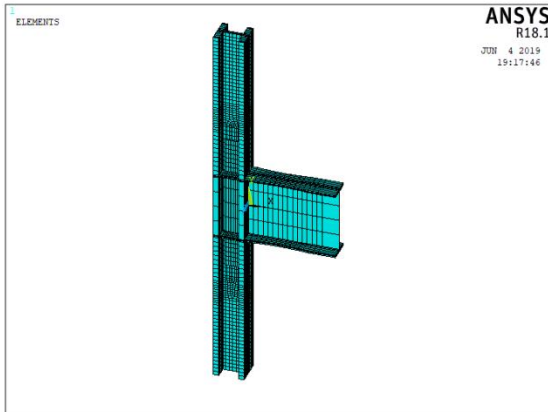


Figure A2: FEA Model for Specimen RBS-8

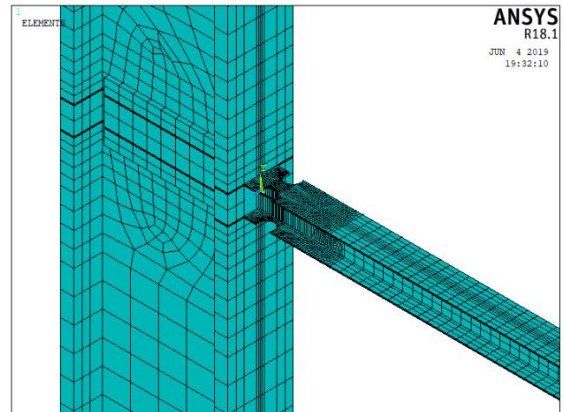
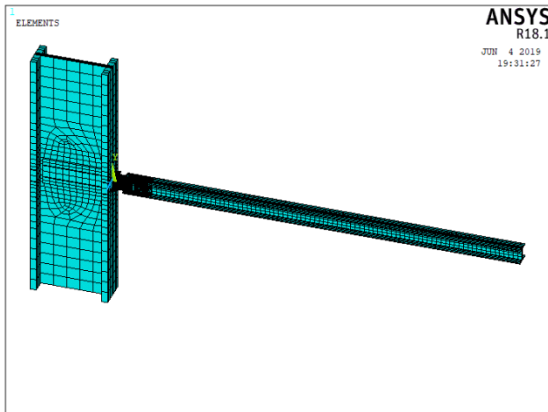


Figure A3: FEA Model for Specimen RBS-9

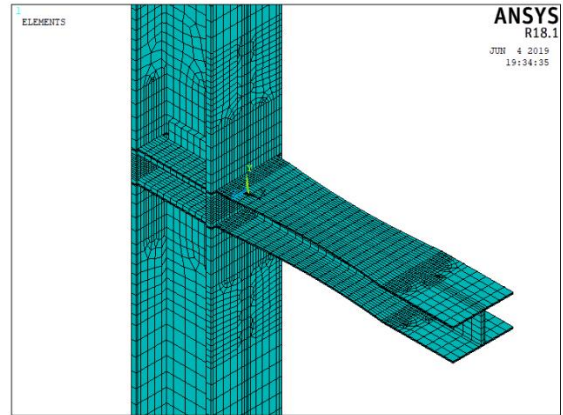
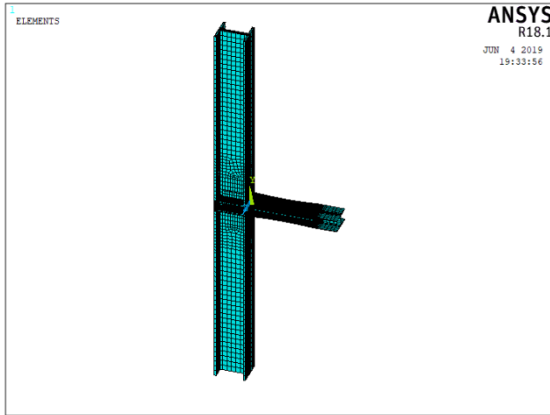


Figure A4: FEA Model for Specimen RBS-10

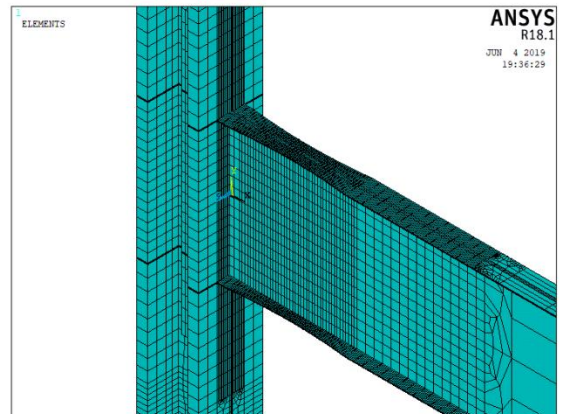
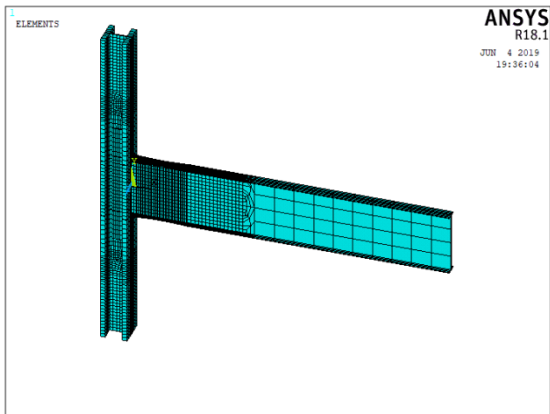


Figure A5: FEA Model for Specimen RBS-11

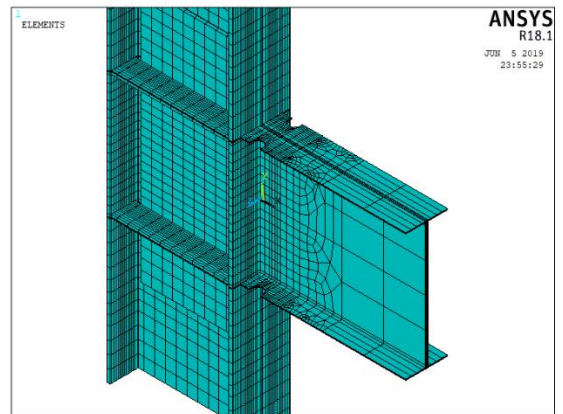
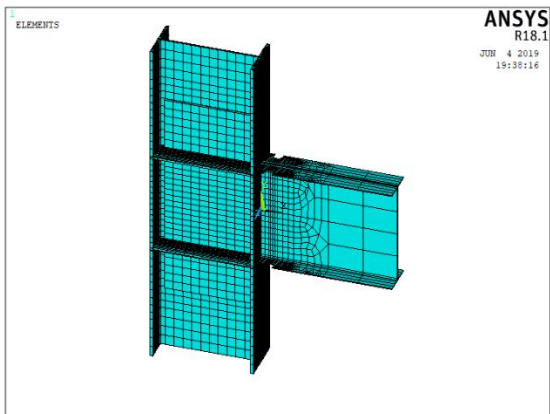


Figure A6: FEA Model for Specimen RBS-12

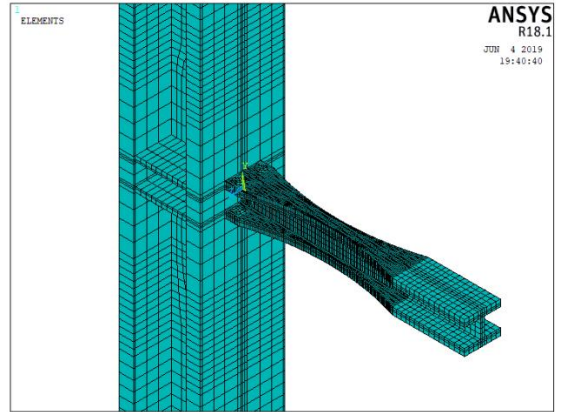
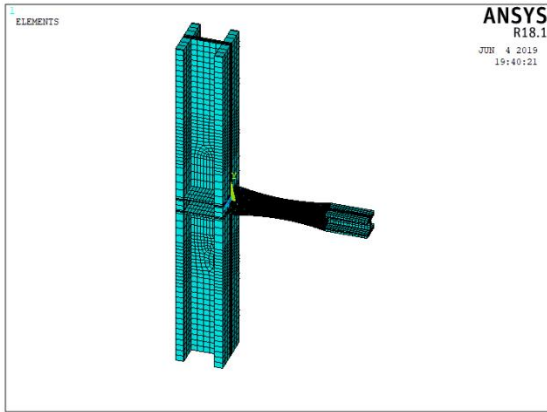


Figure A7: FEA Model for Specimen RBS-13

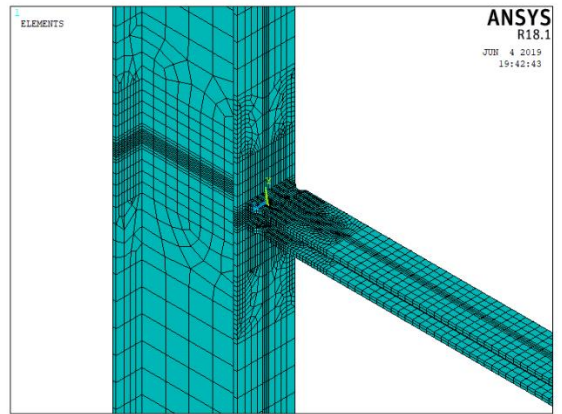
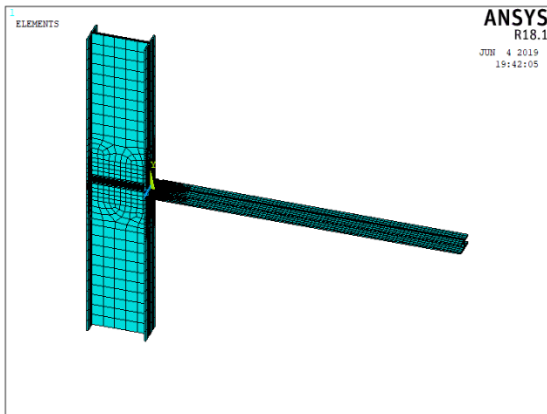


Figure A8: FEA Model for Specimen RBS-14

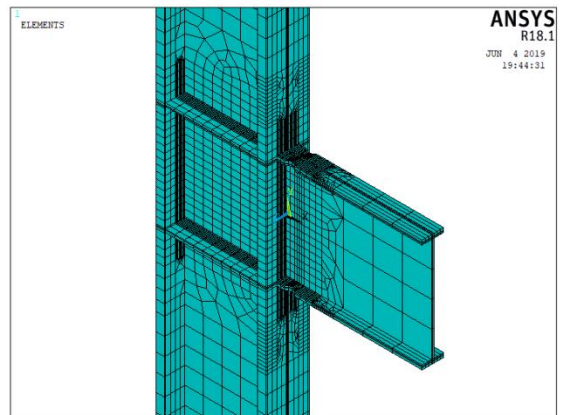
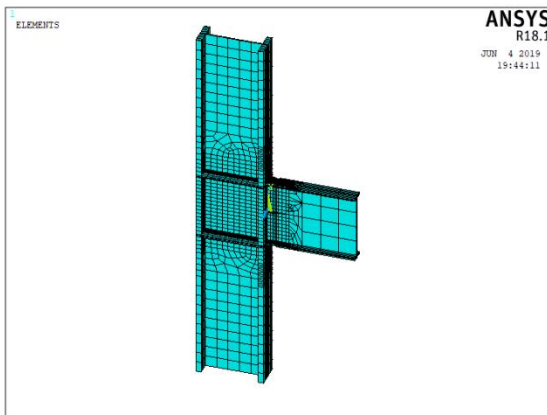


Figure A9: FEA Model for Specimen RBS-15

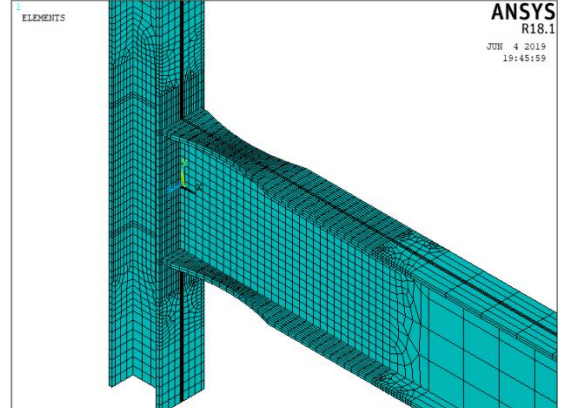
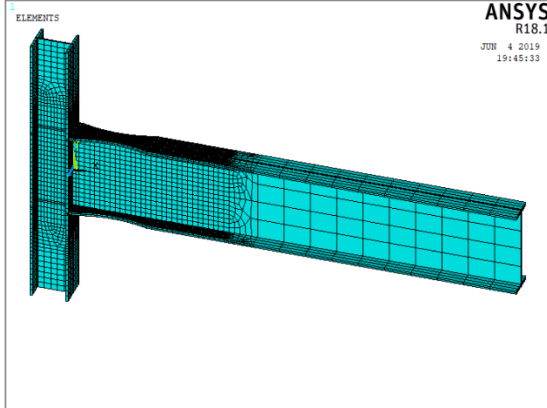


Figure A10: FEA Model for Specimen RBS-16

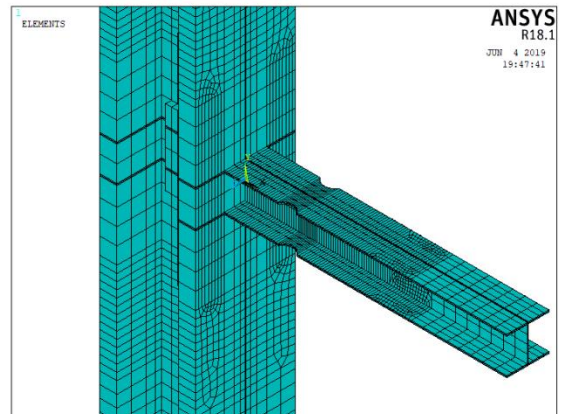
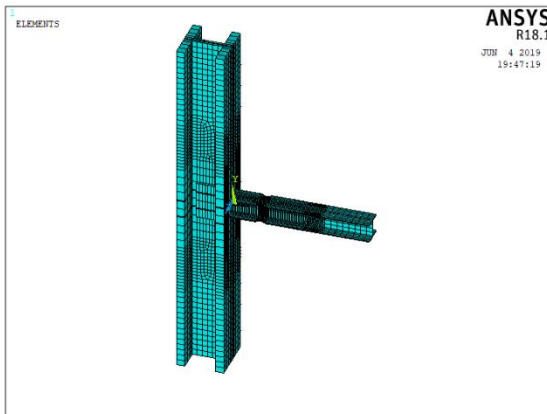


Figure A11: FEA Model for Specimen RBS-17

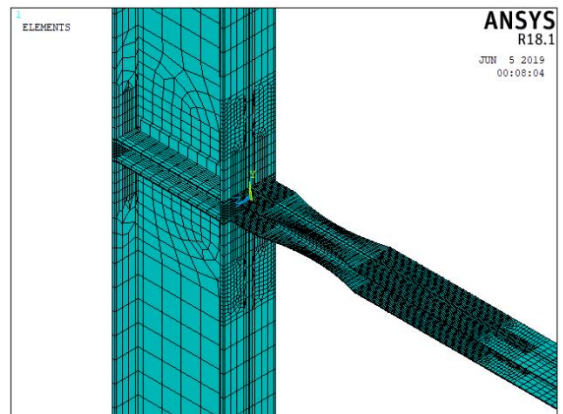
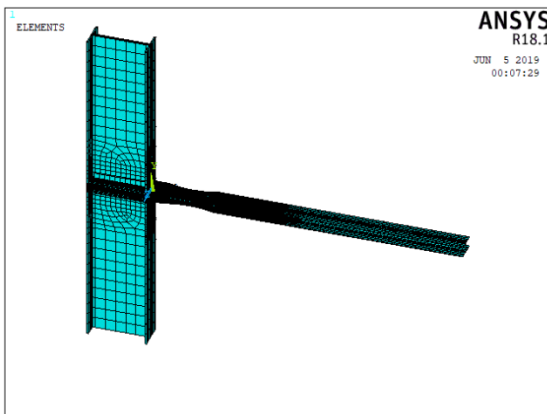


Figure A12: FEA Model for Specimen RBS-18

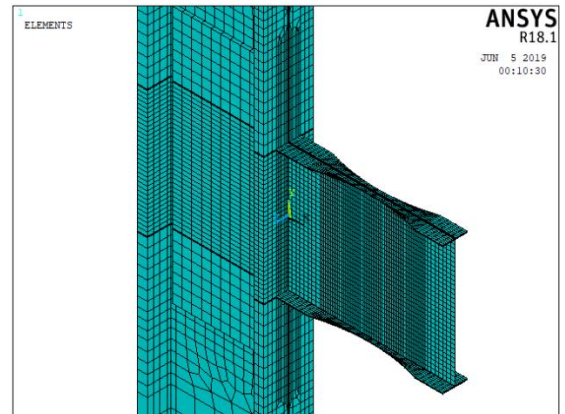
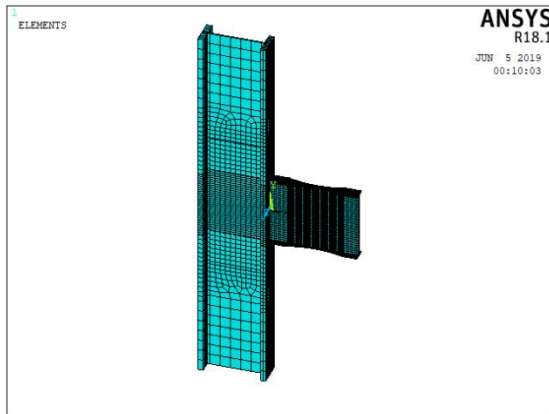


Figure A13: FEA Model for Specimen RBS-19

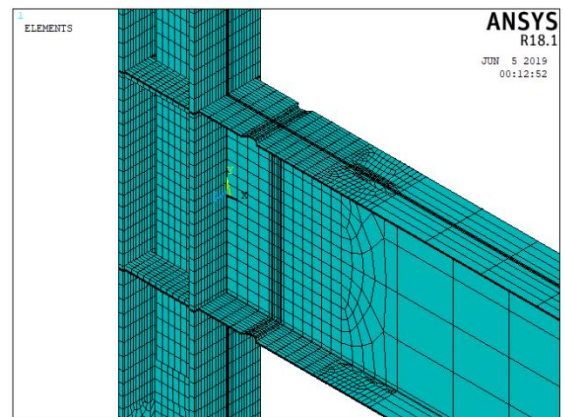
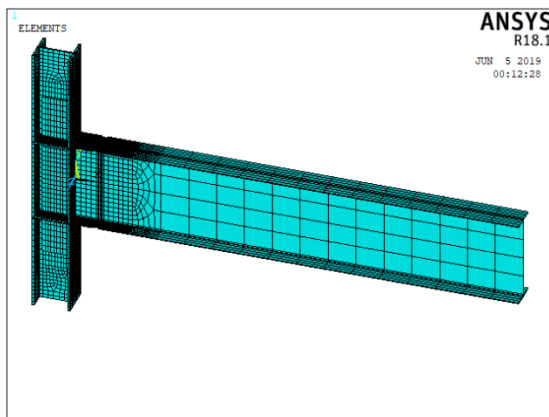


Figure A14: FEA Model for Specimen RBS-20

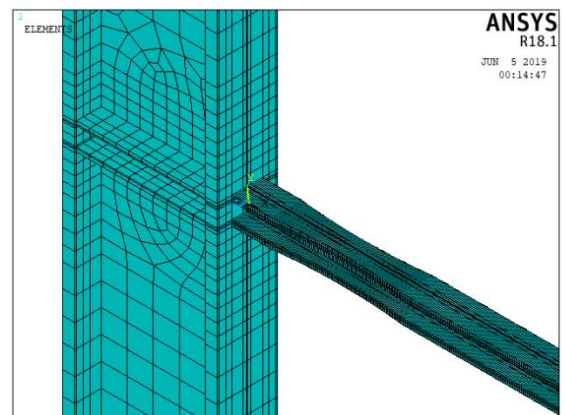
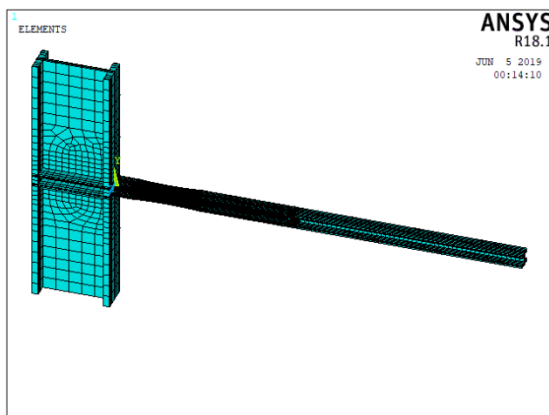


Figure A15: FEA Model for Specimen RBS-21

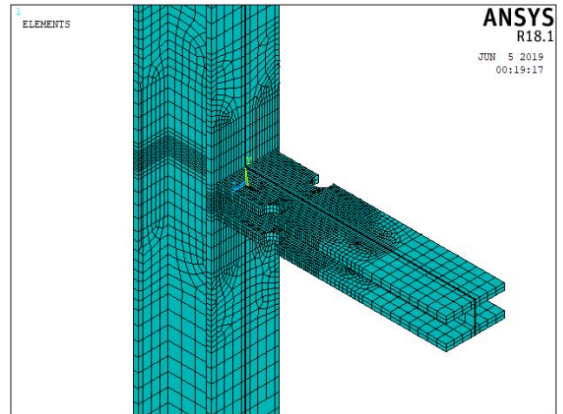
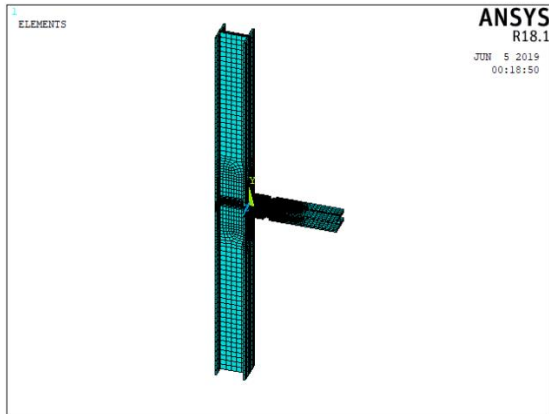


Figure A16: FEA Model for Specimen RBS-22

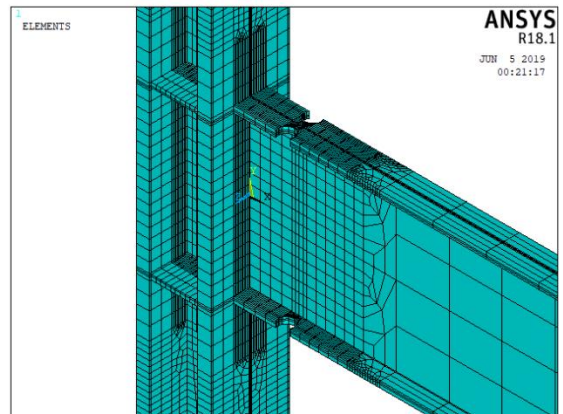
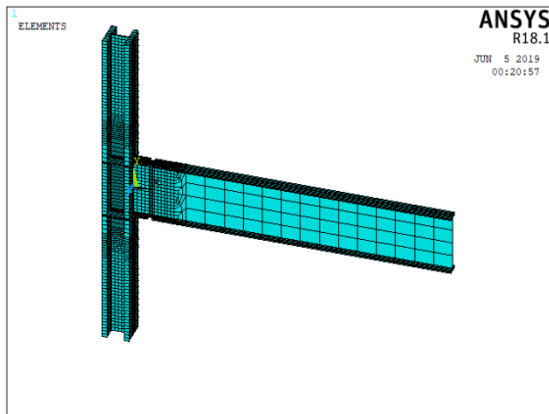


Figure A17: FEA Model for Specimen RBS-23

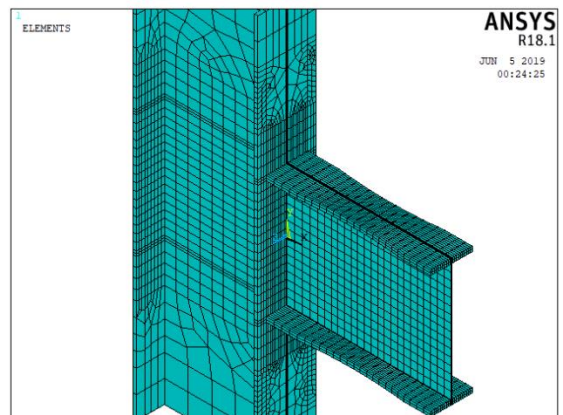
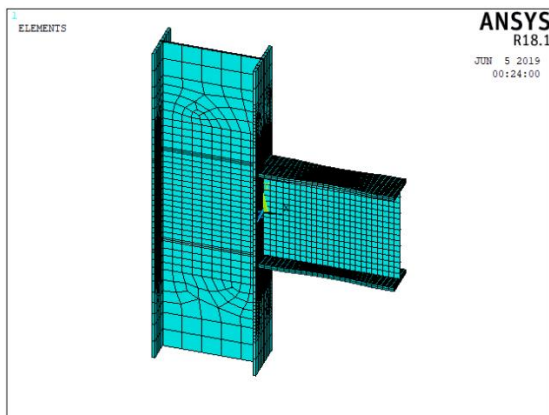


Figure A18: FEA Model for Specimen RBS-24

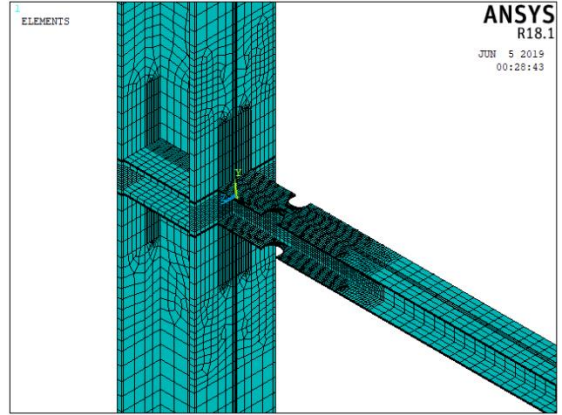
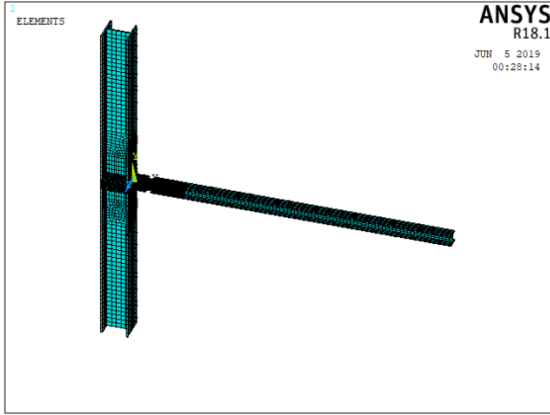


Figure A19: FEA Model for Specimen RBS-25

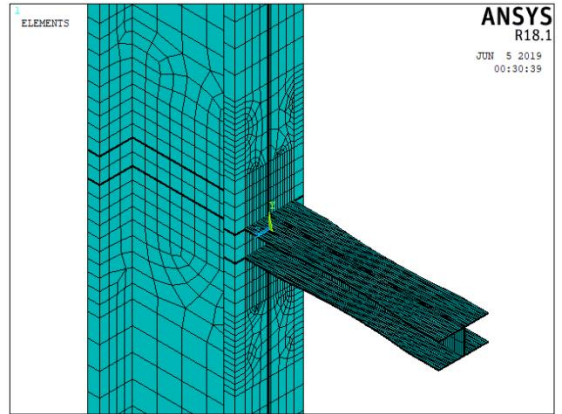
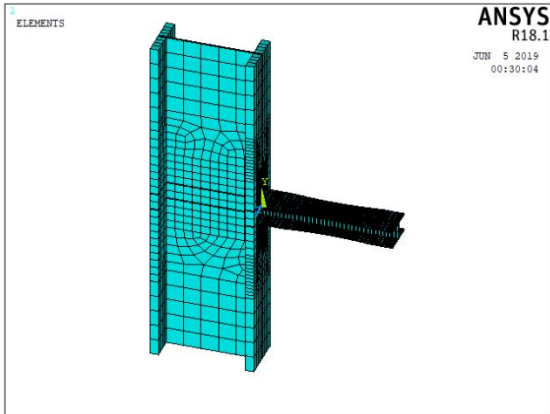


Figure A20: FEA Model for Specimen RBS-26

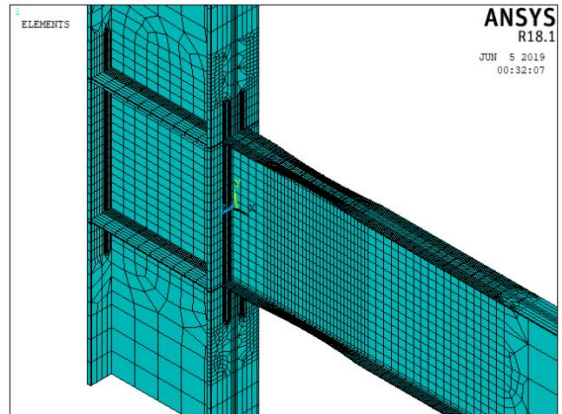
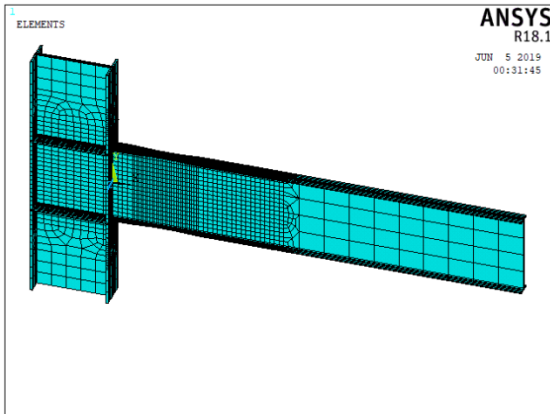


Figure A21: FEA Model for Specimen RBS-27

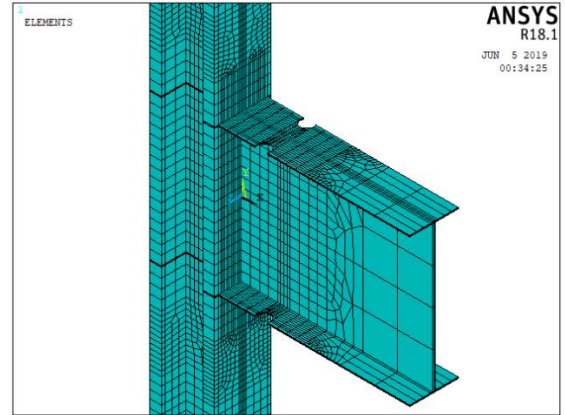
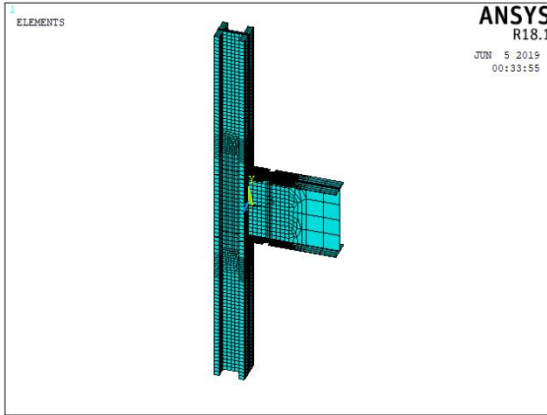


Figure A22: FEA Model for Specimen RBS-28

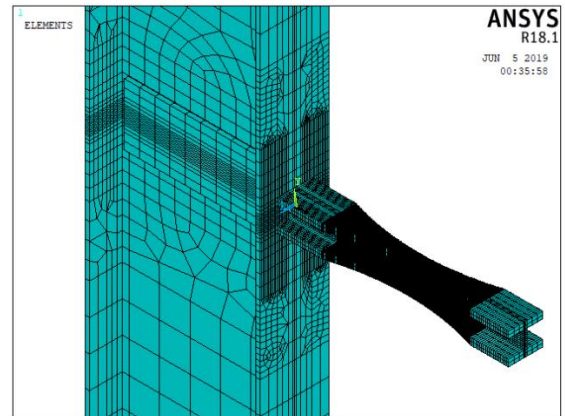
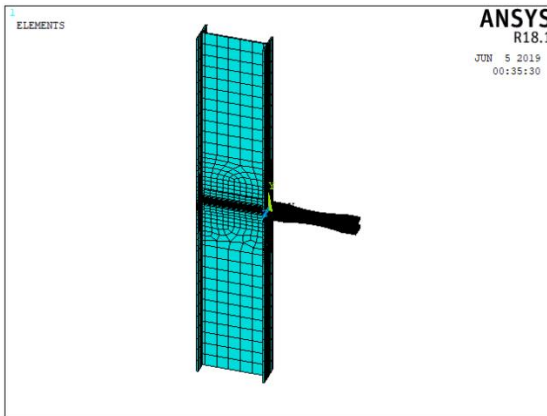


Figure A23: FEA Model for Specimen RBS-29

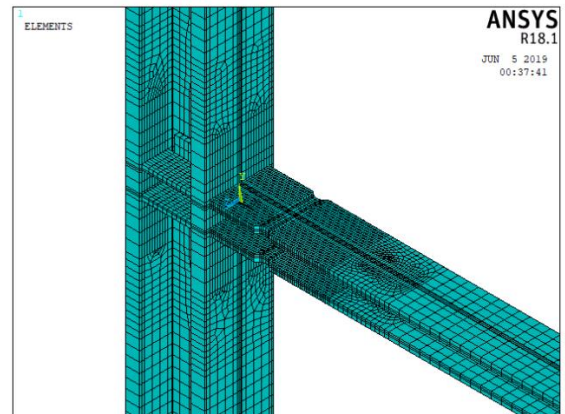
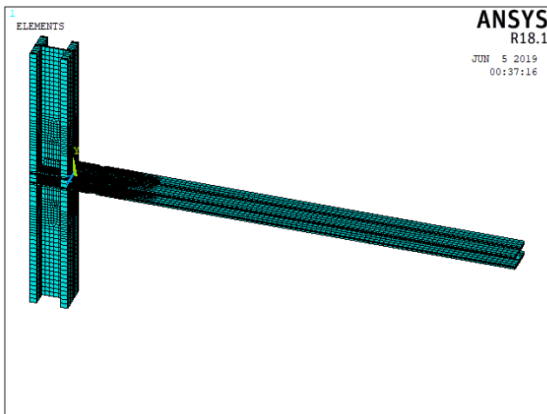


Figure A24: FEA Model for Specimen RBS-30

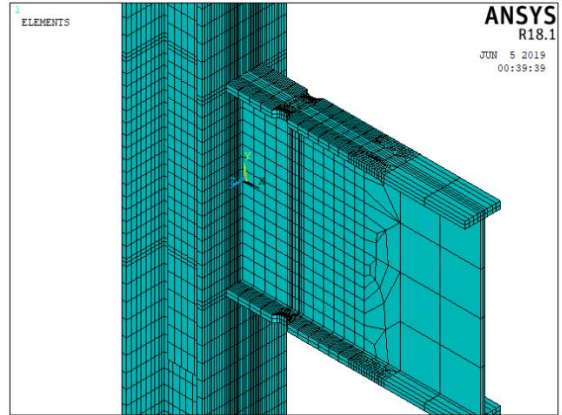
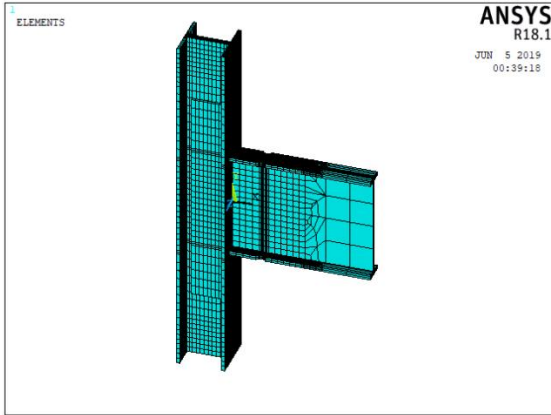


Figure A25: FEA Model for Specimen RBS-31

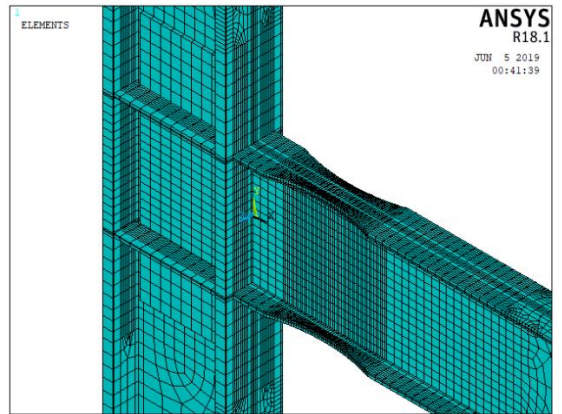
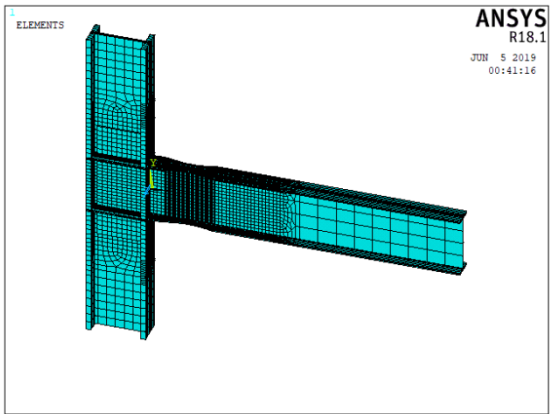


Figure A26: FEA Model for Specimen RBS-32

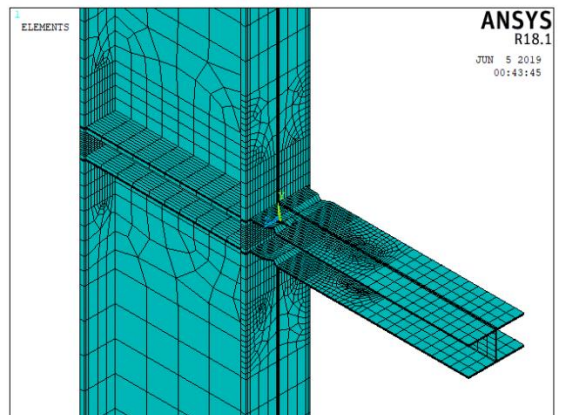
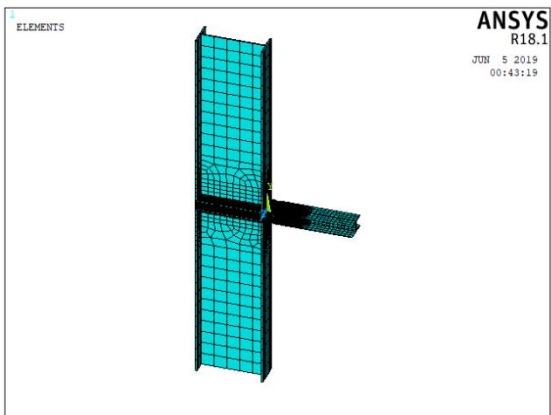


Figure A27: FEA Model for Specimen RBS-33

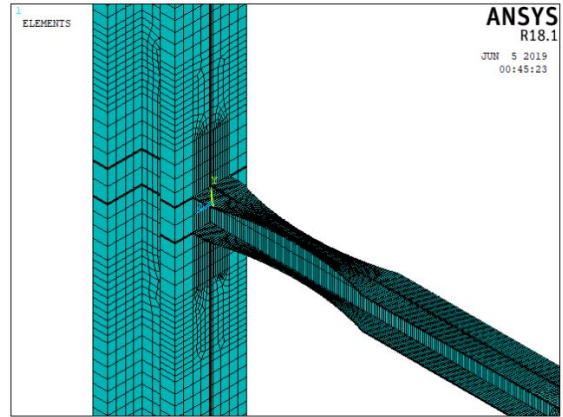
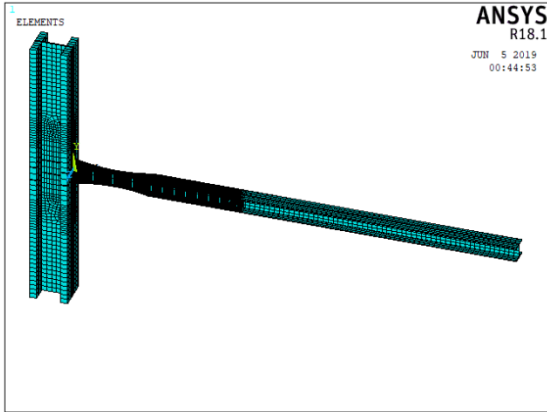


Figure A28: FEA Model for Specimen RBS-34

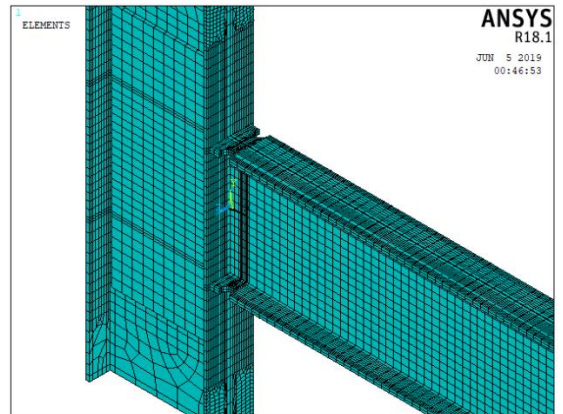
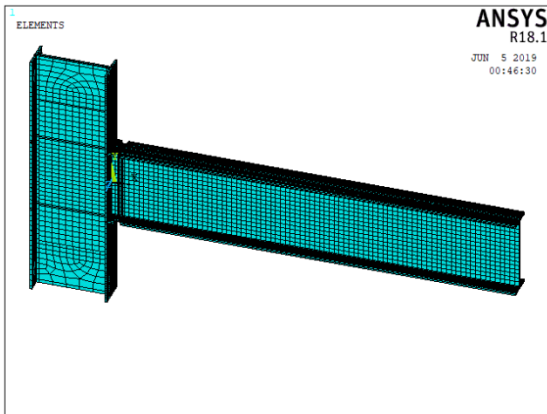


Figure A29: FEA Model for Specimen RBS-35

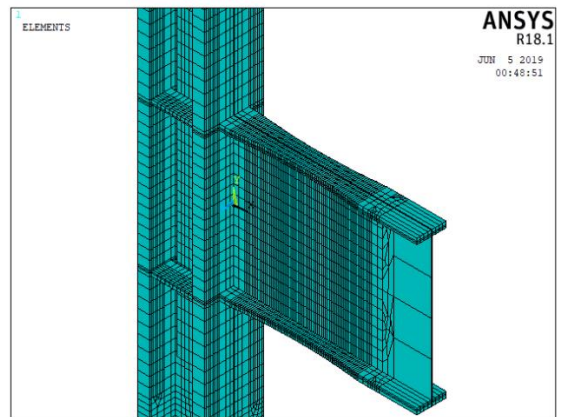
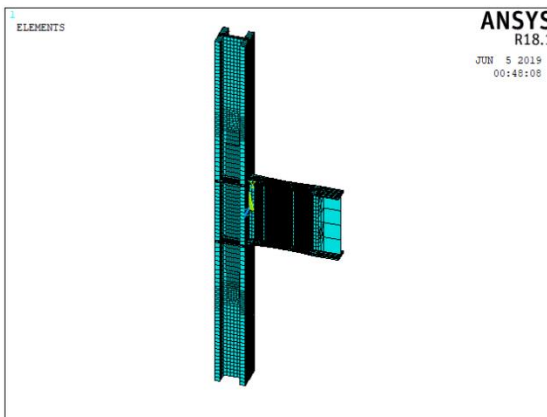


Figure A30: FEA Model for Specimen RBS-36

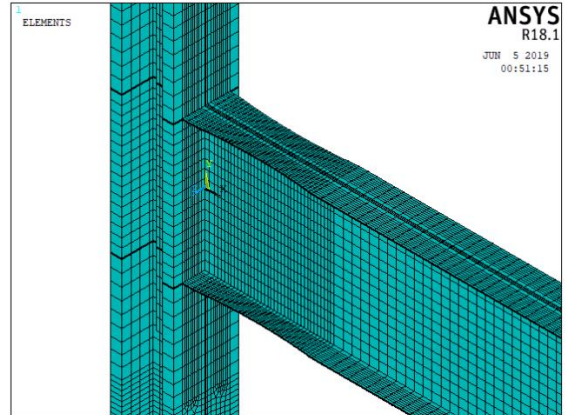
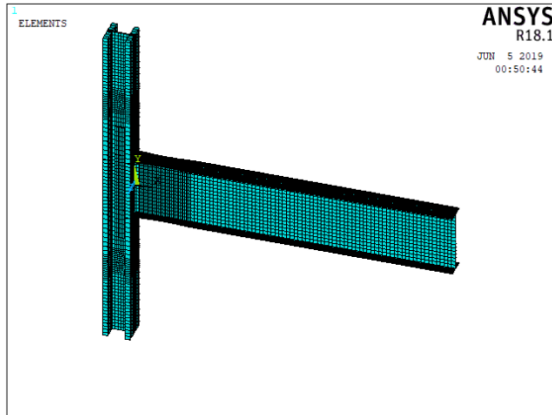


Figure A31: FEA Model for Specimen RBS-37

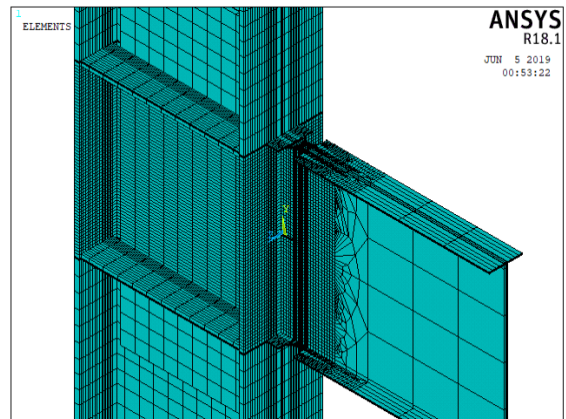
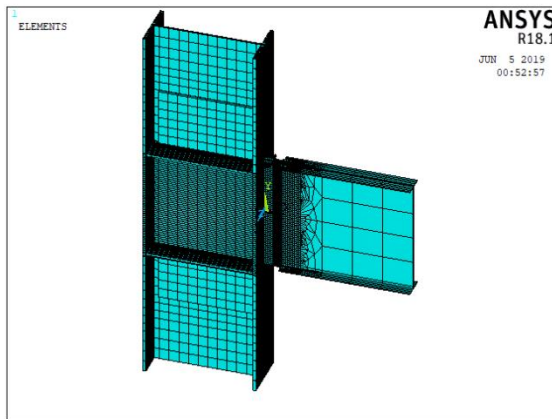


Figure A32: FEA Model for Specimen RBS-38

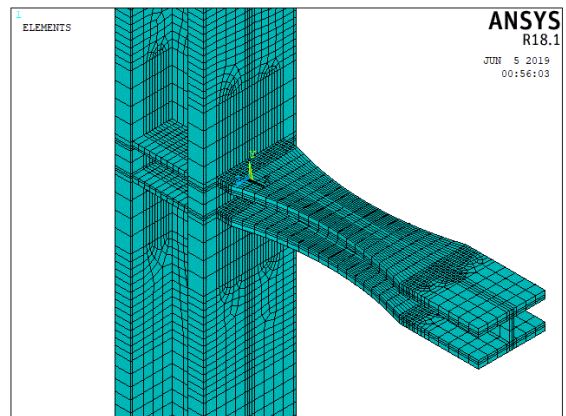
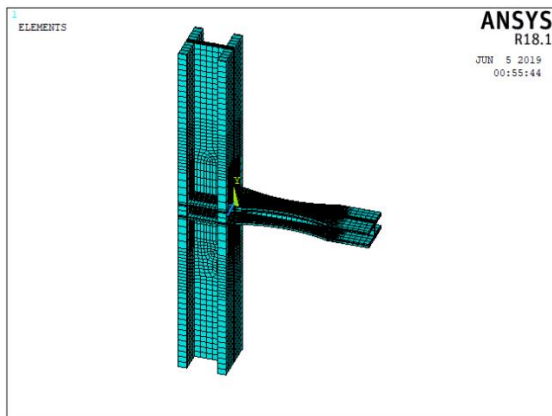


Figure A33: FEA Model for Specimen RBS-39

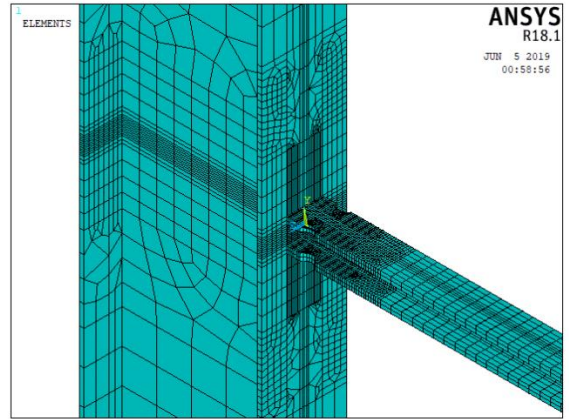
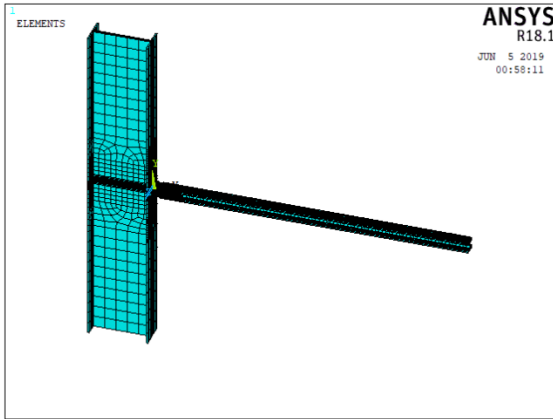


Figure A34: FEA Model for Specimen RBS-40

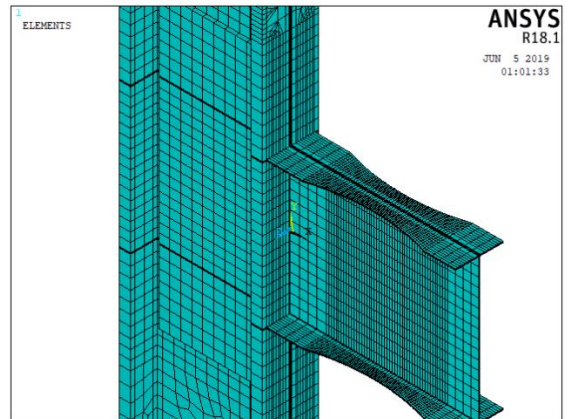
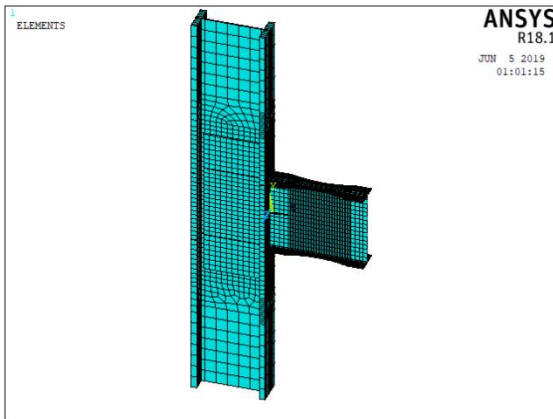


Figure A35: FEA Model for Specimen RBS-41

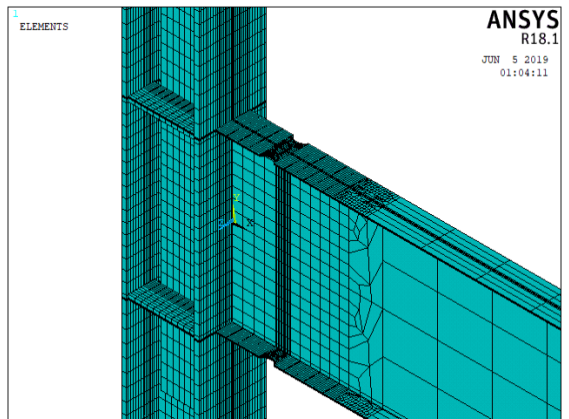
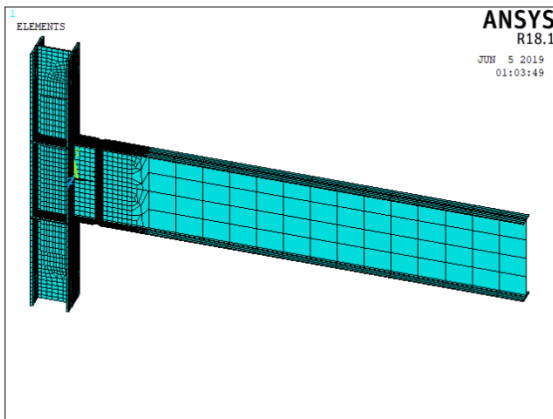


Figure A36: FEA Model for Specimen RBS-42

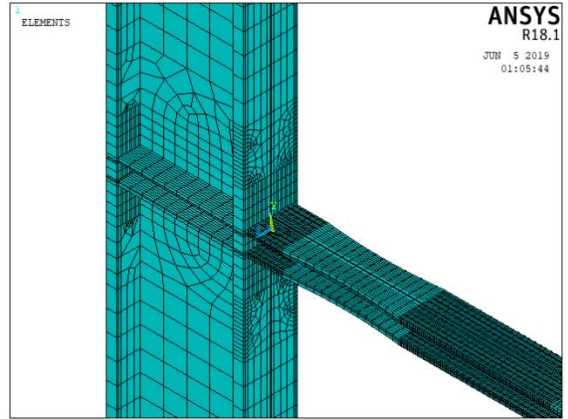
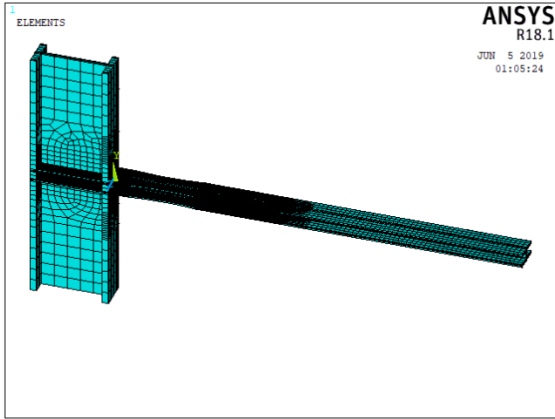


Figure A37: FEA Model for Specimen RBS-43

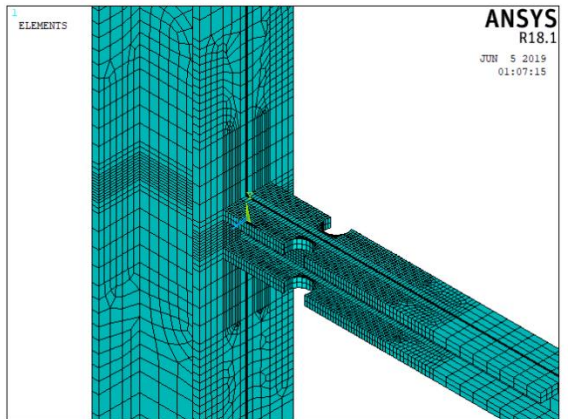
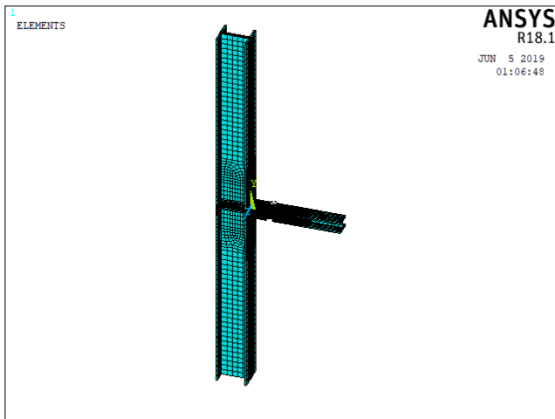


Figure A1: FEA Model for Specimen RBS-44

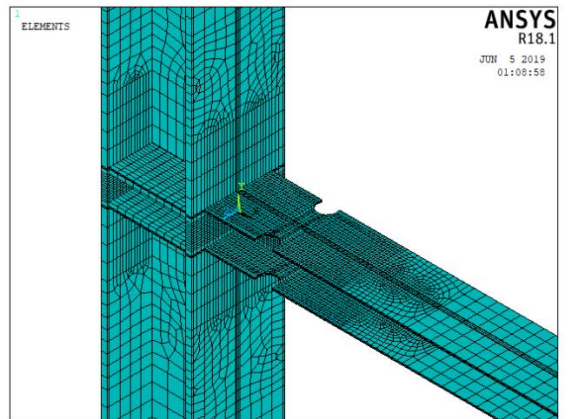
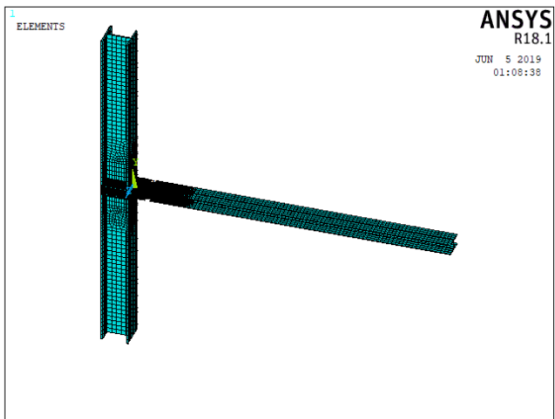


Figure A38: FEA Model for Specimen RBS-45

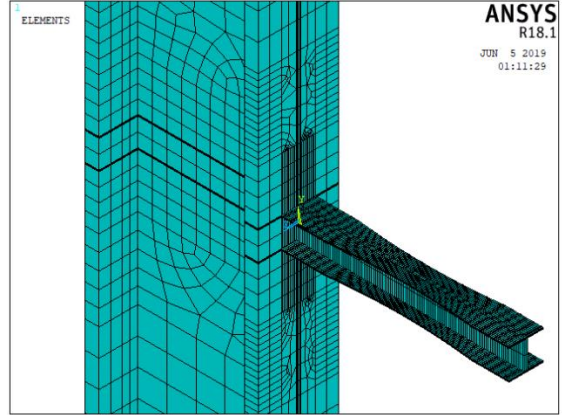
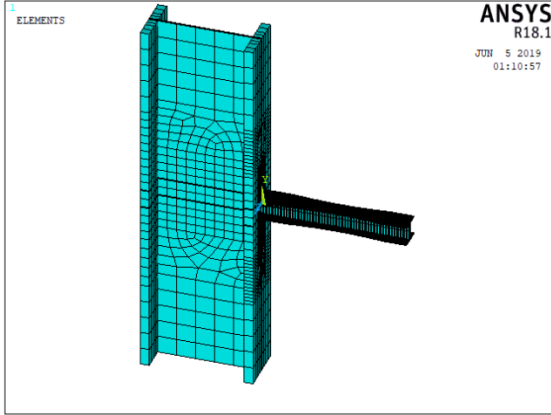


Figure A39: FEA Model for Specimen RBS-46

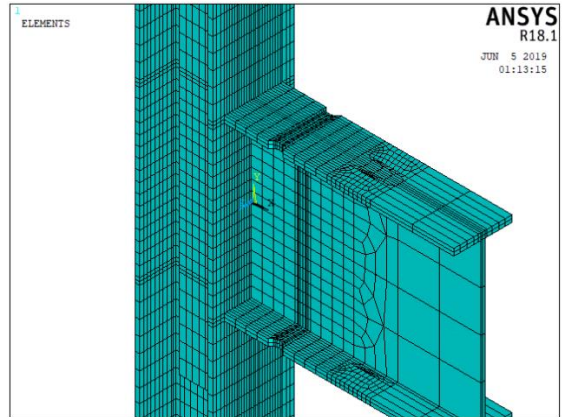
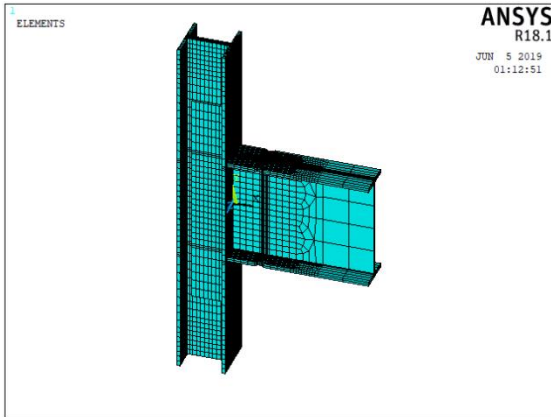


Figure A40: FEA Model for Specimen RBS-47

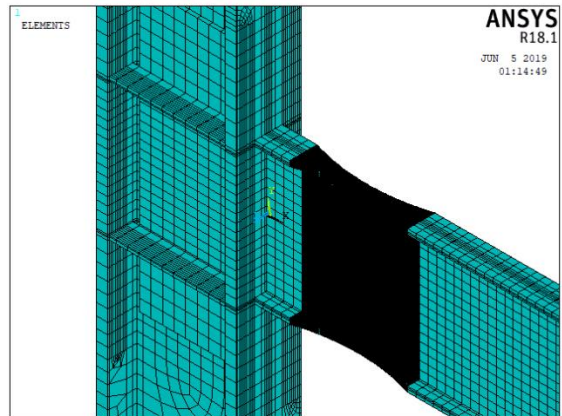
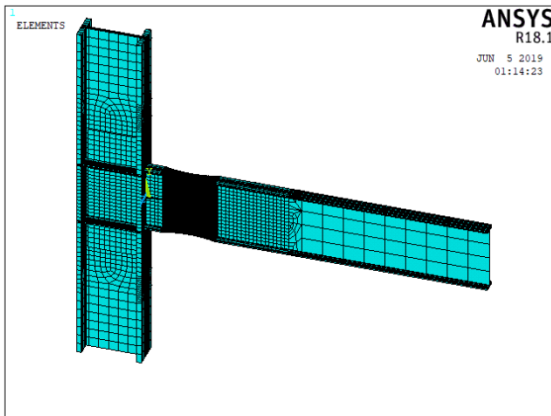


Figure A41: FEA Model for Specimen RBS

APPENDIX B: Response Plots

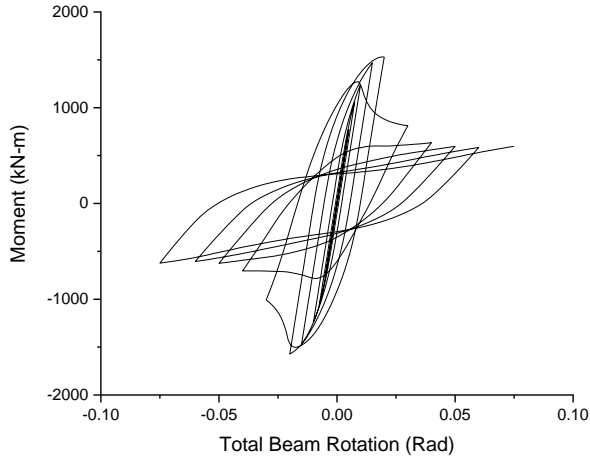


Figure B1: Experimental Moment vs Rotation Curve for RBS-11

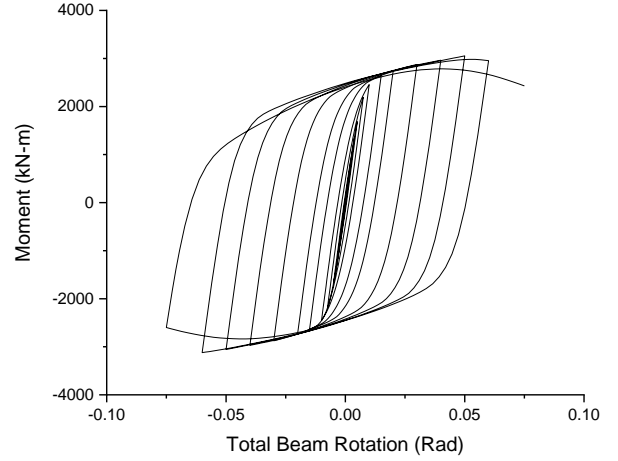


Figure B2: Experimental Moment vs Rotation Curve for RBS-12

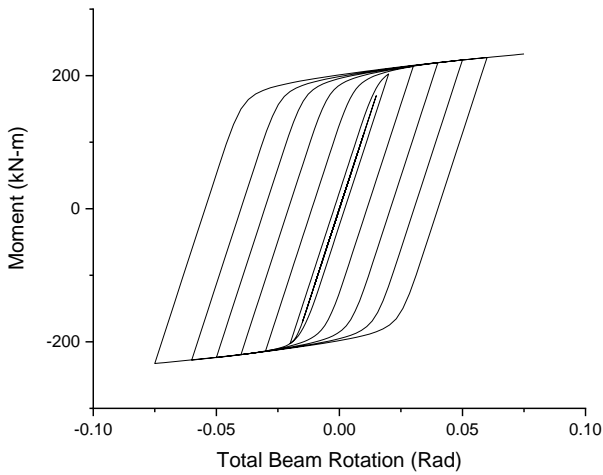


Figure B3: Experimental Moment vs Rotation Curve for RBS-13

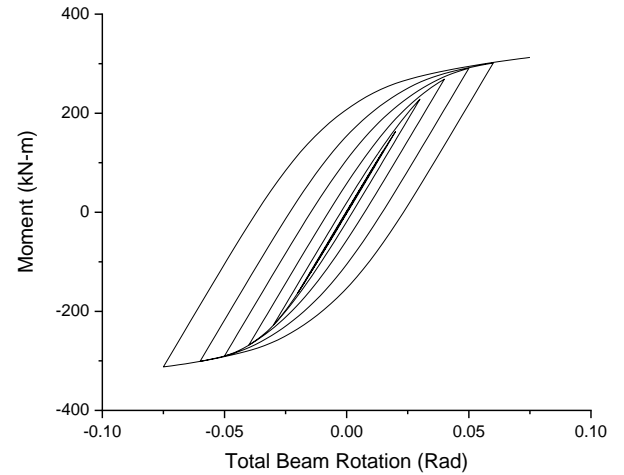


Figure B4: Experimental Moment vs Rotation Curve for RBS-14

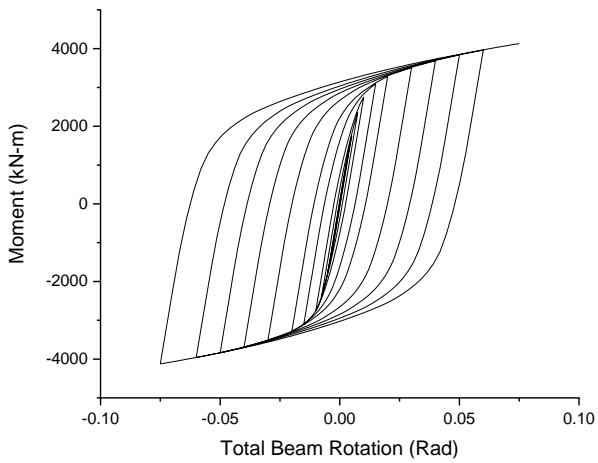


Figure B5: Experimental Moment vs Rotation Curve for RBS-15

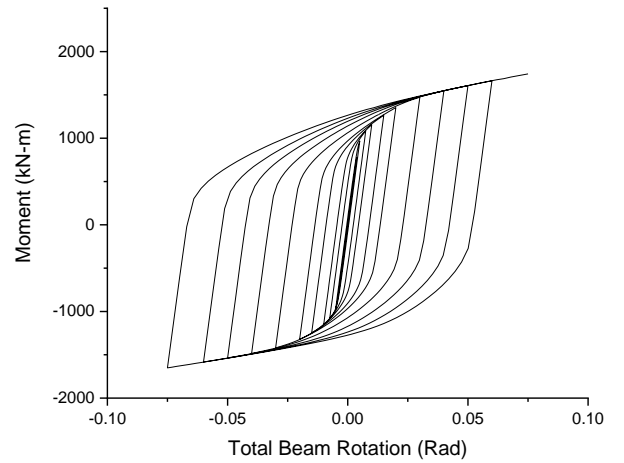


Figure B6: Experimental Moment vs Rotation Curve for RBS-16

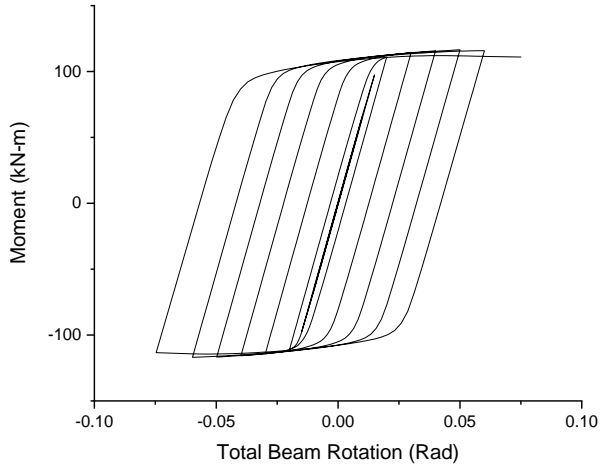


Figure B7: Experimental Moment vs Rotation Curve for RBS-17

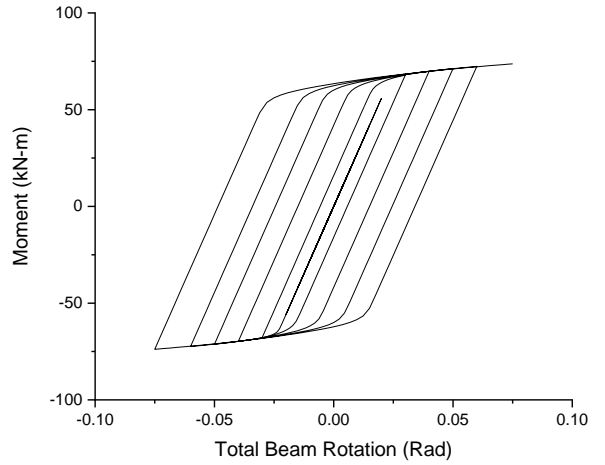


Figure B8: Experimental Moment vs Rotation Curve for RBS-18

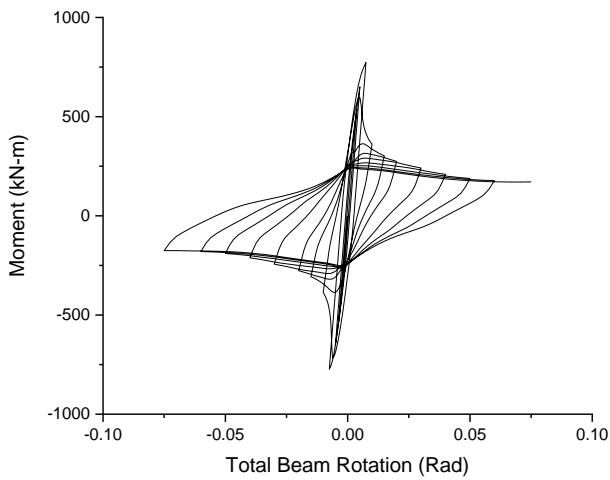


Figure B9: Experimental Moment vs Rotation Curve for RBS-19

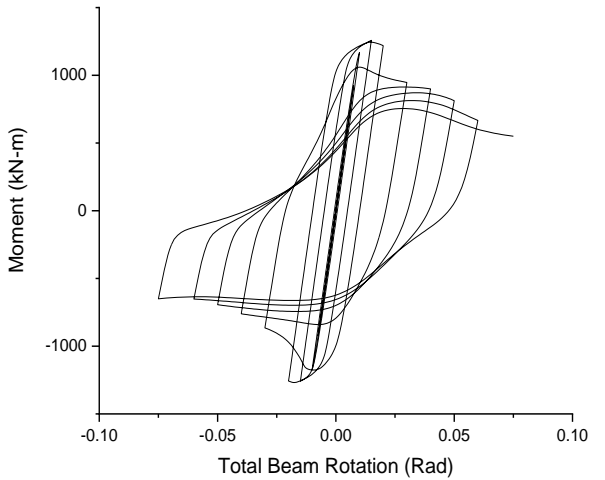


Figure B10: Experimental Moment vs Rotation Curve for RBS-20

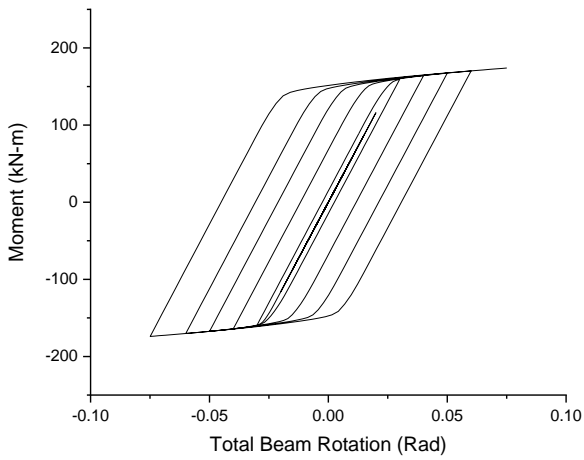


Figure B11: Experimental Moment vs Rotation Curve for RBS-21

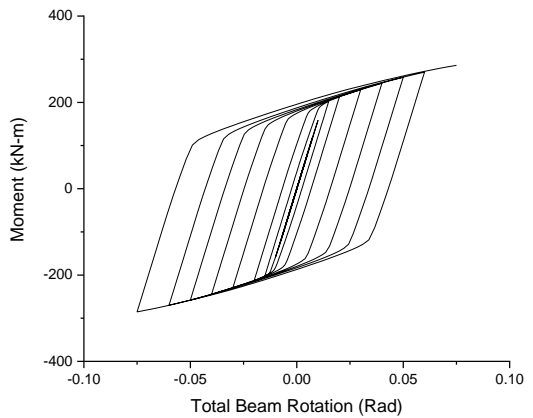


Figure B12: Experimental Moment vs Rotation Curve for RBS-22

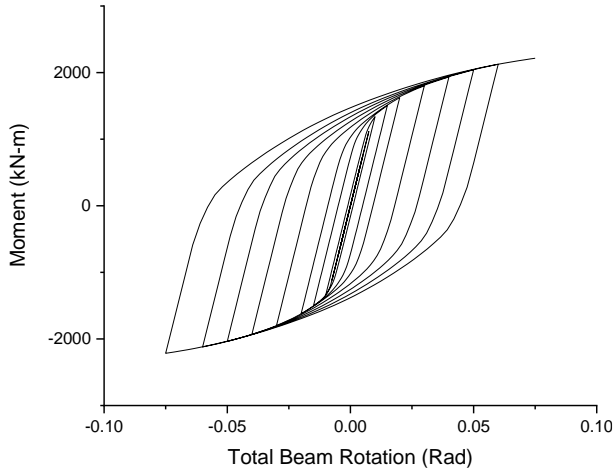


Figure B13: Experimental Moment vs Rotation Curve for RBS-23

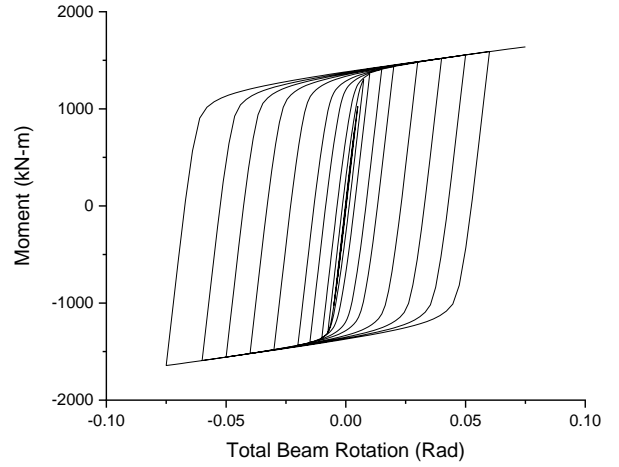


Figure B14: Experimental Moment vs Rotation Curve for RBS-24

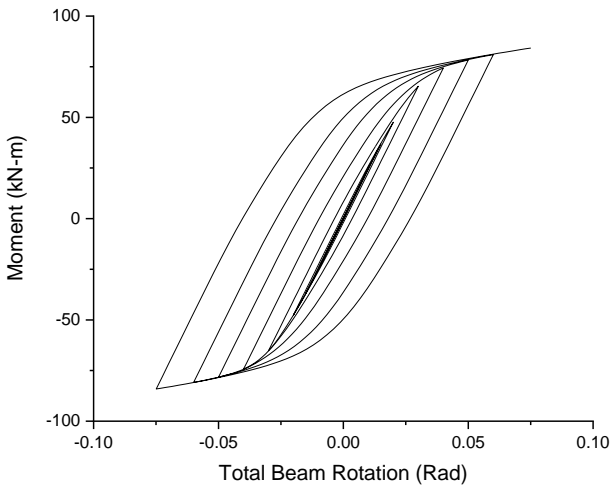


Figure B15: Experimental Moment vs Rotation Curve for RBS-25

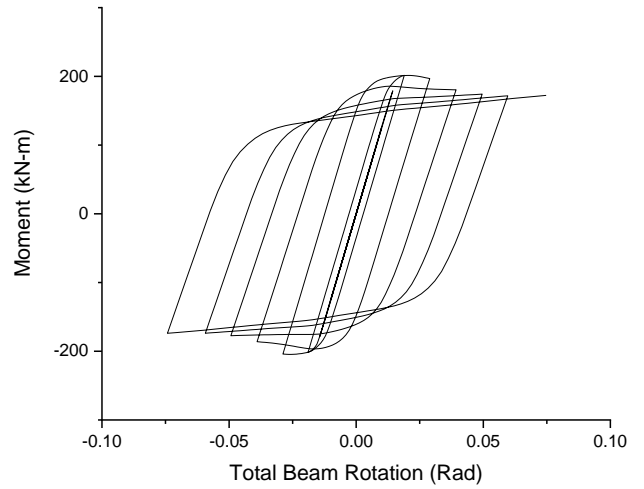


Figure B16: Experimental Moment vs Rotation Curve for RBS-26

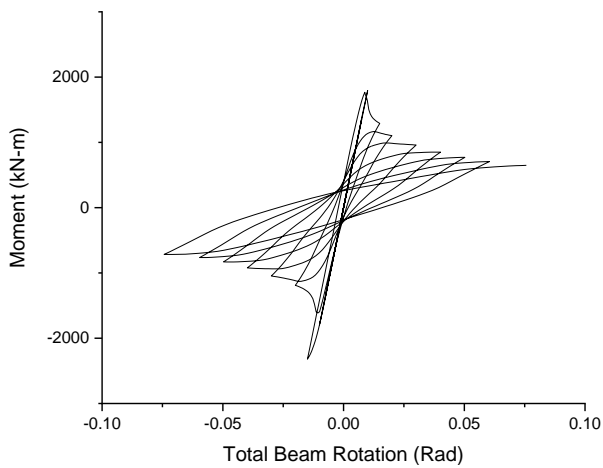


Figure B17: Experimental Moment vs Rotation Curve for RBS-27

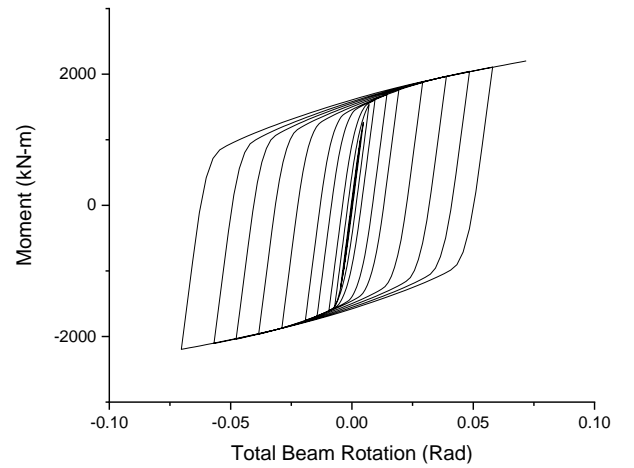


Figure B18: Experimental Moment vs Rotation Curve for RBS-28

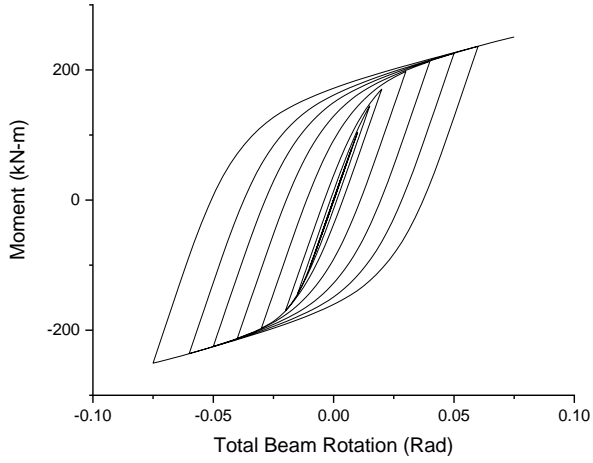


Figure B19: Experimental Moment vs Rotation Curve for RBS-29

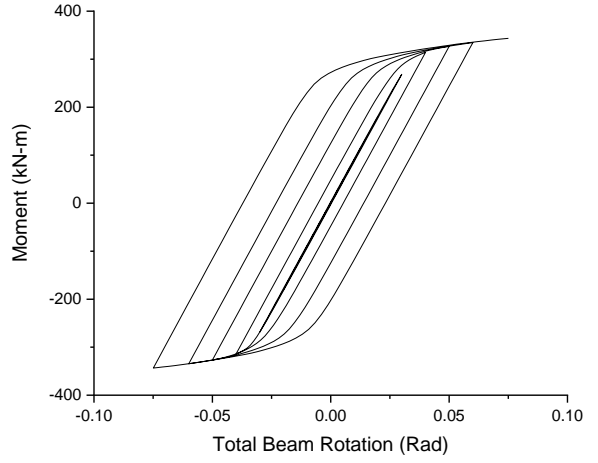


Figure B20: Experimental Moment vs Rotation Curve for RBS-30

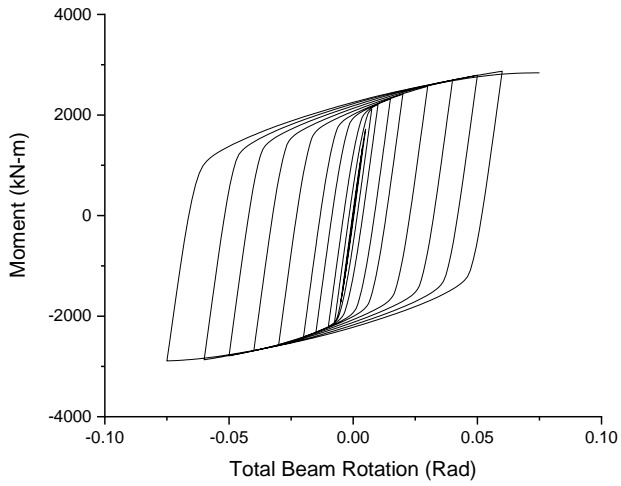


Figure 21: Experimental Moment vs Rotation Curve for RBS-31

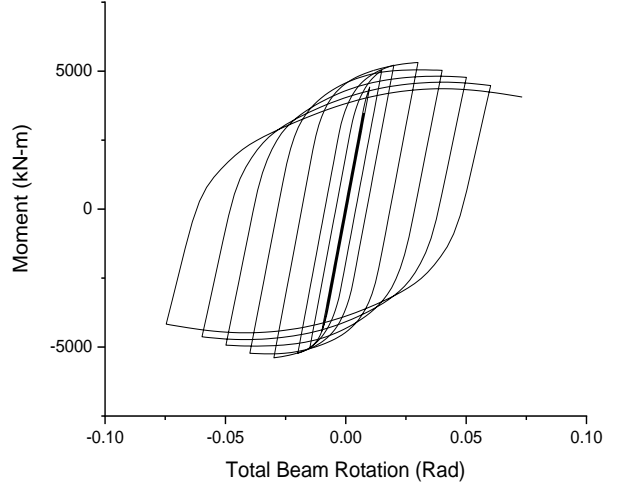


Figure 22: Experimental Moment vs Rotation Curve for RBS-32

APPENDIX C: Deflected Geometries of Specimen

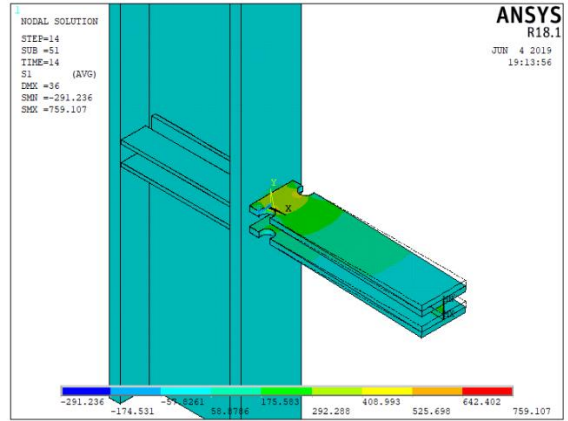
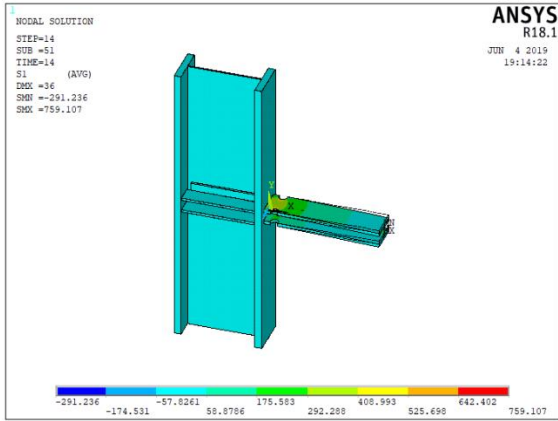


Figure C1: Deflected Geometry of Specimen RBS-6

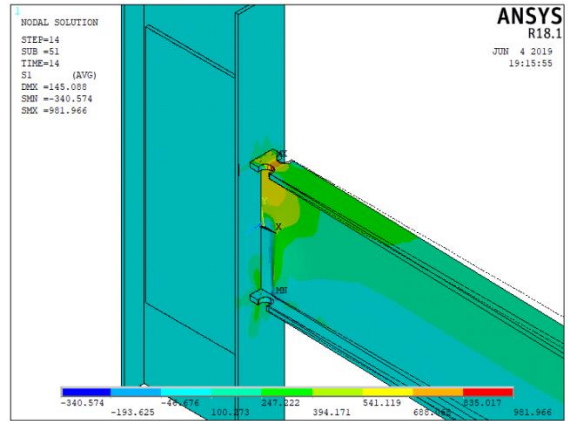
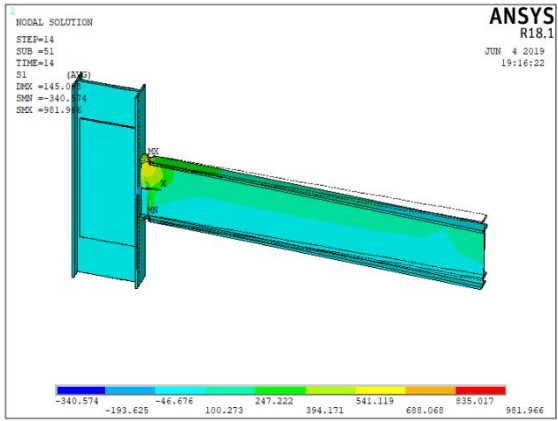


Figure C2: Deflected Geometry of Specimen RBS-7

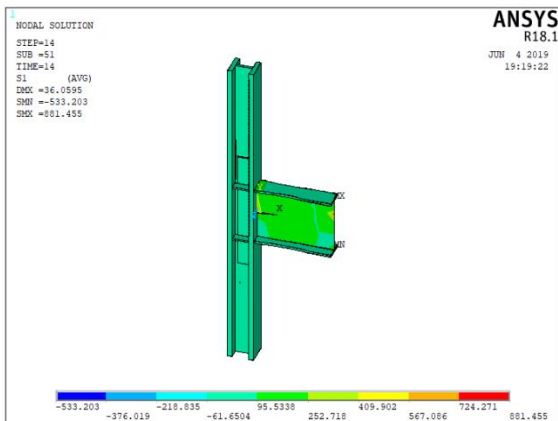


Figure C3: Deflected Geometry of Specimen RBS-8

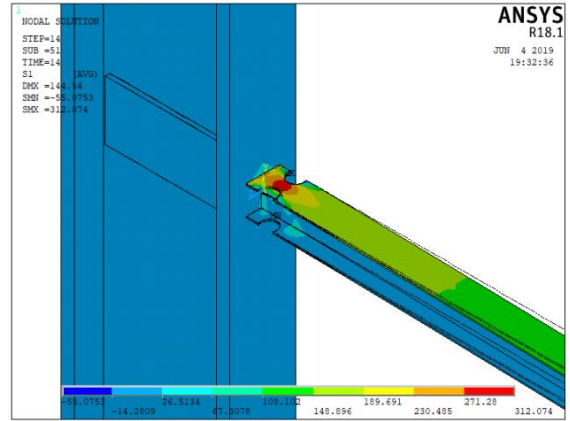
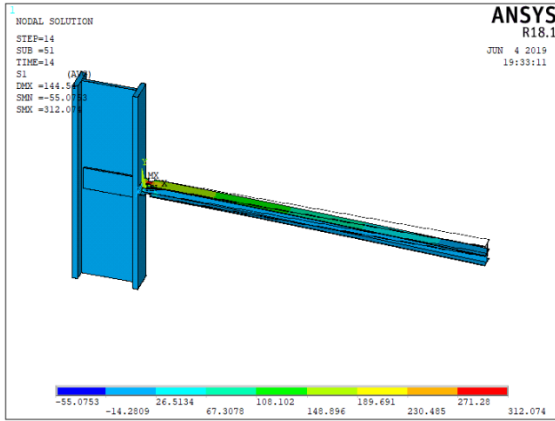


Figure C4: Deflected Geometry of Specimen RBS-9

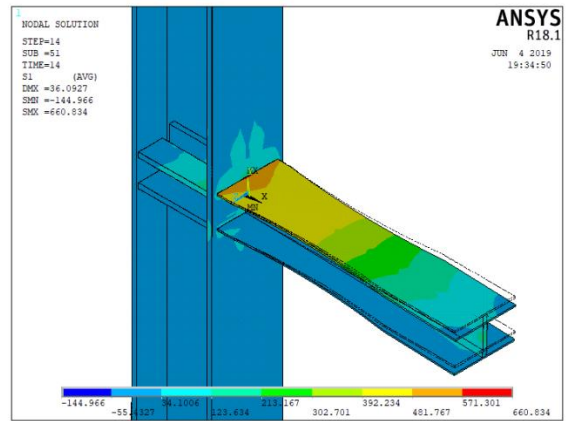
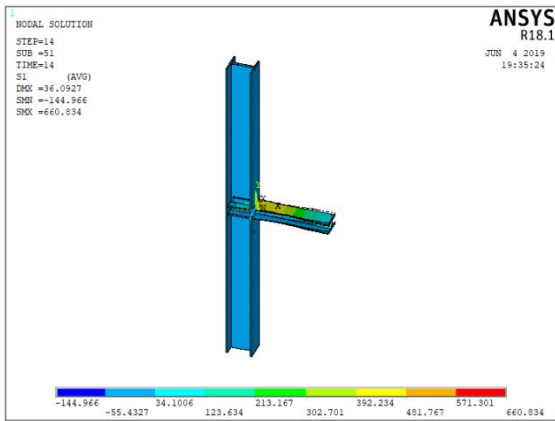


Figure C5: Deflected Geometry of Specimen RBS-10

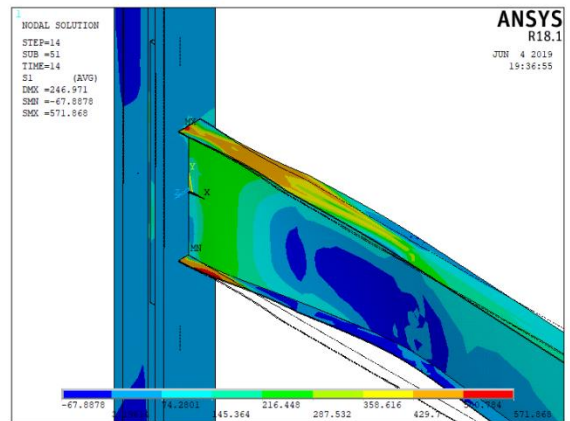
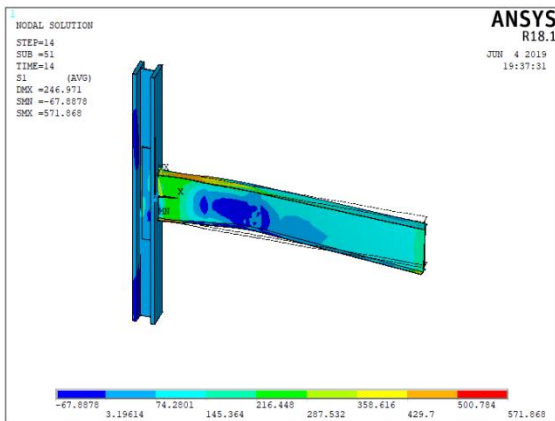


Figure C6: Deflected Geometry of Specimen RBS-11

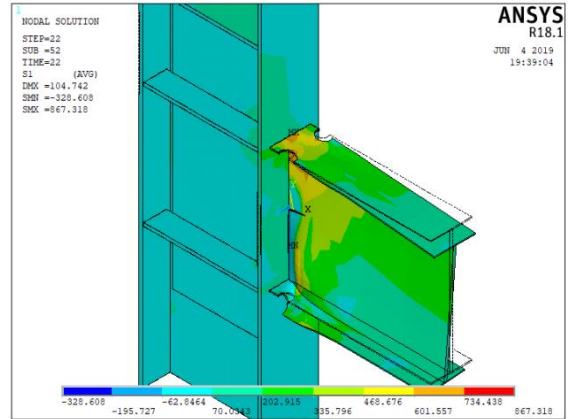
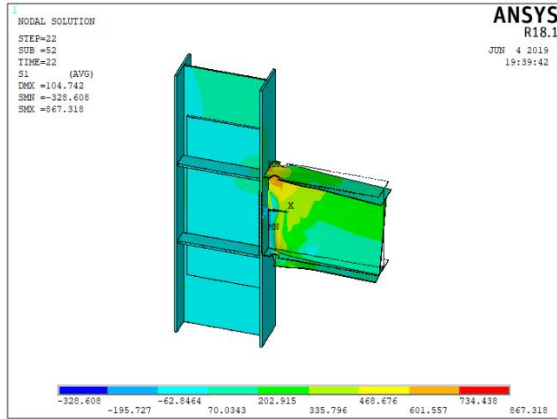


Figure C7: Deflected Geometry of Specimen RBS-12

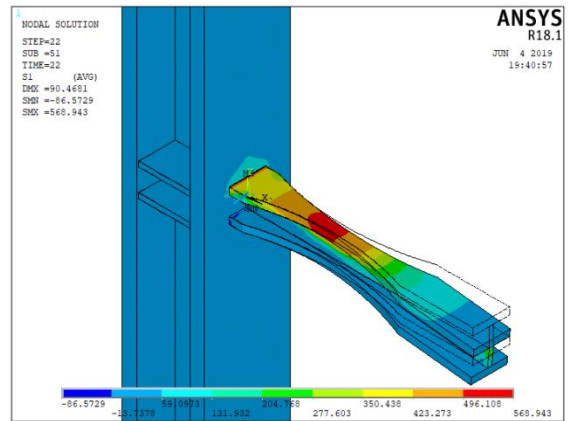
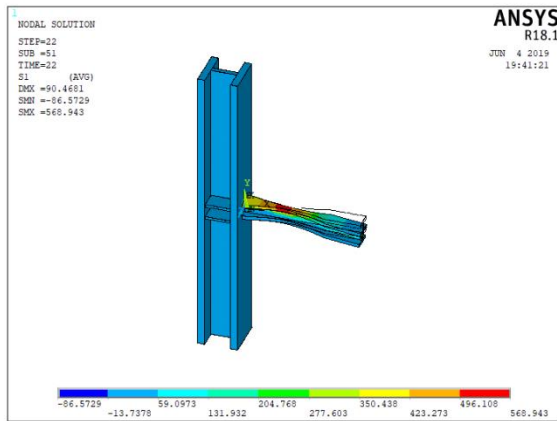


Figure C8: Deflected Geometry of Specimen RBS-13

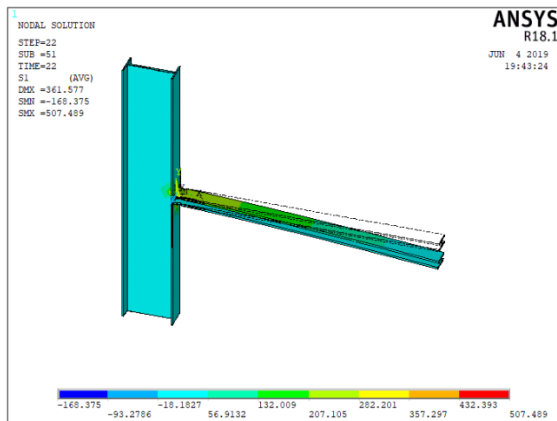


Figure C9: Deflected Geometry of Specimen RBS-14

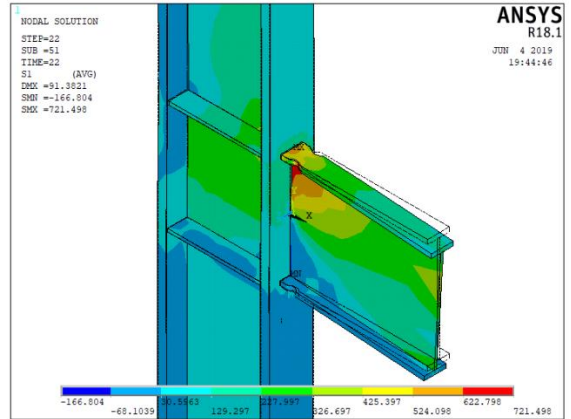
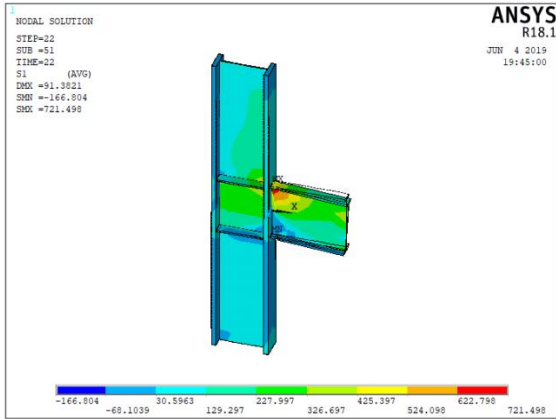


Figure C10: Deflected Geometry of Specimen RBS-15

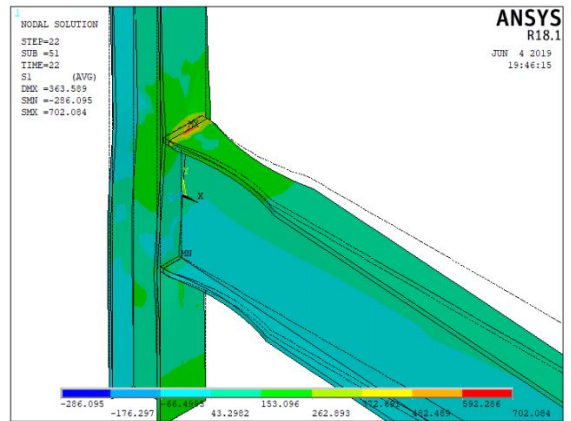
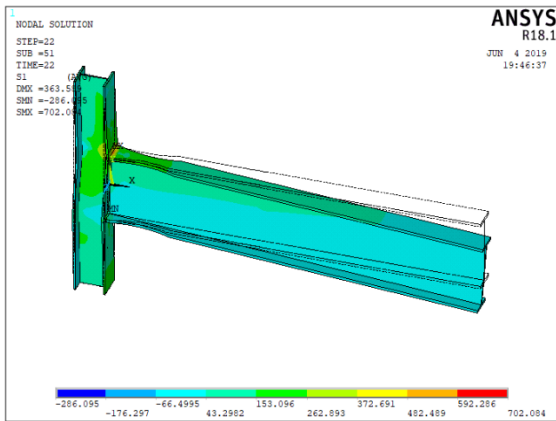


Figure C11: Deflected Geometry of Specimen RBS-16

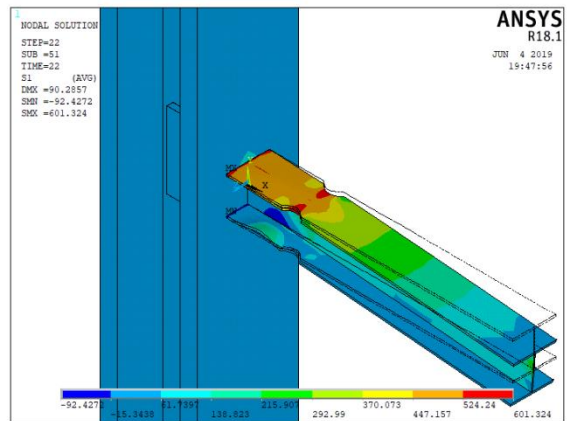
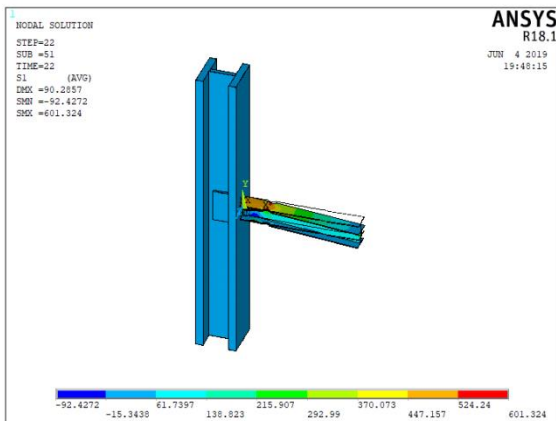


Figure C12: Deflected Geometry of Specimen RBS-17

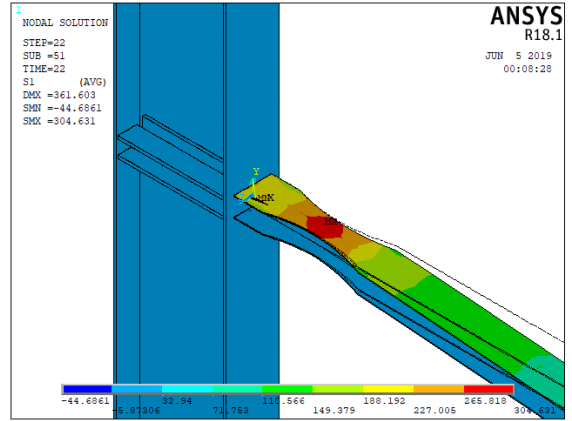
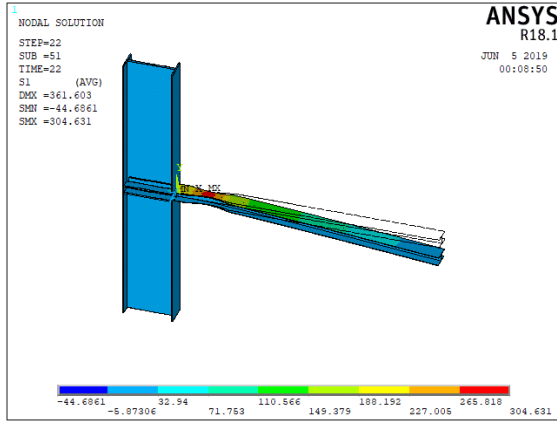


Figure C13: Deflected Geometry of Specimen RBS-18

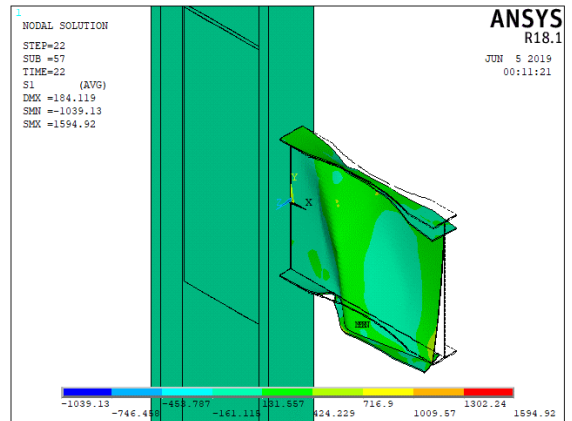
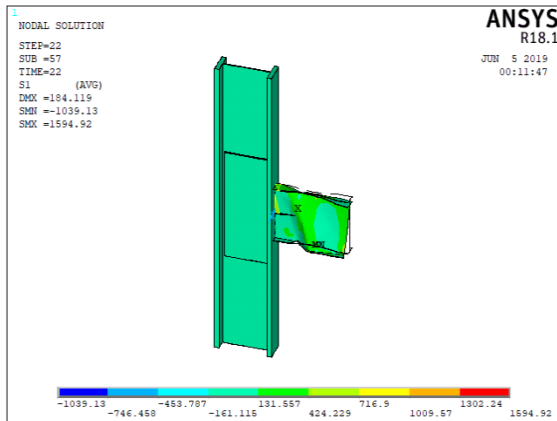


Figure C14: Deflected Geometry of Specimen RBS-19

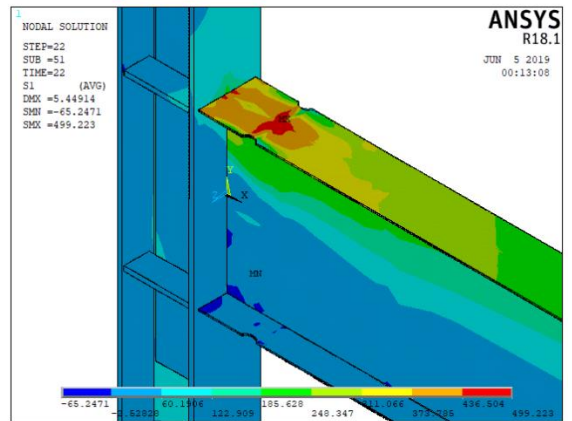
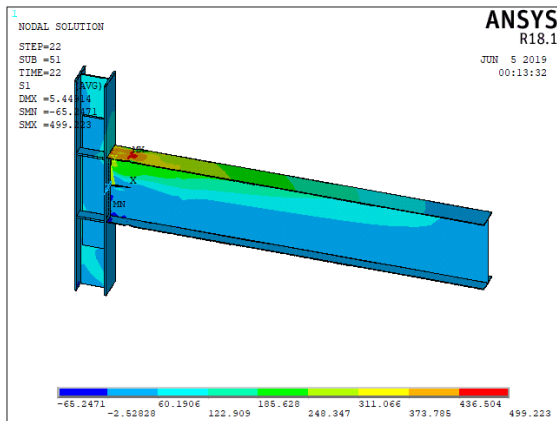


Figure C15: Deflected Geometry of Specimen RBS-20

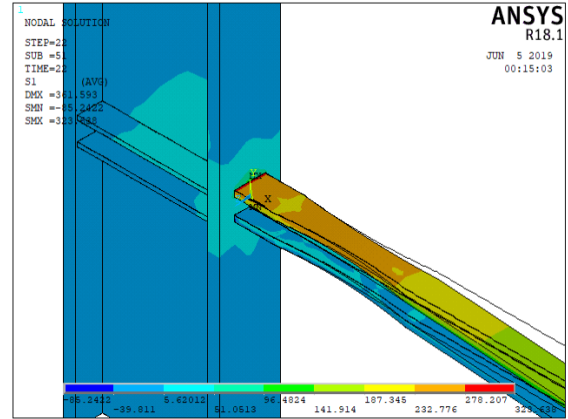
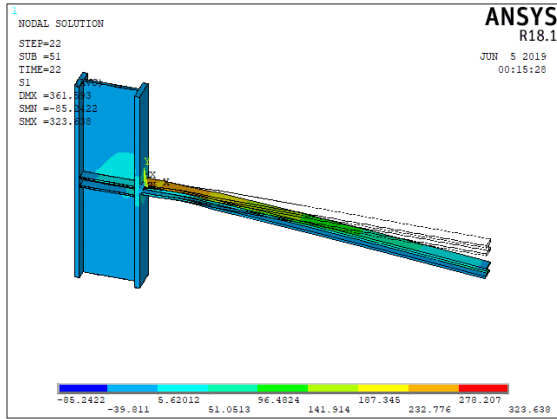


Figure C16: Deflected Geometry of Specimen RBS-21

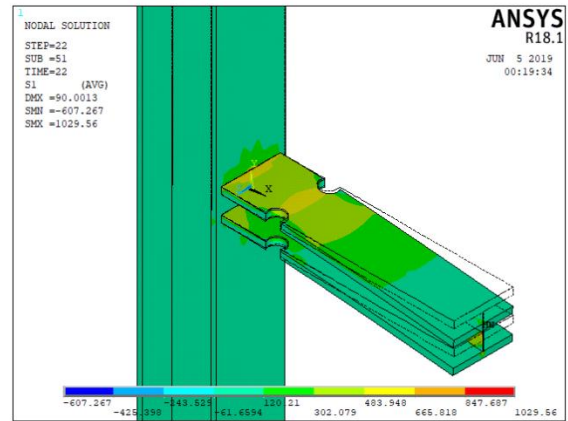
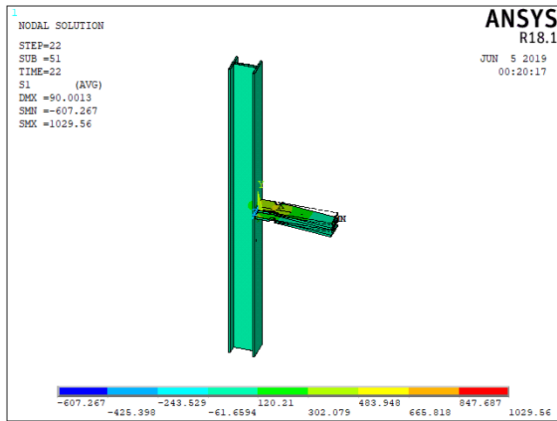


Figure C17: Deflected Geometry of Specimen RBS-22

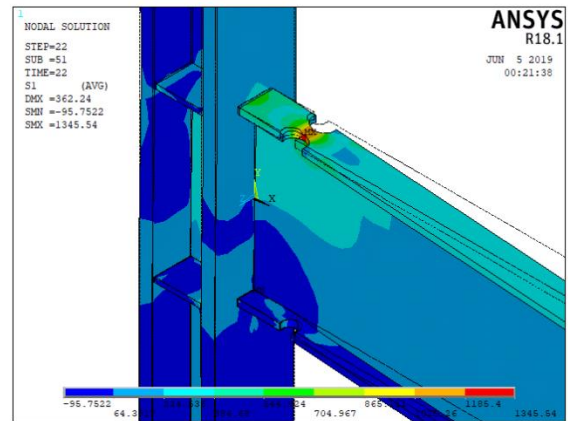
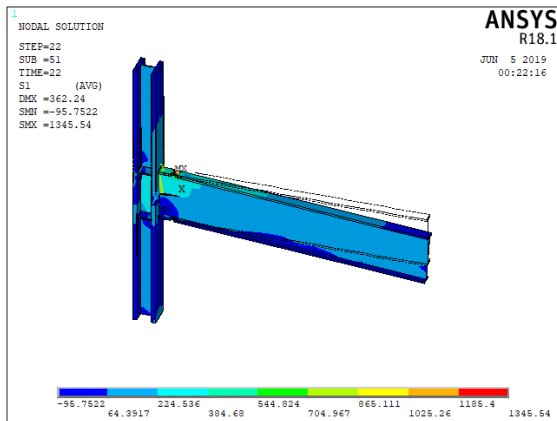


Figure C18: Deflected Geometry of Specimen RBS-23

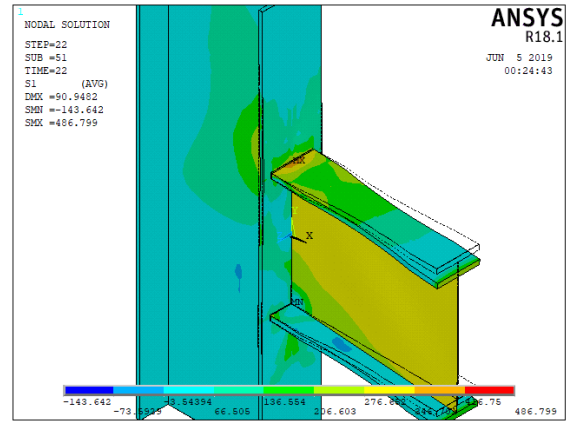
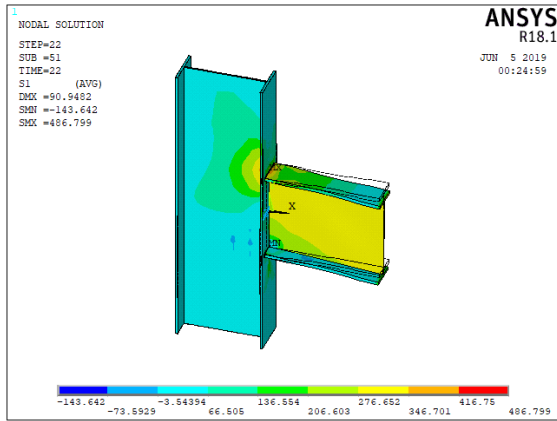


Figure C19: Deflected Geometry of Specimen RBS-24

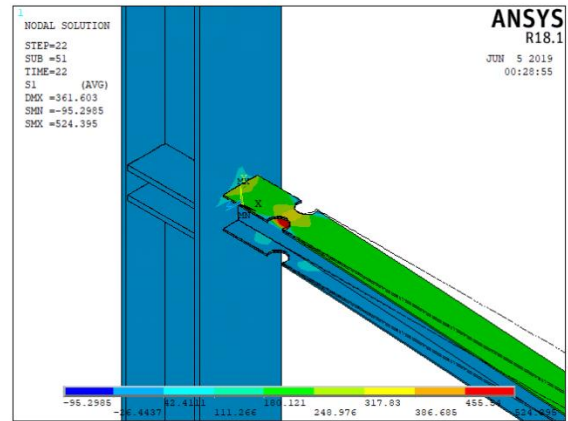
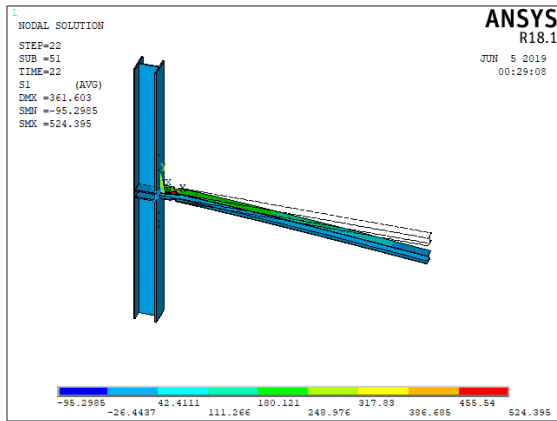


Figure C20: Deflected Geometry of Specimen RBS-25

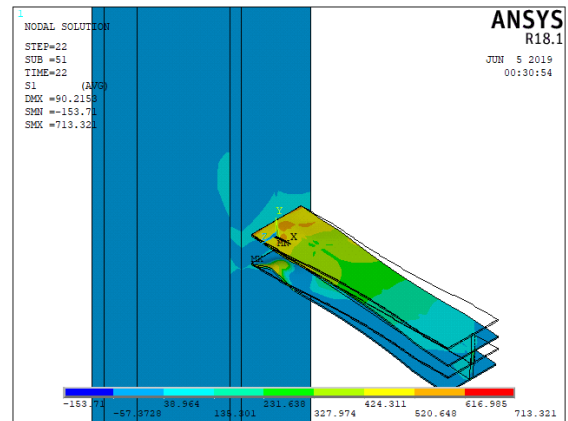
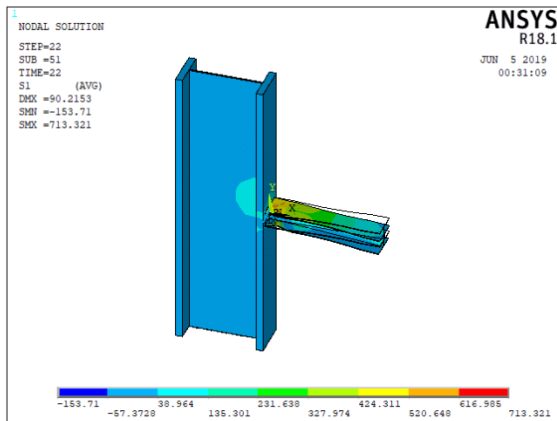


Figure C21: Deflected Geometry of Specimen RBS-26

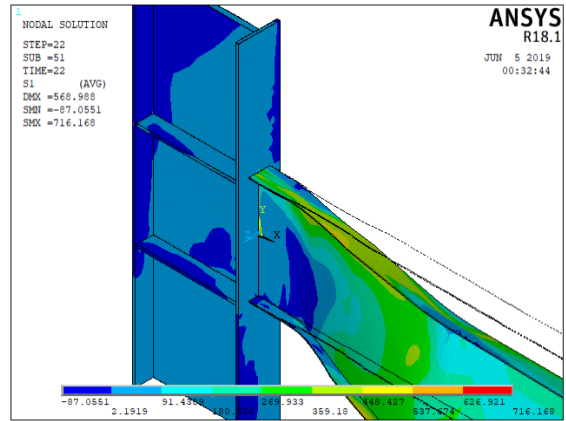
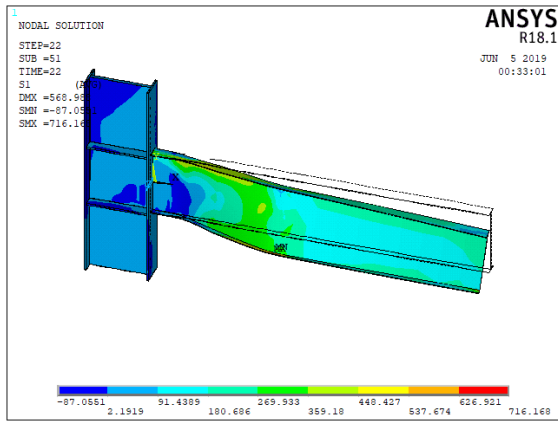


Figure C22: Deflected Geometry of Specimen RBS-27

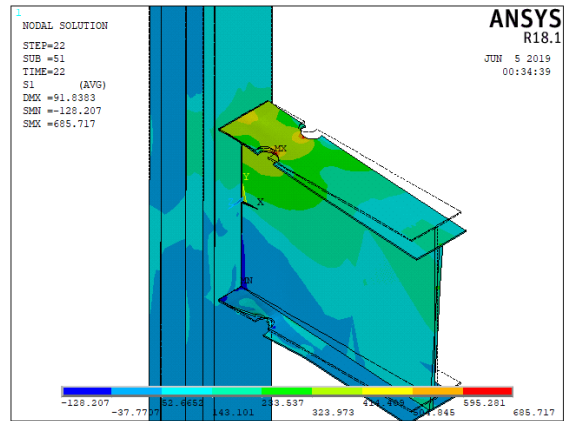
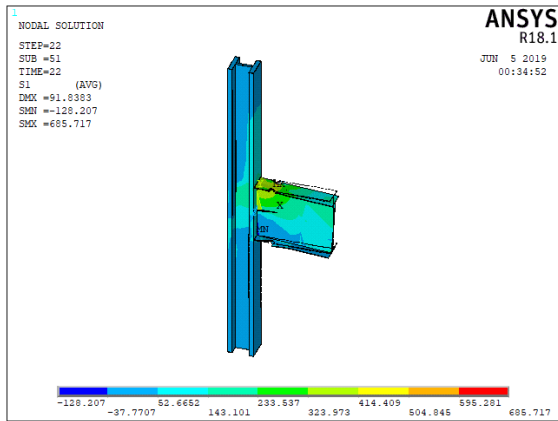


Figure C23: Deflected Geometry of Specimen RBS-28

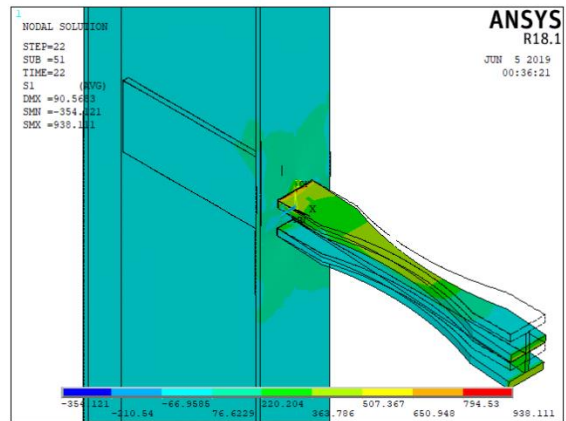
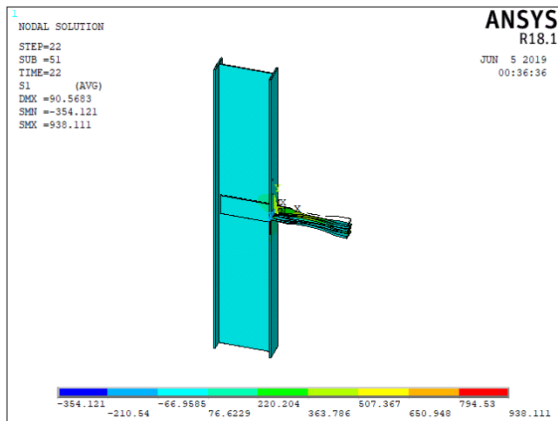


Figure C24: Deflected Geometry of Specimen RBS-29

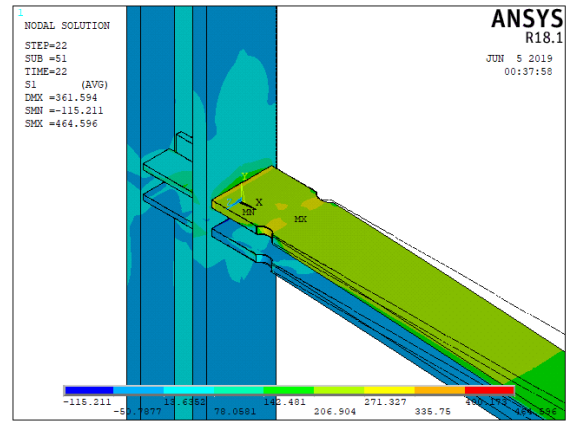
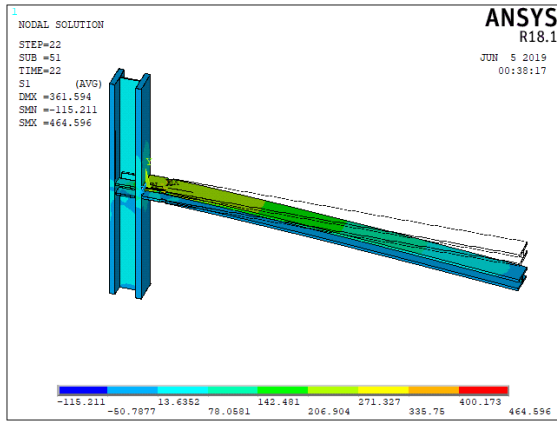


Figure C25: Deflected Geometry of Specimen RBS-30

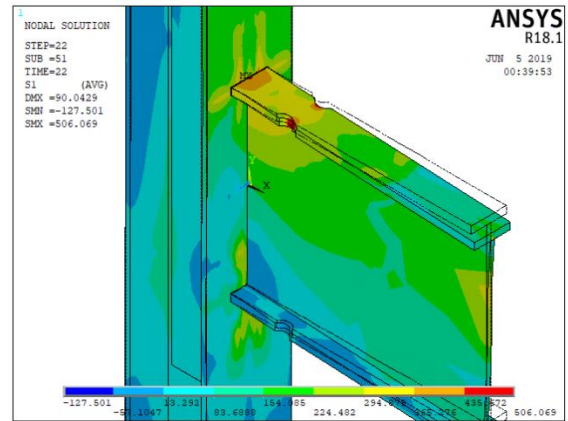
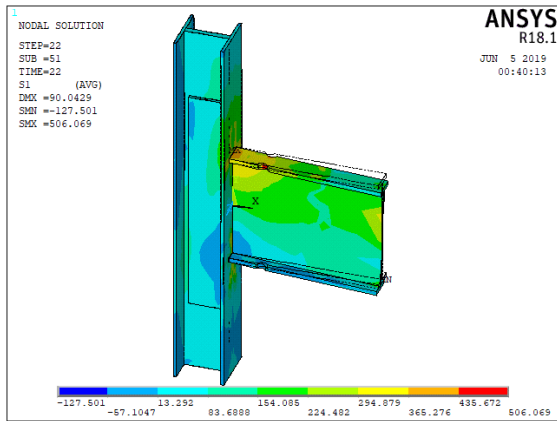


Figure C26: Deflected Geometry of Specimen RBS-31

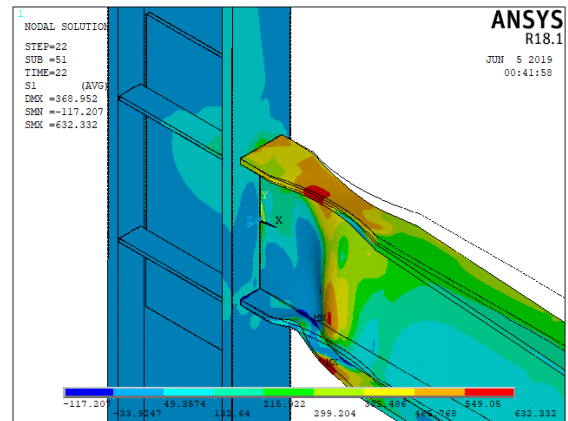
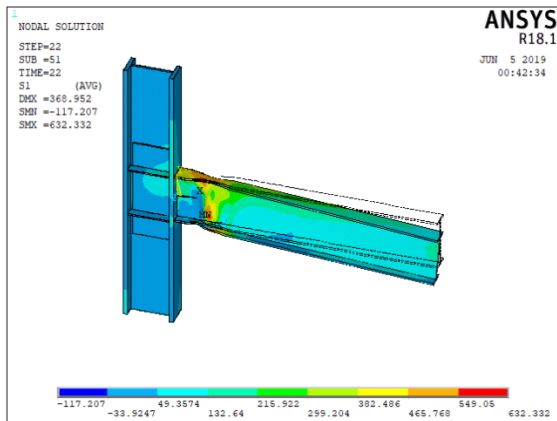


Figure C27: Deflected Geometry of Specimen RBS-32

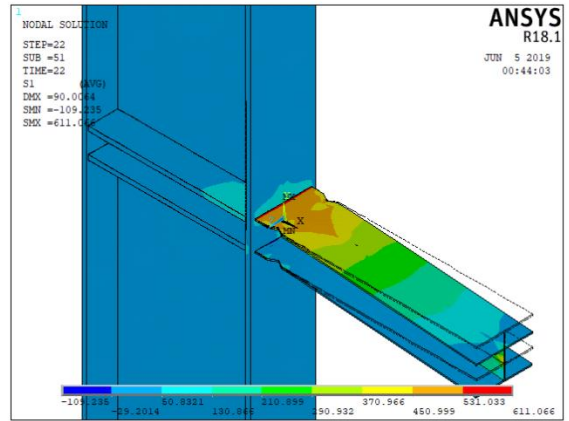
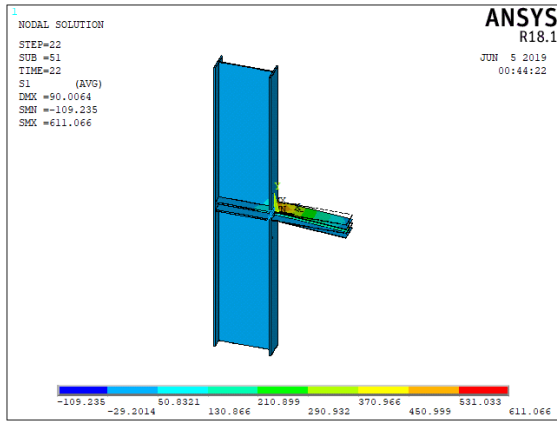


Figure C28: Deflected Geometry of Specimen RBS-33

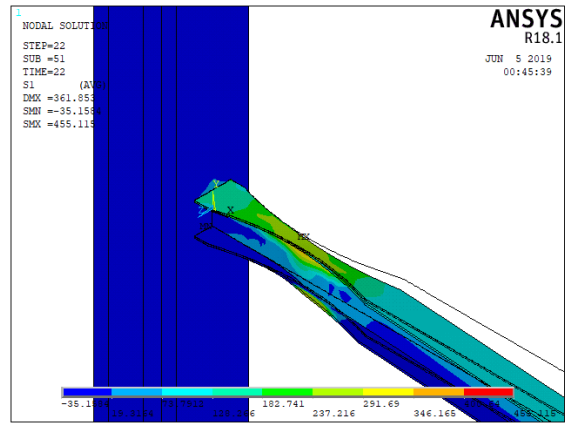
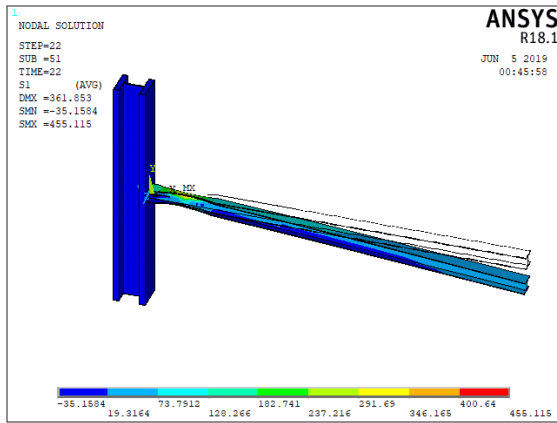


Figure C29: Deflected Geometry of Specimen RBS-34

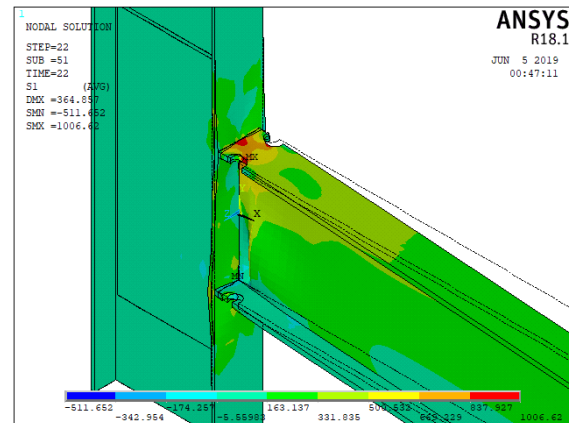
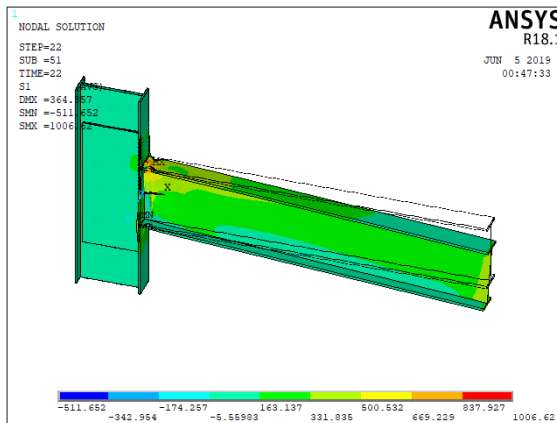


Figure C30: Deflected Geometry of Specimen RBS-35

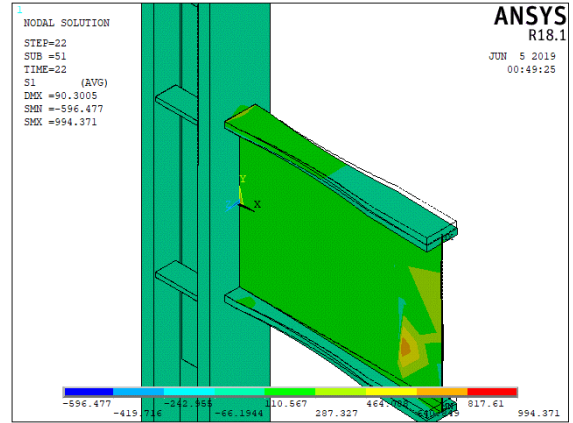
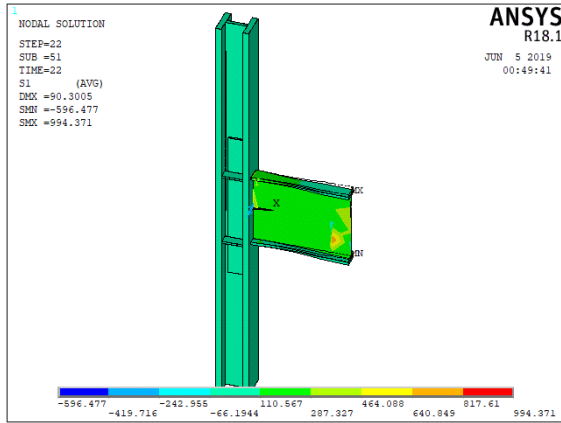


Figure C31: Deflected Geometry of Specimen RBS-36

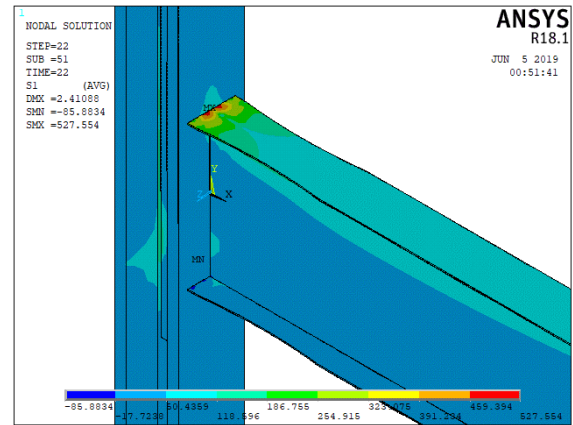
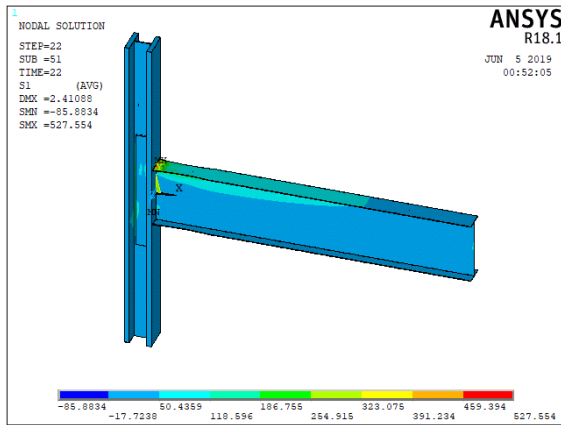


Figure C32: Deflected Geometry of Specimen RBS-37

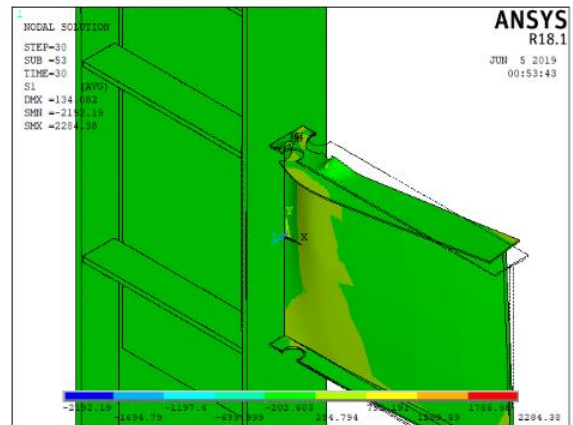
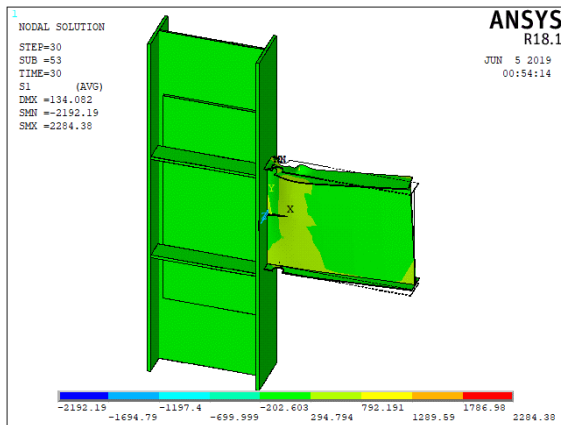


Figure C33: Deflected Geometry of Specimen RBS-38

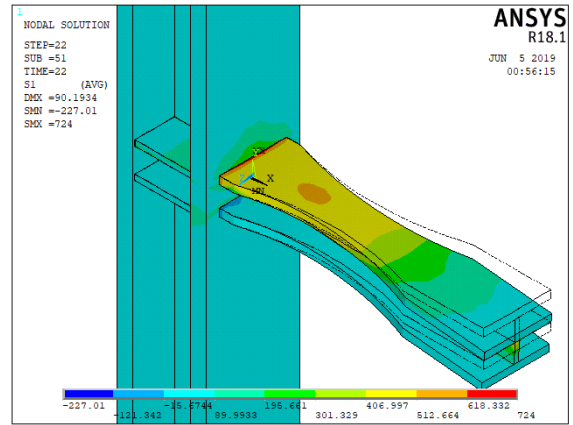
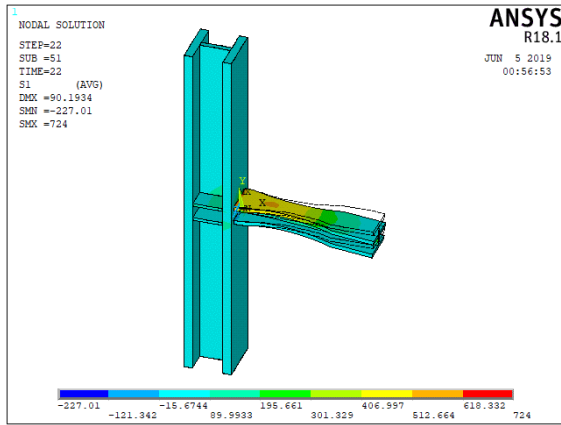


Figure C34: Deflected Geometry of Specimen RBS-39

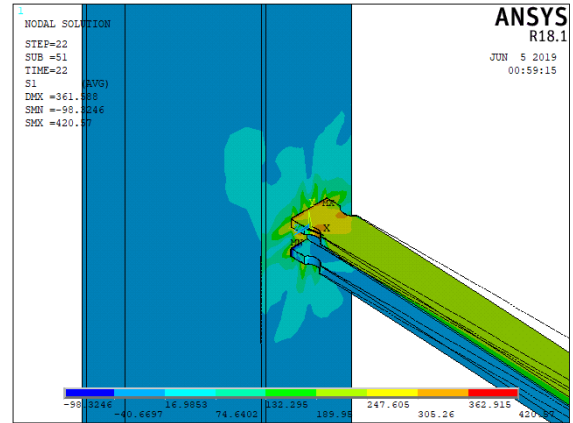
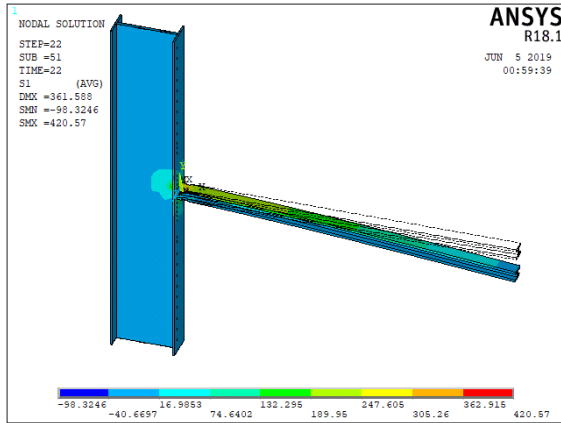


Figure C35: Deflected Geometry of Specimen RBS-40

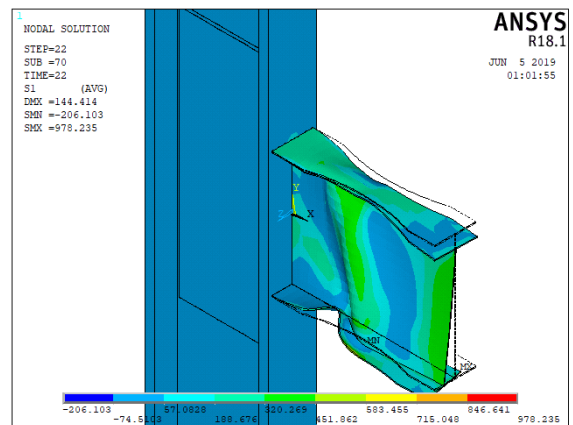
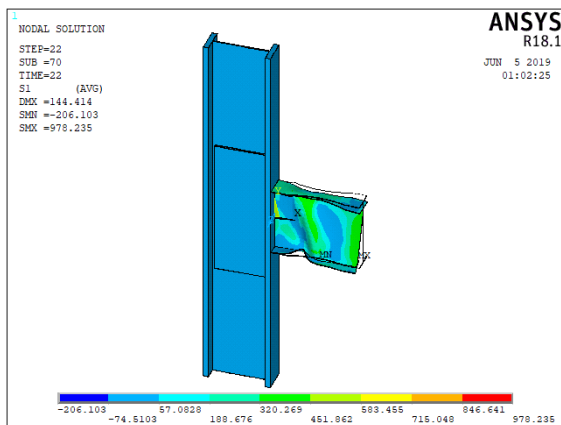


Figure C36: Deflected Geometry of Specimen RBS-41

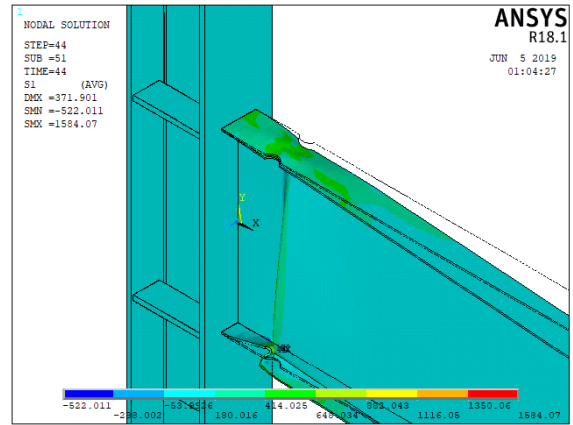
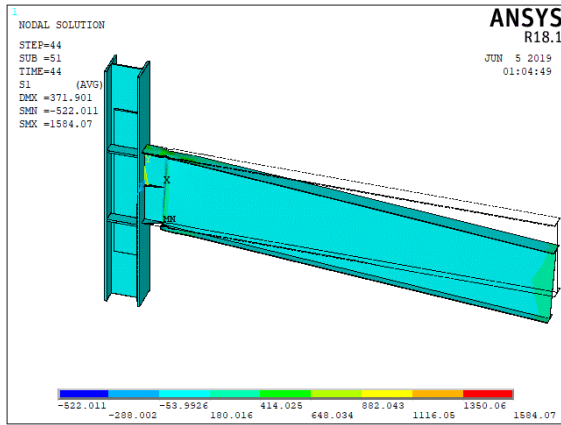


Figure C37: Deflected Geometry of Specimen RBS-42

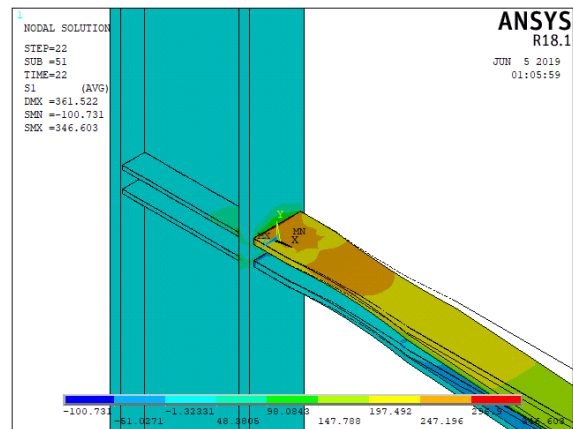
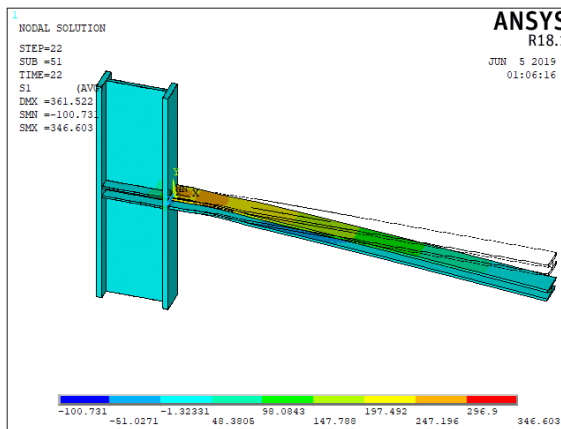


Figure C38: Deflected Geometry of Specimen RBS-43

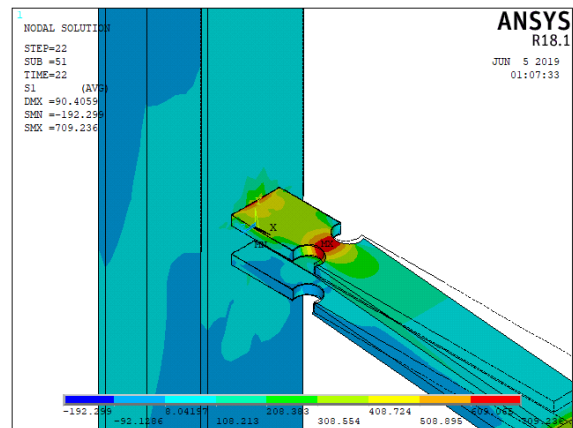
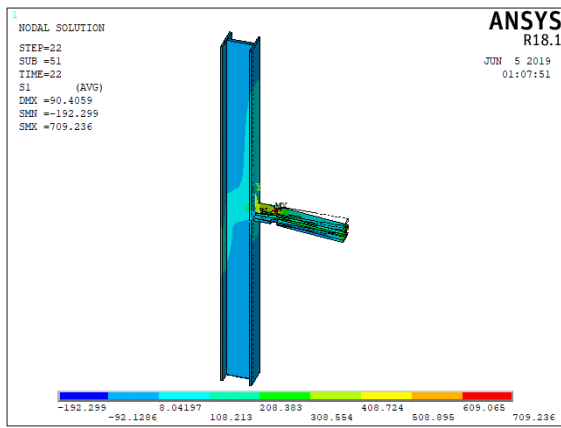


Figure C39: Deflected Geometry of Specimen RBS-44

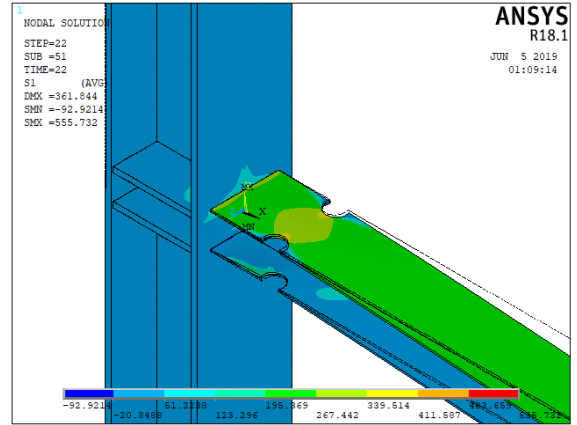
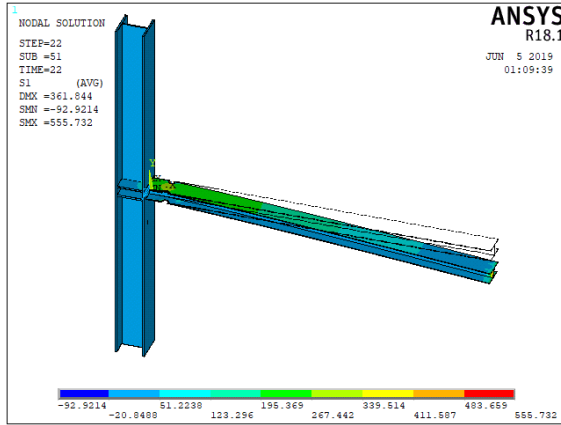


Figure C40: Deflected Geometry of Specimen RBS-45

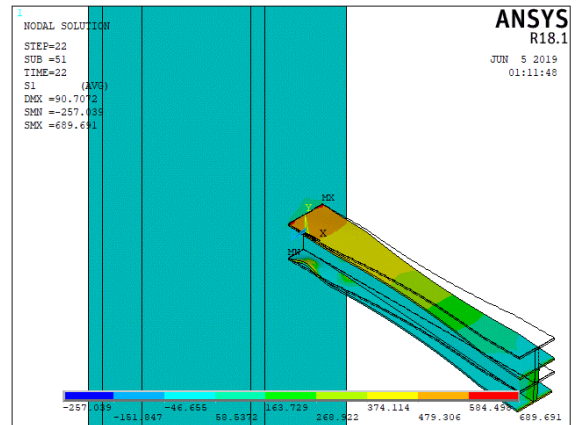
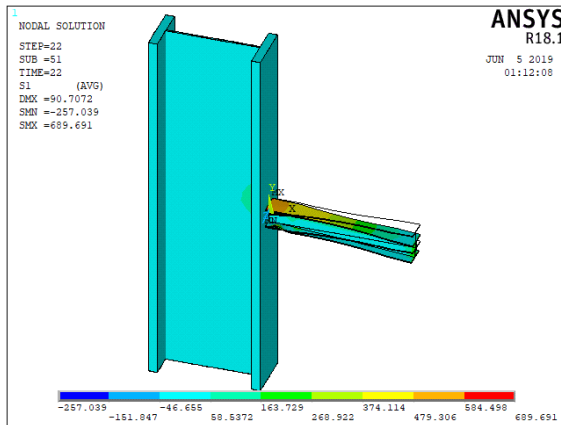


Figure C41: Deflected Geometry of Specimen RBS-46

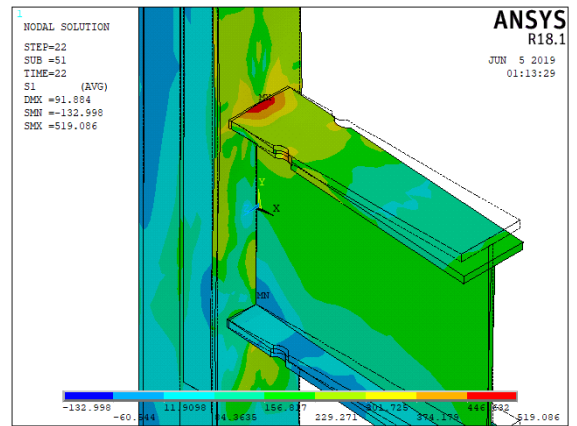
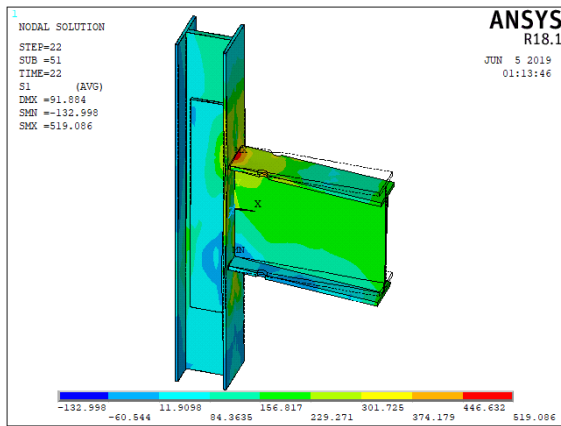


Figure C42: Deflected Geometry of Specimen RBS-47

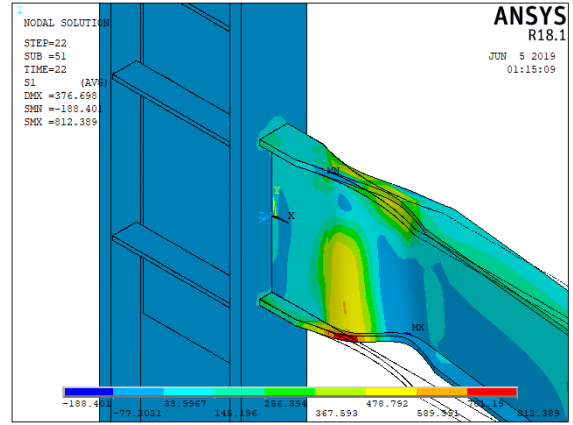
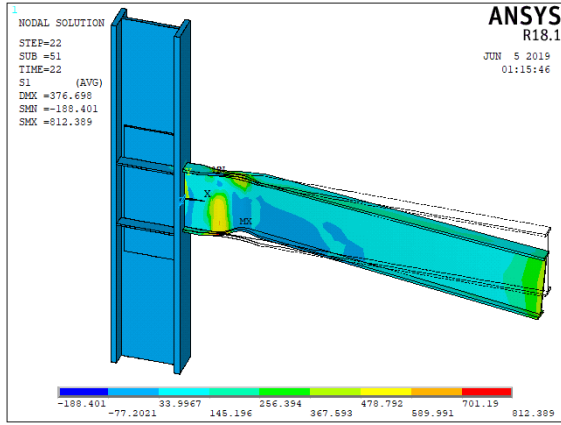


Figure C43: Deflected Geometry of Specimen RBS-48

REFERENCES

- Anderson, M.J., Whitcomb, P.J., Kraber, S.L., and Adams, W. 2017. Stat-Ease Handbook for Experimenters. Stat-Ease, Inc., **11**(27): 1–5.
- Bruneau, M., Uang, C.-M., and Rafael Sabelli. 2011. Ductile Design of Steel Structures.
- Canonsburg, T.D. 2012. ANSYS Mechanical APDL Verification Manual. Knowledge Creation Diffusion Utilization, **15317**(October): 724–746. doi:www.ansys.com.
- Chen, B.S., and Chu, M. 1996. DUCTILE STEEL BEAM-TO-COLUMN CONNECTIONS FOR SEISMIC RESISTANCE. **122**(11): 1292–1299.
- Chi, B., and Uang, C. 2002. Cyclic Response and Design Recommendations of Reduced Beam Section Moment Connections with Deep Columns. **128**(April): 464–473.
- Chou, C., and Wu, C. 2007. Performance evaluation of steel reduced flange plate moment connections. (June): 2083–2097. doi:10.1002/eqe.
- Dastfan, M., Asce, A.M., Driver, R., and Asce, M. 2018. Test of a Steel Plate Shear Wall with Partially Encased Composite Columns and RBS Frame Connections. **144**(2): 1–9. doi:10.1061/(ASCE)ST.1943-541X.0001954.
- Engelhardt, M.D. 1999. The 1999 T. R. Higgins lecture: design of reduced beam section moment connections. 1999 North American Steel Construction Conference(NASCC),: 1999.
- Gilton, C.S., and Uang, C.M. 2002. Cyclic response and design recommendations of weak-axis reduced beam section moment connections. Journal of Structural Engineering-Asce, **128**(4): 452–463. doi:Doi 10.1061/(Asce)0733-9445(2002)128:4(452).
- Jones, S.L., Fry, G.T., and Engelhardt, M.D. 2002. Experimental Evaluation of Cyclically Loaded Reduced Beam Section Moment Connections. Journal of Structural Engineering, **128**(4): 441–51. doi:10.1061/ASCE0733-9445(2002)128:4(441).
- Kim, K., Engelhardt, M.D., and Asce, M. 2007. Nonprismatic Beam Element for Beams with RBS Connections in Steel Moment Frames. **133**(February): 176–184.
- Lee, C., Jeon, S., Kim, J., and Uang, C. 2005. Effects of Panel Zone Strength and Beam Web Connection Method on Seismic Performance of Reduced Beam Section Steel Moment Connections. **131**(December 2005): 1854–1865.

- Lee, C.H., and Kim, J.H. 2007. Seismic design of reduced beam section steel moment connections with bolted web attachment. *Journal of Constructional Steel Research*, **63**(4): 522–531. doi:10.1016/j.jcsr.2006.06.030.
- Li, F.-X., Kanao, I., Li, J., and Morisako, K. 2009. Local buckling of RBS beams subjected to cyclic loading. *Journal of structural engineering*, **135**(12): 1491–1498. doi:10.1061/(ASCE)ST.1943-541X.0000073.
- Li, R., Samali, B., Tao, Z., and Kamrul Hassan, M. 2017. Cyclic behaviour of composite joints with reduced beam sections. *Engineering Structures*, **136**: 329–344. Elsevier Ltd. doi:10.1016/j.engstruct.2017.01.025.
- Montgomery, D.C. 2013. *Design and Analysis of Experiments Eighth Edition*.
- Moradi, S., and Alam, M.S. 2017. Lateral load-drift response and limit states of posttensioned steel beam-column connections: parametric study. *Journal of Structural Engineering (United States)*, **143**(7): 1–13. doi:10.1061/(ASCE)ST.1943-541X.0001772.
- Oh, K., Lee, K., Chen, L., Hong, S., and Yang, Y. 2015. Seismic performance evaluation of weak axis column-beam moment connections with reduced beam section. *JCSR*, **105**: 28–38. Elsevier Ltd. doi:10.1016/j.jcsr.2014.10.005.
- Pachoumis, D.T., Galoussis, E.G., Kalfas, C.N., and Christitsas, A.D. 2009. Reduced beam section moment connections subjected to cyclic loading: Experimental analysis and FEM simulation. *Engineering Structures*, **31**(1): 216–223. Elsevier Ltd. doi:10.1016/j.engstruct.2008.08.007.
- Pachoumis, D.T., Galoussis, E.G., Kalfas, C.N., and Efthimiou, I.Z. 2010. Cyclic performance of steel moment-resisting connections with reduced beam sections - experimental analysis and finite element model simulation. *Engineering Structures*, **32**(9): 2683–2692. Elsevier Ltd. doi:10.1016/j.engstruct.2010.04.038.
- Pantelides, C.P., Eeri, M., Okahashi, Y., Eeri, M., Reaveley, L.D., and Eeri, M. 2004. Experimental Investigation of Reduced Beam Section Moment Connections without Continuity Plates. **20**(4): 1185–1209. doi:10.1193/1.1814369.
- Paul Popov, E., Yang, T.S., and Chang, S.P. 1998. Design of steel MRF connections before and after 1994 Northridge earthquake. *Engineering Structures*, **20**(12): 1030–1038. doi:10.1016/S0141-0296(97)00200-9.
- Prinz, G.S., and Richards, P.W. 2016. Demands on Reduced Beam Section Connections with Out-of-

Plane Skew. *Journal of Structural Engineering*, **142**(1): 04015095. doi:10.1061/(ASCE)ST.1943-541X.0001360.

- Rahnavard, R., Hassanipour, A., and Siahpolo, N. 2015. Case Studies in Structural Engineering Analytical study on new types of reduced beam section moment connections affecting cyclic behavior. *CASE STUDIES IN STRUCTURAL ENGINEERING*, **3**: 33–51. Elsevier Ltd. doi:10.1016/j.csse.2015.03.001.
- Sofias, C.E., Kalfas, C.N., and Pachoumis, D.T. 2014. Experimental and FEM analysis of reduced beam section moment endplate connections under cyclic loading. *Engineering Structures*, **59**: 320–329. Elsevier Ltd. doi:10.1016/j.engstruct.2013.11.010.
- Sophianopoulos, D. 2011. Parameters affecting response and design of Steel Moment Frame Reduced Beam Section connections : An overview Parameters Affecting Response and Design of Steel Moment Frame Reduced Beam Section Connections : An Overview. (June 2011). doi:10.1007/s13296-011-2003-5.
- Sophianopoulos, D.S., and Deri, A.E. 2017. Steel beam-to-column RBS connections with European profiles: I. Static optimization. *Journal of Constructional Steel Research*, **139**: 101–109. Elsevier Ltd. doi:10.1016/j.jcsr.2017.09.028.
- Tabar, A.M., and Deylami, A. 2005. Instability of beams with reduced beam section moment connections emphasizing the effect of column panel zone ductility. *Journal of Constructional Steel Research*, **61**(11): 1475–1491. doi:10.1016/j.jcsr.2005.05.006.
- Uang, B.C., Yu, Q.K., Member, S., Noel, S., and Gross, J. 2000. Cyclic Testing of Steel Moment Connections With RBS or Welded Haunch. *Journal of Structural Engineering*, **126**(January): 57–68. doi:10.1061/(ASCE)0733-9445(2000)126:1(57).
- Uang, C., and Fan, C.-C. 2001. CYCLIC STABILITY CRITERIA FOR STEEL MOMENT CONNECTIONS WITH REDUCED BEAM SECTION. **126**(January): 69–78.
- Zhang, X., and Ricles, J.M. 2006. Experimental Evaluation of Reduced Beam Section Connections to Deep Columns. *Journal of Structural Engineering*, **132**(3): 346–357. doi:10.1061/(ASCE)0733-9445(2006)132:3(346).
- Zhang, X., Ricles, J.M., and Asce, M. 2006. Seismic Behavior of Reduced Beam Section Moment Connections to Deep Columns. **132**(March): 358–367.